Conference program

Book of abstracts

International conference

Functional materials and nanotechnologies 2011

Institute of Solid State Physics
University of Latvia
April 5 - 8

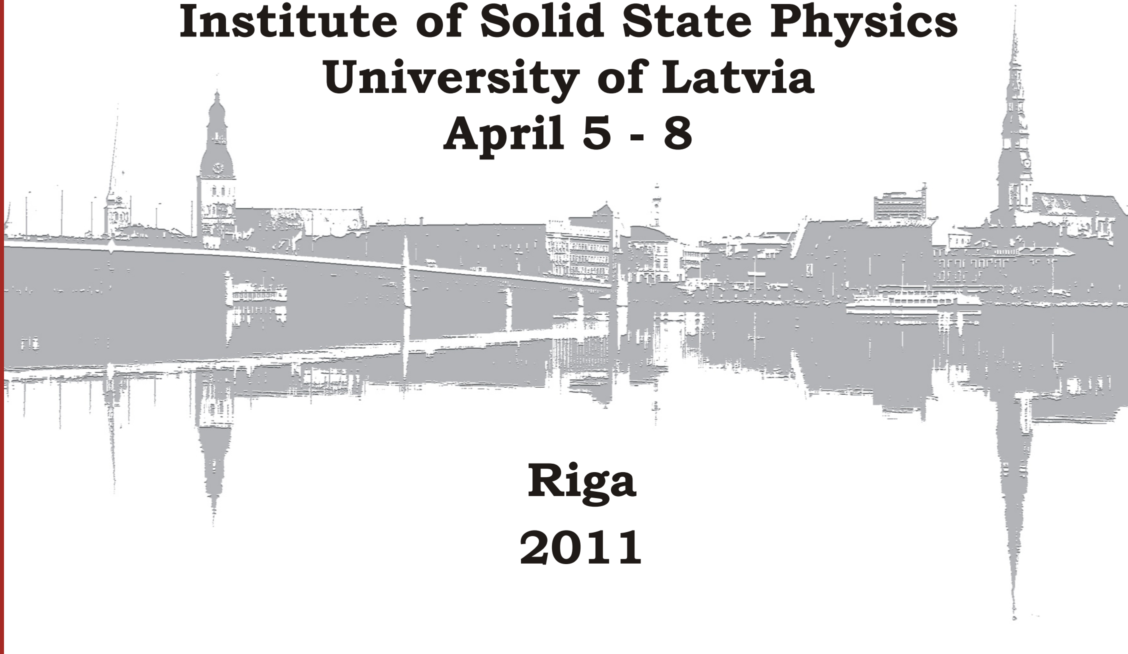

Riga
2011

WELCOME

The Organizing Committee kindly welcomes you to the International Baltic Sea Region conference "Functional materials and nanotechnologies" **FM&NT-2011**. The conference is organized in co-operation with projects **ERANET "MATERA"** and **National Research programme in Materials Science of Latvia.**

The purpose of the conference is to bring together scientists, research staff, engineers, and students from universities, research institutes and related industrial companies aware in the field of advanced material science and materials technologies trends and future activities.

Scientific Themes are following:

- **Theoretical research and modeling of processes and materials;**
- **Materials for energetics, renewable energy technologies and photovoltaics;**
- **Multifunctional inorganic, organic and hybrid materials for photonic, micro and nanoelectronic applications and innovative methods for the research of nanostructures;**
- **Advanced technologies for the synthesis and the research of nanostructured materials, nanoparticles, thin films and coatings;**
- **Applications of innovative materials in science and economics.**

International Organizing Committee

- **Andris Sternberg (chairperson)**, Institute of Solid State Physics, University of Latvia, Latvia, MATERA
- **Juras Banys**, Vilnius University, Lithuania
- **Gunnar Borstel**, University of Osnabrück, Germany
- **Niels E. Christensen**, University of Aarhus, Denmark
- **Robert A. Evarestov**, St. Petersburg State University, Russia
- **Claes-Goran Granqvist**, Uppsala University, Sweden
- **Dag Høvik**, The Research Council of Norway, Norway, MATERA
- **Marco Kirm**, Institute of Physics, University of Tartu, Estonia
- **Vladislav Lemanov**, Ioffe Physical Technical Institute, Russia
- **Witold Łojkowski**, Institute of High Pressure Physics, Poland
- **Ergo Nommiste**, University of Tartu, Estonia
- **Helmut Schober,** Institut Laue-Langevin, France
- **Sisko Sipilä**, Finnish Funding Agency for Technology and Innovation, Finland, MATERA
- **Ingólfur Torbjörnsson**, Icelandic Centre for Research, Iceland, MATERA
- **Marcel H. Van de Voorde**, University of Technology Delft, The Netherlands

International Program Committee

- **Inta Muzikante (chairperson),** Institute of Solid State Physics, University of Latvia, Latvia, MATERA
- **Liga Berzina-Cimdina,** Institute of Biomaterials and Biomechanics, Riga Technical University, Latvia
- **Janis Grabis,** Institute of Inorganic Chemistry, Riga Technical University, Latvia
- **Leonid V. Maksimov,** Vavilov State Optical Institute, Russia
- **Linards Skuja,** Institute of Solid State Physics, University of Latvia, Latvia
- **Maris Springis,** Institute of Solid State Physics, University of Latvia, Latvia
- **Ilmars Zalite,** Institute of Inorganic Chemistry, Riga Technical University, Latvia
- **Janis Zicans,** Institute of Polymers, Riga Technical University

Local Committee:

Liga Grinberga, Anatolijs Sarakovskis, Jurgis Grube, Raitis Siatkovskis, Maris Kundzins, Anna Muratova, Gunita Garda, Maris Springis, Aivars Vembris, Krisjanis Smits, Andris Fedotovs, Dmitrijs Bocarovs, Anastasija Jozepa, Andris Krumins.

The Organizing Committee sincerely hopes that the Conference will give all the participants new insights into the wide spread development of functional materials and nanotechnologies and will enhance the circulation of information released at the meeting.

On behalf of FM&NT-2011 organizers thank you all for coming and we wish you most successful and enjoyable Conference.

Edited by: Andris Sternberg, Inta Muzikante, Liga Grinberga (ISSP UL)
Typesetting: Anatolijs Sarakovskis, Jurgis Grube (ISSP UL)
Printed by “Latgales Druka”
ISBN: 978-9984-45-334-7
Institute of Solid State Physics, University of Latvia
8 Kengaraga Street, LV-1063, Riga, Latvija
Phone: +371-67187816
Fax: +371-67132778
e-mail: issp@cfi.lu.lv
web: http://www.cfi.lu.lv

Riga, 2011

PARTNERS

ERAF

Atbalsts starptautiskās sadarbības
projektiem zinātnē un tehnoloģijās LU CFI

LZP

UNIVERSITAS LATVIENSIS

SCIENTIAE ET PATRIAE

IMIS

IZGLĪTĪBAS un ZINĀTNES
MINISTRIJA

HH
Hanja Hotel

Taylor & Francis
Taylor & Francis Group

AMERICAN
ELEMENTS ®
America's Leading Manufacturer of Engineered and Advanced Material Products

SIDRABE

THORLABS

MATERA

LMPB

EXHIBITORS

FANEX, THORLABS


THORLABS
Optical Spectrum Analyzer
INPUT FC/APC
POWER


THORLABS
LMH-20X-532

Fanex is established in 1993 as a solution provider for laboratories and industry, especially in the field of analytical chemistry and microfiltration.

Fanex activites are based on deep knowledge of our staff with vast experienced in various fields of research and industry.

Today Fanex employs 15 people and is active in Latvia, Lithuania and Estonia.

We operate a calibration laboratory accredited according to ISO 17025. Fanex is certified according to ISO 9001.

Some of the companies we represent in the field of physics and their products:

- Edwards – vacuum equipment
- UniTemp – rapid thermal process ovens
- Jacomex – glove boxes
- Spectro – optical emission spectrometers
- Various vacuum deposition equipment
- Gas detectors
- Reagents and materials

Contacts:
Fanex
Kalna 17-1
LV 1003
Riga
Latvia
Phone: +371 67334747
Fax: +371 67830438
faneks@faneks.lv
www.faneks.lv

April 5

16:00	Registration
17:00 18:30	Welcome party

- Materials for fuel cells and membranes (Joint session with workshop on ceramic membranes FP7 NASA-OTM project)
- Spectroscopy and optical properties
- Advanced nuclear energy materials
- Materials for alternative energetics
- Theory and modeling
- Perspective new materials
- Nanomaterials and nanostructures
- Technologies and methods
- Ferroelectrics and related materials

April 6

8:00	Registration		
9:00	Opening		
9:30	M. Bundule European projects		
9:50	**R. Merkle**		
10:30	Technical information		
10:40	Conference photo		
10:50	**Coffee 10:50 - 11:20**		
	HALL 1 (NASA)		**HALL 2 (Opt)**
11:20	W. Meulenberg	**11:20**	N. Christensen
11:50	J. Serra	**11:50**	I. Tale
12:20	V. Hendriksen	**12:10**	A. Kaminska
		12:30	B. Berzina
12:50	E. Kotomin	**12:50**	J. Piqueras
13:20	D. Gryaznov	**13:10**	C. Leonelli
13:40	**Lunch 13:40 - 14:40**		
	HALL 1 (Nucl)		**HALL 2 (Opt)**
14:40	M. Freyss	**14:40**	W. Lojkowski
15:10	Y. Zhukovskii	**15:10**	D. Millers
15:40	O. Dumbrajs	**15:30**	K. Joy
		15:50	M. Kirm
16:10	A. Shugai	**16:10**	T. Shalapska
16:30	B. Kolbasov	**16:30**	M. Barczak
16:50	J. Kalnins	**16:50**	L. Dolgov
17:10	**Coffee&snacks 17:10 - 17:30**		
17:30 **19:30**	**Poster session**		

April 7

8:00	Registration		
	HALL 1 (Ener)		**HALL 2 (Theo)**
8:50	Technical info	**8:50**	Technical info
9:00	C. G. Granqvist	**9:00**	R. Evarestov
9:30	O. Yanush	**9:30**	E. Blokhin
9:50	L. Frolova	**9:50**	A. Bandura
10:10	A. Ukshe	**10:10**	R. Eglitis
10:30	**Coffee 10:30 - 11:00**		
11:00		**11:00**	S. Kulkova
11:20	A. Kalle		
11:40	G. Chikvaidze	**11:30**	M. Brik
12:00	P. Fursikov	**11:50**	Y. Shunin
12:20	**Lunch 12:20 - 13:20**		
	HALL 1 (Mat)		**HALL 2 (Nano)**
13:20	J. Zimmermann	**13:20**	S. Rols
13:50	L. Skuja	**13:50**	
14:10	A. Fedotovs	**14:10**	V. Bogdanov
14:30	S. Jursenas	**14:30**	D. Erts
		14:50	J. Andzane
15:00	J. Teteris	**15:10**	L. Dorogin
15:20	I. Strazdina	**15:30**	
15:40	A. Mychko	**15:50**	J. Zicans
16:10	**Coffee 16:10 - 16:30**		
16:30 **22:30**	**Excursion & Conference dinner**		

April 8

	HALL 1 (Tech)		**HALL 2 (Ferro)**
9:30	K. Schwartz	**9:30**	V. Trepakov
10:00	D. Tonneau	**10:00**	J. Petzelt
10:20	J. K. Thomas	**10:30**	A. Dejneka
10:40	P. Onufrijevs	**10:50**	O. Malyshkina
11:00	A. Ozols	**11:10**	J. Dec
11:30	**Coffee 11:30 - 12:00**		
12:00	V. Fateev	**12:00**	R. Dittmann
12:20			
12:40	E. Palcevskis	**12:30**	W. Kleemann
13:00	B. Polyakov	**13:00**	J. Banys
	HALL 1		
13:40	**Closing**		
14:00	**Goodbye lunch 14:00 - 15:00**		

DURING THE CONFERENCE THE EXHIBITION OF SEVERAL COMPANIES WILL BE HELD

Plenary - 40 min
Invited - 30 min
Oral - 20 min

International Conference Functional Materials and Nanotechnologies
‘FMNT – 2011’
PROGRAM

Tuesday, April 5

16:00 - 17:00	**REGISTRATION**		
17:00 - 18:30	**WELCOME PARTY**		

Wednesday, April 6

08:00 - 09:00	**REGISTRATION**		
HALL 1	**OPENING**		
Chairman of the conference: A. Sternberg			
09:00 – 09:30	A. Sternberg	Opening	
09:30 – 09:50	M. Bundule	European projects	
09:50 – 10:30	R. Merkle	Mechanistic Insight into Oxygen Exchange on Mixed Conducting Oxides from Experiments and Theory	PL - 1
10:30 – 10:40	**Technical Information**		
10:40 – 10:50	**CONFERENCE PHOTO**		
10:50 – 11:20	**Coffee**		
HALL 1	**MATERIALS FOR FUEL CELLS AND MEMBRANES**		
11:20 – 11:50	W. Meulenberg	Thin Film Mixed Ionic Electronic Conducting Membranes for Oxygen Separation	INV – 1
11:50 – 12:20	J. Serra	Catalytic Surface Activation of Oxygen Transport Membranes	INV – 2
12:20 – 12:50	P. Hendriksen	Oxygen Transport Membranes – from Material Parameters to Application Oriented Devices	INV – 3
12:50 – 13:20	E. Kotomin	First Principles Modeling of Oxygen Incorporation into Oxygen Permeation Membranes and Sofc Cathodes	INV – 4
13:20 – 13:40	D. Gryaznov	Thermodynamic Calculations on Defects in Perovskites: DFT and Frozen Phonon Method	OR – 1
HALL 2	**SPECTROSCOPY AND OPTICAL PROPERTIES**		
11:20 – 11:50	N. Christensen	Band-gap “Design” of Semiconducting Nitride Alloys	INV – 8
11:50 – 12:10	I. Tale	Dynamics of Exciton Creation and Decay Processes in Composition – Disordered InGaN Thin Films	OR – 5
12:10 – 12:30	A. Kaminska	Spectroscopy of Yb^{3+}-doped III-V Semiconductors At Ambient At High Pressure: Experiment, *Ab-initio* and Crystal Field Studies	OR – 6
12:30 – 12:50	B. Berzina	Defect luminescence of III group element nitrides AlN and hBN	OR – 7
12:50 – 13:10	J. Piqueras	Structure, Fe Solubility and Luminescence of Fe Doped ZnO Nanowires and Nanorods	OR – 8
13:10 – 13:40	C. Leonelli	Industrial Scale Microwave-Assisted Production of Nanoparticles	INV – 9
13:40 – 14:40	**LUNCH**		

Wednesday, April 6

HALL 1	**ADVANCED NUCLEAR ENERGY MATERIALS**		
14:40 – 15:10	M. Freyss	First-Principles Study of Uranium and Oxygen Diffusion in Uranium Dioxide UO_2	INV – 5
15:10 – 15:40	Y. Zhukovskii	First-Principles Simulations on Initial Stage of Uranium Nitride Surface Oxidation	INV – 6
15:40 – 16:10	O. Dumbrajs	European Gyrotrons for ITER	INV – 7
16:10 – 16:30	A. Shugai	Radiation Damage Induced by Swift Heavy Ions in $Lu_2Al_5O_{12}$ Crystals	OR – 2
16:30 – 16:50	B. Kolbasov	Studies of Nanostructures Formed in T-10 Tokamak	OR – 3
16:50 – 17:10	J. Kalnin	Effective Diffusion Coefficient in One Dimensional Model	OR – 4
HALL 2	**SPECTROSCOPY AND OPTICAL PROPERTIES**		
14:40 – 15:10	W. Łojkowski	Optical Oxygen Nano-sensor	INV – 10
15:10 – 15:30	D. Millers	Short Lived and Stable Defects in Yttrium Stabilized Zirconia Single Crystal	OR – 9
15:30 – 15:50	K. Joy	Photoluminescence of oxygen related defects in sol gel derived nanocrystalline ZrO_2 thin films	OR – 10
15:50 – 16:10	M. Kirm	Luminescence Spectroscopy of Ca-Apatites under VUV Excitation	OR – 11
16:10 – 16:30	T. Shalapska	5*d*-4*f* Luminescence of Lanthanide Ions in $LiYP_4O_{12}$	OR – 12
16:30 – 16:50	M. Barczak	Microstructure and optical properties of TiO_2 doped with ytterbium synthesized by sol-gel and solar physical vapour deposition process	OR – 13
16:50 – 17:10	L. Dolgov	Plasmon-Coupled Emission From the TiO_2:Sm^{3+} Sol-Gel Film	OR – 14
17:10 – 17:30	**Coffee & Snacks**		

17:30 – 19:30	**POSTER SESSION**

DURING THE CONFERENCE THE EXHIBITION OF COMPANIES
FANEX and THORLABS
WILL BE HELD

Thursday, April 7

08:00 – 08:50	**REGISTRATION**		
HALL 1	**MATERIALS FOR ALTERNATIVE ENERGETICS**		
08:50 – 09:00	**Technical Information**		
09:00 – 09:30	C. G. Granqvist	Green Nanotechnologies for Energy Efficient Buildings: A Sketch	INV – 11
09:30 – 09:50	O. Yanush	Thermochromic Glazing Materials for “Zero Net Energy” Houses	OR – 15
09:50 – 10:10	L. Frolova	Nanostructured Pt/ $Ti_xMe_{1-x}O_2$ (Me = Nb, Ru) Electrocatalysts for Direct Alcohol Fuel Cells	OR – 16
10:10 – 10:30	A. Ukshe	Cluster Approach to Macroscopic Superprotonic Conductivity	OR – 17
HALL 2	**THEORY AND MODELING**		
08:50 – 09:00	**Technical Information**		
09:00 – 09:30	R. Evarestov	Symmetry and Structure of $SrTiO_3$ Nanotubes	INV – 14
09:30 – 09:50	E. Blokhin	Phonon Calculations in Perfect and Defective $SrTiO_3$ perovskites	OR – 27
09:50 – 10:10	A. Bandura	LCAO Calculations of $SrTiO_3$ Nanotubes	OR – 28
10:10 – 10:30	R. Eglitis	Ab initio Calculations of $SrTiO_3$, $BaTiO_3$, $PbTiO_3$, $CaTiO_3$, $BaZrO_3$, $SrZrO_3$ and $PbZrO_3$ (001) and (011) Surfaces as well as Nb Impurity Segregation towards the $SrTiO_3$ Surface	OR – 29
10:30 – 11:00	**Coffee**		
HALL 1	**MATERIALS FOR ALTERNATIVE ENERGETICS**		
11:00 – 11:20			
11:20 – 11:40	A. Kalle	Innovative Method of Solar Grade Silicon Production	OR – 19
11:40 – 12:00	G. Chikvaidze	Electron-beam Refining of UMG-Si for Solar Energetics	OR – 20
12:00 – 12:20	P. Fursikov	Hydrogen Sorption Properties of Nanocomposites Mg-RE-Ni and Mg-RE-Ni-C	OR – 21
HALL 2	**THEORY AND MODELING**		
11:00 – 11:30	S. Kulkova	Halogen Adsorption on III-V Semiconductor (001) Surface	INV – 15
11:30 – 11:50	M. Brik	*Ab Initio* Calculations of Electronic, Optical, Elastic Properties and Microscopic Treatment of Crystal Field Effects for Some Cubic Crystals	OR – 30
11:50 – 12:10	Y. Shunin	Theoretical Simulations of Fundamental Properties of CNT-Me and GRN-Me Interconnects for Novel Electronic Nanodevices	OR – 31
12:20 – 13:20	**Lunch**		

Thursday, April 7

HALL 1	**PERSPECTIVE NEW MATERIALS**		
13:20 - 13:50	J. Zimmermann	Role of Oxygen and the Fluorine-bromine Ratio in the Storage Mechanism of $BaFBr:Eu^{2+}$	INV – 12
13:50 – 14:10	L. Skuja	Effects of Temperature on Electron Paramagnetic Resonance of Dangling Oxygen Bonds in Amorphous Silicon Dioxide	OR – 22
14:10 – 14:30	A. Fedotovs	Paramagnetic Impurities for Studies of the Oxyfluoride Glass Ceramics Structure	OR – 23
14:30 – 15:00	S. Jursenas	Tailoring the Photophysical Properties of Multifunctional Molecular Systems	INV – 13
15:00 – 15:20	J. Teteris	Photoinduced Mass Transport in Soft Materials	OR – 24
15:20 – 15:40	I. Strazdina	Deposition of ZnO:Al Transparent Conductive Layers on Polymer Substrate by Magnetron Sputtering	OR – 25
15:40 – 16:00	A. Mychko	NanoCones Formation on a Surface of CdZnTe by Laser Radiation: Exciton Quantum Confinement Effect	OR – 26
HALL 2	**NANOMATERIALS AND NANOSTRUCTURES**		
13:20 – 13:50	S. Rols	Selected Examples of Molecular Confinement Using Nanocarbon Hosts	INV – 16
13:50 – 14:10			
14:10 – 14:30	V. Bogdanov	Nano Structure of Lead-Germanate Glasses and Their Melts	OR – 33
14:30 – 14:50	D. Erts	Fabrication of Ultrathin Anodized Aluminum Membranes for Deposition of Nanodot Arrays	OR – 34
14:50 – 15:10	J. Andzane	Application of Individual Semiconductor Nanowires in Gateless Bistable Nanoelectromechanical Switch	OR – 35
15:10 – 15:30	L. Dorogin	Measurements of Static and Kinetic Friction of ZnO Nanowires on a Flat Surface	OR – 36
15:30 – 15:50			
15:50 – 16:10	J. Zicans	Structure and Electrical Properties of Styrene Acrylonitrile Copolymer Nanocomposites	OR – 38
16:10 – 16:30	**Coffee**		
16:30 – 22:30	**EXCURSION AND CONFERENCE DINNER**		

Friday, April 8

HALL 1	**TECHNOLOGIES AND METHODS**		
09:30 – 10:00	K. Schwartz	Swift Heavy Ion Tracks in Dielectrics and Their Possible Applications for Nanotechnology	INV – 17
10:00 - 10:20	D. Tonneau	Coupling X-ray Spectroscopy and Scanning Probe Microscopy for Simultaneous Sample Topography and Chemical mapping	OR – 39
10:20 - 10:40	J. K. Thomas	Structural, Dielectric and Optical Characterization of $BaMoO_4$ Nano powder Synthesized Through an Auto-Igniting Combustion Technique	OR – 40
10:40 - 11:00	P. Onufrijevs	Two-Stage Mechanism of Nano-Cones Formation by Laser Radiation on a Surface of Elementary Semiconductors and Semiconductor Solid Solutions	OR – 41
11:00 - 11:20	A. Ozols	Self-Enhancement of Scalar and Vector Holographic Gratings in Azobenzene Molecular Glassy Films	OR – 42

HALL 2	**FERROELECTRICS AND RELATED MATERIALS**		
09:30 – 10:00	V. Trepakov	Chromium Centers in $SrTiO_3$: Properties, Problems and New Data	INV – 18
10:00 - 10:30	J. Petzelt	Wide-range Dielectric Spectroscopy of $BaTiO_3$-based Nanoceramics and Various Nanocomposites	INV – 19
10:30 - 10:50	A. Dejneka	Strain Effects in Epitaxial $SrTiO_3$ and $KTaO_3$ Films	OR – 47
10:50 - 11:10	O. Malyshkina	Determination of Thermal Diffusivity Coefficients of Thin Films by TSWM	OR – 48
11:10 - 11:30	J. Dec	Multifunctionality of Strontium-Barium Niobate	OR – 49

11:30 -12:00	**Coffee**

HALL 1	**TECHNOLOGIES AND METHODS**		
12:00 – 12:20	V. Fateev	Development of Plasma Technologies for Nanostructured Materials: Nanoparticles, Thin Films and Coatings in NRC «Kurchatov Institute»	OR – 43
12:20 - 12:40			
12:40 - 13:00	E. Palcevskis	Formation of Alpha Phase in Nanosized Plasma Processed Alumina Powder	OR – 45
13:00 - 13:20	B. Polyakov	Manipulation of Gold Nanoparticles Inside Scanning Electron Microscope	OR – 46

HALL 2	**FERROELECTRICS AND RELATED MATERIALS**		
12:00 – 12:30	R. Dittmann	Scaling Potential of Local Redox-Processes in Memristive $SrTiO_3$ Thin Film Devices	INV – 20
12:30 – 13:00	W. Kleemann	Supermagnetic States of Nanoparticles	INV – 21
13:00 - 13:30	J. Banys	Two Dimensional Distribution of the Relaxation Times	INV – 22

HALL 1	**CLOSING**
Chairperson: A. Sternberg	
13:40 – 14:00	**Closing of the conference**
14:00 – 15:00	**GOODBYE REFRESHMENTS**

Abstracts of the plenary presentations

PL-1

Mechanistic Insight into Oxygen Exchange on Mixed Conducting Oxides from Experiments and Theory

R. Merkle[1], L. Wang[2], Yu.A. Mastrikov[3], E.A. Kotomin[1], J. Maier[1]
[1]Max-Planck Institute for Solid State Research, Stuttgart, Germany
[2]Electrochemical Energy Laboratory, MIT, Cambridge, USA
[3]Materials Science and Eng. Dept., University of Maryland, College Park, USA
e-mail: r.merkle@fkf.mpg.de

The oxygen incorporation surface reaction into mixed conducting oxides is important for adjusting the oxygen stoichiometry of a material (and thus its electrical, optical, magnetic properties etc.) as well as for oxidation catalysis and (electro)chemical devices such as fuel cells, permeation membranes and sensors [1]. Nevertheless, a detailed mechanistic understanding in terms of reaction pathways and rate-determining steps is difficult to achieve.

Effective rate constants k^q for the oxygen incorporation reaction were determined by impedance spectroscopy on PLD-deposited thin-film microelectrodes on YSZ substrates. This method allows us to measure k^q values for different materials [2] without interference from different morphologies that could arise when studying porous films. The comparison of k^q for $(La,Sr)MnO_{3\pm d}$, $(La,Sr)(Co,Fe)O_{3-d}$ and $(Ba,Sr)(Co,Fe)O_{3-d}$ perovskites and the correlation with vacancy diffusion coefficients suggests that not only the concentration of oxygen vacancies but also their mobility plays a crucial role in oxygen exchange kinetics [3].

For the mechanistic understanding, ab-initio DFT calculations are a valuable tool which supplies information difficult to obtain from experiments, e.g. adsorption enthalpies, energies of intermediates, and reaction barriers. In combination with experimental data this allowed us to suggest a reaction mechanism for oxygen incorporation into $(La,Sr)MnO_{3\pm d}$ [4].

This work was partly supported by the EC FP7 NASA-OTM project, GIF research project #1-1025-5-10/2009 and National Science Foundation.

References

1. R. Merkle, J. Maier, Angew. Chemie Int. Ed. **47**, 2 (2008)
2. F. S. Baumann, J. Fleig, G. Cristiani, B. Stuhlhofer, H.-U. Habermeier, J. Maier, J. Electrochem. Soc. **154**, B931 (2007)
3. L. Wang, R. Merkle, J. Maier, J. Electrochem. Soc. **157**, B1802 (2010)
4. Y. A. Mastrikov, R. Merkle, E. Heifets, E. A. Kotomin, M. M. Kuklja, J. Maier, J. Phys. Chem. C **114**, 3017 (2010)

Abstracts of the invited presentations

INV-1

Thin Film Mixed Ionic Electronic Conducting Membranes for Oxygen Separation

W.A. Meulenberg, S. Baumann, S. Uhlenbruck
Forschungszentrum Jülich GmbH, Institute of Energy and Climate Research IEK-1
e-mail: w.a.meulenberg@fz-juelich.de

Oxygen transport membranes consist of gas-tight Mixed Ionic Electronic Conductors (MIEC), which allow oxygen ion diffusion through vacancies in the crystal lattice and simultaneous transport of electrons in the opposite direction. Their major advantage is infinite oxygen selectivity, assuming no leakage through the membrane layer or the sealing, resulting in high purity oxygen, which can directly be provided to e.g. Oxyfuel power plants. Furthermore, these membranes can be used in membrane reactors in order to facilitate chemical reaction requiring oxygen. Thin membranes are favorable to obtain high permeation rates. However, a thickness reduction becomes more and more ineffective below a characteristic thickness L_c due to slow surface exchange kinetics. In order to use the potentially high fluxes of a thin membrane a fast incorporation/excorporation of the oxygen into/out of the membrane is necessary by using high surface porous catalyst layers.

As consequence an optimized membrane assembly is characterized by (i) high oxygen permeation rate, (ii) infinite oxygen selectivity, and (iii) low degradation rate. In order to address all of these goals at the same time, the development of nano-structured surface activated thin oxygen transport membranes is essential. Modeling activities, e.g. atomistic modeling of transport and surface phenomena, are necessary to support the experimental membrane development.

Therefore, an EU-FP7-project (CP-FP 228701-2 NASA-OTM) following the approach described above was set up by the partners Forschungszentrum Jülich (D), Risø National Laboratory (DK), Consejo Superior de Investigaciones Científicas (E), University of Hannover (D), ISSP/University of Latvia (LV), BASF AG (D), Instalaciones Inabensa, S.A. (E), and University of Queensland (AUS).

INV-2

Catalytic Surface Activation of Oxygen Transport Membranes

J.M. Serra, P. Lobera, S. Escolástico
[1]Instituto de Tecnología Química, Universidad Politécnica de Valencia – Consejo Superior de Investigaciones
Científicas, Avda. Naranjos s/n, E-46022 Valencia, Spain
e-mail: jmserra@itq.upv.es

Oxygen transport membranes (OTM) based on mixed ionic–electronic conducting (MIEC) oxides allow the selective oxygen separation at high temperature, which could be integrate in oxyfuel power plants and in the chemical industry. The principle of oxygen separation through this kind of membranes is the ambipolar diffusion of electrons/ holes and oxide ions/vacancies through the metal oxide lattice. Consequently, a gastight MIEC membrane allows theoretically achieving an infinite selectivity. If the membrane thickness and the material diffusivity are sufficiently high, bulk transport is not the unique limiting transport. Typically, bulk oxygen ionic diffusion and surface exchange steps are particularly important but other important limitations could appear due to gas concentration polarization in the module compartment and in the porous structures of the membrane. In this presentation, we discussed on the possible permeation limitations and focused on the development of catalytic surface activation, which enables to increase substantially the permeation of thin supported membranes when other external limitations are minimized.

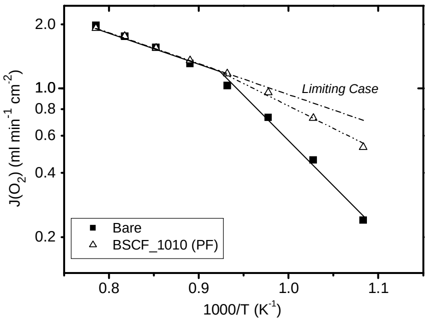

Fig.1 Temperature dependence of oxygen permeation flux through catalytic MIEC membranes. QAr = 65 ml/min, QAir = 60 ml/min (pO_2=0.21).

References

1. J. Sunarso, S. Baumann, J.M. Serra, W.A. Meulenberg, S. Liu, Y.S. Lin and J.C. Diniz da Costa, *J. Membrane Sci.*, 2008, **320**, 13-41
2. J M. Serra, V.B. Vert, O.Büchler, W.A. Meulenberg and H.P. Buchkremer, *Chem. Mater.*, 2009, **20**, 3867-3875.
3. M. Czyperek, P. Zapp, H.J.M. Bouwmeester, M. Modigell, K. Ebert, I. Voigt, W.A. Meulenberg, L. Singheiser and D. Stöver, *J. Membrane Sci.*, 2010, **359,** 149–159.
4. T. Schiestel, M. Kilgus, S. Peter, K.J. Caspary, H. Wang and J. Caro, J. Membrane Sci., 2005, 258, 1-4

INV-3

Oxygen Transport Membranes – from Material Parameters to Application Oriented Devices

P.V. Hendriksen, M. Søgaard
Fuel Cells and Solid State Chemistry Division, Risø National Laboratory for Sustainable Energy, Technical University of Denmark, Denmark
e-mail: msqg@risoe.dtu.dk

Oxygen transport membranes (OTMs) consists of a dense layer that can conduct both oxide ions and electrons. This allows for a net selective transport of oxygen through the membrane. Different techniques for evaluating membrane materials will be discussed including electrical conductivity relaxation, coulometric titration, electrolyte probe method and thin film methods. The methods are applied to perovskite type materials such as strontium doped lanthanum cobaltite ($La_{1-x}Sr_xCoO_{3-\delta}$, $x = 0.4$ and $x = 0.15$). The derived materials parameters will be used in combination with a model that includes oxygen ion diffusion through the dense membrane, the kinetics of the surface layers and also the gas transport through porous structures. The model will be used in order to define optimal membrane architectures depending on the application. The developed model will be applied both to perovskite and ceria based membranes and the importance of activation layers will be highlighted. Particularly the activation layer for the oxygen reduction needs a very high activity in order not to limit the overall performance of the membrane. Examples of different type activation layers ranging from materials studies on dense thin film perovskites to highly active infiltration layers will be presented.

INV-4

First Principles Modeling of Oxygen Incorporation into Oxygen Permeation Membranes and Sofc Cathodes

E.A. Kotomin[1, 2], R. Merkle[1], Yu.A. Mastrikov[2, 3], M.M. Kuklja[3], D. Fuks[4], J. Maier[1]

[1]Max Planck Institute for Solid State Research, Heisenbergstr, Stuttgart, Germany
[2]Institute for Solid State Physics, University of Latvia, Kengaraga str. 8, Latvia
[3]Materials Science and Eng. Dept., University of Maryland, College Park, USA
[4]Materials Engineering Dept, Ben-Gurion University of the Negev, Beer-Sheva, Israel

Currently, $Ba_{0.5}Sr_{0.5}Co_{0.75}Fe_{0.25}O_{3-d}$ (BSCF) shows the best oxygen exchange kinetics among mixed conducting perovskites (despite other drawbacks) and is a candidate for permeation membranes and solid oxide fuel cell (SOFC) cathodes [1]. As it is well established now, the two key factors, which control the oxygen reduction, are the high oxygen vacancy (Vo) concentration at the cathode surface and the high vacancy mobility.

In this talk, we discuss calculated from first principles the atomic and electronic structure of oxygen vacancies, their formation and migration energies in the bulk and in the surface layer, the defect-induced electronic density redistribution, and dependence of defect properties on the chemical composition of the BSCF (Fe/Co ratio) [2,3]. Additionally, the adsorption energies of an oxygen molecule and an O atom were obtained. Our calculations confirm that the O-vacancy formation and, in particular, migration energies in BSCF are considerably smaller than in similar LSM and LSCF perovskites [2,3] which explains its good performance. The gradual increase of these energies with an increase of the iron content is explained by analysis of the relevant density of the states.

We predict that in both $(La,Sr)(Co,Fe)O_3$ (LSCF) and BSCF perovskites the dissociation of surface peroxide or superoxide ion occurs with assistance of V_O, their encounter being the *rate-determining step*. The estimated reaction rate for this mechanism is significantly higher than in other perovskites, in good agreement with the experimental observations.

This work was partly supported by the EC FP7 NASA-OTM project, GIF research project # 1-1025-5-10/2009 and National Science Foundation.

References

1. L.Wang et al, J.Electrochem. Soc., **157**, B1802 (2010).
2. Yu.Mastrikov et al, Energy Env. Sci., **3**, 1544 (2010).
3. E.A. Kotomin et al, Sol. St. Ionics, 2010, in press.
4. E.A.Kotomin et al, Phys Chem Chem Phys **10**, 4644 (2008).
5. Yu.Mastrikov et al, J.Phys.Chem. C **114**, 3017 (2010).

INV-5

First-Principles Study of Uranium and Oxygen Diffusion in Uranium Dioxide UO_2

B. Dorado, M. Freyss, M. Bertolus

CEA, DEN, DEC, Centre de Cadarache , 13108 Saint Paul Lez Durance Cedex, France

Uranium dioxide (UO_2) attracts much interest due to its technological value as the standard nuclear fuel for pressurized water reactors. In order to get some comprehension in the evolution of the fuel properties under irradiation, the study of point defects and fission products is central. In particular, obtaining accurate formation and migration energies of point defects is essential in order to model the evolution of the microstructure of the material. First-principles electronic structure calculations can give direct insight into elementary transport processes at the atomic scale and the results can be used as input data in a multi-scale modeling scheme of the material properties, with direct links to modeling techniques such as classical molecular dynamics, kinetic Monte Carlo.

We will present here a first-principles study of uranium and oxygen diffusion in uranium dioxide. The activation energies obtained will be compared to recent experimental results [1, 2] for oxygen diffusion in UO_2.

Within standard Density Functional Theory (DFT), the strong correlations between the *5f* electrons of uranium in UO_2 are significantly underestimated and it still remains a challenge to accurately describe the electronic structure of UO_2. We will show that the addition of a Hubbard-like term in the so-called DFT+U [3] formalism improves the treatment of these electrons and succeeds in describing several bulk properties of UO_2, as well as the behaviour of its point defects [4, 5].

This study is supported by the F-BRIDGE project of the European Commission.

References

1. P. Garcia, M. Fraczkiewicz, C. Davoisne, G. Carlot, B. Pasquet, G. Baldinozzi, D. Siméone, C. Petot, J. Nucl. Mat. **400**, 112 (2010).
2. B. Dorado, P. Garcia, G. Carlot, M. Fraczkiewicz, B. Pasquet, M. Freyss, M. Bertolus, G. Baldinozzi, D. Siméone, to appear in Phys. Rev. B (2011).
3. S.L. Dudarev, G.A. Botton, S.Y. Savrasov, Z. Szotek, W.M. Temmerman, A.P. Sutton, Phys. Stat. Sol. A **166**, 429 (1998).
4. B. Dorado, B. Amadon, M. Freyss, M. Bertolus, Phys. Rev. B **79**, 235125 (2009).
5. B. Dorado, G. Jomard, M. Freyss, M. Bertolus, Phys. Rev. B **82**, 035114 (2010).

INV-6

First-Principles Simulations on Initial Stage of Uranium Nitride Surface Oxidation

Yu.F. Zhukovskii[1], D. Bocharov[1, 2, 3], D. Gryaznov[1], E.A. Kotomin[1]
[1]Institute for Solid State Physics, University of Latvia, Kengaraga 8, Riga LV-1063
[2]Faculty of Computing, University of Latvia, Raina blvd. 19, Riga LV-1586
[3]Faculty of Physics and Mathematics, University of Latvia, Zellu 8, Riga LV-1002
e-mail: quantzh@latnet.lv

As a promising fuel material for the Generation-IV fast reactors, uranium mononitride (UN) reveals unwanted oxidation in air, which greatly affects its properties, in contrast to a "traditional" UO2 nuclear fuel. Thus, it is important to understand the mechanism of UN oxidation and possible steps for inhibition of this process. In this study, we present results of large-scale first-principles atomistic simulations of oxygen adsorption [1], dissociation [2] and diffusion upon the UN(001) surface (both perfect and defective, with regularly distributed single vacancies [3]).

The plane-wave DFT spin-polarized calculations (using the VASP computational package [4]) for basic properties, e.g., reactivity, of the UN(001) surface have been performed on various 3D slab models [1-3]. Obtained results clearly demonstrate: (i) metallic-covalent inter-atomic bonding inside the substrate, (ii) possibility of spontaneous dissociation of oxygen molecule adsorbed upon the appropriate surface sites, (iii) further localization of oxygen adatoms, released after dissociation, upon the surface U atoms, (iv) high mobility of O adatoms along the surface, due to low migration barriers (~0.5 eV) between the two neighbouring adsorption sites upon the surface uranium atoms. The oxygen adatom atop the surface U atom nearest to the N vacancy can be spontaneously captured by the latter. Possibilities of further oxygen adatom migration between the adjacent vacancies on the UN(001) surface are discussed too. The results for O atom penetration into UN bulk [5] and surface layer are compared and verified (using experimental UPS data).

References

1. Yu.F. Zhukovskii, D. Bocharov, E.A. Kotomin, R.A. Evarestov, and A.V. Bandura, *Surf. Sci.*, 2009, **603**, 50-53.
2. Yu.F. Zhukovskii, D. Bocharov, and E.A. Kotomin, *J. Nucl. Mater.*, 2009, **393**, 504-507.
3. D. Bocharov, D. Gryaznov, Yu.F. Zhukovskii, and E.A. Kotomin, *Surf. Sci.*, 2011, **605**, 396-400.
4. G. Kresse and J. Furthmller, *VASP the Guide*, University of Vienna (2009).
5. E.A. Kotomin and Yu.A. Mastrikov, *J. Nucl. Mater.*, 2008, **377**, 492-495.

INV-7

European Gyrotrons for ITER

O. Dumbrajs
Institute of Solid State Physics, University of Latvia, Latvia
e-mail: olgerts.dumbrajs@lu.lv

Gyrotron is a microwave source whose operation is based on the stimulated cyclotron radiation of electrons oscillating in a static magnetic field. The radio frequency radiation is excited by gyrating electrons bunched near the phase in which they yield their energy to the high-frequency field. The phase bunching is due to the relativistic dependence of the electron mass on its velocity. This makes rotation of decelerated electrons faster and that of the accelerated ones slower. The typical frequency range of gyrotrons working at the fundamental harmonic is between 20-200 GHz.

Operating mode	$TE_{34,19}$
Frequency	170 GHz
RF output power	2 MW
Beam current	75 A
Accelerating voltage	90 kV
Velocity ratio	1.3
Cavity magnetic field	6.87 T
RF output efficiency	50%

European gyrotron design specifications

Powerful gyrotrons can be used to heat nuclear fusion plasma. In addition, they have found a wide utility in plasma diagnostic, plasma chemistry, radars, high-temperature processing of materials, extra-high-resolution spectroscopy, and medicine. However, the main application of gyrotrons is the electron cyclotron resonance heating in tokamaks and stellarators. For example, for its heating system with power up to 20 MW, the international thermonuclear experimental reactor (ITER) will need about 20 continuous wave ordinary gyrotrons at a frequency 170 GHz with output power per tube or about 10 coaxial gyrotrons with 2 MW output power per tube. Coaxial gyrotrons are developed only in Europe: at Karlsruher Institut für Technologie, Germany, and Ecole Polytechnique Fédérale de Lausanne, Centre de Recherches en Physique des Plasmas, Switzerland. Theoretical work is done also at the Institute of Solid State Physics, University of Latvia.

References

1. O. Dumbrajs and G.S. Nusinovich, *“Coaxial gyrotrons: past, present and future,”* invited review article, IEEE Transactions on Plasma Science, **32**, 934 (2004).
2. O. Dumbrajs, *„Influence of possible reflections on the operation of European ITER gyrotrons,”*
J. Infrared Milli. Terahz. Waves **31**, 892 (2010).

INV-8

Band-gap “Design” of Semiconducting Nitride Alloys

I. Gorczyca[1], A. Svane[2], N.E. Christensen[2]
[1]Institute of High Pressure Physics, Polish Academy of Science, Warsaw, Poland
[2]Deppartmen of Physics and Astronomy, Aarhus University, Aarhus, Denmark
e-mail: nec@phys.au.dk

Band-gap tailoring, creation of semiconducting materials by alloying two binary compounds, AC and BC, to form a ternary alloy, $A_xB_{1-x}C$, is a widely used method to obtain band gap values which satisfy the requirements of specific applications such as production of light emitting diodes, solid state lasers, solar cells etc. operating in desired frequency ranges. Often a rather smooth and reproducible variation of the gap with composition x is found, and in some cases even a nearly linear x dependence has been observed. The III-nitrides AlN, GaN, and InN are materials of great importance for such “gap design” because their gaps span a wide energy range, 6.4 eV (AlN), 3.5 eV GaN down to 0.7 eV in InN, and the present work summarizes results [1,2] of theoretical calculations of the composition dependence of the gaps in ternary and quaternary semiconducting nitride alloys. The calculations are based on the density-functional theory, including approximations to obtain not only reliable ground state properties but also energies of excited states [3]. The calculated energy gaps, as well as their pressure coefficients, are compared to experimental data. The measured results as obtained from different research groups exhibit a strong scatter, exceeding the quoted error bars. From the calculations it is shown that the gaps in the III-nitride alloys depend sensitively on the geometrical arrangement of the cations in the lattice. Formation in In clusters produces a significant gap reduction, and with reasonable definition of “uniform” and “clustered” geometries it is possible essentially to span all available experimental data. This shows that for the alloys containing InN the gap values depend sensitively on the sample growth conditions. The anomalously large band gap bowing found in the In-containing nitrides can be related to specific properties of InN which do not follow [4] the trends observed in several other binaries (note, for example, its very small energy gap, 0.7 eV).

References

1. I. Gorczyca, S.P. Lepkowski, T, Suski, N.E. Christensen, A. Svane, Phys.Rev **80**, 075202 (2009)
2. I. Gorczyca, T. Suski, A. Kaminska, G. Staszcak, H.P.D. Schenk, N.E. Christensen, A. Svane, Appl. Phys. Lett. **96**, 101907 (2010)
3. A. Svane, N.E. Christensen, I. Gorczyca, M. van Schilfgaarde, A.N. Chantis, T. Kotani, Phys. Rev. B. **82,** 115102 (2010).
4. I. Gorczyca, T. Suski, N.E. Christensen, and A. Svane, Phys. Rev. B. In print (2011).

INV-9

Industrial Scale Microwave-Assisted Production of Nanoparticles

C. Leonelli, P. Veronesi

Department of Materials and Environmental Engineering, University of Modena and Reggio Emilia, Modena, Italy

e-mail: cristina.leonelli@unimore.it

Achieving a narrow temperature distribution in the reaction volume contributes to reaction selectivity or, in case of nucleation and growth processes, to control particle size [1]. The possibility of volumetrically heat the reaction volume by means of microwaves can originate a temperature distribution completely different from a conventionally heated reaction volume. Many researchers identified this difference in the presence of "hot spots" which locally enhance or promote some selected reactions or transformations.

In case of nucleation and growth of nanoparticels (microwave hydrothermal synthesis), the narrow temperature distribution obtained by simulation can justify why nanoparticles are formed, having a narrower particle size distribution with respect to conventionally heated synthetic routes [2]. The large scale production of nanoparticles requires the development of microwave reactors which can reflect the laboratory temperature profile homogeneity.

It will be presented a new dedicated continuous-flow reactor, made of two twin prismatic applicators for a microwave-assisted process in aqueous solution. The reactor can produce up to 1000 liters/day of nanoparticles colloidal suspension at ambient pressure and relatively low temperature hence conducted using a "green chemistry" approach.

References

1. C. Leonelli, W. Lojkowksi, Chem. Today, **26,** 26 (2008).
2. C. Leonelli, A.Rizzuti, R. Rosa, A. Corradi, P.Veronesi, Proceedings of IMPI 44th Annual Symposium, Denver, Colorado, USA, July 14-16 (2010).

INV-10

Optical Oxygen Nano-sensor

A. Świderska-Środa[1], K. Gałązka[1], W. Łojkowski[1], T. Chudoba[1], A. Opalińska[1], K. Smits[2],
L. Grigorjeva[2], D. Millers[2], C. Leonelli[3]
[1]Institute of High Pressure Physics, Polish Academy of Sciences, Poland
[2]Institute of Solid State Physics, University of Latvia
[3]Universita' degli Studi di Modena e Reggio Emilia, Italy
e-mail: annas@unipress.waw.pl

Detection of oxygen content in gases is important for health protection and engines operation. Commonly used oxygen sensors exploit the dependence of electric resistance of ZrO_2 ceramics on oxygen content in the analyzed gas. The ceramic needs to be heated up to about 700°C. There are optical sensors where changes of luminescence of organic materials are exploited. For them direct contact with a hot gas has to be avoided. We developed nano-zirconia particles whose photoluminescence strongly depends on oxygen content in nitrogen/oxygen gas mixtures. The nano $ZrO_2:Eu^{3+}$ particles are produced in a microwave hydrothermal synthesis process. They are doped uniformly with Eu^{3+} ions, and the optimum content is 8%. Their grain size distribution is narrow and for 8 at.% Eu the average size is 19 nm. The material temperature can range from room temperature to 300°C, but the optimal conditions are 100°C. We designed a prototype of the sensor of a very simple construction. An example of the influence of oxygen partial pressure on the luminescence intensity is presented in Fig 1. This work was supported by the project Eranet– MATERA-OXYNANOSEN.

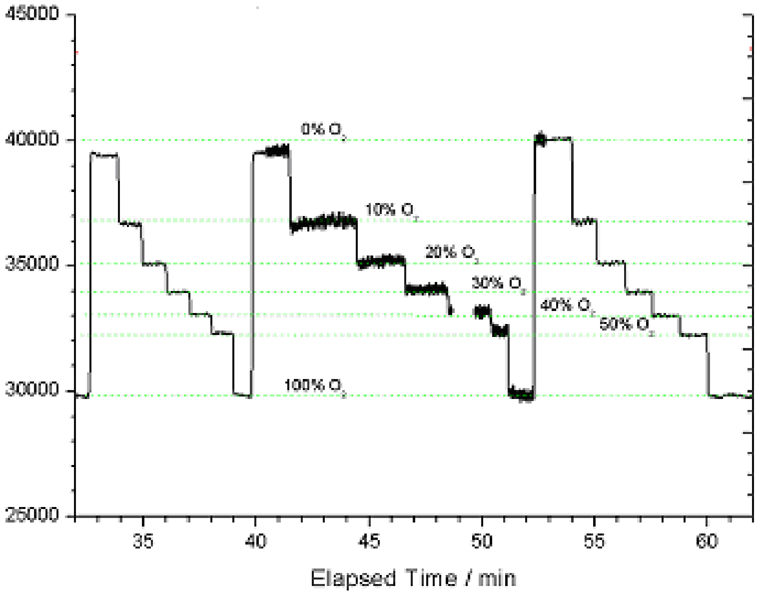

Fig.1 The influence of O_2 partial pressure on the luminescence intensity of ZrO_2-8 at.% Eu nano-sensor. The plot shows the time dependence of the integral of luminescence in the range 600 – 640 nm excited by a 402 nm LED. Temperature is 100°C.

INV-11

Green Nanotechnologies for Energy Efficient Buildings: A Sketch

C.G Granqvist

Department of Engineering Sciences, The Ångström Laboratory, Uppsala University, Uppsala, Sweden

e-mail: claes-goran.granqvist@angstrom.uu.se

This talk attempts to give a rapid overview over a number of recent research activities aimed at developing more energy efficient buildings.[1] I explain why we need more energy efficient buildings, and how many of the desired technologies can be discussed from the perspective of the thermal and solar energy around us, how this energy is modified by the atmosphere, and the luminous sensitivity of the eye. New technologies for windows are discussed, with foci of low-emittance coatings, solar control coatings, and chromogenic (electrochromic and thermochromic) solutions. I also present some information on luminaires, solar collectors and solar cells, and cooling via high-albedo paints and via exposure to the clear sky ("sky cooling"). The talk is ended with some information on sensors for air quality, photocatalytic air cleaning, and thermal insulation via nanomaterials.

Reference

1. G. B. Smith and C. G. Granqvist, Green Nanotechnology: Solutions for Sustainability and Energy in the Built Environment (CRC Press, Boca Raton, USA, 2010).

INV-12

Role of Oxygen and the Fluorine-bromine Ratio in the Storage Mechanism of BaFBr:Eu^{2+}

J. Zimmermann, S. Hesse, H. von Seggern
Institute of Materials- and Geo Science, Darmstadt University of Technology, Darmstadt, Germany
e-mail: zimmermann@e-mat.tu-darmstadt.de

The role of oxygen in the storage mechanism of the storage phosphor BaFBr:Eu^{2+} is investigated. It is known for BaFBr:Eu^{2+} that a divalent oxide is located on an anion site keeping an anion vacancy in its vicinity for charge compensation. Electrons generated upon x-ray absorption are trapped in these vacancies forming F-centers whereas simultaneously generated V_k centers are trapped at Eu^{2+} [1]. Upon photostimulation, electrons are liberated from their traps and subsequently recombine with trapped holes resulting in the characteristic Eu^{2+} luminescence at 390nm. This read out process is called photostimulated luminescence (PSL).

In the present investigation it is shown that even though oxygen seems to be essential to provide sufficient vacancies and thus F-centers, a maximum of the PSL efficiency occurs at a comparatively low content of oxygen. It is assumed that a surplus of oxygen leads to the increased trapping of hole centers at oxygen competing with the hole trapping at Eu^{2+}. It is shown that the oxygen fraction is theoretically controllable together with the F-center lattice site (bromine F_{Br} or fluorine F_F) by a tiny unbalance of the employed halides and the ratio of cation and anion precursors in which the cation precursor is the oxygen source additionally. For the controlled introduction of bromine, fluorine and oxide a one-step synthesis with the precursors $BaCO_3$, NH_4Br, and NH_4F [2] was utilized. Thus micron sized powders of BaFBr:Eu^{2+} powders were obtained and analyzed by photoluminescence, PSL, and remission measurements.

References

1. F. K. Koschnik, J.-M. Spaeth, R. S. Eachus, W. G. McDugle, R. H. D. Nuttall, Phys. Rev. Let. **67**, 3571 (1991)
2. S. Hesse, J. Zimmermann, H. von Seggern, X. Meng, C. Fasel, R. Riedel, J. Appl. Phys. **105,** 063505 (2009)

INV-13

Tailoring the Photophysical Properties of Multifunctional Molecular Systems

S. Jursenas, K. Kazlauskas
Institute of Applied Research, Vilnius University, Lithuania
e-mail: saulius.jursenas@ff.vu.lt

Search for the new materials with advanced properties is one of the major tasks of the rapidly developing field of organic optoelectronics. Currently much attention is being focused on the multifunctional compounds, i.e. molecules composed of several fragments carrying different functionalities. Multifunctional materials are expected not only to increase the device performance but also to simplify their architectures and fabrication procedures.

On the other hand, multifunctionality unavoidably involves an increase in complexity of their properties giving rise to new collective effects, such as intramolecular charge transfer, intramolecular twisting and isomerization, formation of complexes etc. In a solid state, molecular complexity results in different packing morphology, and thus, in various intermolecular interactions, which considerably affect excitation localization, energy transfer and emission properties. Hence, further development of the multifunction molecular compounds for device applications requires thorough analysis and optimization of the emerged collective properties.

Here we review our recent work on tailoring the photophysical properties of various multifunctional emissive systems. We start with glass-forming carbazole dyad and triad systems displaying excellent electron and hole transport properties, and emphasize variation of their photophysical properties invoked by different linking topology, e.g., by 2-, 2,7- or 3-, 3,6-substitution of the carbazole. Further we discuss properties of highly fluorescent novel compounds containing singly bonded carbazole, fluorene and benzothiadiazole functional units in one core. The sterically hindered donor-acceptor compounds are shown to exhibit well-expressed intramolecular charge-transfer and flattening upon excitation resulting in unusual emission properties. We also introduce more complex fluorescent pyrrolopyrimidine derivatives with various molecular rotors attached for biosensing applications. Additionally, we debate properties of a series of multifunctional iridium-based triplet emitters featuring a different number (from 0 to 28) of hole-transporting carbazole moieties for OLED applications. Finally, a few examples of new fluorescence sensing systems based on the aggregation induced emission color and intensity changes are presented.

INV-14

Symmetry and Structure of $SrTiO_3$ Nanotubes

R. Evarestov[1]

[1]Department of Quantum Chemistry, St. Petersburg State University, Russia

e-mail: re1973@re1973.spb.edu

The line symmetry group $L=ZP$ (a product of one axial point group P and one infinite cyclic group Z of generalized translations) of single-walled (SW) and double-walled (DW) $SrTiO_3$ nanotubes (NT) is considered. The nanotube is defined by the square lattice translation vector $\mathbf{L} = l_1\mathbf{a} + l_2\mathbf{b}$ and chiral vector $\mathbf{R} = n_1\mathbf{a} + n_2\mathbf{b}$, ($l_1$, l_2, n_1 and n_2 are integers). The nanotube of the chirality (n_1, n_2) is obtained by folding the (001) layer (with the layer group P4*mm*) in a way that the chiral vector **R** becomes circumference of the nanotube.

For SW (n,0) NTs the line symmetry groups belong to family 11 (T^D_{nh}) and are n/mmm or $\overline{2n}\,2m$ for even and odd n, respectively. For SW (n,n) NTs the line symmetry groups $(2n)_n/mcm$ belong to family 13 ($T_{2n}^{1}D_{nh}$).

The line symmetry group of a double-wall nanotube can be found as intersection $L_2 = Z_2P_2 = (L \cap L')$ of the symmetry groups L and L' of its single-wall constituents as earlier considered for DW CNTs [1, 2].

In particular case of the commensurate $(n,n)@M(n,n)$ and $(n,0)@M(n,0)$ DW perovskite nanotubes with square morphology the DW NT symmetry group depends on the parity of M. For DW NTs with odd M, the line symmetry groups are the same as for their SW constituents and belong to families 13 and 11 respectively. For even M, the rotations about screw axis of order $2M$ are changed by rotations around pure rotation axis of order M so that DW NT line symmetry groups belong to family 11 for both chiralities.

The results of the first principles LCAO-PBE0 calculations of SW and DW $SrTiO_3$ NTs are presented. CRYSTAL-09 computer code [3] is used, the rod subgroups of line groups are applied allowing the large scale computations for NTs. The DW nanotubes strain energy is estimated relatively to the sum of their constituents energies.

The author is grateful for the support of Saint-Petersburg State University, grant 12.37.142.2011 for fundamental research.

References

1. Damnjanovic, M.; Milosevic, I.; Vukovic, T.; Sredanovic, R. *Phys Rev B* **1999**, 60, 2728.
2. Damnjanovic, M.; Dobradzic, E.; Milosevic, I.; Vukovic, T.; Nicolic, B. New J. Phys. **2003**, 5, 148.
3. R. Dovesi, et al., CRYSTAL09 User's Manual, University of Torino, Torino, 2010.

INV-15

Halogen Adsorption on III-V Semiconductor (001) Surface

S. Kulkova[1, 2], A. Bakulin[2], S. Eremeev[1, 2], O. Tereshchenko[3]
[1]Institute of Strength Physics and Materials Science SB RAS, Russia
[2]Tomsk State University, Russia
[3]Institute of Semiconductor Physics, Novosibirsk, Russia
e-mail: kulkova@ms.tsc.ru

For modern technology it is very important to develop techniques such as layer by layer removal of a semiconductor, keeping well-ordered, atomically flat and stoichiometric semiconductor surface. Since III-V semiconductors (001) surface represents alternating layers of anion and cation, these semiconductors are ideal candidate for making such atomically abrupt structures. Digital etching of III-V semiconductors can be realized by means surface reactions with adsorbates interacting selectively with atoms of group III or group V.

We present comparative *ab-initio* study of the halogens (F, Cl, I) adsorption on the cation-rich GaAs and InAs ζ–(001)-(4×2) surface as well as Cl adsorption on InAs β3′-(4×2) performed by means of the pseudopotential plane-wave method within density functional theory. The most preferable position for halogens were found above dimerized Ga (In) atoms in the case of ζ– (001)-(4×2) surface. As seen from Fig. 1 the accumulation of a large negative charge between cation dimer atom and halogen occurs upon adsorption at M_1 (the same trend takes place for M_2, M_3, S_1 sites also), whereas the charge depletion is observed between cation and anion surface atoms. The opposite trend occurs when halogen is adsorbed above As-trench edge atom (S_7) - the depletion of charge occurs in the region of halogen-As bond. Atomic and electronic structure of new β3′-InAs(001)-(4×2) reconstruction is discussed. It was show that independently on surface reconstruction, halogen prefers to bond with In dimerized atoms. In general, halogen interaction with semiconductor surface leads to the weakening of the chemical bonds between surface atoms that determines the initial stage of surface etching.

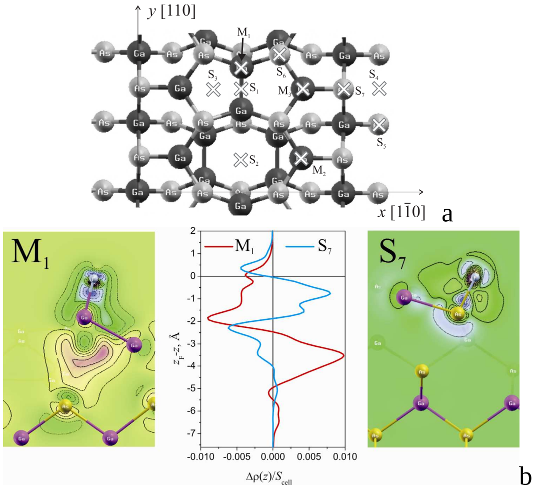

Fig. 1 Atomic structure of ζ-(001)-(4×2) surface and adsorbate sites (a). Charge density difference $\Delta\rho(r)=\rho_{Ga(In)As}(r)+\rho_{Halogen}(r)-\rho_{Halogen/Ga(In)As}(r)$ for M_1 and S_7 fluorine adsorption sites and integrated Δρ in the direction parallel to surface as a function of Z into the bulk (b).

INV-16

Selected Examples of Molecular Confinement Using Nanocarbon Hosts

S. Rols[1], C. Bousige[1, 2], P. Launois[2]

[1]Institut Laue Langevin, France

[2]Laboratoire de Physique des Solides, France

e-mail: rols@ill.fr

In this contribution I will present some recent results on the dynamics of a selection of molecules confined inside different nanocarbon hosts: fullerene C_{60} and carbon nanotubes. The results are essentially derived from a large panel of neutron investigations at different time/energy scales.

Quantum confinement will be illustrated by the case of molecular H_2 confined inside C_{60} [1, 2].

The effect of interstitial insertion of a cubic like molecule C_8H_8 (further referred as cubane) on the dynamic of the C_{60} lattice will be discussed in the light of textbooks results issued from inelastic neutron scattering investigations [3].

The mixed effects of confinement and low dimensionality will be illustrated by the case of peapods which are made from 1D C_{60} chains inserted inside single walled nanotubes [4].

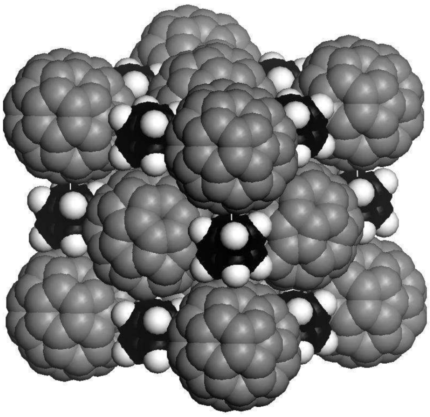

Fig.1 The fullerene-cubane “rotor stator” molecular system: at ambient conditions, the fullerene molecule is a rotor- rotating freely around its center- while the stator cubane acts as static bearings.

References

1. A. J. Horsewill *et al.*, Phys. Rev. Lett. **102,** 013001 (2009)
2. A.J. Horsewill *et al.*, Phys. Rev. B **82**, 081410 (2010)
3. C. Bousige *et al.*, Phys. Rev. B **82** 195413 (2010)
4. S. Rols et al, Phys. Rev. Lett. **101**, 065507 (2008)

INV-17

Swift Heavy Ion Tracks in Dielectrics and Their Possible Applications for Nanotechnology

K. Schwartz[1], M.V. Sorokin[2], A.E. Volkov[2]

[1]GSI Helmholtz Zentrum für Schwerionen Forschung (GSI), Planckstr. 1, 64201, Darmstadt, Germany

[2]Russian Research Center “Kurchatov Institute”, Kurchatov Squere 1, 123182 Moscow; Russia

e-mail: k.schwartz@gsi.de

Swift heavy ions (SHI) with energies (E_{ion}) higher than 1 MeV per nucleon (MeV/u) and masses higher than 20 nucleons can produce structure and phase transformations in solids in nanometric vicinities of their trajectories. These effects occur, when the electronic stopping power (*dE/dx*) of the ion overcomes a critical threshold (~ 1 keV/nm). For SHI with $E_{ion} < 1$ MeV/u the elastic energy loss resulting from collisions with target atoms is to low and can not explained the observed structural modifications [1, 2]. The damage structure of SHI tracks in various solids depends on chemical binding, the ion energy E_{ion} and *dE/dx*, as well as on the irradiation temperature [2 – 5].

SHI effects in solids open new possibilities for nanotechnology due to the nanometric damage scales, the extremely high ratio of the track diameter (10 nm) to the length (100 nm),, and specific structure modifications along the ion path. Developed applications are conductive nanochannels in solids and nanopores in polymers for molecular biology and nanowire technology [5]. New tunable electronic devices are developed for information processing [6]. Damage creation mechanisms and physical limitations for applications are analyzed.

References

1. N. Itoh, D. N. Dufly, S. Khadshouri, A. M. Stoneham, J. Phys.: Condens. Matter **21**, 474205 (2009)
2. K. Schwartz, A. E.Volkov, M. V. Sorokin, C. Trautmann, K.-O.Voss, R. Neumann, M. Lang, Phys. Rev. B **78**,024120 (2008)
3. S. J. Zinkle, V. A. Skuratov, Nucl. Instr. Meth. **B** 191, 758 (2002)
4. Maik Lang, Jie Lian, Jiaming Zhang, William J. Weber, Christina Trautmann, Rodney C. Ewing, Phys. Rev. B **79**, 224105 (2009)
5. J. L. Duan, T. W. Cornelius, J. Liu, S. Karim, H. J. Yao, O. Picht, M. Rauber, S. Müller, R. Neumann, J.Phys.Chem.C **113**, 13583 (2009)
6. D. Fink, A. Saad, S. Dhamodaran, A. Chandra, W. R. Fahner, K. Hoppe, L. T. Chadderton, , Rad. Measurements **43**, S546 (2008)

INV-18

Chromium Centers in $SrTiO_3$: Properties, Problems and New Data

V. Trepakov[1, 2], A. Badalyan[2], D. Azamat[1], A. Dejneka[1], L. Jastrabik[1], P. Galinetto[3]
[1]Institute of Physics AS CR, Czech Republic
[2]Ioffe Physical-Technical Institute RAS, Russia
[3]IFMN- Dipartimento di Fisica “A. Volta” Universita di Pavia, Italy
e-mail: trevl@fzu.cz

Doping by spectroscopic and functional impurities is widely used in a number of studies and applications of ABO_3 perovskite-like oxides. We present a review of the most significant results and new studies of the popular model representative of ABO_3 ferroelectric (FE) oxides with TO1 soft phonon mode: $SrTiO_3$ (STO) doped by Cr^{3+} (3d) model TrM impurities. Presence of the low-lying temperature-dependent TO1 soft mode and orbital degeneracy of the ^2E_g state of Cr^{3+} lead to very unusual “dielectric related” temperature shift of the zero-phonon emission *R*- line ($^2E_g \rightarrow {}^4A_{2g}$) and local configuration instability of Cr^{3+} in photo-excited ^2E_g state [1,2]. Valuable information about phonon modes can be obtained from investigations of vibronic sidebands of *R*- lines. Because Cr unavoidably contaminates STO, the temperature shift of the *R* lines can be used for detection and studies of phase transition in STO based crystals, ceramics, thin films (e.g. [3] for STO:Ca). Just recently the instability and low-temperature minimum of the *R*-emission line energy was found in STO:Cr nanoparticles of the size ~ 13 and 20 nm [4]. This feature can be connected to FE transition in the particle surfaces with the formation of a closed configuration of spontaneous polarization. An important effect of Cr doping was shown in the recent EPR studies of Cr centers controlling a reproducible bistable switching of the leakage current in STO:Cr based structures [5]. We also present new EPR studies of the Cr centers structure depending on thermal treatment of crystals, ratio and stoichiometry of batched Sr and Ti host ions [6].

References

1. S. E. Stokowski and A. L. Schawlow, Phys. Rev. **178**, 457 (1969)
2. V. Vikhnin, V. Trepakov, F. Smutny, L. Jastrabik, Ferroelectrics **176**, 7 (1996)
3. V. A. Trepakov, S. Kapphan, J. G. Bednorz, I. Gregora, L. Jastrabik, Ferroelectrics **304**, 83 (2004)
4. V. A. Trepakov, Z. Potucek, M. V. Makarova, A. Dejneka, P. Sazama, L. Jastrabik, Z. Bryknar, J. Phys.: Condens. Matter **21**, 375 303 (2009)
5. F. La Mattina, J. G. Bednorz, S. F. Alvarado, A. Shengelaya, K. A. Müller, H. Keller, Phys. Rev. B. **80**, 075122 (2009)
6. A. G. Badalyan, D. Azamat, A. Dejneka, P. Galinetto, M. C. Mozzati, V. A. Trepakov, J. Rosa. L. Jastrabik, under preparation for Sol. State. Commun.

INV-19

Wide-range Dielectric Spectroscopy of $BaTiO_3$-based Nanoceramics and Various Nanocomposites

J. Petzelt, D. Nuzhnyy, T. Ostapchuk, P. Vanek, V. Bovtun, M. Savinov

Institute of Physics, Acad. Sci. Czech Rep.

e-mail: petzelt@fzu.cz

New data on dielectric spectroscopy and critical dynamics of pure $BaTiO_3$ (BT) crystals [1], ceramics and nanoceramics [2] are briefly reviewed, including the dielectric grain-size effect on the permittivity and its frequency dispersion up to the infrared range [3]. In addition, various BT core - dielectric nano-shell composites were studied in a similar frequency range and modeled by appropriate models based on effective medium approximation (EMA) [4-6]. An unexpected strong dielectric dispersion was revealed below the THz frequency range in all sufficiently dense samples, not obtained by modeling using EMA. We assign it to partial interdiffusion of BT into the shells. The dispersion is presumably connected with bound charges present in these gradient layers, which create a strong interfacial polarization [6].

Another type of nanoconfined BT was obtained by infiltration of BT sol into the nanoporous Vycor and opal silica glasses [7]. It was shown that in the pores of 4-6 nm diameter (Vycor), BT remains amorphous, but with ferroelectrically distorted TiO_6 octahedra. In larger pores of opals (up to ~50 nm) partial crystallization of BT occurs without macroscopic percolation, but displaying a diffuse ferroelectric transition.

The work was supported by the Czech Science Foundation (project 202/09/0430).

References

1. J. Hlinka, T. Ostapchuk, D. Nuzhnyy, J. Petzelt, P. Kuzel, C. Kadlec, P. Vanek, I. Ponomareva, L. Bellaiche, Phys. Rev. Lett. **101**, 167402 (2008).
2. T. Ostapchuk, J. Petzelt, M. Savinov, V. Buscaglia, L. Mitoseriu, Phase Transitions **79**, 361 (2006).
3. J. Petzelt, Ferroelectrics **400,** 117 (2010).
4. D. Nuzhnyy, J. Petzelt, I. Rychetsky, V. Buscaglia, M. T. Buscaglia, P. Nanni, J. Phys. D **42** 155408 (2009).
5. J. Petzelt, Proc. Appl. Ceram.**3**, 145 (2009).
6. D. Nuzhnyy, J. Petzelt, V. Bovtun, M. Kempa, M. Savinov, C. Elissalde, U.-C. Chung. D. Michau, C. Estournes, M. Maglione, submitted to J. Adv. Dielectrics.
7. D. Nuzhnyy, P. Vanek, J. Petzelt, V. Bovtun, M. Kempa, I. Gregora, M. Savinov, R. Krupkova, V. Studnicka, J. Bursik, M. I. Samoylovich, W. Schranz, Proc. Appl. Ceram., **4**, 215 (2010).

INV-20

Scaling Potential of Local Redox-Processes in Memristive $SrTiO_3$ Thin Film Devices

R. Dittmann

Peter Grünberg Institut, Forschungszentrum Jülich GmbH, Jülich, Germany

e-mail: r.dittmann@fz-juelich.de

A large variety of binary and ternary oxides exhibit resistive switching phenomena, or so called memristive behavior [1]. In the search for promising oxide materials for future non-volatile memories, special attention has to be paid to their scaling capabilities. The issue of scaling is strongly linked to the question of, whether the switching current is distributed homogeneously across the device area or localized to one or a few conducting filaments. In this work, we addressed the question where resistive switching takes places in single crystalline Fe-doped $SrTiO_3$ thin films and memristive devices. We compared resistive switching induced by the tip of the AFM, acting as virtual electrode on the bare thin film surface, with the switching properties observed in memristive devices with Pt top electrode. In order close the gap between these two approaches, we combined conductive AFM with a delamination technique to remove the top electrode of Fe-doped $SrTiO_3$ MIM structures to gain insights into the active switching interface with nanoscale lateral resolution. This enabled us to prove the coexistence of a filamentary and an area-dependent switching process with opposite switching polarities in the same sample (Figure 1) [2]. The spatially resolved analysis by transmission electron microscopy and photelectron spectromicroscopy gave us some hints that the two switching types take place in device areas with different defect density and significant stoichiometry.

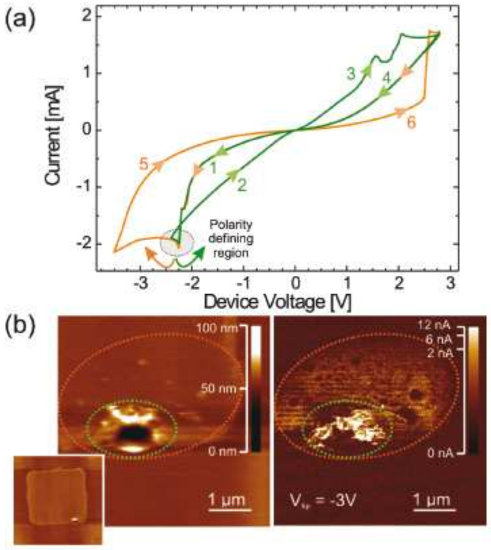

Fig.1 a) *I–V* - characteristic of a Fe-doped $SrTiO_3$ thin film. (b) Conductive AFM topography and current image of a junction after electroforming and top electrode removal. [2]

References

1. R. Waser, R. Dittmann, G. Staikov, K. Szot, Advanced Materials 21, 1-32 (2009)
2. R. Münstermann, T. Menke, R. Dittmann, R. Waser, Adv. Mat. **22**, 4819 (2010)

INV-21

Supermagnetic States of Nanoparticles

W. Kleemann[1], S. Bedanta[1, 2]

[1]Angewandte Physik, Universität Duisburg-Essen, 47048 Duisburg, Germany

[2]School of Physics, National Institute of Science Education and Research (NISER), Bhubaneswar-751 005, India

e-mail: wolfgang.kleemann@uni-due.de

Ensembles of single domained ferromagnetic (FM) nanoparticles, in which magnetic interparticle interactions are sufficiently weak, show *superparamagnetic* (SPM) behavior. However, at increased interactions the system eventually shows collective behavior, which overcomes the individual anisotropy properties of the particles. Different collective states of magnetism were first recognized [1] on so-called *discontinuous magnetic metal-insulator multilayers* (DMIM) consisting of focused ion-beam grown $Co_{80}Fe_{20}$ nanoparticles on glassy Al_2O_3 (Fig. 1). At sufficiently small interparticle distances as controlled by the nominal $Co_{80}Fe_{20}$ film thickness, 0.5 nm $< t_n <$ 1.1 nm, dipolar interaction enables *superspin glass* (SSG) properties. Similar to atomic spin glasses they reveal chaotic *SSG* ground states as corroborated by aging properties such as memory and rejuvenation. At increased concen-tration, but still below physical percolation, 1.1 nm $< t_n <$ 1.4 nm, stronger interactions give rise to *superferromagnetic* (SFM) states with domain formation (Fig. 2) similar to that in conventional FM films [2]. At $t_n > 1.4$ nm the *metal-insulator multilayers* (MIM) become continuous owing to physical interparticle percolation. Owing to inherent layer roughness competing ANNNI-type dipolar interactions give rise to modulated magnetization profiles as evidenced by polarized neutron reflectivity and MOKE microscopy [3].

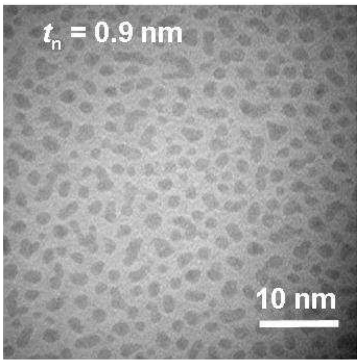

Fig.1 TEM image of $Co_{80}Fe_{20}$ nanoparticles making up a SSG.

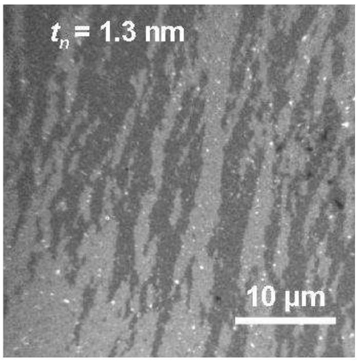

Fig.2 SFM domains in a DMIM $[Co_{80}Fe_{20}(1.3nm)/Al_2O_3(3nm)]_{10}$ imaged by XPEEM [2].

The talk will highlight the most important developments in the field of '*supermagnetism'* [4] comprising *superparamagnetism*, *superspin glass*, *super*- and *percolated ferromagnetism.*

References

1. W. Kleemann, O. Petracic, Ch. Binek, G. N. Kakazei, Yu. G. Pogorelov, J. B. Sousa, S. Cardoso, P. P. Freitas, *Phys. Rev.* B **63** 134423 (2001)
2. S. Bedanta, T. Eimüller, W. Kleemann, J. Rhensius, F. Stromberg, E. Amaladass, S. Cardoso, P. P. Freitas, *Phys. Rev. Lett.* **98** , 176601 (2007)
3. S. Bedanta, E. Kentzinger, A. Scholl, W. Kleemann *et al., J. Phys.* D: *Appl. Phys.* **43**, 474002 (2010)
4. S. Bedanta, W. Kleemann, *J. Phys.* D: *Appl. Phys.* **42**, 013001 (2009)

INV-22

Two Dimensional Distribution of the Relaxation Times

J. Banys[1], A. Mikonis[1], R. Grigalaitis[1], V. Zauls[2], A. Kania[3]
[1]Faculty of Physics, Vilnius University, Lithuania
[2]Institute of Solid State Physics, University of Latvia, Latvia
[3]August Chelkowski Institute of Physics, University of Silesia, Poland
e-mail: juras.banys@ff.vu.lt

Relaxors and dipolar glasses show very broad distribution of the relaxation times. Due to that the usual models, such as Cole – Cole equation or Davidson – Cole or Havriliak – Negami equations are working not very well especially at low temperatures, where the distribution of the relaxation times becomes extremely broad. To address these shortcomings a calculation program was created, which allowed to extract one dimensional distribution of the relaxation times. If we assume, that each relaxation time follows the Arrhenius law, with certain activation energy and attempt relaxation time, we can obtain two dimensional distribution function of attempt relaxation times and activation energies.

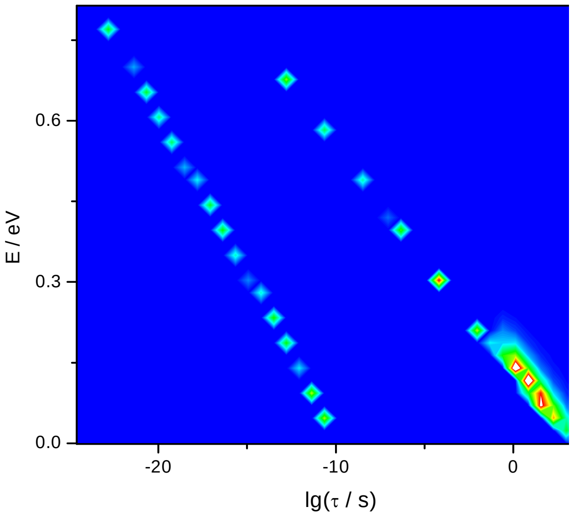

Fig.1 Two dimensional distribution of activation energies and attempt relaxation time of PMN crystal measured from 10^{-3} Hz to GHz frequency range.

Such calculations have been performed for different materials, such as classical dipolar glasses BP/BPI, classical relaxors PMN (Fig.1) and PLZT. The graphs allow us to distinguish between dipolar glasses and relaxors. Also, the results confirmed Meyer – Neldel law [1] with different values of the linear coefficients. The differences and common features of these two classes of materials will be presented.

References

1. A.Yelon, B.Movaghar and H.M.Branz, , Phys. Rev. B **46**, 12244 (1992)

Abstracts of the oral presentations

OR-1

Thermodynamic Calculations on Defects in Perovskites: DFT and Frozen Phonon Method

D. Gryaznov[1, 2], M. Finnis[3], R. Evarestov[4], J. Maier[2]
[1]Max Planck Institute for Solid State Research, Stuttgart, Germany
[2]Institute of Solid State Physics, University of Latvia, Latvia
[3]Imperial College London, London, United Kingdom
[4]St. Petersburg State University, Russia
e-mail: d.gryaznov@fkf.mpg.de

The ABO_3-type perovskites with Co are widely used as cathodes in solid oxide fuel cells. Thermodynamic aspects for calculating point and impurity defects in $LaCoO_3$ are discussed on the basis of first principles calculations. The thermodynamic analysis included 1) phonon symmetry considerations in $LaCoO_3$ and $(La,Sr)CoO_3$, and 2) formation energy of oxygen vacancy in $(La,Sr)(Co,Fe)O_3$ with respect to the chemical potential and phonon contribution. The calculations were done using *ab initio* simulation package VASP [1-2] within spin-polarized density functional theory (DFT) and the supercell method. An analysis of the phonon spectrum in pure $LaCoO_3$ as well as the solid solution is performed using the frozen-phonon method as implemented into the VASP code. The oxygen vacancy behavior is carefully analyzed within the DFT formalism by calculating its formation energy as a function of temperature and oxygen partial pressure [3]. These are two key parameters controlling performance of a SOFC cathode. The formation energies were calculated by taking into account the variation in oxygen chemical potential. The vacancy formation energy decreases from 3.0 eV to 1.8 eV at an oxygen partial pressure of 0.2at over the temperature range from 0 to 1000 K, being very close to that in a pure $LaCoO_3$ [4]. The role of strong electron correlation effects is also considered.

References

1. G. Kresse, J. Furthmüller, Comput. Mater. Sci., 6, 15 (1996).
2. Kresse, J. Furthmüller, VASP, The Guide, University of Vienna, 2009.
3. M. W. Finnis, A. Y. Lozovoi, A. Alavi, Annu. Rev. Mater. Res. 35, 167 (2005).
4. Y-L. Lee, J. Kleis, J. Rossmeisl, D. Morgan, Phys. Rev B 80, 224101 (2009).

OR-2

Radiation Damage Induced by Swift Heavy Ions in $Lu_2Al_5O_{12}$ Crystals

A. Shugai[1], A. Lushchik[1], M. Nikl[2], F. Savikhin[1], K. Schwartz[3], E. Vasil'chenko[1]

[1]Institute of Physics, University of Tartu, Estonia

[2]Institute of Physics AS CR, Prague, Czech Republic

[3]Gesellschaft für Schwerionenforschung (GSI), Darmstadt, German

e-mail: annasu@ut.ee

The creation processes of radiation defects have been investigated in $Lu_3Al_5O_{12}$:Ce^{3+} (used as fast scintillators [1]) and $Lu_3Al_5O_{12}$ (5N purity) single crystals. The irradiation of these crystals by swift heavy ions (SHIs, 2.14-GeV, U^{238}) at 300 K has been performed at GSI, Darmstadt for the first time. About 99% of SHIs energy is spent on electronic energy losses, while small nuclear losses are maximum at the end of ion range (46.2 μm). After fast ($<10^{-13}$ s) intermediate processes there arise an extremely high density of different electronic excitations (EEs, 10^{-12}-10^{-2} s), including hot and relaxed e-h pairs, excitons etc. The energy of EEs either is transferred to Ce^{3+} luminescence centres, as-grown anti-site defects etc., or is spent on the creation of Frenkel defects in oxygen sublattice and their various nano- and micro-associations. It is established that in contrast to more resistant Al_2O_3 crystals the irradiation of LuAG with SHIs at fluence of 10^{12} U/cm^2 causes mechanical stresses, related expansion of a lattice in the direction perpendicular to SHI tracks and even the beginning of crystal cracking. The optical characteristics of ion-irradiated LuAG (in comparison with virgin samples) have been detected via the spectra of optical absorption, reflection and excitation for various emissions as well as the spectra of tunnel phosphorescence at 10 K and thermally stimulated luminescence (10-700 K) in the samples additionally irradiated by 6–10-keV electrons. Similar to Al_2O_3, ion-irradiation of LuAG causes the creation of F^+, F and some other defects absorbing close to the energy gap, $E_g = 8.2$ eV. Hot e-h recombinations are undoubtedly responsible for the creation of these defects in the materials, where the formation energy of a Frenkel pair exceeds E_g. The creation mechanisms not only of Frenkel defects and their nanosize associations, but also of more complex defects, for instance, cluster readjustment of a crystal lattice due to the decay of cooperative EEs, are discussed.

References

1. M. Nikl, E. Mihokova, J. Pejchal, et al., IEEE trans. Nucl. Sci. **55**, 1035 (2008)

OR-3

Studies of Nanostructures Formed in T-10 Tokamak

V.G. Stankevich[1], N.Yu. Svechnikov[1], B.N. Kolbasov[1], A.M. Lebedev[1], K.A. Menshikov[1],
D. Rajarathnam[2], V.A. Somenkov[1], A.A. Veligzhanin[1], Y.V. Zubavichus[1]

[1]Russian Research Center “Kurchatov Institute”, 123182 Moscow, Russia

[2]CERAR, University of South Australia, 5095 Australia

e-mail: kolbasov@nfi.kiae.ru

Hydrocarbon films and flakes are formed under deuterium plasma discharges in T-10 tokamak. Homogenous 20-30 μm thick films, redeposited inside the vacuum vessel far from graphite plasma facing components, may have atomic ratio D/C up to 0.9 and higher. The properties of such films were studied with application of small-angle X-ray scattering using synchrotron radiation, wide-angle X-ray scattering measurements, neutron diffraction and other techniques. According to the X-ray diffraction (XRD) studies, the overall structural pattern of the films resembles the pattern for an amorphous solid, with graphene-like sheets composed of aromatic rings oriented mainly parallel to the film surface. The XRD peak positions showed the presence of structural defects with interplane distances of 0.12, 0.24 and 0.66 nm. The peak widths gave the in-plane sizes of the scattering structures equal to about 1 nm. Comparison of X-ray and neutron diffractograms suggests that the film structure is strongly disturbed by broken bonds of carbon network and by nanopores filled with atomic deuterium. The combination (Raman) scattering studies did not reveal presence of molecular deuterium and protium in the films. The experiments performed using near-edge X-ray absorption fine structure (NEXAFS) spectroscopy have shown that the films contain about 63% of sp^3 and ~37% of sp^2 states. The films display the properties of a wide-band semiconductor with a gap of about 3 eV. X-ray fluorescence spectroscopy employing synchrotron radiation revealed that the films contain at least 12 impurities of Fe, Mo, Cr, Ni, Nb and other transition metals. The studies using electron paramagnetic resonance spectroscopy revealed defects with unpaired spins that refer to unpaired π-bonds in Csp^2-nano-clusters which size is ~4 nm and spin orientation is non-isotropic.

Difference between film properties on its opposite sides was revealed using Fourier-transform infrared spectroscopy and analysis of current-voltage characteristics (CVC). On the wall facing side of the film, aromatic rings Csp^2 dominate, carbon network is distorted. Amount of metallic impurities on this side is higher and concentration of hydrogen isotopes, hydroxyls and C=O groups is smaller than on the wall facing side. CVC is of semiconductor type with resistivity $\rho = 10^5$-10^7 Ω·cm. On the plasma facing side, diamond-like Csp^3 structures prevail, $\rho = 10^8$-10^9 Ω·cm, while CVC is quasi-ohmic. Different types of CVC hysteresis are observed on the opposite sides of the films. They are caused by different types of charge traps, i.e. structural defects serving as centers for hydrogen isotope and hydrocarbon adsorption. Difference in properties of opposite film sides, apparently, is determined by the process of film formation under discharges.

Deuterium retention can be monitored by two groups of vibrational sp^3 modes with different oscillator strengths, depending on the amount of deuterium in films.

OR-4

Effective Diffusion Coefficient in One Dimensional Model

J.R. Kalnin

Ventspils University College, Latvia

e-mail: simts@latnet.lv

The effective diffusion coefficient in two-phase one-dimensional model with periodical distribution of inclusions is calculated. Effective medium approximation is used (Fig.1). Region I is inclusion and region II - matrix with diffusion coefficients D_1, D_2 and particle concentrations C_1, C_2 respectively. These two regions are embedded into the third region acting as an effective medium with the concentration c_{eff} and diffusion coefficient D_{eff}. It is assumed that concentration leap on the boundary matrix – inclusion occurs. Representative region is immersed in linear diffusion field *–gx*. Diffusion equation in the regions I-III were solved with the appropriate boundary conditions. For concentrations were used $c_{eff}\big|_{x=x_1} = \chi^{-1} c_1\big|_{x=x_1}$, $c_1\big|_{x=x_2} = k^{-1} c_2\big|_{x=x_2}$, $c_2\big|_{x=x_3} = k\, c_3\big|_{x=x_3}, c_3\big|_{x=x_1} = \chi\, c_{eff}\big|_{x=x_1}$.

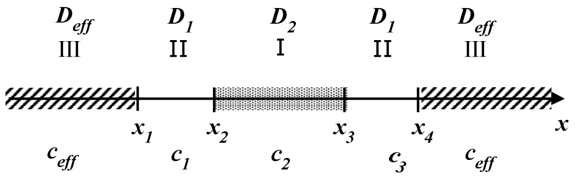

Fig.1. 1D system in mean field approximation. II-I-II - representative elementary cell, III- effective media

Widely discussed [1-2] multiplier $\chi = \left(1 - f + \frac{c_1}{c_2} f\right)^{-1}$, where *f* is inclusion volume fraction, was received without any other additional assumptions about the averaging of concentrations. It is shown that $k = \frac{D_2 l_1}{D_1 l_2}$, where l_1 and l_2 mean free path in I and II respectively.

References

1. J. R. Kalnin, E.A. Kotomin, J. Maier. J. Phys. Chem. Solids. **63**, 449 (2002)
2. J. Jamnik, J.R.Kalnin, J.A. Kotomin, J. Maier. Phys. Chem. Chem. Phys. **8**, 1310 (2006).

OR-5

Dynamics of Exciton Creation and Decay Processes in Composition – Disordered InGaN Thin Films

L. Dimitrocenko, P. Kulis, A. Sarakovskis, I. Tale, A. Voitkans
Institute of Solid State Physics, University of Latvia
e-mail: iatale@latnet.lv

In the GaN-based ternary alloys, InGaN crystals have been recognized as key materials for e-h plasmas-exciton dynamics, because of large exciton binding energies (24.8 meV in GaN). The localization of biexcitons have been investigated in $In_xGa_{1-x}N$ (x=0.05) sample using time-integrated PL spectra measurements as a function of the excitation density [1]. We report experimental data showing that dynamics of exciton decay involves formation of localized single excitons, biexcitons and triexcitons.

Picosecond time resolved photoluminescence (PL) spectroscopy in MOCVD grown $In_xG_{1-x}N$ mixed films with In concentration in range from x=0.1 to 0.18 under the band-to-band excitation have been investigated. It has been found that the band-band photo excitation at 8 K in wide composition range results in creating of complex luminescence band represented by three close overlapping Gaussian shape bands, (2.946, 2.929 and 2.918 eV, having FWHM 26.9, 13.40 and 16.1 meV respectively, sample x=0.18). Increase of the excitation density results first in super linear growth of 2.946 eV band followed by preferential sharp increase of 2.918 eV band. All three luminescence bands show close exponential 10-14 ps decay time constants. Formation of biexciton band is delayed with respect to the exciton band for ~35 ps, triexciton band for ~30 ps with respect to the biexciton band indicating that the dynamics involves step-by-step creation mechanism. At increased In content up to 18% both the localized excitons, biexcitons and triexcitons are represented by Gaussian type luminescence bands being non-uniformly broadened at the high energy side.

Acknowledgments: L.D., A.S., P. K. and A. V. were supported by ESF Grant 2009/0202/1DP/1.1.1.2.0/09/APIA/VIAA/141

References

1. Kanemitsu Y, Hirano D 2008 *J. Luminiscence* 128 712

OR-6

Spectroscopy of Yb^{3+}-doped III-V Semiconductors at Ambient at High Pressure: Experiment, *ab-initio* and Crystal Field Studies

C.-G. Ma[1], M.G. Brik[1], A. Kaminska[2], A. Suchocki[2, 3]

[1]Institute of Physics, University of Tartu, Riia 142, Tartu 51014, Estonia

[2]Institute of Physics, Polish Academy of Sciences, Al. Lotników 32/46, 02-668 Warsaw, Poland

[3]Institute of Physics, University of Bydgoszcz, Weyssenhoffa 11, Bydgoszcz 85-072, Poland

e-mail: kaminska@ifpan.edu.pl

Rare earths (RE) doped semiconductors are nowadays attracting a lot of attention due to their unique optical and electrical properties and high potential of these materials in new optoelectronic device applications, for instance in electrically-pumped light-emitting diodes or lasers [1 and references therein]. Among the RE doped III–V semiconductors InP:Yb is one of the most intensively studied material for its strong Yb-related luminescence at about 1 µm. Yb^{3+} ions ($4f^{13}$ electron configuration) have a simple energy level scheme, which consists of two states only: $^2F_{7/2}$ and $^2F_{5/2}$ separated by about 10000 cm^{-1}. Such a scheme excludes excited state absorption and all related energy losses. From this point of view, Yb^{3+} ion is now the most promising for use as a non-Nd lasing center in the infrared spectral region [2]. On the other hand, InP and GaN – typical representatives of the III-V semiconductors – can be relatively easily and cheaply synthesized in the laboratory by different growth techniques and doped with ytterbium ions.

In the present work we report on combination of the high-pressure measurements with use of diamond anvil cell (DAC) of the luminescence spectra of InP:Yb^{3+} and GaN:Yb^{3+} crystals with *ab initio* calculations of the electronic (band structure, density of states, Mulliken effective charges), optical (absorption spectra, refractive index, dielectric functions), elastic (bulk modulus and its pressure derivative) properties of these systems. The CASTEP module [4] of the Materials Studio was used to calculate the optimized crystal structure data, electronic and optical properties at ambient at elevated pressure. In addition, crystal field analysis of splitting of the $^2F_{7/2}$ and $^2F_{5/2}$ states has been performed as well, with an aim of assigning all features of the experimental luminescence spectra.

A thorough analysis of the pressure behavior of the Yb^{3+} luminescence lines in InP [6] reveals interesting effects, namely: after 6 GPa blue shift of the luminescence tends to saturation, which was explained by pressure-induced shift of the InP valence band approaching the energies of the Yb 4f-4f transitions [7]. This overlap behaves exactly as the luminescence lines with pressure. Detailed Raman investigations along with polarized luminescence spectra measurements of GaN:Yb^{3+} samples allowed to determine positions of the zero-phonon lines, which then were used for modeling the Yb^{3+} energy levels in the trigonal crystal field Hamiltonian.

Acknowledgements: This work was partly supported by the European Union within European Regional Development Fund, through the Innovative Economy grant (POIG.01.01.02-00-108/2009/2) and the project no N N202 010134 of Polish Ministry of Science and Higher Education.

References:

1. H.J. Lozykowski, W.M. Jadwisienczak, J. Han, I.G. Brown, Appl. Phys. Lett. 77 (2000) 767.
2. E. Montoya, J. A. Sanz-Garcia, J. Capmany, L. E. Bausá, A. Diening, T. Kellner, G. Huber, J. Appl. Phys. 87 (2000) 4056.
3. M. Godlewski, A. Kozanecki, J.P. Bergman, B. Monemar, Appl. Phys. Lett. 66 (1995) 493.
4. M. D. Segall, P. J. D. Lindan, M. J. Probert, C. J. Pickard, P. J. Hasnip, S. J. Clark, M. C. Payne, J. Phys.: Condens. Matter 14 (2002) 2717.
5. G.K. Liu, in: G.K. Liu and B. Jacquier (Eds.), Spectroscopic Properties of Rare Earths in Optical Materials, Tsinghua University Press & Springer-Verlag (Berlin), Heidelberg, 2005, p. 1.
6. A. Kaminska, A. Kozanecki, S. Trushkin, A. Suchocki, Phys. Rev. B 81 (2010) 165209.
7. M.G. Brik, A. Kaminska, A. Suchocki, J. Appl. Phys. 108 (2010) 103520.

OR-7

Defect Luminescence of III Group Element Nitrides AlN and hBN

B. Berzina, V. Korsaks, L. Trinkler, J. Grigorjeva
Institute of Solid State Physics, University of Latvia, Latvia
e-mail: baiber@latnet.lv

III group element nitrides are promising materials for future optoelectronics and interests of physicists from many world laboratories are focused on research of their optical properties. Recently it was found that AlN and hBN are prospective light emitters in the far UV region around 200 nm based on excitonic processes. The present report is devoted to investigation of native defect luminescence processes and mechanisms in AlN and hBN with bulk and nanosize structures within the UV spectral region from 250 nm up to visible light at 700 nm and wide temperature range from 8 K up to 300 K.

It was found that for AlN as well as for hBN the same defect structures are characteristic for both the bulk material and nanosize ones. In the case of AlN the main native defects are the oxygen-related ones (O_N) with characteristic luminescence around the 400 nm from the bulk material and around 480 nm from the surface defects. The recombination character of 400 nm luminescence and its mechanism was also proposed [1].

In the case of hBN – bulk powder and multiwall nanotubes (BNNTs), there are two main luminescence bands at 320 nm and 400 nm both with well-pronounced phonon structure [2], which intensities increase with temperature decrease down to 8 K. According to our results and data reported from other authors the 320 nm luminescence in hBN can be credibly caused by the C impurity (C_N) substituting for the N. The mechanism of this luminescence is of inter-center type, when excitation and emission processes cover the same defect. The 400 nm luminescence could be related to the processes with recombination character. Taking into account the results obtained and close analogy of both materials the AlN and hBN the origin of the 400 nm luminescence in hBN can also be related to the oxygen related defects located near the surface of the material. The 400 nm luminescence mechanism is proposed.

The defect luminescence from AlN and hBN located within the visible range of the spectra is important for elaborating new white light sources.

References

1.B.Berzina,L.Trinkler, D.Jakimovica, V.Korsaks, J.Grabis. I.Steins, E.Palcevskis, S.Bellucci, Li-Chyong Chen, Surojit Chattopadhyay, Kuei-Hsien Chen, Journal of Nanophotonics **1**, 031950 (2009)

2. R.T.Williams, K.B.Ucer, D.L.Carroll, B.Berzina, L.Trinkler, V.Korsak, and R.Krutohvostov, Journal of Nanoscience and Nanotechnology **8,** 1 (2008)

OR-8

Structure, Fe Solubility and Luminescence of Fe Doped ZnO Nanowires and Nanorods

B. Alemán[1], Y. Ortega[1], J.A. García[2], P. Fernández[1], J. Piqueras[1]
[1]Department of Materials Physics, University Complutense of Madrid, Spain
[2]Department of Applied Physics II, University of Basque Country, Spain
e-mail: piqueras@fis.ucm.es

Fe doped ZnO nanowires, nanorods and urchin-like nanostructures have been grown by an evaporation-deposition method [1] with compacted mixtures of ZnS and Fe_2O_3 powders, with different Fe contents as precursors. Treatments at 950 ºC under argon flow lead to the growth of iron doped nanowires, nanorods and other nanostructures on the surface of the compacted sample. The incorporation of iron into the nanostructures has been investigated by energy dispersive spectroscopy as well as by cathodoluminescence (CL) in the scanning electron microscope and photoluminescence (PL) in an optical microscope. The content of iron in the structures is limited to the range 0.5-0.7 at. % and does not depend on the content in the precursor, which was in the range 0.6-6 at. %.

CL and PL of the nanowires show Fe^{3+} intraionic transitions at 1.71 eV and 1.79 eV respectively, and an enhanced green band relative to undoped material. Fe incorporation also causes a red shift of the near band gap and of the main defect emission band.

Transmission electron microscopy of the nanowires shows dark contours perpendicular to the growth axis. Bright and dark field TEM analysis indicate that these features are twist contours. The results are compatible with twist contours related to a dislocation-driven growth mechanism, as reported for other semiconducting nanowires [2].

References

1 B. Alemán, P. Fernández and J. Piqueras, Appl. Phys. Lett. **95**, 013111 (2009)
2 S. A. Morin and S. Jin, Nano Letters, **10,** 3459 (2010)

OR-9

Short Lived and Stable Defects in Yttrium Stabilized Zirconia Single Crystal

D. Millers, K. Smits, L. Grigorjeva
Institute of Solid State Physics, University of Latvia, Latvia
e-mail: dmillers@latnet.lv

The study of zirconia luminescence showed that in the oxygen deficient samples the efficient charge traps exist [1]. The trapping of charge carriers could result in absorption change – the induced absorption can appear. Therefore the attempt to detect the induced absorption in zirconia was carried out. The yttrium stabilized zirconia single crystal was irradiated with a pulsed electron beam and induced absorption was observed. The wide induced absorption band covered spectral region from 1.15 eV up to 3.6 eV. The decay of absorption take place after irradiation pulse and the decay rate was different within band detected. The origin of induced short lived absorption in general could be (I) due to the absorption of intrinsic and/or bound polaron states; (II) absorption from the excited states, e.g., luminescence center excited state might be responsible; (III) due to recharging of pre-irradiation defects. The comparison of luminescence and absorption decay kinetics showed that contribution in absorption from luminescence excited states is insignificant. The different decay rate of absorption within band indicated that the absorption band is complex, several bands overlaps. The use of time – resolved techniques allow to make decomposition of the wide absorption band on several components. Therefore several kinds of centers were responsible for induced absorption. The dependence of induced absorption decay rate on temperature led to the conclusion that a fraction of absorption arises due to recharging of pre- irradiation defects and the activation energies for charge release from traps were estimated. These estimations allow to predict the temperature range for existence of stable defects. It is supposed that at liquid nitrogen temperature both the polarons and recharged defects contributed in induced absorption, whereas at room temperature the contributions from recharged defects dominate.

References

1. K. Smits, L. Grigorjeva, D. Millers, J.D. Fidelus, W. Lojkowski, IEEE Transactions on Nuclear Science **55** (3), art. no. 4545213, p. 1523, (2008)

OR-10

Photoluminescence of Oxygen Related Defects in Sol Gel derived Nanocrystalline ZrO_2 Thin Films

K. Joy, J.S. Lakshmi, J.K. Thomas, P.V. Thomas

Thin film Lab, Post Graduate and Research Department of Physics, Mar Ivanios College, Thiruvananthapuram 695015, India

e-mail: *jolly2jolly@gmail.com*

ZrO_2 is an interesting material because of its outstanding thermal, mechanical and optical and electrical properties. Advanced materials for luminescent oxygen sensors require modified surface with excellent oxygen exchange property and transparency high enough for luminescent light output [1]. Zirconia in the thin film form attracts special interest owing to its advantageous properties of being highly homogenous and transparency. Highly transparent and homogeneous nanocrystalline ZrO_2 thin films were prepared by sol-gel dip coating method. XRD pattern of ZrO_2 thin films calcined in air and O_2 shows the formation of tetragonal phase with varying crystallite size (7.3nm and 11.3nm) at 500°C. X-ray photoelectron spectroscopy (XPS) (Fig.1) shows O1s and Zr3d spectra of thin film annealed in air which reveals zirconium suboxide component (ZrO_x, $0 < x < 2$) , Zr-O bond and surface defects [2]. An average transmittance of > 85 % (in UV-Vis region) was observed for all calcined samples. Photoluminescence (PL) reveals an intense emission peak at 379nm and weak peaks at 294, 586 and 754nm for ZrO_2 film calcined in air. A 2 fold increase in the PL intensity and a red shift is observed in film calcined in O_2 atmosphere. The oxygen deficient defect, which is the distorted Zr-O bond, is suggested to be responsible for photoluminescence. The defect states in the nanocrystalline zirconia thin films play an important role in the energy transfer process. The luminescence dependence on defects in the film makes it suitable for luminescent oxygen-sensor development.

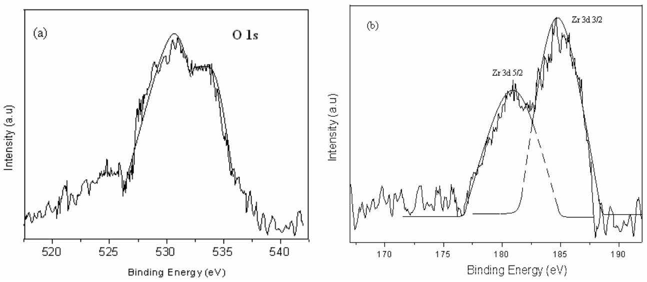

Fig.1. XPS spectra of ZrO_2 thin film calcined in air at 500˚C: (a) O 1s and (b) Zr 3d

References

1. Francisco Trivinho-Strixino , Francisco E.G. Guimarães , Ernesto C. Pereira , Chemical Physics Letters **461,** 82 (2008)
2. Latha Kumari, W.Z.Li, J.M. Xu, R.M.Leblanc, D.Z.Wang, Yi Li, Haizhong Guo, Jiandi Zhang Crystal Growth and Design **9,** 3874 (2009)

OR-11

Luminescence Spectroscopy of Ca-Apatites under VUV Excitation

E. Feldbach, H. Mägi, M. Kirm
Institute of Physics, University of Tartu, Estonia
e-mail: marco.kirm@ut.ee

Apatites represent the class of materials with very wide functionality found in nature. Chemical formula of any apatite can be written generally as $M_4^{I}M_6^{II}(TO_4)_6X_2$, where M denotes metal ions occupying two non-equivalent positions (I and II) in crystal lattice, TO_4 refers to oxyanions with tetrahedron structure (PO_4, SiO_4, GeO_4, etc) and X anions (OH^-, F^-, Cl^-, etc). Consequently, chemical composition of apatites is highly variable, which opens extraordinary possibilities for the synthesis of novel functional materials. Apatites have hexagonal crystal structure where tetrahedrons (TO_4) and metals (M) form positively charged framework with open channels along the hexagonal axis. Electroneutrality of crystal structure is provided by anions (X), which makes apatites family analogous to nanoporous compound of $12CaO\cdot7Al_2O_3$, investigated by us earlier [1]. Pure hydroxyapatite (HAP) $Ca_{10}(PO_4)_6(OH)_2$ and its fluorine-substituted modification (FAP) are obviously the most well-known apatites, being the main inorganic constituent of all mammalian bones and teeth. Despite of very high potential for various applications basic optical properties of these apatite hosts remain still to be investigated - even energy gap width of HAP is not reliably determined yet.

We applied luminesecnce spectroscopy at SUPERLUMI station of HASYLAB to study electronic properties of HAP and FAP, the band-gap energy was determined in MAX-LAB by photostimulated luminescence method used earlier in [2]. Samples of HAP were prepared from commercial powder (Sigma-Aldrich, 99.999%). The FAP ceramics resulted from solid state reaction of $Ca_3(PO_4)_2$ and CaF_2. The revealed intrinsic UV emissions in both systems are due to radiative decay of Frenkel excitons localized on the PO_4 oxyanions, well excited within excitation bands peaked at 7.2 eV and 7.5 eV in HAP and FAP, respectively. Both bands are located below band-gap energy, identified for pure HAP as $E_g\approx7.7$ eV by excitation onsets of photoluminescence and afterglow spectra. Luminescence properties and the electronic structure of pure HAP and FAP will be discussed taking into account results of theoretical and earlier experimental studies, mostly carried out for rare earth doped hosts.

References

1. E. Feldbach, V. P. Denks, M. Kirm, K. Kunnus, A. Maaroos, Radiat. Meas. **45** (2010) 281.
2. V. Nagirnyi, L. Jönsson, M. Kirm, *et al*. Radiat. Meas. **38** (2004) 519.

OR-12

5*d*-4*f* Luminescence of Lanthanide Ions in $LiYP_4O_{12}$

T. Shalapska[1], G. Stryganyuk[2], A. Voloshinovskii[1], P. Dorenbos[3]
[1]Ivan Franko National University of Lviv, Str. Kyryla i Mefodiya, 8, Lviv, 79005, Ukraine
[2]Institute for Scintillation Materials NAS of Ukraine, 60 Lenin ave., 61001 Kharkiv, Ukraine
[3]Faculty of Applied Sciences, Delft University of Technology, Mekelweg 15, Delft, 2629 JB, Netherlands
e-mail: t_shalapska@ukr.net

Study of stoichiometric polyphosphate compounds containing lanthanide ions is increasing mainly for numerous modern applications in light-emitting devices. The conversion of VUV radiation, scintillator materials, tunable UVV-UV microlaser sources etc. rely on lanthanide luminescence upon high-energy electron excitation. The inorganic polyphosphates with general formula $ALnP_4O_{12}$ (A=Li, Na, K, Cs, Ln - lanthanide ions) have been extensively investigated in the past years due to their lighting application perspective. The high concentration and the large distance between the Ln^{3+} ions (~5,6Å) facilitate the decreasing of concentration quenching and the achieving of high luminescence emission intensity [1,2]. The relatively large band gap (~9 eV) of $ALnP_4O_{12}$ polyphosphates provides favourable conditions for the investigation of luminescent processes in oxide compounds taking into consideration the energy relaxation processes involving a broad series of Ln^{3+} ions. This circumstance allowed to carry out the comprehensive study of $LiLnP_4O_{12}$ luminescence caused by the intra- $4f^N \leftrightarrow 4f^N$, interconfigurational $4f^N \leftrightarrow 4f^{N-1}5d$ and charge transfer $O^{2-} \rightarrow Ln^{3+}$ electronic transitions upon excitation with synchrotron VUV-UV radiation from the DORIS III storage ring with use of the SUPERLUMI experimental facility (Beamline I) at HASYLAB (DESY, Hamburg) and laboratory nanosecond pulse X-ray source [3].

A considerable part of our study was focused at the spectroscopy of Ce^{3+} ion since its energy state parameters have been used as a basis for construction of the energy level diagram for the entire series of Ln^{3+} ions. Much attention was paid to the investigation of charge transfer transition in Eu^{3+} ions to estimate the location of 4f ground states of Ln^{2+} ions. Basing on the Ln^{3+} emission, their excitation spectra and the empirical relationships between spectroscopy of Ce^{3+} and Ln^{3+} ions we have constructed the energy levels diagram in absolute energy scale for 4f and 5d states of Ln^{3+}, Ln^{2+} ions in $LiYP_4O_{12}$.

References

1. T Shalapska, et.al. J Phys: Conds. Matter, **21**, 445901 (2009)
2. J. Zhong, et. al. Optical Materials, **32**, 378 (2009)
3. G Zimmerer, Radiations Measurements. **42**, 859 (2007)

OR-13

Microstructure and Optical Properties of TiO_2 Doped with Ytterbium Synthesized by Sol-Gel and Solar Physical Vapour Deposition Process

J.D. Fidelus[1, 2], M. Barczak[3], A. Dużyńska[1], C.J. Monty[4], P. Sybilski[1], P. Nowakowski[1], A. Suchocki[1]

[1]Institute of Physics, Polish Academy of Sciences, Al. Lotników 32/46, 02-668 Warszawa, Poland
[2]Institute of High Pressure Physics, Polish Academy of Sciences, Sokołowska 29/37, 01-142, Warsaw, Poland
[3]Faculty of Chemistry, Maria Curie-Skłodowska University, Maria Curie-Sklodowska Sq. 5, 20-031 Lublin, Poland
[4]CNRS, PROMES laboratory, Odeillo, 66120 Font-Romeu, France
e-mail: mbarczak@umcs.pl

The photoelectrolysis of water (to split water into hydrogen and oxygen) as a result of the absorption of sunlight is considered to be the most important unconventional future energy source. This process is conducted in a photoelectrochemical cell (PEC) composed of an aqueous electrolyte and two electrodes [1]. Currently, TiO_2 is one of the most appropriate candidate for the photo-anode material in the PEC due to its high resistance to corrosion, stability and a negative flat band potential.

The band gap of TiO_2 is ~3 eV, too high for the efficient absorption of the sunlight. However, the light absorption of TiO_2 may be increased substantially by modification of its semiconducting and electrochemical properties through doping with aliovalent ions and producing solid-solutions with other oxides [2]. Additionally, incorporating rare-earth ions into titania matrix, can up-convert infrared radiation into various shorter wavelengths. This process plays an important role in enhancing optical detection and display devices.

In present work, the differences appearing from the synthesis process of initial materials and nanopowders obtained in a solar reactor have been studied. Initial titania nanopowders doped with different amounts of ytterbium were obtained by sol-gel technique according procedure reported elsewhere [3]. Further, the pelletized nanopowders were processed by fusion and vaporization-condensation process in medium size solar furnace with HELIOTRON solar reactor in Odeillo (France).

The structure and selected optical properties of obtained materials have been studied by broad range of instrumental techniques including: X-ray diffractometry, scanning electron microscopy, atomic force microscopy, thermogravimetry, infrared spectroscopy, nitrogen sorption measurements, spectrofluorimetry and spectrophotometry.

Acknowledgements
This work was supported by the project “Nanomaterials for renewable energy applications” (RENANOS, 2010) within the framework of the EU-DG RTD's 'Solar Facilities for the European Research Area (SFERA), and partly supported by the European Union within European Regional Development Fund, through the Innovative Economy grant POIG.01.01.02-00-108/2009/2.

References

1. A. K. Fujishima, H. Honda, *Nature* ***238*** (1972) 37.
2. T. Bak, J. Nowotny, M. Rekas, C.C. Sorrell, *Int. J. Hydrogen Energy* ***27*** (2002) 991.
3. X. An-Wu, G. Yuan, L. Han-Qin, *Journal of Catalysis* ***207*** (2002) 151.

OR-14

Plasmon-Coupled Emission from the TiO_2:Sm^{3+} Sol-Gel Film

L. Dolgov, V. Kiisk, I. Sildos
Institute of Physics, University of Tartu, Estonia
e-mail: dolgov@fi.tartu.ee

Sol-gel derived oxides doped with rare-earth ions are perspective luminescent, laser, waveguide and sensory media. Coupling of fluorescence with surface plasmon-polaritons can crucially enhance intensity and polarization of emission, provide necessary direction of beams.

Previous experiments with plasmon-coupled rare-earth emission were mainly realized in composites of rare earths with noble metal nanoparticles [1-3]. Here we present another approach, where the rare-earth emission couples with plasmon-polariton wave induced in thin smooth gold layer. TiO_2 film (~100 nm) doped with 6 wt. % of Sm was spin-coated on a gold layer (50 nm) deposited on glass substrate. This sample was attached by index matching oil to a semi-cylindrical prism. The sample was excited by UV laser light (λ=355 nm) (Fig. 1, a). It was revealed that Sm^{3+} fluorescence was preferentially directed at certain angles and strongly polarized. Moreover, the longer wavelengths were directed at smaller angles θ, which testifies about the plasmonic origin of the directional emission. The obtained directional emission of Sm^{3+} ions is promising for using in waveguiding, suppression of undesirable background emission and optical sensors based on the effect of surface plasmon coupled emission.

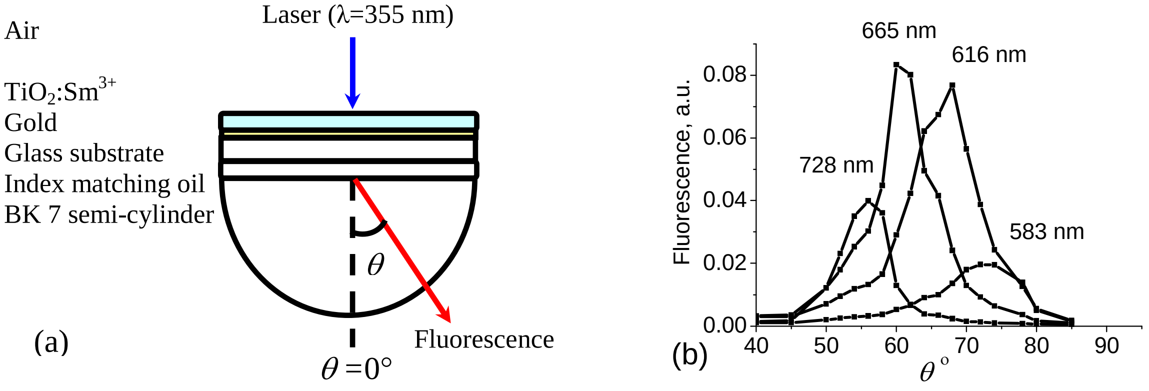

Fig. 1. Scheme of experiment (a). Angular dependence of fluorescence from different Sm^{3+} bands (b).

References

1. J. Zhang, Yi Fu, J. R. Lakowicz, J. Phys. Chem. C **113**, 19404 (2009)
2. R. Reisfeld, Ts. Saraidarov, V. Levchenko, J Sol-Gel Sci. Technol. **50**, 194 (2009)
3. L. Dolgov, V. Reedo, V. Kiisk, S. Pikker, I. Sildos, J. Kikas, Opt. Mat. **32**, 1540 (2010)

OR-15

Thermochromic Glazing Materials for “Zero Net Energy” Houses

O. Yanush, T. Markova
Saint Petersburg State Technological University of Plant Polymers, Russia
e-mail: o.v.yanush@inbox.ru

Energy consumption for heating and air conditioning of buildings can be significantly reduced by means of “smart windows” capable to vary its daylight transmission. In spite of long-term research efforts of many well-established companies, the larger scale production of inexpensive and effective “smart windows” is not created up to now.

Results of R&D of novel thermochromic substance have been presented. It is a polymer doped with complexes of some transition metals. The change of the complexes coordination occurs under the influence of light or heat fluxes, that results in reversible change of transmittance and/or color of the polymer from: light gray ⇆ dark gray, light brown ⇆ dark brown, rosy ⇆ blue, yellow ⇆ green, light green ⇆ blue.

Thermochromic polymer is characterized by high (1-20 kg/cm) adhesion to window surface. The polymer layer of 0.3-1 mm thickness ensures the reversible reduction of daylight transmittance from 80% to 20% when its temperature grows from 20 to 70°C.

Chief advantages of thermochromic laminated glazing (TLG) are as follows: daylight regulation adapted on a programmable and automatic basis without using of any electrical power or driving unit, no blinding effect; simple design, cheap raw materials, feasibility of large glazing area production, high UV-stability of TLG material established by UV-testing, cyclic recurrence unlimited in number, storage in a wide range of temperature from -50^0C to $+80^0$C. Toxic-free manufacturing, exploitation and utilization of TLG having a life time of over dozen years. TLG opens the way to design new type of stained glass panels assembled out of coloured TLG, which will change its image during a day. A high-performance thermochromic insulated-glass unit (TGU) consisting of TLG as the outer pane and Low Emissivity glass (Low E) as the inner pane will make possible to create regulated cover heating for “zero net energy” houses (“intelligent facades”). In summer TGU will operate with high efficiency because TLG absorbs visible and near IR rays and then Low E glass reradiates energy in far infrared region only (without blinding effect). In winter TLG will constantly have the maximum light transmittance because of the low temperature outside ($T<20^0$C).

This work was supported by grants from the RFBR (Projects N09-03-00755-a, N10-03-00323-a).

OR-16

Nanostructured Pt/ $Ti_xMe_{1-x}O_2$ (Me = Nb, Ru) Electrocatalysts for Direct Alcohol Fuel Cells

L. Frolova, Yu. Dobrovolsky
Institute of Problem Physical Chemistry, RAS, Russia
e-mail: laf@icp.ac.ru

Our research purpose was to develop effective nanostructured platinum electrocatalysts supported on $Ti_xMe_{1-x}O_2$ (Me = Nb, Ru; where Me = 1 ÷ 12 % mol.) and to study the influence of their composition, electro-physical properties and size effects on the electrocatalytic activity and stability in the oxidation of methanol and ethanol. Our mark is also aimed at investigation the influence of structure of an active layer of electrodes on electrochemical parameters of the above mentioned processes in fuel cells.

The corrosion stable supports $Ti_xMe_{1-x}O_2$ with high specific surface (~100 m^2/g), narrow distribution of particles on the size (20-25 nm) were obtained. $Ti_xMe_{1-x}O_2$ (Me = Nb, Ru; Me = 7 ÷ 12 % mol.) characterized by high electronic conductivity (~ 2 Sm/cm).

Pt colloidal particles were deposited on oxide supports with various amounts of Pt loading (2-35 mass. %). The electrocatalytic catalysts activities for methanol and ethanol oxidation reaction (MOR and EOR) have been investigated in half cell experiments, by cyclic voltammetry and stationary current–voltage measurements. The results were compared with commercial catalyst - 20%PtRu/C (E-Tek). It was found that the catalysts containing about 5 mass percents of platinum are the most effective. They demonstrated highest specific active surface of the catalysts (~ 70 $m_{(Pt)}^2/g$). Electrochemical experiments carried out in steady-state conditions demonstrate that using the oxide supported platinum Pt/ $Ti_{0.9}Me_{0.1}O_2$ (Me = Nb, Ru) produces a very reactive electrocatalyst that possibly adsorbs and/or dissociate methanol and ethanol more efficiently than pure Pt changing the onset potential of the reaction by 200mV toward less positive potentials. These synergic effects indicate that the using the oxide supports inhibits the poisoning effect caused by strongly adsorbed intermediary species. The specific activities of the 5%Pt/ $Ti_{0.9}Me_{0.1}O_2$ catalysts are higher than those of the commercial catalysts 20%PtRu/C (E-TEK). Specific power capacities of alcohol fuel cells in case of using the optimized structures of catalytic active layers (Pt/ $Ti_{0.9}Me_{0.1}O_2$ /«Nafion») as the anode were amount 30-40 mW/cm^2 (1 mg_{Pt}/cm^2). These results can indicate that the catalysts Pt/$Ti_xMe_{1-x}O_2$ are the promising catalytic system which can be applied in direct methanol and ethanol fuel cells.

This work was supported by Ministry of Education and Science of the Russian Federation (State-Contract № 16.740.11.0251).

OR-17

Cluster Approach to Macroscopic Superprotonic Conductivity

A.E. Ukshe, A.V. Pisareva, R.V. Pisarev, Y.A. Dobrovolsky
Institute of Problems of Chemical Physics Russian Academy of Sciences
e-mail: anyuta@icp.ac.ru

It is well-known fact that the proton conductivity of low-temperature superprotonic conductors strongly depends on moisture. This dependence apparently corresponds to the Grotthuss mechanism of proton transport in solids. Indeed, if the oxonium ions H_3O^+ (or $H_5O_2^+$, $H_9O_4^+$) are the charge carriers, increasing the water content will only lead to an increase in the number of carriers and linear increase in conductivity $\sigma = \mu \cdot n$. However, in reality the growth of the conductivity is much faster and closely to exponential manner [1–3]. Moreover, it is known, that even the conductivity of wet fibers exponentially increases with increasing of water content [4]. Obviously, it means that the dependence of proton conductivity on the humidity is not associated with changes in carrier concentration. But in the "box of logical possibilities" one can find only an increase in the number of transport routes other than the number of carriers.

In generalized form the proton conductor can be represented as a structure containing acid residues serving as "proton-generating centers" (hereinafter “p^+-centers”), and water clusters serving as routes for fast proton transport through self-organization in solid or polymer matrix. The results of self-organization correspond to logistic equation with water as limited resource. On the other hand, the dependence of conductivity on the increase of the number of transport routes in heterogeneous environments can be described by the Percolation theory.

The semiquantitative model based on this approach, describing the exponential increase in proton conductivity with water content increasing in the mesostructure, is proposed.

References

1. Y. M. Li and K. Hinokuma, Solid State Ionics **150**, 309 (2002)
2. Y. Ozawa, N. Miura, N. Yamazoe and T. Seiyama, Chem. Lett. **11**, 1741 (1982)
3. A. V. Pisareva R. V. Pisarev and Y. A. Dobrovol’skii, Russ. J. Electrochem. **45**, 693 (2009)
4. E. J. Murphy and A. C. Walker, J. Phys. Chem. **32**, 1761 (1928)

OR-19

Innovative Method of Solar Grade Silicon Production

A. Kalle
Xeron AG , Switzerland
e-mail:alexkalle@aim.com

Solar Grade Silicon SG-Si is becoming today very highly demanded due to the very fast growing market of photovoltaic. Therefore, the creation of a new special technology of solar grade polysilicon feedstock production is of high value. Today, Semiconductor-grade polysilicon is produced with trichlorosilane ($SiHCl_3$) technology. The feed-stock for trichlorosilane is metallurgical-grade silicon, which is the product of reduction of natural quartzite. The trichlorsilane polysilicone production is characterized by high energy consumption and large amounts of wastes, containing environmentally harmful chlorine based compounds. Innovative double step metallurgical refining techniques: EBM (electron beam melting) and Bridgman crystallisation process, are being developed for use by production of SG- Si from metallurgical grade (MG) silicon. By this means, MG silicon that is refined in first step can be used as solar grade (SoG) silicon feedstock for directional solidification in Bridgman process and is qualitative acceptable for photovoltaic applications. The most problematic impurity elements are B and P because of their high segregation coefficients. Electron beam refining processes with evacuation, formation of impurity complexes and oxidation of impurities is effective in removal of impurities from MG silicon. Charge sizes have been scaled up to 80 kg. Impurity analysis of 400 kg charge after refining and Bridgman directional solidification has shown reduction of most impurities to <0,1 ppma B and P to 1ppma level. It has been demonstrated that B and P as well as other impurities can be reduced from MG silicon. Further reduction of impurities is possible; With developed procedures it is possible to reach a larger charge sizes and to use it as technology for SG Si production plant. Therefore, SoG silicon production using these procedures should be at low cost and high efficiency. The first production facility using the above described technology is being built now in Jelgava, Latvia.

OR-20

Electron-beam Refining of UMG-Si for Solar Energetics

G. Chikvaidze[1], V. Zauls[1], K. Kundzins[1], M. Kundzins[1], V. Ogorodniks[1], A. Viksna[2], V. Evteev[3],
N. Zhandayev[4], V. Osokin[5], V. Panibratskiy[5]

[1]Institute of Solid State Physics, University of Latvia

[2]Faculty of Chemistry, University of Latvia

[3]State Pedagogical University of Vinnitsa, Ukraine

[4]Association with the limited liability" Scientific Productive Center "Ulba", Kazakhstan

[5]The State Scientific Research Institute “Helium”, Vinnitsa, Ukraine

e-mail: georgc@cfi.lu.lv

The process of refining and purification of Upgraded Metallurgical Grade Silicon (UMG-Si) with purity of 4N (99,99) by electron-beam remelting was investigated to obtain Solar Grade Silicon. The advantage of starting material (UMG-Si) produced by company «KazSilicon» (Kazakhstan) in comparison with earlier studied [1] materials manufactured by the companies Timminco (Canada), Rimi (Brazil) and Elkem Solar (Norway) has demonstrated.

The advantages of the oxidative refining using electron-beam remelting for the purification of silicon are proved by the result of the study the initial and final products. Analytical technique for investigation of the samples included Mass Spectrometry (ICP-MS), Scanning Electron Microscope (SEM) and Energy- dispersive X-ray spectroscopy (EDS) for the elemental analysis of the samples.

Raman spectra of the final product indicate that when the refining of metallurgical silicon is made using electron-beam vacuum oxidation method, then coagulation of impurities takes place. This allows us to control the distribution of particle impurities in the silicon melt by the choice of method for refining and cooling rate of melt.

Our results indicate that technology of oxidation refining in a vacuum that performed using electron-beam remelting can provide a high-purity silicon with purity of 6N (99,9999) that can be used for solar energetics.

References:

1. **Осокин В.А., Панибрацкий В.А.** Рафинирование металлургического кремния методом электронно-лучевого воздействия в вакууме // Вимірювальна та обчислювальна техніка в технологічних процесах. № 2. 2010. С. 30-41.

OR-21

Hydrogen Sorption Properties of Nanocomposites Mg-RE-Ni and Mg-RE-Ni-C

P.V. Fursikov, D.N. Borisov, B.P. Tarasov

Institute of Problems of Chemical Physics RAS, Russia

e-mail: fpv@icp.ac.ru

Recently we reported [1] that additions of cabon nanomaterials improved the hydrogen sorption performances of composites based on ternary eutectic alloys Mg-La(Mm)-Ni. To elucidate the role of carbonaceous additives in the hydrogen interaction with the composites we studied hydrogen desorption (HD) by hydrided Mg-Mm-Ni alloys and by the hydrided composites Mg-Mm-Ni + 10 mass % of carbon nanofibers. The experimental data were processed using the Avrami-Erofeev equation, which is widely employed, in particular to describe thermal decomposition of hydride phases [2]: $a = 1 - \exp(-(kt)^n)$, where a is the part of desorbed hydrogen (the total amount equals unity), t – time, k is the rate constant, and the exponent n, which relates to the reaction mechanism, may be derived (Fig. 1) from the linear approximation of HD curves in the coordinates $\ln t$ — $\ln(-\ln(1-a))$.

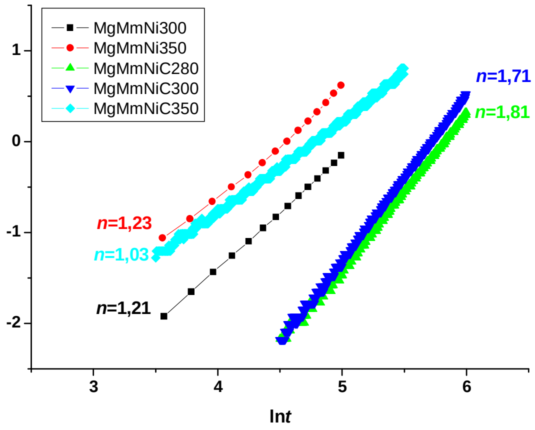

Fig.1 Curves of hydrogen desorption by hydrided materials, Mg-Mm-Ni alloy and its composite Mg-Mm-Ni-C, at various temperatures. The curves are plotted in coordinates, where the term $\ln t$ linearly enters to the Avrami-Erofeev equation

At high (> 300°C) temperatures the n values range within 1.0–1.2, both for hydrided alloys Mg-Mm-Ni and for their composites with carbon nanofibers. At temperatures ≤ 300°C the n values for the composites change significantly (n = 1.7–1.8), while those for the hydrides of Mg-Mm-Ni practically do not.

The carbon additions seem to alter the mechanism of hydrogen desorption from the Mg hydride phase in composites Mg-Mm-Ni-C at low (≤ 300°C) temperatures. The obtained results are discussed.

References

1. D.N. Borisov, P.V. Fursikov, and B.P. Tarasov, Int. J. Hydrogen Energy **36**, 1326 (2011).
2. S. Løken, J. Solberg, J. Maehlen, R. Denys, M. Lototsky, B. Tarasov, and V. Yartys, J. Alloys Comp., **446-447**, 114 (2007).

OR-22

Effects of Temperature on Electron Paramagnetic Resonance of Dangling Oxygen Bonds in Amorphous Silicon Dioxide

L. Skuja[1], K. Kajihara[2], M. Hirano[3], A. Silins[1], H. Hosono[3, 4]
[1]Institute of Solid State Physics, University of Latvia, Latvia
[2]Department of Applied Chemistry, Graduate School of Urban Environmental Sciences, Tokyo Metropolitan University, Japan
[3]Frontier Research Center, Tokyo Institute of Technology, Japan
[4]Materials and Structures Laboratory, Tokyo Institute of Technology
e-mail: skuja@latnet.lv

Amorphous silicon dioxide (a-SiO_2) has numerous properties, useful to modern technologies. One of them is an extremely high optical transparency, ranging from near infrared (optical fibers) to vacuum ultraviolet (UV) (high-power and UV laser optics). Among all known point defects in a-SiO_2, dangling oxygen bonds (usually denoted as non-bridging oxygen hole centers, NBOHC) have the strongest detrimental effect on optical properties. Electron paramagnetic resonance (EPR) has been a key tool for their detection for over 3 decades, and many aspects of NBOHC EPR signal are well-understood [1]. However, one difficulty, important to practical applications still remains: the EPR-based estimates of NBOHC concentration are in many cases not consistent with the intensities of optical bands, in some kinds of a-SiO_2 where „EPR-silent" NBOHCs exist. This problem in part can be attributed to the near orbital degeneracy of the ground state of the defect and disorder in a-SiO_2 network around it.

In the present work we studied temperature dependence of X-band CW NBOHC EPR signal in excimer laser-irradiated synthetic SiO_2 glasses in the range down to liquid He temperatures. It is demonstrated that due to motional efects, temperatures below the routinely used liquid nitrogen temperature are necessary for correct concentration measurements. Concentration estimates, based on these measurements are compared to current estimates of the oscillator strengths of NBOHC optical absorption bands, based on the luminescence decay kinetics. The reasons for existence of "EPR-silent" NBOHCs will be discussed.

References

1. D.L. Griscom, in Defects in SiO_2 and Related Dielectrics: Science and Technology, G. Pacchioni, L. Skuja, and D.L. Griscom, Eds., (Kluwer Academic, The Netherlands, 2000) pp. 117-159.

OR-23

Paramagnetic Impurities for Studies of the Oxyfluoride Glass Ceramics Structure

A. Fedotovs, Dz. Berzins, O. Kiselova, A. Sarakovskis, U. Rogulis
Institute of Solid State Physics, University of Latvia, Latvia
e-mail: andris-f@navigator.lv

Crystallization of the fluoride crystal phases in the oxyfluoride glass ceramics materials could be investigated with electron paramagnetic resonance (EPR) techniques by doping with paramagnetic impurities [1]. Considerable changes in the EPR spectra of impurity ions are observed if they enter in the fluoride crystallites [1, 2].

We investigated the crystalline phases of glass ceramics doped with transition metal impurity ions Mn^{2+}, Fe^{3+} and Cu^{2+} by the X-band EPR techniques. The EPR measurements at 77K showed presence of the probe ions in the crystalline structures of the oxyfluoride glass ceramics samples containing crystallites of CaF_2, BaF_2, LaF_3 and $LiYF_4$.

It is shown that the most suitable impurity for CaF_2 and BaF_2 is Mn^{2+}, while trivalent transition element ion Fe^{3+} - for the more complex fluorides LaF_3, $LiYF_4$. The experimental and theoretical EPR studies of the CaF_2, BaF_2, LaF_3 and $LiYF_4$ crystalline phases in the oxyfluoride glass ceramics doped with paramagnetic impurities will be discussed.

The financial support of ESF project 2009/0202/1DP/1.1.1.2.0/09/APIA/VIAA/141 is greatly acknowledged.

References

1. R.W.A. Franco, J.F. Lima, C.J. Magona, J.P. Donoso and Y. Messaddeq, J. Non-Cryst. Sol. **352**, 3414 (2006)
2. A. Fedotovs, Dz. Berzins, A. Sarakovskis, U. Rogulis and G. Doke, IOP Conf. Ser.: Mater. Sci. Eng. **15**, 012068 (2010)

OR-24

Photoinduced Mass Transport in Soft Materials

J. Teteris, J. Aleksejeva, U. Gertners
Institute of Solid State Physics, University of Latvia, Latvia
e-mail: teteris@latnet.lv

In this report an interaction between laser light beam with high intensity gradient and soft materials (amorphous chalcogenide and organic polymer films) was studied. The single light beam focusing and two beam interference were used for high light intensity gradient formation. Under intensive illumination the formation of relief structures on the surface of amorphous films due to lateral mass transport regarding the light propagation direction has been observed. The possibility to apply this phenomenon in surface nanopatterning of the materials has been discussed.

The amorphous films of chalcogenides (As-S, As-S-Se and As-Se systems) and azo-dye doped organic polymers (PMMA, PVA, PS) were used for studies. The influence of the amorphous film thickness, recording laser wavelength (248 nm, 266 nm, 325 nm, 441.6 nm, 532 nm, and 632.8 nm), grating period, light intensity and polarization state on the relief formation process in amorphous inorganic and organic films was studied. It was shown that the efficiency of the surface-relief formation strongly depends on the recording light polarization state (two *p*-linear, *s*-linear, identical circular or orthogonal circular polarized beams) [1]. We have found that in *s-s* and *p-p* polarized writing conditions, a significant grating modulation enhancement can be achieved if an incoherent assisting light beam with orthogonal polarization is used. The relief grating profile on amorphous films was analyzed by means of atomic force microscope (AFM).

A strong relationship between surface relief grating (SRG) and polarization holographic grating formation was observed and studied. The study of the phase relationship between the exciting light field and the resulting surface deformation is crucial in understanding the mechanism of SRG formation. It was observed that the peak of the SRG on chalcogenide films was formed at the position of p-polarization state in the polarization modulation pattern. The peak formation of the surface relief on organic azobenzene doped polymers was observed at the position of s-polarization state.

The mechanism of the direct recording of surface-relief on amorphous chalcogenide and organic polymer films based on the photo-induced anisotropic plasticity of amorphous films and the optical gradient force induced mass transport has been discussed.

OR-25

Deposition of ZnO:Al Transparent Conductive Layers on Polymer Substrate by Magnetron Sputtering

V. Klykov[1], I. Strazdina[2], V. Kozlov[1]

[1]"Sidrabe" Inc, 17 Krustpils str., Riga, Latvia

[2]Riga Technical University, Latvia

Aluminum doped zinc oxide (ZnO:Al) is an attractive inexpensive material for transparent conductive electrodes and IR reflective coatings. ZnO:Al layers were deposited on 100 μm thick PET (polyethylene terephthalate) film by magnetron sputtering of ZnO/Al_2O_3 2 wt.% planar ceramic target (225x100) mm^2 in Ar/H_2 atmosphere under $(1–5)\cdot10^{-3}$ Torr pressure in the vacuum chamber. RF (13.56 MHz) and DC power sources were used separately. The PET film was fixed on a rotated water-cooled drum. The substrate surface was cleaned by an ion gun before ZnO deposition.

The investigation shows that properties of ZnO layers depend mainly on the type of power source, power levels applied to the target and concentration of hydrogen in the gas mixture.

ZnO layers must be structured in order to get maximum conductivity. When depositing zinc oxide on glass [1] this goal is achieved both by heating the substrate and by increasing sputtering power. Contrariwise, during the deposition of ZnO layers on the polymer film we observed the opposite trend. For both types of the sources resistivity of ZnO layers decreased while reducing sputtering power until it reached a certain limit. Optimum levels of power were 200 W for RF-source and 100 W for DC-source. Unbalancing of the magnetron allowed additional reducing of ZnO resistivity while working in the optimum range of the power level. A further decrease of power did not lead to resistivity decreasing.

Adding H_2 to the gas mixture initially caused a relatively rapid decrease of resistivity of ZnO layers. The optimum concentrations of hydrogen were about 1 vol. % and (10-12) vol. % for the RF- and DC-sources respectively. Further increasing of hydrogen content led to slow raise of resistivity. It is known [2] that hydrogen incorporated into ZnO can act as a donor. The fact that the optimum concentration of H_2 is much lower when the RF-source is used could probably serve as indirect evidence that in this case the crystal structure of ZnO layers is more perfect.

As a result ZnO layers on the PET film of conductivity 7×10^{-4} Ω.cm (RF-source) and 1.3×10^{-3} Ω.cm (DC-source) were obtained. The best samples have optical transmittance (82-83)% for λ (360-600) nm and ZnO thickness (350-400) nm. The layers are crack-free and have good adhesion to the substrate.

References

1. O.Graw, U.Schreiber. Transparent conductive zinc oxide film and production method thereof, EP 2180529 A1, 2010
2. C. van de Walle. Hydrogen as a cause of doping in ZnO, Am.Phys.Soc., Ann. March Meeting, March 12-16, 2001, abstr.#c5.004

OR-26

NanoCones Formation on a Surface of CdZnTe by Laser Radiation: Exciton Quantum Confinement Effect

A. Medvid[1], A. Mychko[1], Y. Naseka[2]
[1]Riga Technical University, LV 1048, Riga, Azenes Str.12, Latvia
[2]Institute of Semiconductor Physics, Ukraine
e-mail: mychko@latnet.lv

Nanocones formation on a surface of $Cd_xZn_{1-x}Te$ solid solution with x = 0.1 after irradiation by strongly absorbed Nd:YAG laser radiation (LR) with intensity I = 10.0 MW/cm^2 was observed. Studying of the nanocones optical properties using the low temperature 5 K photoluminescence (PL) method a new exciton band at energy up to 1.872 eV and at the same time, shift of A^0X and D^0X exciton bands on 2.5 meV toward the higher energy of quantum, the so-called “blue shift” for the first time were observed. Appearance of a new PL band and “blue shift” of the exciton bands are explained by Exciton quantum confinement (EQC) effect in nanocones and mechanical compressive stress of CdTe top layer formed on the irradiated surface of the solid solution, correspondingly. Appearance of the nanocones leads to rise of a new band in PL spectrum of the structure and decrease of A^0X and D^0X exciton bands “blue shift” in PL spectrum. Reconstruction of this band shows that it consists of three lines which look like A^0X, D^0X and A^0X–LO lines (the distance between the lines and their width FWHM are the same) in non irradiated PL spectrum of the semiconductor. Therefore, we connect the appearance of both the new band in PL spectrum and nanocones formation on the irradiated surface of the semiconductor with EQC in nanocones and denote them as A^0XQC and D^0XQC lines. Calculation of quantum dot diameter using formula from paper [1] and shift of PL spectrum on 0.23 eV gives diameter of the quantum dots up to 10.0 nm. This data corresponds to the size of nanocones: height and diameter of cones bottom are 10.0 nm, measured using 3D image of AFM. An evidence of the EQC nature of the new band is decreasing of LO phonon energy on 0.7 meV that is the so-called Phonon quantum confinement effect [2].

References

1. Y.Kayanuma, *Phys.Rev.* B 38 (1988) 9797.
2. H. Campbell and P.M. Fauchet. *Solid State Commun.* **58** (1986) 739.

OR-27

Phonon Calculations in Perfect and Defective $SrTiO_3$ Perovskites

E. Blokhin[1], D. Gryaznov[1, 2], E. Kotomin[1, 2], R. Evarestov[3], J. Maier[1]

[1]Max-Planck Institute for Solid State Research, Stuttgart, Germany

[2]Institute for Solid State Physics, University of Latvia, Riga, Latvia

[3]Department of Quantum Chemistry, St. Petersburg State University, Peterhof, Russia

e-mail: e.blokhin@fkf.mpg.de

$SrTiO_3$ perovskite is an excellent model of mixed electronic-ionic conductor [1]. In the present study the hybrid Hartree-Fock – density functional theory simulations of perfect and defective $SrTiO_3$ crystals are performed using CRYSTAL06 [2] computer code within the method of linear combination of atomic orbitals. The calculations of atomic vibrations (phonons) are of great importance as they provide the key to describe thermodynamic properties within *ab-initio* framework. The direct frozen-phonon method [3] is used for phonon calculations. The concurrent character of two known soft phonon modes in perfect $SrTiO_3$ cubic crystal was illustrated. The detailed calculations of phonon frequencies in the tetragonal phase have been performed. Lastly, the experimental temperature dependence of the $SrTiO_3$ heat capacity was successfully reproduced [4].

Based on the experience for defect-free crystal, the same computational approach was applied for further thermodynamic study of $SrTiO_3$ with oxygen vacancies under finite temperatures. The defects are examined at different concentrations in neutral charge state with an emphasis on atomic geometry, electronic structure and vibrational properties. Incorporation of oxygen vacancy does not affect significantly the band gap of the crystal and induces the local state in the band gap. The atomic relaxation around the defect is shown to be relatively small. The corresponding phonon spectra are obtained and spectra changes due to point defects are analyzed. The comparison of free energy and heat capacity for defect-free and defective crystals is presented.

References

1. R. Merkle and J. Maier, *Angew. Chem. Int. Ed.* 2008, 47, 3874
2. R. Dovesi, et al., CRYSTAL06 User's Manual, University of Torino, Torino, 2006
3. K. Parlinski, Z. Li, Y. Kawazoe, *Phys. Rev. Lett.* 1997, 78, 4063
4. R. Evarestov, E. Blokhin, D. Gryaznov, E. Kotomin, J. Maier, *Phys. Rev. B.* 2011, in press

OR-28

LCAO Calculations of $SrTiO_3$ Nanotubes

A. Bandura, R. Evarestov, A. Oranskaya
Department of Quantum Chemistry, St. Petersburg State University, Russia
e-mail: andrei@ab1955.spb.edu

The $SrTiO_3$ nanotubes (NT) have been obtained recently with low-temperature hydrochemical method [1]. They have a cubic perovskite structure with the unit cell parameter slightly smaller than the lattice constant of the corresponding cubic bulk phase. Such materials have a potential application as nanosized ferroelectrics and memory elements. In this work the large-scale first-principles simulation of the structure and stability of $SrTiO_3$ nanotubes is performed for the first time. All calculations have been made using the periodic PBE0 LCAO method via CRYSTAL-2009 [2] computer code.

The initial structures of the nanotubes have been obtained by the rolling up of the stoichiometric $SrTiO_3$ slabs consisting of two or four alternating (001) SrO and TiO_2 atomic planes. The initial slab symmetry is described by square plane lattice and layer group P4*mm*. Nanotubes with chiralities (*n*,0) and (*n*,*n*) have been studied. The line group families for considered NT initial structures are 11 (L*n*/*mmm*) and 13 ($L(2n)_n/mcm$), correspondingly. Two different NT can be constructed for each chirality: (*oti*) with TiO_2 outer shell, and (*osr*) with SrO outer shell; the inner shell has alternate composition for the adopted even number of planes in the slab.

Positions of all atoms have been optimized to obtain the most stable NT structure with preserving the rototranslational symmetry only. In the most of considered cases the inner or outer TiO_2 shells of NT undergo a considerable reconstruction due to shrinkage or stretching of interatomic distances in the initial cubic perovskite structure. There were found two types of surface reconstruction: (1) breaking of Ti–O bonds with creating of Ti=O titanyl groups in outer surface; (2) inner surface folding due to Ti–O–Ti bending. Based on formation and strain energy calculations the largest stability was found for *oti*-(*n*,0) NTs.

The authors are grateful for the support of Saint Petersburg State University grant 12.37.142.2011 for fundamental research.

References

1. Y. Mao, S. Banerjee, S. S. Wong, Chem. Comm., 2003, 408.
2. R. Dovesi, et al., CRYSTAL09 User's Manual, University of Torino, Torino, 2010.

OR-29

Ab initio Calculations of $SrTiO_3$, $BaTiO_3$, $PbTiO_3$, $CaTiO_3$, $BaZrO_3$, $SrZrO_3$ and $PbZrO_3$ (001) and (011) Surfaces As Well As Nb Impurity Segregation towards the $SrTiO_3$ Surface

R. I. Eglitis
Institute of Solid State Physics, University of Latvia, Latvia
e-mail: reglitis@yahoo.com

While the (001) surfaces of ABO_3 perovskites, such as $SrTiO_3$, $BaTiO_3$, $PbTiO_3$, $CaTiO_3$, $SrZrO_3$, $PbZrO_3$ and $BaZrO_3$ have been extensively studied [1-5], much less is known about the (011) surfaces. On the (001) surfaces, I consider both AO (A=Sr, Ba, Pb or Ca) and BO_2 (B=Ti or Zr) terminations. The (001) surface AO layer is found to relax inward for all seven materials with the sole exception of SrO-terminated $SrTiO_3$ (001) surface first layer O atom.

My calculated surface rumplings of 6.77 % for the SrO-terminated $SrZrO_3$ (001) and 3.32 % for the PbO-terminated $PbZrO_3$ (001) surfaces are almost ten times larger than those of the corresponding ZrO_2-terminated $SrZrO_3$ and $PbZrO_3$ (001) surfaces [5].

As for the (011) surfaces, I consider three types of surfaces, terminating on a BO layer, A layer and O layer. Turning now to the surface energies, I find that both the AO and BO_2-terminated (001) surfaces are about equally energetically favorable and may co-exist. In contrast, I see very large differences in the surface energies on the ABO_3 (011) surfaces. I demonstrate that Nb is a shallow donor in $SrTiO_3$ and discuss also its segregation towards the $SrTiO_3$ surface [6].

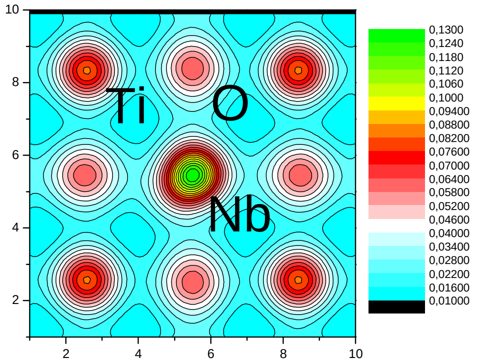

Fig. 1 Total charge density map for Nb doped $SrTiO_3$ calculated by means of hybrid B3PW method.

References

1. R. I. Eglitis, J. Phys.: Condens. Matter **19**, 356004 (2007).
2. R. I. Eglitis and D. Vanderbilt, Phys. Rev. B **76**, 155439 (2007).
3. R. I. Eglitis and D. Vanderbilt, Phys. Rev. B **77**, 195408 (2008).
4. R. I. Eglitis and D. Vanderbilt, Phys. Rev. B **78**, 155420 (2008).
5. R. I. Eglitis and M. Rohlfing, J. Phys.: Condens. Matter **22**, 415901 (2010).
6. R. I. Eglitis and E. A. Kotomin, Physica B **405**, 3164 (2010).

OR-30

Ab Initio Calculations of Electronic, Optical, Elastic Properties and Microscopic Treatment of Crystal Field Effects for Some Cubic Crystals

M.G. Brik, I. Sildos, C.-G. Ma, V. Kiisk
Institute of Physics, University of Tartu, Estonia
e-mail: brik@fi.tartu.ee

In the present paper we give a review of the recently obtained results on *ab initio* calculations of the structural, electronic, optical and elastic properties of several cubic crystals. The considered examples are: Cs_2SiF_6 and Cs_2GeF_6 [1], $Y_2Ti_2O_7$ and $Y_2Sn_2O_7$ [2], Rb_2CrF_6 [3]. Special attention has been paid to the properties of chemical bonds between atoms and effects of hydrostatic pressure on the band structure and interionic distances.

Using an original approach developed in Ref. [4], the microscopic crystal field effects for Cr^{4+} in Rb_2CrF_6 were considered in details. Analyzing pressure dependence of the chromium 3d electrons' density of states, we succeeded in getting analytical dependences of the crystal field strength 10*Dq* [5] on pressure and Cr – F distance (Fig. 1).

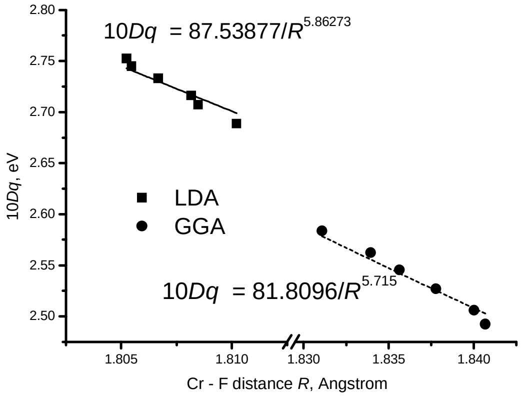

Fig.1. Dependence of the crystal field strength 10*Dq* on Cr – F distance in Rb_2CrF_6. In all equations *R* is the Cr – F distance in Å and the calculated result is the 10*Dq* value in cm^{-1}.

All obtained results were compared with available experimental data; good agreement between the calculated and experimental results confirms validity of the performed calculations. The presented analysis can be readily extended for applications to other hosts.

References

1. M.G. Brik, Solid State Commun. **150**, 1529 (2010)
2. A.M. Srivastava, M.G. Brik, J. Lumin. **130,** 2368 (2010)
3. M.G. Brik, N.M. Avram (in preparation)
4. M.G. Brik, I. Sildos, V. Kiisk, J. Lumin. (in press, doi:10.1016/j.jlumin.2010.09.024)
5. S. Sugano, Y. Tanabe, H. Kamimura, Multiplets of Transition-Metal Ions in Crystals (Academic Press, New York, 1970).

OR-31

Theoretical Simulations of Fundamental Properties of CNT-Me and GRN-Me Interconnects for Novel Electronic Nanodevices

Yu.N. Shunin[1, 2], Yu.F. Zhukovskii[2], N. Burlutskaya[1], V.I. Gopeyenko[1], S. Bellucci[3]
[1]Information Systems Management Institute, Riga, Latvia
[2]Institute of Solid State Physics, University of Latvia, Riga, Latvia
[3]INFN - Laboratori Nazionali di Frascati, Frascati (Rome), Italy
e-mail: shunin@isma.lv

Unique physical properties, especially due to a ballistic (without losses) mechanism of conductivity, carbon nanotubes (CNTs) and graphene nanoribbons (GNRs) attract permanently growing technological interest, for example, as promising candidates for nanointerconnects in a high-speed electronics. However, formation of either CNT-Me or GRN-Me contacts is technologically different. For CNT-Me interconnects, this can be provided by a catalytic growth procedure [1]. At the same time, full integration of graphene into conventional device circuitry would require a reproducible large scale graphene synthesis that is compatible with conventional thin film technology.

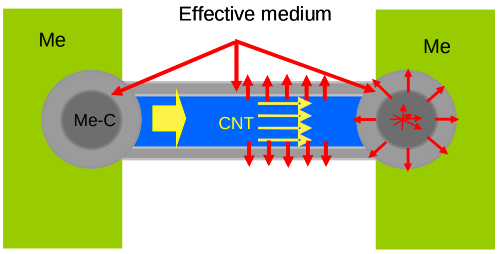

Fig. 1. Model of CNT-Me interconnect as a prototype of nanodevice.

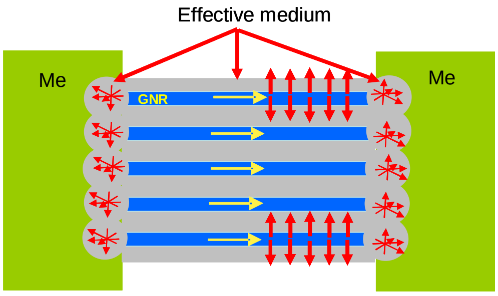

Fig. 2. Model of multilayered GNR-Me interconnect as a prototype of nanodevice.

Theoretical simulations of essential fundamental properties (electronic, electric, mechanical, magnetic, temperature, frequency) of interconnect are actual as both in time of formation of C-Me contacts formation and exploitation in the framework of possible electronic nanodevices [2]. Results of presented theoretical simulations are discussed from the point of technological priorities of a wide class of C-Me contacts (Me: Ni, Cu, Ag, Au, Pd, Pt).

References

1. Yu.N. Shunin, Yu.F. Zhukovskii, N. Burlutskaya, S. Bellucci. Central European Journal of Physics (2011), DOI: 10.2478/s11534-010-0086-9.
2. Yu.N. Shunin, In: *GENNESYS White Paper*. Eds. H. Dosch and M.H. Van de Voorde, Max-Planck-Institut für Metallforschung, Stuttgart, Ch.2, 8-29 (2009)

OR-32

Carbon-Ceramic Composites Based on Alumina and Carbon Nanotubes

A.A. Volodin, B.P. Tarasov
Institute of Problems of Chemical Physics of RAS, Russia
e-mail: alexvol@icp.ac.ru

Due to high electric and thermal conductivity, chemical and thermal stability, as well as high mechanical strength, carbon nanotubes may be used for reinforcement of ceramics in order to enhance their hardness, fracture strength, wear resistance, and electric conductivity [1-2]. We have elaborated the manufacturing schemes for synthesis of composites with carbon nanotubes and ceramic matrices. The schemes are based on hot-pressure treatment of initial mixtures that may be prepared by two methods: growing nanotubes in the volume of ceramic powder and mixing nanotubes and the powder in an ultrasonic bath. The elaborated schemes allow us to obtain samples of various composition suitable for mechanical attestation, investigation of microstructure, and measuring electric and thermal conductivity. Our investigations of the microstructure of the composites have show that growing carbon nanotubes in the volume of ceramic powder leads to rather uniform nanotubes, enabling their percolation, and therefore high transport properties of the composites (Fig.1).

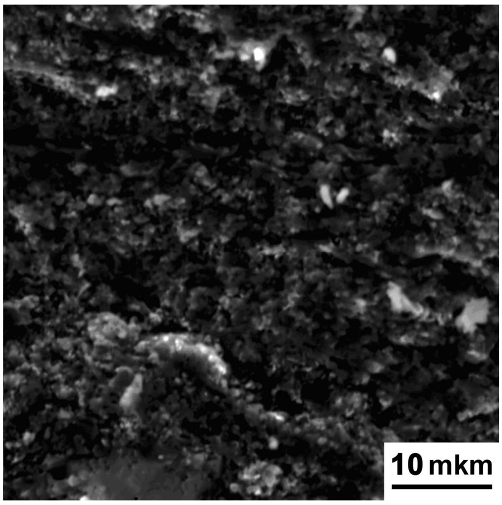

Fig.1 SEM image of CNT/Al_2O_3 (1% mass), prepared by the hot-pressure at 1500ºC and 40 MPa.

The composites prepared via the alternative manufacturing scheme, i.e. by mixing the nanotubes and the powders in an ultrasonic bath, contain rather isolated conglomerates of nanotubes that seem to not have expecting transport properties. We anticipate that variation of the manufacturing scheme would improve the transport properties. For example, we found the growth of grains of the ceramic matrices with increasing the temperature of hot-pressure treatment. In the areas containing the conglomerates of carbon nanotubes we observed inhibition of recrystallization of the matrix grains.

References

1. J. Lee, Sh. Mahendra, P.J.J. Alvarez, ACS Nano, **4**, 3580 (2010)
2. A. K. Keshri, J. Huang, V. Singh, W. Choi, S. Seal, A. Agarwal, Carbon, **48**, 431 (2010)

OR-33

Nano Structure of Lead-Germanate Glasses and Their Melts

V. Bogdanov[1], A. Anan'ev[2], V. Golubkov[3], L. Maksimov[2]

[1]Saint Petersburg State University, Russia

[2]Research and Technological Institute of Optical Material Science, Russia

[3]Silicate Chemistry Institute, Russia

e-mail: v.n.bogdanov@mail.ru

At present PbO-GeO_2 glasses attract attention of glass scientists and photonic device designers because of their properties which were found valuable for modern applications in information transmitting and processing systems. [1] The paper is aimed at investigation of nanoscaled fluctuation inhomogeneities of PbO-GeO_2 glasses. The glasses were studied by Rayleigh and Mandel'shtam-Brillouin scattering (RMBS) spectroscopy that resulted in glass composition dependences of Landau-Placzek ratio reflecting the ratio of contributions of “frozen-in” and equilibrium fluctuations into Rayleigh scattering (RS) by glasses. Temperature and frequency dependences of ultrasonic velocity in the glass melts allowed to independently estimate contributions from “frozen-in density and concentration fluctuations into RS intensity by the Macedo-Schroeder formulation [2]. The small-angle X ray (SAXS) scattering was used to estimate average dimensions of light scattering centers. Analysis of RMBS data for glasses and ultrasonic data for glass melts evidenced that chemical inhomogeneity, that is “frozen-in” concentration fluctuations, dominated in Rayleigh scattering by the glasses. Similarity of glass composition dependences of Landau-Placzek ratio, Rayleigh scattering and SAXS intensities with the maximum in PbO 5-20 mol.% range showed that the dimensions of light scattering fluctuation inhomogeneities in glasses were on the nanometer scale. The latter corresponds with the results for glass forming oxides [3]

PbO activities of PbO-GeO_2 melts were determined from electrochemical data and used for independent calculations of concentration fluctuations contribution into light and X-ray scattering. It was found that the glass melt composition dependence of calculated concentration fluctuations correlated with the data of RMBS and SAXS obtained for the glasses. Therefore, the latter confirms that a glass inherits its fluctuation nanostructure of a melt.

The study was partially supported by RFBR (Grant # 10-03-00323).

References

1. A. Cereyon, B.Champagnon, V.Martinez, L.Maksimov, O.Yanush, V.Bogdanov. Optical Materials 28, 1301 (2006)
2. J. Schroeder, Light Scattering of Glass. Treatise on Material Science and Technology, 12, Glass 1, − New York, N. Y. Academic Press (1977)
3. I.Zh. Bus'ko, V.V.Golubkov. Glass Physics and Chemistry, 29, No. 5, 438 (2003)

OR-34

Fabrication of Ultrathin Anodized Aluminum Membranes for Deposition of Nanodot Arrays

R. Poplausks[1], V. Rutkovskis[1], I. Apsite[1], I. Pastare[1], F. Lombardi[2], D. Erts[1]

[1]Institute of Chemical Physics, University of Latvia

[2]Chalmers University of technology, Goteborg, Sweden

e-mail: donats.erts@lu.lv

Quantum dot (QD) formation technology is an important step in development of nanometer size devices. QD arrays have perspective for novel sensor development and applications in electronic circuits. One of the nanosize particle production technique is use of porous ultra thin anodized aluminum oxide (AAO) template (mask) through witch material is evaporated and deposited to form arrays of 50-80 nm diameter nanoparticles on a substrate [1,2]. AAO layer preparation is a controllable process, which results in a highly ordered nanoporous structure with pore diameter range 10 – 400 nm and density ~10^{11} pores/cm^2.

The aim of this work is fabrication of ultra thin AAO masks for production of QDs. Typically AAO nanoparticles are deposited through masks with thickness of 200-700 nm and pore diameter 60-100 nm. However, deposition of quantum dots with diameter below 20 nm requires thinner masks. A two step anodization process of aluminum surface in a sulphuric acid was adapted for production of AAO membranes with thickness below 200 nm and pore diameters 10-30 nm using DC voltage of 10 - 24 V. After AAO formation on aluminum surface the next step is removal of aluminum substrate and opening of barrier layer without breaking the membrane mechanically. Aluminium was removed with mercury (II) chloride and barrier layer was removed by chemical method. Obtained ultra thin AAO membranes and nanodot arrays on the surface were analyzed with Scanning Electron Microscope. Chromium nanodot arrays with particle size below 20 nm were created on the surface by ion evaporation.

References:

1. Ding G. Q., Zheng M. J, Xu W. L. Shen W. Z., *Nanotechnology,* 2005, Vol. 16 , 1285–1289

2. Woo L., Hee H., Lotnyki A., Schubert M., Hesse D., Baik S., Gosele U., *Nature Nanotechnology,* 2008, Vol. 3 402-407.

OR-35

Application of Individual Semiconductor Nanowires in Gateless Bistable Nanoelectromechanical Switch

R. Meija[1], J. Andzane[1], J. Prikulis[1], L. Jasulaneca[1], J.D. Holmes[2], D.Erts[1]
[1]Institute of Chemical Physics, University of Latvia, Latvia
[2]Department of Chemistry, University College Cork, Ireland
e-mail: Raimonds.Meija@lu.lv

Nanoelectromechanical systems (NEMS) are a rapidly growing area of research with considerable potential for future applications. The basic idea underlying NEMS is the strong electromechanical coupling in devices on the nanometer scale in which the Coulomb forces associated with device operation are comparable with the chemical binding forces. Nanowires are excellent candidates for NEMS devices because of their well-characterized chemical and physical structures, low mass and dimensions and range of electronic properties. Nanowire-based NEMS potentially have internal operating frequencies above 10^{10} Hz range and may reach extremely high integration level, approaching 10^{12} elements per cm^2 (Rueckes et al. 2000), which makes them suitable for a number of applications.

Recently, two-terminal (gateless) nanowire-based NEMS device prototypes have been demonstrated, e.g., a germanium nanowire based nanoelectromechanical programmable read-only memory (NEMPROM) was reported by Ziegler et al. (2004). The NEMPROM device could be switched OFF by mechanical motion or by heating the device above the stability limit to overcome the van der Waals attractive forces. Two-terminal bistable devices, having both ON and OFF regimes, were also reported. C.-H. Ke and H.D. Espinosa presented a feedback controlled nanocantilever device based on carbon nanotubes (2004). Our group demonstrated two-terminal devices based on individual free standing Ge nanowires (J.Andzane et al.2009) and $Mo_6S_3I_6$ nanowire bundles (2010) using an *in situ* TEM-STM technique. In this work we present an *in situ* SEM investigation of the operational conditions of a mechanically stable gateless nanoelectromechanical switch using Ge nanowires as the active components.

In contrast to the two-terminal ON/OFF devices reported before, which were working due to large elastic force of the nanowire and were very dependent on distance between the counter electrode and the nanowire, the gateless bistable device in this case achieves OFF switching by controlled reduction of adhesion/friction force in the nanowire-electrode contact place. Different methods of the adhesion force reduction were investigated and compared.

OR-36

Measurements of Static and Kinetic Friction of ZnO Nanowires on a Flat Surface

L.M. Dorogin[1], B. Polyakov[1, 2], A. Petruhins[2], A. Lõhmus[1], A.E. Romanov[1, 3], I. Kink[1], R. Lõhmus[1]
[1]Institute of Physics, University of Tartu, Estonia
[2]Institute of Solid State Physics, University of Latvia, Latvia
[3]Ioffe Physical Technical Institute, RAS, Russia
e-mail: dorogin@ut.ee

A nanowire (NW) lying on a flat surface (substrate) and being held in bent state by friction forces is experimentally and theoretically investigated. Zinc oxide NWs on highly oriented pyrolytic graphite (HOPG) and oxidized silicon wafer are used in the experiment inside a scanning electron microscope (SEM). A model based on the elastic beam theory for interpretation of the elastic deformation of NWs is proposed. Calculation of distributed friction force along the NW's length from experimentally obtained bending profile is demonstrated.

Two main cases are considered: a) NW is statically fixed by friction force on the surface; b) NW is being loaded by a constant force at its midpoint and dragged over the surface. In the first case a SEM image of a NW is being analyzed and distributed static friction force is calculated. In the second case a nanomanipulation device as an actuator and an atomic force microscope (AFM) tip attached to it as a probe are used in order to push and drag the NW at its midpoint. Kinetic friction force between the NW and the substrate is then found from the shape of the NW during the manipulation.

References

1. M. Bordag, A. Ribayrol, G. Conache, L. Fröberg, S. Gray, L. Samuelson, L. Montelius and H. Pettersson, Small **3**, 1398 (2007)
2. G. Conache, S. Gray, A. Ribayrol, L. Froberg, L. Samuelson, H. Pettersson and K. Montelius, Small **5**, 203 (2009)

OR-38

Structure and Electrical Properties of Styrene Acrylonitrile Copolymer Nanocomposites

J. Zicans[1], R. Merijs Meri[1], T. Ivanova[1], J. Bitenieks[1], M. Knite[2]
[1]Institute of Polymer Materials, Riga Technical University, Latvia
[2]Institute of Technical Physics, Riga Technical University, Latvia
e-mail: zicans@ktf.rtu.lv

In this research physicomechanical and electrical properties of styrene acrylonitrile copolymer (SAN) modified with additions of *Bayer C 150 P* multi-walled carbon nanotubes (CNT) are investigated.

To obtain test specimens, CNT were first dispersed in distilled water by using an ultrasonic generator. The resulting dispersion was subjected to intensive mixing with the corresponding amount of SAN water suspension. Then the prepared mixture was cast in Teflon dishes and dried at ambient temperature. By changing the ratio of the amount of mixed components, specimens with different CNT content (W_f), varying from 0 to 2 wt. %, were obtained.

Results of tensile stress-strain properties of the nanocomposites (Fig. 1) let us conclude that introduction of small (to 0.5%) amount of CNT causes dramatic growth of σ_Y and E modulus. At higher CNT contents the increase of the elastic modulus and the yield point slows down. Stress at break σ_B varies nonmonotonically, however, these changes are not so significant. The effect of CNT content on ultimate elongation is more pronounced. Thus ultimate elongation ε_B of the nanocomposite with W_f = 2% of CNTs is 3 times lower than that of unfilled SAN.

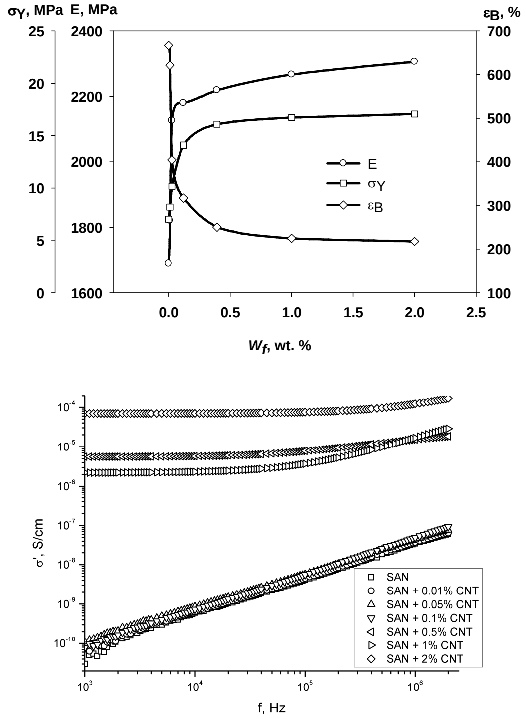

Fig.1. Tensile elastic modulus *E*, stress at yield σ_Y, strain at break ε_B, AC conductivity σ' of SAN/CNT composites as functions of CNT weight content W_f.

The effect of CNT on AC conductivity and permittivity of the nanocomposites is shown in Fig. 1. As one can see considerable increase of these characteristics is observed above CNT content of 0.5 wt. %.

OR-39

Coupling X-ray Spectroscopy and Scanning Probe Microscopy for Simultaneous Sample Topography and Chemical mapping

M. Dehlinger[1], C. Fauquet[1], F. Jandard[1], J. Purans[2], D. Pailharey[3], S. Ferrero[3], B. Dahmani[4],
A. Bjeoumikhov[5], I. Zizak[6], A. Erko[6], D. Tonneau[1]
[1]Centre Interdisciplinaire de NAnosciences de Marseille, Université de la méditerranée, France
[2]Institute of Solid State Physics, University of Latvia, Latvia
[3]Cie Axess Tech, Saint Cannat, France
[4]Cie Lovalite, Besançon, France
[5]IFG-GmbH, Berlin, Germany
[6]HZB-BESSY, Berlin, Germany
e-mail: fauquet@cinam.univ-mrs.fr

Scanning Probe Microscopies (Scanning Tunnelling Microscopes (STM), Atomic Force Microscopes (AFM), Shear Force Microscopes (SFM)…) are powerful tools for surface topography analysis at high lateral resolution. However, these equipments cannot provide a priori chemical mapping of the analysed surface. X-Ray Spectroscopy is a fine surface analysis technique allowing to define chemical and structural properties of a material. The lateral resolution for chemical mapping is limited by the X-ray primary beam focusing optics in the range of 20-50 nm for soft X-rays (<4 keV) and 100-1000 nm for hard X-rays (>4 keV). However, in these experiments it is not possible to simultaneously acquire the sample topography and thus it is not possible to perform a spectroscopy on a given micro- or nano-object somewhere on the surface.

We have designed and fabricated a Shear Force Microscope head allowing to obtain simultaneously with the same apparatus and in ambient conditions, the sample topography and chemical mapping by XRF or XAFS-XEOL [1, 2]. In the former case, a sharp optical fibre is used as shear force probe for sample topography and for simultaneous collection of the visible luminescence under focused X-ray excitation (resolution 50 to 100 nm for both topography and chemical analysis). In the latter configuration, an X-ray capillary replaces the optical fibre to collect the X-ray sample fluorescence (resolution of 100 nm expected).

References

1. M. Dehlinger et al., Small, to be published (2011).
2. C. Fauquet et al., Nanoscale Research Letters, accepted for publication (2011).

OR-40

Structural, Dielectric and Optical Characterization of $BaMoO_4$ Nano powder Synthesized through an Auto-Igniting Combustion Technique

J.K. Thomas, S. Vidya, K. Joy, S. Solomon
Electronic Materials Research Laboratory, Department of Physics, Mar Ivanios College, Thiruvananthapuram- 695 015,
Kerala, India
e-mail: jkthomasemrl@yahoo.com

Scheelite-structured compounds belonging to the molybdate family possess interesting structural features and attractive luminescence properties [1, 2].In this paper we report for the first time, the synthesis of phase pure nanocrystalline scheelite-type BaMoO4 which is an LTCC semiconducting material, using an auto-igniting combustion of a precursor solution containing metal ions, oxidant, and a fuel with citric acid as complexing agent and Urea as fuel. The XRD pattern of as prepared nano powder of particle size 20 nm, shows tetragonal structure. The DTA/TGA curve shows sample is thermally stable with minimum weight loss. The optical band gap determined from the UV-Vis absorption spectra is 3.20eV indicate that the material is a wide band semiconductor. The photo luminescent spectra shows a broad green emission band along with a small peak at red region The nano powder is pelletized and sintered at 750^{o}C up to 95% density. The surface morphology of the sample examined using SEM indicates the sample posses minimum porosity. The dielectric constant and loss factor of the sample at 1 MHz is found to be 9.75 and 1.38×10^{-2}.Thus $BaMoO_4$ an LTCC material with high thermal stability, good dielectric properties and excellent optical character could be synthesized as nanopowder in single step combustion and further sintered relatively at a very low temperature of 750^{o}C.

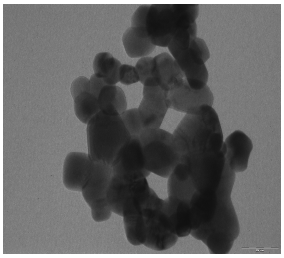

Fig 1. TEM Micrograph of $BaMoO_4$

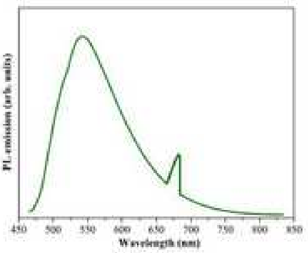

Fig 2. Photoluminiscent spectra of $BaMoO_4$

References

1. Ryu J H, Yoon J W, Lim CS, Shim KB. Mater Res Bull 40, 468 (2005)
2. P. Yang, G.Q. Yao, J.H. Lin, Inorg. Chem. Commun. 7, 389 (2004).

OR-41

Two-Stage Mechanism of Nano-Cones Formation by Laser Radiation on a Surface of Elementary Semiconductors and Semiconductor Solid Solutions

A. Medvid, P. Onufrijevs, A. Mychko

Research Laboratory of Semiconductor Physics, Riga Technical University, Riga, 14 Azenes Str., LV-1048, Latvia

e-mail: onufrijevs@latnet.lv

The basic model used today for description of laser radiation (LR) effects in semiconductors is the thermal model, at least for laser pulse duration till picoseconds [1]. It implies that energy of light is transformed into thermal energy. But it is only the first step in the understanding of this process. So, irradiation of a semiconductor by LR can lead to different results, but sometimes even to opposite results.

Experimental results on investigation of the mechanism of nano-cones formation on the irradiated surface of $Si_{1-x}Ge_x$ and $Cd_{1-x}Zn_xTe$ solid solutions have shown that this process is characterized by two stages – Laser Redistribution of Atoms (LRA) and Selective Laser Annealing (SLA).

At the first stage of the process, - LRA - formation of hetero-structures takes place, such as: Ge/Si due to Ge and Si atoms separation in $Si_{1-x}Ge_x$ sample and $CdTe/Cd_{1-x1}Zn_{x1}Te$ in $Cd_{1-x0}Zn_{x0}Te$ (x1>x0) solid solutions due to separation of Cd and Zn atoms in gradient of temperature takes place. LRA is non linear optical effect: concentration of the redistributed atoms (Ge in the case of GeSi and Cd in the case of CdZnTe) increase with number of laser pulses and in the same time- increase absorption coefficient of the formed top layer.

At the second stage, SLA - formation of nanocones on the irradiated surface of a semiconductor takes place by mechanical plastic deformation of the top layer due to relaxation of the mechanical compressive stress arising between these layers due to mismatch of their crystal lattices and mostly heating of the top layer. SLA occurs due to higher absorption of the laser radiation by the top layer than layer under it.

The evidences of these stages will be presented by experimental investigation of $Si_{1-x}Ge_x$ and $Cd_{1-x}Zn_xTe$ solid solutions irradiated by laser radiation using following methods: microhardness, photoluminescence, Raman back scattering and atomic force microscopy.

References

1. D.K. Biegelsen, G.A. Rozgonyi and C.V. Shank, Energy Beam-Solid Interactions and Transient Thermal Processing, **35** (Pittsburgh:Mater.Res.Soc., (1985).

OR-42

Self-Enhancement of Scalar and Vector Holographic Gratings in Azobenzene Molecular Glassy Films

A. Ozols, V. Kokars, P. Augustovs, Dm. Malinovskis, K. Traskovskis, E. Zarins
Faculty of Material Science and Applied Chemistry, Riga Technical University, Azenes iela 14/24, LV-1007, Riga, Latvia
e-mail: aozols@latnet.lv

Organic materials, especially azobenzene compounds, are of a wide interest for applications in holography and nonlinear optics because they enable much easier tailoring of their properties than inorganic ones [1]. In this paper, we have studied self-enhancement (SE) possibility of vector and scalar holographic gratings (HG) in azobenzene molecular glassy films produced in our Faculty. SE of vector gratings has not been studied until now, as far as we know. However, it can have practical importance as an alternative method of hologram recording.[2,3].SE properties in reflection mode also are studied for the first time.

SE of a nonstationary hologram is the increase in its diffraction efficiency (DE) over time under the stimulus of a single beam light irradiation or simply in the dark [2,3,]. We have experimentally studied SE in transmission and reflection mode at 532 and 633 nm for *p-p* and *s-p* linear recording beam polarizations. DE increase up to 42 times was achieved for *p-p* HG in the sample **8a** , and up to 4.3 times for vector *s-p* HG in the sample **W-50** (see also Fig.1).Thus SE of vector holograms have been observed for the first time, to our knowledge.. More detailed results and their analysis will be presented at the conference.

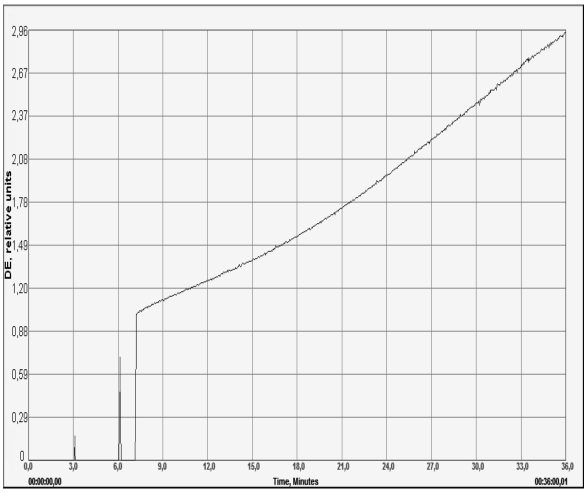

Fig.1 Coherent SE of the vector HG recorded in the sample **W-50** with orthogonally polarized *s*- and *p*-beams**.** Transmission mode, 532 nm, HG period is 2μm. The first peaks and the relative DE=1.00 correspond to the initial HG recording with two beams. Coherent SE excitation and readout is simultaneously made with the *s*-polarized beam.

References

1. Y.Zhao and T.Ikeda, Smart light-responsive materials (John Wiley&Sons, Inc., Hoboken, New Jersey, 2009).
2. K.Schwartz, The Physics of Optical Recording (Springer Verlag, Berlin, 1993).
3. A.Ozols, O.Salminen, and M.Reinfelde, *J.Appl.Phys.,* **75,** 3326 (1994).

OR-43

Development of Plasma Technologies for Nanostructured Materials: Nanoparticles, Thin Films and Coatings in NRC «Kurchatov Institute»

V.N. Fateev, O.I. Obrezkov, V.M. Kuligin, A.A. Fedotov

NRC “Kurchatov institute”, Russia, Moscow

e-mail: fat@hepti.kiae.ru

Such technologies as arc evaporation, magnetron-ion sputtering, ion implantation and pulsed ion implantation are widely used in our Center for nanoparticle (electrocatalysts and so on) and nanostructured films and coatings production. These methods permit to create any type of crystalline or even amorphous structure of metals and their compounds and to produce thermodynamically unstable compositions and nanostructures.

Important results were obtained in improvement of corrosion resistance, thermal and mechanical strength, friction force improvement. Magnetron sputtering assisted by ion (gas and metal ions with energy 1,0-100 keV) implantation permitted to create different types of nanostructured coatings. For example coatings with 5 µm thickness containing up to 1000 nanolayers on TiAlN of different composition resulted in improvement of mechanical strength of metal-working tools and increase of their life-time in 3-5 times and increase of tool efficiency for 25-35% (for example, drilling tools). Special installation “Kremen” was designed and produced in NRC “Kurchatov institute” for surface layers application.

Magnetron-sputtering or sputtering assisted by ion implantation was successfully used for catalyst and electrocatalyst synthesis. Sputtering of Ni, Pd, Pt and their application on carbon particles (including nanotubes and nanofibers) permitted to obtain electrocatalysts for PEM fuel cells and PEM and alkaline electrolysers. Average particle size could be easier varied due to ion current and time of sputtering. Additional high energy gas ion treatment gives possibility to increase the specific activity (up to 10%) and lifetime (up to 30-40%) of the catalysts by modification of catalyst particles (radiation defects production) and carbon carrier surface (purification). Pt catalyst with average particle size about 5-10 nm (specific surface up to 60 m^2/g) demonstrated same activity at lower Pt loadings in electrolyzers as chemically synthesized catalysts. Pt catalyst (particles and films with dimensions less then 100 nm) on porous metals (Ti, Zr) were developed for hydrogen in air oxidation for hydrogen safety systems. Plasmachemical processes in a gas phase permit to produce different types of nanoparticles for example solar grade silicon nanoparticles from SiO_2 by SiO gas phase reduction ($2\ SiO + 2\ CH_4 = 2Si + 2\ CO + 4\ H_2$) what is developed in our Center.

OR-44

Experiments on Application of High Power Microwave Radiation to Biomedicine Using Micro- and Nanoparticles

S.P. Besedin[1], A.K. Kaminsky[2], O.V. Komova[2], E.A. Krasavin[2], I.A. Krjachko[2], E.A. Perelstein[2],
S.N. Sedykh[2], V.N. Shaljapin[2], N.L. Shmakova[2], S.I. Tjutjunnikov[2]
[1]Joint Institute for Nuclear Research, Dubna, Moscow region, Russia
[2]Russian Scientific Center “Kurchatov Institute”, Moscow, Russia
e-mail: tsi@sunse.jinr.ru

High pulsed power microwave radiation gives new possibilities in the biomedicine, particularly to cancer cell damage study. Cooperative influence of microwaves and conducting micro- or nanoparticles provides local and selective action of microwaves on cancer cells. First results of JINR successful experiment are reported on cancer cells killing with the help of high power microwaves propagating through the thin gold layer. The microwave source was the JINR free electron maser with the power of 20 MW and frequency of 30 GHz. The microwave energy dencity was about 1 J/cm^2 during cell irradiation, number of pulses was 300 -1000. In the culture medium there are the cancer cells located on an object glass near the golden layer. The cell disruption was observed through 30-60 minutes after irradiation. The cells leaved the glass in the form of large conglomerates. Through 12 hours there were no irradiated cancer cells on the object glass. The preliminary study of processes leading to cancer cell damages were performed to estimate the perspective of such technique.

OR-45

Formation of Alpha Phase in Nanosized Plasma Processed Alumina Powder

E. Palcevskis, A. Lipe, A. Krumina, J. Krastiņš
Institute of Inorganic Chemistry, Riga Technical University, Latvia
e-mail: eriksp@nki.lv

The peculiarity of plasma processed fine alumina powders is that such powders contain δ- and θ-Al_2O_3 chrystallographic phases and problems arise to achieve high density ceramics because:

- the density of δ- and θ-Al_2O_3 is lower than density of α-Al_2O_3 ;
- δ- and θ-Al_2O_3 phase transition into α-Al_2O_3 occurs in the temperature range of 1000-1200 ^{o}C simultaneously with the particles growth, therefore the particle size increases and the sintering occurs already among relatively coarse α-Al_2O_3 particles, resulting in building of vermicular microstructure [1].

In this study the formation of α-Al_2O_3 by thermal treatment of granulated nanosized alumina powder (with the average particle size of 30-50 nm) prepared by spray-draying technique was investigated depending on used surfactant/suspension preparation conditions. It is shown that the granulation of plasma processed alumina powder promotes the formation of alpha phase in the temperature range of 1050–1150 ^{o}C.

The surfactant and the solution for preparation of suspensions have an effect on the kinetics of δ- and θ-Al_2O_3 phase transition into α-Al_2O_3, especially at lower temperatures and shortest thermal treatment times.

The peculiarity of plasma processed fine alumina powders is used for manufacturing of porous materials. The average pore size for such materials could be changed in the range of 80-300 nm at the open porosity in the range of 30-40 vol. %.

The possible application fields of obtained materials are the thermal insulator materials, recycling filter materials, ceramic membranes and catalyst carriers for chemical and pharmacy engineering, materials for manufacturing of medical implants etc.

References

1. C.Legros, C.Carry, P.Bowen, H.Hofmann. J. Euro. Ceram. Soc., 1999, v. 19, No. 11, pp. 1967-1978.

OR-46

Manipulation of Gold Nanoparticles inside Scanning Electron Microscope

B. Polyakov[1, 2], S. Vlassov[1], L. Dorogin[1], A. Romanov[1, 3], A. Lohmus[1], R. Lohmus[1]
[1]Institute of Physics, University of Tartu, Estonia
[2]Institute of Solid State Physics, University of Latvia, Latvia
[3]Ioffe Physical Technical Institute, RAS, Russia
e-mail: celbic@yahoo.com

Nanodevice engineering requires precise and deep understanding of nanomanipulation of small objects on different surfaces. Most nanoparticle manipulation experiments have been done by atomic force microscope (AFM) in contact or tapping mode [1, 2]. We studied the forces needed to overcome static friction and move individual Au nanoparticles of approximately 150 nm in diameter on an oxidized Si substrate inside a scanning electron microscope (SEM) in real time. The experimental setup consisted of a quartz tuning fork (QTF) mounted onto a high-precision 3D nanomanipulator used with a glued silicon tip as a force sensor.

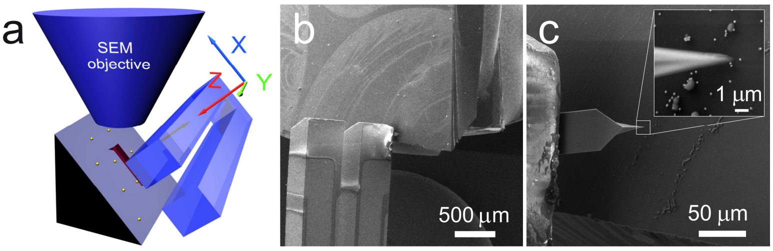

(a) Schematics of the experiment: QTF and sample are tilted at 45 degrees relative to the SEM objective. (b, c) SEM images of the sample and QTF with AFM cantilever at different magnification.

Static friction was found to range from tens of nN to several hundred nN. Large variations in static friction values were observed with differences in particle shape. Kinetic friction tended to be close to the detection limit and in most cases did not exceed several nN. The influence of thermal treatment in reducing the static friction of nanoparticles was observed.

References

1. K. Mougin, E. Gnecco, A. Rao, M. Cuberes, S. Jayaramaņ, E. McFarland, H. Haidara, E. Meyer. *Langmuir* 24, 1577, 2008
2. D. Dietzel, M.Feldmann, H. Fuchs, U. Schwarz, A.Schirmeisen. *Appl. Phys. Lett.* 95, 053104, 2009

OR-47

Strain Effects in Epitaxial $SrTiO_3$ and $KTaO_3$ Films

A. Dejneka[1], V. Trepakov[1, 2], D. Chvostova[1], L. Jastrabik[1], J. Narkilahti[3], M. Tyunina[3]
[1]Institute of Physics, ASCR, Na Slovance 2, 182 21 Prague 8, Czech Republic
[2]Ioffe Physical-Technical Institute of the RAS, 194 021 St.-Petersburg, Russia
[3]Microelectronics and Materials Physics Laboratories, University of Oulu, FI-90014 Oulun Yliopisto, Finland
e-mail: dejneka@fzu.cz

Principal possibility to control the properties of ABO_3 perovskite-type ferroelectrics by varying of strain in 2D clamped heteroepitaxial films has attracted a special attention today. Through the series of theoretical and experimental works (e.g., [1–5]) it is believed today that structure, polarization response and tunability of such films are influenced crucially by misfit strains.

We report on strain effects on properties and phase state of heteroepitaxial $SrTiO_3$ (STO) and $KTaO_3$ (KTO) films fabricated by pulsed laser deposition on 2D clamping straining and compressing substrates. Our attention have been mainly focused on spectral ellipsometry, thermooptics and dielectric studies of epitaxial 2.2% tensile strained 12 nm thick STO films deposited on (100) KTO single crystalline substrates (STO/KTO films) and on 2.2% compressive in-plane strained KTO/STO epitaxial 13 nm thick films. We present explicit experimental manifestations and proves that strain induced polar state is realized in epitaxial films of perovskite-like quantum paraelectrics STO and KTO under large enough in-plane epitaxial strains [see e.g. 6,7].

References

1. N. A. Pertsev, A. G. Zembilgotov, and A. K. Tagantsev, Phys. Rev. Lett. **80**, 1988 (1998).
2. N. A. Pertsev, A. K. Tagantsev, and N. Setter, Phys. Rev. B **61**, R825 (2000); Phys. Rev. B **65**, 219901 (2002).
3. Z. G. Ban and S. P. Alpau, J. Appl. Phys. **91**, 9288 (2002).
4. W. Chang, S. W. Kichoefer, K. M. Pond, J. A. Bellotti, S. D. Quadri, D. G. Schlom, J. H. Haeni, J. Appl. Phys., **96**, 6629 (2004).
5. J. H. Haeni, P. Irvin, W. Chang, R. Uecker, P. Roiche, Y. L. Li, S. Shoudhury, W. Tian, M. E. Hawiey, B. Graigo, A. K. Tagantsev, X. Q. Pan, S. K. Steffer, L. Q. Chen, S. W. Kirchoofer, J. Levy, and D. G. Schlom, Nature (London) **430**, 758 (2004).
6. M. Tyunina, J. Narkilahti, M.Plekh, R.Oja, R.M. Nieminen, A. Dejneka, V. Trepakov, Phys. Rev. Lett. 104 , 227601 (2010).
7. A.Dejneka, M.Tyunina, J.Narkilahti, J.Levoska, D.Chvostova, L.Jastrabik, V.A Trepakov, Physics of the Solid State 52, 2082 (2010).

OR-48

Determination of Thermal Diffusivity Coefficients of Thin Films by TSWM

O. Malyshkina, A. Movchikova, O. Kalugina
Department of Physics of Piezo- and Ferroelectrics, Tver State University, Russia
e-mail: Olga.Malyskina@mail.ru

The three thermal properties of a solid material are related with each other. The thermal diffusivity is the thermal conductivity divided by the volumetric heat capacity. Knowledge of the thermal diffusivity is necessary to evaluate of both the response time of the pyroelectric detector to an external thermal impact and for the reconstruction of the spatial distribution of polarization in ferroelectrics by the Laser Intensity Modulation Method (LIMM) [1] or by the Thermal Square Wave Method at single-frequency (TSWM) [2].

In this work, we describe a new measurement technique that is related to several recent pyroelectric methods [3-5], but which uses a similar theory and an identical experimental setup to the TSWM experiments [2]. We have considered two types of systems: 1) dielectric film deposited on a ferroelectric crystal, 2) the ferroelectric film - a metallic substrate. For both case the surface of the investigating film was periodically heated by rectangular modulated heat flux. The thermal diffusivity coefficients were estimated when the calculated forms of the pyroelectric response were completely identical to those obtained experimentally.

Approbation of the technique was carried out on unannealed PZT film deposited on a lithium tantalate crystal and on polarized PZT film. The decrease of the thermal diffusivity coefficient (from $1{,}5 \cdot 10^{-7}$ to $0{,}006 \cdot 10^{-7}$ m^2/s) with the decreasing of the film thickness (from 240 to 0,4 μm, respectively) was observed. The difference between the values of the thermal diffusivity coefficient of PZT films and of PZT bulk ceramics [5, 6] can be attribute to the fact that thin polycrystalline films are more porous than the bulk samples. Also the existence of size effect in the propagation of heat in the body should be taken into account.

This work was performed within the Federal Target Program "Research and Research-Pedagogical Personnel of Innovation Russia for 2009-2013"

References:

1. S. B. Lang, D. K Das-Gupta. J. Appl. Phys. **59**, 2151-2160 (1986).
2. O. V. Malyshkina, A.A. Movchikova, R.M. Grechishkin, et al. Ferroelectrics. **400**, 63-75 (2010).
3. H. Coufal, P. Hefferle. Appl. Phys. A**, 38,** 213 (1985).
4. P. K. John, L. C. M. Miranda, A. C. Rastogi. Phys. Rev. B. **34,** 4342 (1986).
5. S. B. Lang. Ferroelectrics. **93**, 87-93 (1989).
6. S. Bauer, B. Ploss. IEEE Transactions on Electrical Insulation. 27, 861-866 (1992).

OR-49

Multifunctionality of Strontium-Barium Niobate

J. Dec[1], S. Miga[1], K. Wokulska[1], M. Świrkowicz[2], T. Łukasiewicz[2]
[1]Institute of Materials Science, University of Silesia, Katowice, Poland
[2]Institute of Electronic Materials Technology, Warsaw, Poland
e-mail: jan.dec@us.edu.pl

Solid solutions of the strontium-barium niobate $Sr_xBa_{1-x}Nb_2O_6$ where $0 < x < 1$ (SBN) are environmental friendly (lead free) polar materials of oxygen octahedral family. Their potential applications are based on very attractive pyroelectric, electromechanical, electro-optic, photorefractive, and nonlinear optical and dielectric properties. Strontium-barium niobate is distinguished by its open tungsten bronze structure, i.e. the compound contains five AB_2O_6 formula units per tetragonal unit cell in which six *A* sites are occupied by five divalent metal atoms A. As a result the empty sites give rise to quenched electric random fields even in the stoichiometric compound. Consequently, by changing the ratio between strontium and barium components one may tune the system from ferroelectric ($x < 0.5$) to a generic relaxor ($x > 0.6$) behavior while maintaining the structure unchanged [1].

Using the Czochralski method eleven single crystalline compounds with nominal $x = 0.26$, 0.35, 0.40, 0.45, 0.50, 0.45, 0.61, 0.65, 0.70, 0.75, and 0.80 designated hereafter as SBN26, …, SBN80 have been grown. The crystals grown along the [001] tetragonal direction were up to 22 mm in diameter and 40 mm in length with characteristic 24 faces, free from striations and other extended defects. Density of etch pits was found to be of the order of $10^2 – 10^3$ cm^{-2}.

Investigations of the linear dielectric response measured within $10^0 \leq f \leq 10^5$ Hz along the polar c-axis of the obtained single crystals revealed a gradual crossover from ferroelectric (SBN26) to generic relaxor (SBN80) behavior. Complementary, temperature dependences of the lattice parameters confirm existence of structural phase transitions.

Financial support by MNiSW under grant N N507 455034 is gratefully acknowledged.

References

1. A. M. Glass J. Appl. Phys. 40, 4699 (1969).

OR-50

Electric Conductivity of Carbon Nanotube Composite

E.M. Ibragimova, V.N. Sandalov, M.I. Muminov
Institute of Nuclear Physics Academy of Sciences, pos. Ulugbek, Tashkent, 100214, Uzbekistan
e-mail: ibragimova@inp.uz

We studied the effect of ionizing radiation on temperature dependence of the surface resistance (R_s) of carbon powder containing about 70% nanotubes (CNT) glued on polyvinyl acetate (PVA) film of $10\times10\times0.1$ mm. Measurement of R_s were done by volt-ampere technique with Cu electrodes pressed against the film at the applied direct voltage of 0.1 V. The samples were irradiated at 300 K with ^{60}Co gamma-quanta at the dose rate 3.2 Gy/s step-like up to the dose $3\cdot10^5$ Gy, provided R_s measurements after each step. Temperature dependences of R_s shown in Fig.1 are non-linear and close to those occurred in CNT composites [1,2]. Arrhenius plot of these dependences can be divided into 3 regions, each characterized its own activation energy of polaron hopping conductivity, as listed in the table below.

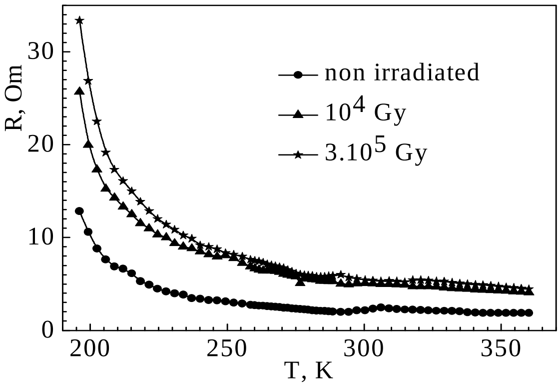

Fig.1 The surface current thermal dependence for UNT-PVA film prior and after gamma irradiation.

Sample	196 – 230 K	220–250 K	260–360 K
Non-irradiated	0.123	0.064	0.010
Irradiated to 10^4 Gy	0.138	0.077	0.030
Irradiated to $3\cdot10^5$ Gy	0.224	0.096	0.055

Gamma-irradiation results in dissolving of small clusters, the graphene nanoparticle and CNT concentration growth. Consequently, both the polaron hopping frequency and $R_s(T)$ values increase. Both CNT and PVA matrix, where quite strong intrinsic electric fields may be created [3], are suggested to contribute in the electric conductivity at $T < 250$ K.

References

1. M.M. Tomishko, O.V. Demicheva et al. Multilayer carbon nanotubes and their applications Russian Chem.J. vol. LII, No 5, 39 (2008).
2. J.E Fisher, W. Zhou, J. Vavro et al. Magnetically aligned single wall carbon nanotube films: preferred orientation and anisotropic transport properties. J. Appl. Phys. 93, 2157 (2003).
3. Yu.V. Kornyushin. On effective conductivity of composite materials. Letters to J.Techn.Phys. vol. 36, No 9, 50 (2010).

Abstracts of the poster presentations

PO-1

Luminescence in GeO_2-SiO_2 Films Fabricated by SPCVD

A. Trukhin[1], K. Golant[2], J. Teteris[1]
[1]Institute of Solid State Physics, University of Latvia, Latvia
[2]Kotel’nikov Institute of Radio-engineering and Electronics of RAS, Russia
e-mail: truhins@cfi.lu.lv

A line of Ge-doped silica films 10-20μ in thickness were synthesized by the surface-plasma chemical vapor deposition (SPCVD) on silica substrates [1]. The content of Ge in different films was varied as n·GeO_2-(1-n) ·SiO_2 with n changing from 0.02 to 1. No luminescence was observed in as received films under the excitation by 5 eV UV photons. It was the reason to conclude that the twofold coordinated germanium center is not formed immediately during the film preparation by SPCVD [2]. However, subsequent heat treatment of the films by a CO_2 laser beam leads to the appearance of luminescence as well as to a huge grows of the absorption band at 5 eV, which indicates to the presence of twofold coordinated germanium centers. This observation correlates with the case of Ge implanted silicon dioxide thin films, in which luminescence of the twofold coordinated germanium was found to increase several hundreds times after the heat treatment [3]. In pure (without silicon) GeO_2 SPCVD films the twofold coordinated germanium centers were not revealed even after heat treatment. However, under an ArF excimer laser (193 nm wavelength) excitation some luminescence is observed in the non-treated films with intensity increase at cooling down to 80 – 60 K. The decay kinetics of this luminescence significantly differs from that of the twofold coordinated germanium center, although its spectral content is similar.

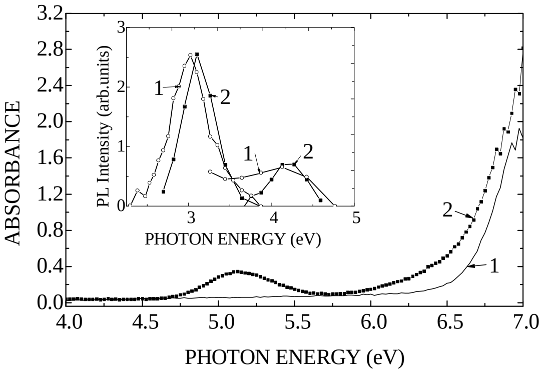

Fig.1 Absorption and (insertion) time resolved photoluminescence spectra under ArF laser pulses in a SPCVD 0.5·GeO_2-0.5·SiO_2 film on KU-1 silica substrate. 1 - as received. 2 - sample annealed with CO_2 laser. Time constants are for blue band 1~ 5 μs, 2 ~ 100 μs; for UV band 1 ~ 2 ns, 2 ~ 6 ns.

References

1. K. M. Golant,1 O. V. Butov, A. N. Denisov, V. M. Mashinsky, O. D. Sazhin, C. M. Smith, S. V. Muraviov, Proc. XIX Int. Congr. Glass, Edinburgh, UK (2001); Phys. Chem. Glasses, 43C, 131(2002)
2. D.Y. Kislitsyn, et al, 21 Intern. Congress on Glass, Strasbourg, France, 110 (2007)
3. H.J.Fitting et al, Journal of Non-Crystalline Solids 303, 218 (2002)

PO-2

γ-Ray Induced GeODC(II) Centers in Germanium Doped α-Quartz Crystal

A. Trukhin[1], A. Boukenter[2], Y. Ouerdane[2], S. Girard[3]
[1]Institute of Solid State Physics, University of Latvia, Latvia
[2]Laboratoire H. Curien, UMR CNRS 5516, France
[3]CEA, DAM, DIF, France
e-mail: truhins@cfi.lu.lv

Main luminescence of Ge-doped α-quartz crystal is known to be due to self-trapped exciton located near germanium atoms [1]. The characteristic luminescence of Ge-doped silica glass [2] associated with the so called GeODC has never been observed in Ge-doped α-quartz crystal. We performed experiments to check whether the GeODC-like-luminescence appear after γ-irradiation of such crystals. This is indeed the case as a new luminescence with two bands is detected under pulsed light of ArF laser (193 nm). The first emission corresponds to a blue luminescence with time constant of about 100 μs. The second one corresponds to a UV luminescence with fast decay time of ~1.5 ns. This last emission looks similar to the GeODC luminescence of silica glass. Besides, the old STE luminescence remains in the irradiated sample when an F_2 excimer laser (157 nm) is used as a probe excitation. However, clear differences are obtained regarding the induced center with respect to the well known twofold coordinated Ge center. The excitation under KrF laser does not provide decay time constant of about 100 μs but generates blue luminescence with a fast decay time of about 4 μs. The ArF laser pulses also excite this blue band component. The observed organization is connected to the multiformity of γ-ray created centers in amorphous areas of the Ge-doped crystal.

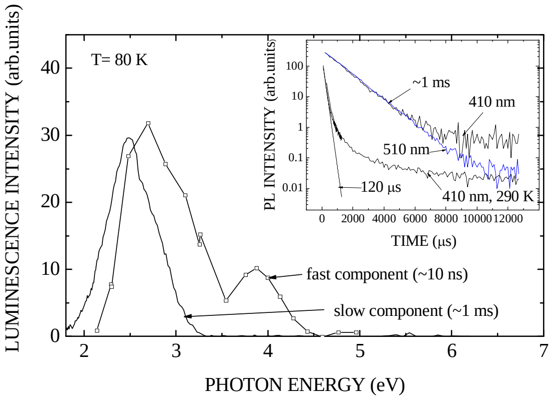

Fig.1 Photoluminescence spectra and decay curves (insertion) of γ-ray irradiated Ge-doped α-quartz under F_2 excimer laser (157 nm). The decay with τ ~1 ms corresponds to triplet-singlet transitions of the self-trapped exciton near Ge, whereas component with τ ~120 μs corresponds to triplet-singlet transitions in the induced GeODC like luminescence.

References

1. A.N.Trukhin, J.Non-Crystalline Solids **149**, 32 (1992).
1. L.N.Skuja, A.N.Trukhin, A.E.Plaudis, Phys.Stat.Sol.(a) **84** K153 (1984).

PO-3

Heat Treatment Effect on the ZrO_2 + Eu Nanopowder Luminescence

K. Gałązka[1], A. Świderska-Środa[1], W. Łojkowski[1], T. Chudoba[1], A. Opalińska[1], K. Smits[2],
L. Grigorjeva[2], D. Millers[2], C. Leonelli[3]
[1]Institute of High Pressure Physics, Polish Academy of Sciences, Poland
[2]Institute of Solid State Physics, University of Latvia
[3]Universita' degli Studi di Modena e Reggio Emilia, Italy
e-mail: annas@unipress.waw.pl

Investigations of the heat treatment influence on the luminescence of nanocrystalline zirconia doped with europium were performed. ZrO_2 + 10 mol.% Eu nanopowder with an average crystallite size of 5 nm and Specific Surface Area (SSA) of 160 m^2/g was synthesized using hydrothermal-microwave synthesis method [1]. The powder was heated in air at temperatures in range 400-850°C during 1 hour. We ascertained that grain growth and SSA decrease occurred in the samples annealed at temperature higher than 400°C. At 850°C the average crystallite size reached 12 nm and SSA diminished up to 35m^2/g. The higher was the annealing temperature, the lower was the intensity of europium luminescence. The luminescence spectra for nanopowders as a function of the temperature of annealing are presented in Fig.1.

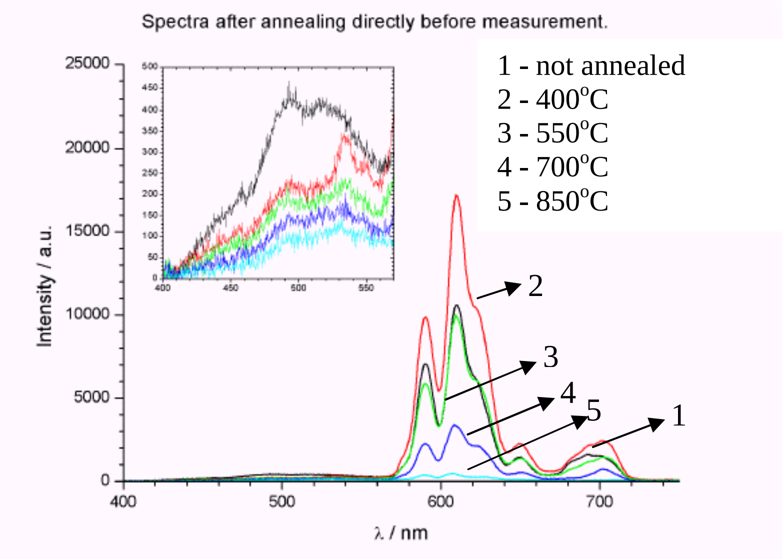

Fig.1. Luminescence of the ZrO_2-10 mol.% Eu heat treated nanopowders excited by a 402 nm LED

This work was supported by the project Eranet – MATERA “OXYNANOSEN”.

References

1 W. Lojkowski, A. Opalinska, T. Strachowski, A. Presz, S. Gierlotka, E. Grzanka, B. Palosz, W Strek, D. Hreniak, L. Grigorjeva, D. Millers, F. Bondioli, C. Leonelli, E. Reszke, *Microwave- Driven Hydrothermal Synthesis of Oxide Nanopowder for Application in Optoelectronics*, (in): "The Nano-Micro Interface: Bridging the Micro and Nano Worlds", edited by H.J. Fecht and M. Werner. Wiley-VCH Verlag GmbH & Co. KGaA, 2004.

PO-4

The Luminescence of Eu Doped ZrO_2 Nanocrystals

K. Smits[1], D. Millers[1], Dz. Jankovica[1], L. Grigorjeva[1]
[1]Institute of Solid State Physics, University of Latvia, Latvia
e-mail: smits@cfi.lu.lv

The time-resolved luminescence of undoped as well as europium doped ZrO_2 free standing nanocrystals (nanopowders) obtained by Sol - Gel method were studied. Samples with Eu concentration from 0.1% mol till 20% were prepared. Contamination of Eu in sample and type of crystalline structure were verified by x-ray fluorescence and XRD methods. The different excitation sources (x-ray, YAG laser (4th harmonic) 4.66 eV, optical parametric oscillator (OPO) laser and deuterium lamp) were used in experiments.

Our previous studies show the activator luminescence and structure dependence on activators concentration [1]. The electronic excitations in zirconia are mobile, so with increasing of activator concentration the intrinsic defects related luminescence band intensity decreases and activator luminescence intensity increases until it reaches the saturation. On the one hand Eu acts as phase stabilizer on the other hand as the luminescent probe.

The main luminescence bands due to transitions $^5D_0$ - $^7F_1$ and $^5D_0$ - $^7F_2$ of the Eu^{3+} and the excitation spectra of these bands where analyzed. Depending on excitation energy energy transfer to ions incorporated in tetragonal or monoclinic phase are possible.

The differences of intra-centre and recombinative luminescence were observed. The use of different excitation sources allow to determine the role of direct excitation of luminescence centers, energy transfer by excitons to these centers and band carriers trapping involved in the creation of excited states of the luminescence centers. The mechanisms of excited state creation and the possible models of luminescence centers in the nanocrystals will be discussed.

Acknowledgment: The financial support of ESF project 2009/0202/1DP/1.1.1.2.0/09/APIA/VIAA/141 is greatly acknowledged

References

1. K. Smits, L. Grigorjeva, D. Millers, A. Sarakovskis, A. Opalinska, J.D. Fidelus, W. Lojkowski, Opt. Mater. 32, 827 (2010).

PO-5

Up-conversion Luminiscence in ZrO_2 Nanocrystals

K. Smits[1], A. Sarakovskis[1], D. Millers[1], Dz. Jankovica[1], L. Grigorjeva[1]
[1]Institute of Solid State Physics, University of Latvia, Latvia
e-mail: smits@cfi.lu.lv

There is a large interest in rare-earth doped the zirconia to obtain up-conversion luminescence material for biological labeling [1] as well as for other applications. This interest is partially because of high chemical and physical stability of zirconia as well as due to relatively low phonon energy of the matrix especially among oxides (about 470 cm^{-1}) which is an important factor for the efficiency of the up-conversion processes in a material.

A set of undoped as well as Er and Yb doped ZrO_2 samples at different concentrations was prepared by sol-gel method. For the synthesized samples the study of both the stationary and time-resolved luminescence was carried out. The dopant concentration impact on the up-conversion luminescence as well as the upconversion luminescence dependence on the temperature was also studied. The correlation between Er and Yb related to tetragonal or even cubic structure stabilization and intrinsic defect concentration change was analyzed.

It will be shown that the incorporation of Er and Yb ions leads to the stabilization of tetragonal and cubic phase of zirconia. The intrinsic defect concentration impact on upconversion luminescence band change is provided. The possible models and mechanisms of upconversion in ZrO_2 was studied using time resolved luminescence measurments. Possible application of the rare-earth doped zirconia in temperature measurements for biological applications will be discussed.

Acknowledgment: The financial support of ESF project 2009/0202/1DP/1.1.1.2.0/09/APIA/VIAA/141 is greatly acknowledged

References

1. 1.G. Chen, G. Somesfalean, Y. Liu, Z. Zhang, Q. Sun, and F. Wang, Phys. Rev. B **75**, 195204 (2007)

PO-6

Cathodoluminescence of Terbium and Cerium Activated Oxyfluorides

E. Elsts, U. Rogulis, J. Jansons, A. Sarakovskis, G. Doke
Institute of Solid State Physics, University of Latvia, Latvia
e-mail: eelsts@cfi.lu.lv

We have studied cathodoluminescence spectra and decay times of the following oxyfluorides:

- Tb activated sodium - containing composition SiO_2 - Al_20_3 - Na_2O - LaF_3 - NaF,
- Tb and Ce activated lithium - containing composition SiO_2 - Al_2O_3 - Li_2O - LaF_3.

Cathodoluminescence decay times of the terbium activated sodium - containing samples are 65 - 330 μs at CL 380 nm band and 815 - 975 μs at 545 nm CL band [1]. Terbium activated lithium - containing sample's decay times are 125 μs at 380 nm band and 910 μs at 545 nm band. Cerium activated lithium - containing sample's decay times are 2.4 μs at 380 nm band.

Li_2O - containing terbium activated glasses have more stable cathodoluminescence than Na_2O - containing glasses. Decay times of cerium activated oxyfluoride glases are considerably faster than terbium activated, but also less intense.

References

1. E. Elsts et al., Latvian Journal of Physics and Technical Sciences, 5 (2010) p. 48.

PO-7

Synthesis and Characterization of Cerium and Europium Doped YAG Nanocrystals

Dz. Jankoviča[1], J. Grabis[1], L. Grigorjeva[2], D. Millers[2], K. Smits[2], L. Bukonte[2]

[1]Institute of Inorganic Chemistry Physics, RTU, Salaspils, Latvia

[2]Institute of Solid State Physics, University of Latvia, Latvia

e-mail: lgrig@latnet.lv

The Yttrium Alumina Garnet (YAG) doped with RE ions is known as a laser host (YAG:Nd; YAG:Yb), as a scintillator material (YAG:Ce, YAG;Pr), as a material for white LED and other photonic applications. The quality of laser ceramic has been improved noticeably since in 1980's the technology of transparent ceramics fabrication was developed [1] and the quality of laser ceramic has been improved noticeably. For the ceramic sintering the nanoscaled YAG material is used as a starting material and its characteristics play important role in the fabrication of laser and luminescent ceramics.

The current study focuses on the YAG nanopowder synthesis process, characterization of obtained powders by XRD, SEM, S_{BET} and EDX analysis. The studies of luminescence properties of YAG nanocrystals were carried out by means of time-resolved spectroscopic methods.

The YAG nanopowders were prepared by the sol-gel low temperature combustion method [2, 3]. The starting materials were aluminum nitrate, yttrium oxide, ethylene glycol, nitric acid and cerium or europium nitrates. The solutions of the precursors were mixed and heated at 80-85^{o}C. The mixture was evaporated at 90-100^{o}C. The dry powder was combusted at temperature 500-550^{o}C for 4 h. The powders were calcinated at 1000^{o}C for 3 h in air obtaining powders with YAG crystalline structure. According the S_{BET} method, the grain sizes of powders are 30-35 nm, however the SEM images shows the agglomeration of nanocrystals.

The spectra of cathodoluminescence, photoluminescence and radioluminescence were studied. The luminescence of intrinsic defects localized excitons (LE), antisite defects (Y_{Al}) were compared in undoped and RE doped YAG nanocrystals. The luminescence spectra and decay times of RE ions luminescence as well as energy transfer efficiency to dopand ions were studied.

References

1. H.Yagi, T.Yanagitani, K.Tankaichi, K.Ueda, A.Kaminskii. Opt.Mater. **29,** 1258 (2007).
2. L.A.Diaz-Tores, E.De la Rosa, P.Salas, H.Desena. Opt.Mater., **27,** 1305 (2005).
3. J.Grabis, D.Jankoviča, I.Šteins, A.Patmalnieks. Material Science Forum,.**636-637**, 697(2010).

PO-8

Multicolor Up-Conversion Luminescence in Rare-Earth Doped $NaLaF_4$

G. Doke, M. Voss, J. Grube, A. Sarakovskis, M. Springis
Institute of Solid State Physics, University of Latvia, Latvia
e-mail: guna.doke@gmail.com

In the past years many scientists have studied up-conversion (UC) processes in the rare-earth doped materials related to the emission of higher-energy photons (VIS and UV) when excited by lower-energy photons (usually IR). By applying particular rare-earth ions in the materials it is possible to get separate red, green and blue luminescence light or mixture of these colors, for example, white light under IR excitation.

In this work we tried to achieve white UC luminescence color based on 1931 CIE diagram. To do that we synthesized $NaLaF_4$ doped with different Er^{3+}, Tm^{3+} and Yb^{3+} concentration. UC luminescence was measured (Fig. 1) and main luminescence bands from Er^{3+} and Tm^{3+} in red, green and blue spectral regions were observed. The relative intensities of the luminescence bands were found to be dependent on the doping levels of rare-earth ions. Moreover minor changes in the UC luminescence color could be achieved by applying different IR pump power density.

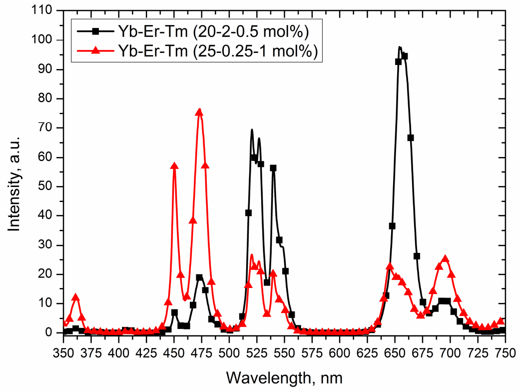

Fig.1 UC luminescence of $NaLaF_4$ with different Yb^{3+}, Er^{3+} and Tm^{3+} ions concentration under 980nm excitation

Acknowledgment: The financial support of ESF project 2009/0202/1DP/1.1.1.2.0/09/APIA/VIAA/141 is greatly acknowledged

PO-9

Novel Synthesis of Up-Conversion Phosphor Based on Rare-Earth Doped $NaLaF_4$

A. Sarakovskis, M. Voss, G. Doke, J. Grube, M. Springis
Institute of Solid State Physics, University of Latvia, Latvia
e-mail: Anatolijs.Sarakovskis@cfi.lu.lv

Fluorides are known to be effective hosts for different rare-earth ions particularly the ones to be used in up-conversion applications. Due to small phonon energy of most fluorides the multi-phonon relaxation in rare-earth ions could be reduced which is important if the material is considered to be used in up-conversion applications. However for an efficient up-conversion process suppression of luminescence quenching by both multi-phonon relaxation and presence of quenching centers is also required.

Our previous results suggested $NaLaF_4:Er^{3+}$ as attractive media for up-conversion luminescence [1]. However the material suffered from different types of oxygen related defects, which are believed to be the common quenching centers of the luminescence in fluorides.

In this report we present a novel, inexpensive and effective synthesis route of oxygen free $NaLaF_4:Er^{3+}$ material without using hazardous hydrofluoric acid for elimination of oxygen impurities. Along with the description of the synthesis route, luminescence spectra and decay kinetics of both traditional and up-conversion luminescence of Er^{3+} will be presented for different Er^{3+} doping levels. It will be shown that the increase of Er^{3+} concentration leads to the shortening of Er^{3+} luminescence lifetime and enhances energy-transfer probability in the up-conversion processes. It will be also shown that the elimination of oxygen impurities strongly influences the up-conversion processes in $NaLaF_4:Er^{3+}$ and improves the efficiency of the up-conversion luminescence.

Acknowledgment: The financial support of ESF project 2009/0202/1DP/1.1.1.2.0/09/APIA/VIAA/141 is greatly acknowledged

References

1. A. Sarakovskis, J. Grube, A. Mishnev, M. Springis, Opt. Mat. **31**, 10 (2009)

PO-10

Evaluation of Commercial Retroreflective Coating Performance in Decreased Visibility Conditions

K. Luse[1, 2], A. Pausus[1], V. Karitans[1, 2], M. Ozoliņš[1], M. Tukisa[1]

[1]University of Latvia, Optometry and Vision Science Dept., Latvia

[2]Institute of Solid State Physics, University of Latvia, Latvia

e-mail: kaiva.luse@gmail.com

Generally commercially available retroreflective (RR) materials lack instructions on usage and the average purchaser lacks knowledge on their performance and constructive differences. Three different types of RR's were evaluated [1 - 3M™ *Scothlite*; 2 - 3M™ *Diamond Grade*; 3 – microprismatic RR (*Chief-light CO, Ltd*)]. Five different colors of microprismatic RR's were compared (white, yellow, green, orange and red). The evaluation was based on finding weather the construction and color of sample significantly affect the retroreflectance optical indicatrix by tilting the RR (Fig.1. A). The performance of samples was evaluated by creating deviated lightning conditions of the RR's. Reflectance spectrum of all samples was measured and compared.

Electron-microscopic estimate of the size of RR's active regions were made (Fig.1. B). Interpretation of diffraction effects has been proposed. In addition to performance detection with technical support, psychophysical studies are scheduled.

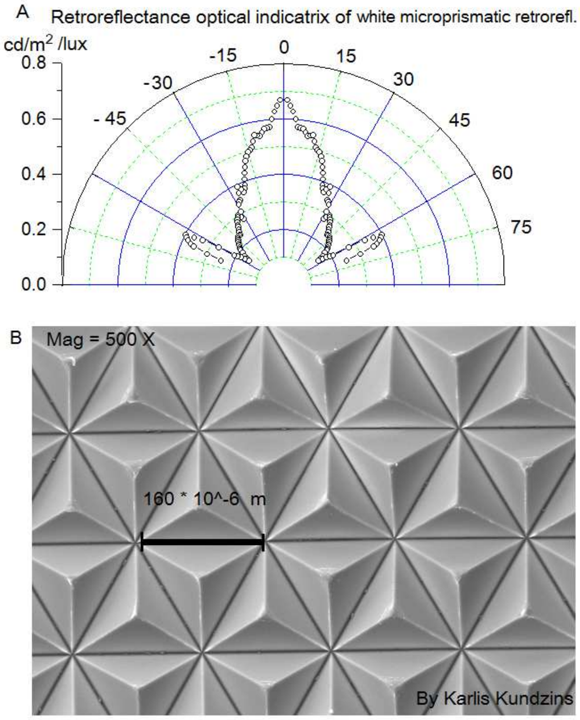

Fig.1 An example of study: A – white microprismatic RR's retroreflectance optical indicatrix; B microscopic size evaluation of the same sample.

Significantly different changes were discovered among different types as well as colors of RR's.

PO-11

Analysis of Rabkin Color Deficiency Test under Different Illumination

S. Fomins[1], M. Ozoliņš[1], G. Krūmiņa[1, 2], I. Lācis[2]

[1]Institute of Solid State Physics, University of Latvia, Latvia

[2]Optometry and Vision Science Department, University of Latvia, Latvia

e-mail: sergejs.fomins@gmail.com

Colorimetric analysis of color deficiency tests is the main technique for analysis of used pigments according to the dichromate confusion lines (Fig.1) [1]. Perception of color is influenced by lighting conditions and spectral characteristics of the illuminant. Many of the pseudoisochromatic plates are designed for daylight illumination [2]. However, there are tests (Rabkin polychromatic plates) with no specialized type of illumination mentioned. Four different illumination sources were chosen for analysis of Rabkin test for color deficiency, including typical halogen light source (~3000K), diffuse daylight (~6500K), modern warm light emitting diode bulb (~3000K), and fluorescent lamps (~4000K). Acquisition of color deficiency test spectral images was provided by CRI Nuance II VIS multispectral camera for 420 to 720 nm range of visible spectrum. Colorimetric data of the each pixel of the test image is calculated and distribution of color coordinates is analyzed for each illumination conditions in CIE x,y chromaticity diagram.

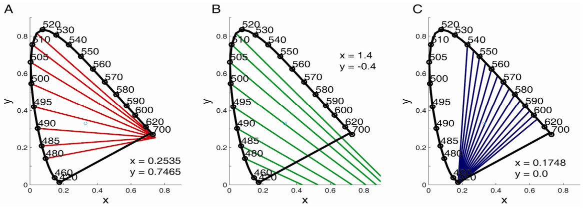

Fig.1 Dichromate confusion lines in CIE x,y chromaticity diagram [3] Coordinates of the copunctal convergence points are given.

References

1. D.Y. Lee, M. Honson. Color research and application. Suppl. **28(4)**, 267-276 (2003).
2. S. Ishihara. Ishihara`s test for colour blindness. Concise Edition, Isshinkai, Tokyo, Japan (1965)..
3. V.C. Smith, J. Pokorny. Vision Research, **15**, 161-171 (1975).

PO-12

Dependence Of Wavefront Aberrations On Spectral Properties Of Shack-Hartmann Wavefront Sensor

V. Karitans[1, 2], M. Ozoliņš[1, 2], K. Luse[2]

[1]Institute of Solid State Physics, University of Latvia, Latvia

[2]Department of Optometry and Vision Science, University of Latvia, Latvia

e-mail: variskaritans@gmail.com

Measurement of optical aberrations requires a referent state against which these aberrations are measured. This referent state is an absolutely planar wavefront. Absolute calibration of the Shack-Hartmann wavefront sensor (SHWS) has been described already previously [1]. The referent state in adaptive optics is created when a collimated beam enters the SHWS. However, the optical system of the SHWS may not be achromatic and spot pattern in the referent state may vary depending on the wavelength at which it is set. We investigated whether the measured wavefront aberrations depend on the wavelength at which the referent state is set. The optical scheme for setting the referent state is shown in Figure 1.

Results reveal variations in measured defocus value when choosing different referent states. Variations are less than 0.1 µm. For a 3 mm pupil like in our case it corresponds to about 0.3 D change in spherical equivalent. The RMS of defocus was the smallest when measured against the referent state set at 532 nm but increased towards the end of the spectrum. This is insignificant refractive error in optometrist’s practice and is about the just noticeable difference in the refractive state of an eye [2].

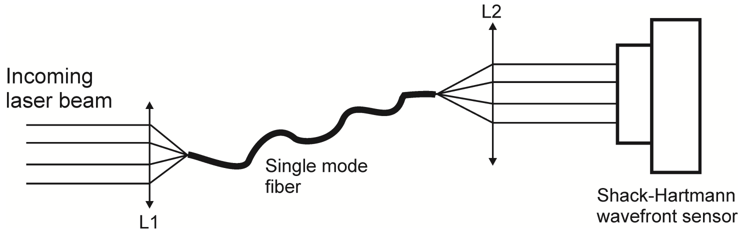

Fig.1 Setting the referent state in adaptive optics for measuring wavefront aberrations. A lens L1 focuses the laser beam on one end of a single-mode fiber while the other end is placed in the focal point of an aspheric lens L2. When a collimated beam enters the wavefront sensor the referent state is set.

A possible source of variations in magnitude of wavefront aberrations may be chromatic dispersion in the lenses of the SHWS – relay lenses and the microlens array.

The authors are thankful to the European Social Fund project “Support of Doctoral Studies at the University of Latvia”. Project No. 1DP/1.1.2.1.2./09/IPIA/VIAA/004.

References

1. A. Chernyshov, U. Sterr, F. Riehle, J. Helmcke, and J. Pfund, Appl. Opt. 44, 6419 – 6425 (2005).
2. R. Legras, N. Chateau and W. N. Charman, Optom. Vis. Sci. 81, 718 – 728 (2004).

PO-13

Photoluminescence of Al_2O_3 Nanopowders of Different Phases

L. Trinkler[1], B. Berzina[1], Z. Jevsjutina[1], J. Grabis[2], I. Steins[2]

[1]Institute of Solid State Physics, University of Latvia, Latvia

[2]Institute of Inorganic Chemistry, Riga technical university, Latvia

e-mail: trinkler@latnet.lv

Photoluminescence (PL) in 8-300 K temperature range has been studied in nominally pure alumina (Al_20_3) nanopowders. Al_2O_3 nanoparticles were prepared by evaporation of commercial available coarse grained alumina in inductively coupled air plasma. The prepared samples were calcinated at 800–1400 ^oC for 2 h. Temperature of calcination determines phase composition and grain size of the samples, which grows from 13 to 80 nm. Accordingly to XRD analysis the as-prepared samples contained weekly crystallized δ-Al_2O_3. Calcination of samples up to 1000 ^oC had a little influence on phase composition. Phase transition and formation of α-Al_2O_3 started at 1200 ^oC but pure α-Al_2O_3 particles were obtained only at 1400 ^oC high temperature. However, from PL measurements it follows that even the sample calcinated at 1400 ^oC besides α phase contains also θ phase.

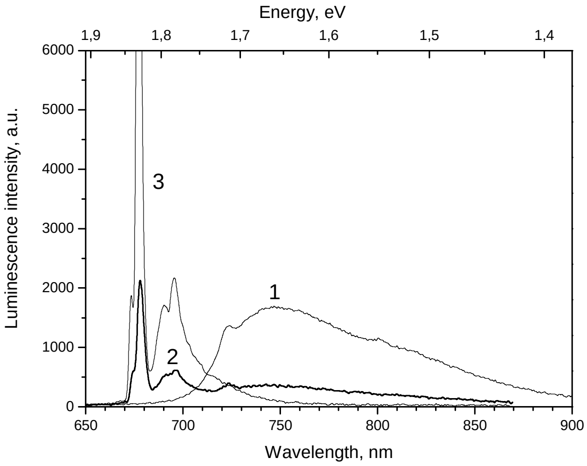

Fig.1.Photoluminescence at 8 K of Al_2O_3 nanopowders calcinated at 800 ºC (1), 1300 ºC (2) and 1400 ºC (1).

It was found out that luminescence properties of alumina powders are determined by uncontrolled impurities, mainly iron and chromium. Luminescence spectra of the samples with δ-Al_2O_3 phase have a broad band in the 700-900 nm region ascribed to emission from Fe^{3+} ions. In the samples with $\theta + \alpha$ phases Fe^{3+} luminescence band diminishes and disappears, instead there emerges two narrow bands corresponding to Cr^{3+} emission in alumina with θ phase (680 nm) and α phase (694 nm). Excitation spectra of Fe^{3+} and Cr^{3+} ions contain bands inherent for absorption transitions of these ions, besides there is a common band at 320 nm. It is assumed that 320 nm excitation band is connected with an exciton type state, which depending on lattice phase causes either titanium or chromium emission.

PO-14

Zirconia Films Doped with PbS Nanodots for Ultraviolet Radiation Dosimetry

Y. Dekhtyar[1], M. Romanova[1], A. Anischenko[1], A. Sudnikovich[1], N. Polyaka[1], R. Reisfeld[2],
T. Saraidarov[2], B. Polyakov[3]
[1]Institute of Biological Engineering and Nanotechnology, Riga Technical University, Latvia
[2]Hebrew University of Jerusalem, Israel
[3]Institute of Solid State Physics, University of Latvia, Latvia
e-mail: marina.romanova@inbox.lv

Due to new technological possibilities to sense and visualize processes at a nanoscale, a new experimental field of bionanophysics has developed. One of its directions deals with nanodosimetry. Since the primary targets of interaction of radiation with biological tissue are DNA and other biomolecular structures which have nanoscale dimensions, it is important to have a sensor of corresponding nanovolume. One approach offers to use a thin film dosimeter, which consists of nanodots embedded in a solid thin film matrix. The nanodots are supposed to be a radiation-sensitive substance.

This experimental research studies the effects of ultraviolet radiation on zirconia films doped with PbS nanodots (ZrO_2:PbS films). The films were fabricated using sol-gel technique. ZrO_2:PbS films were irradiated with UV light with wavelengths 250 – 400 nm during 50 minutes. Photoelectron emission from the surface of the films was studied and band structure of the films was calculated. It was found that quantity of localized states decreased after UV irradiation while density of localized states was dependent on concentration of PbS nanodots. The observed changes in band structure of ZrO_2:PbS films after UV irradiation allow to suggest that the films may be considered as an effective material for UV radiation dosimetry, PbS nanodots being the UV sensitive substance of such a dosimeter.

References

1. A. Sashchiuk, E. Lifshitz, R. Reisfeld, T. Saraidarov, M. Zelner and A. Willenz, J. Sol-Gel Sci. Technol. **24**, 31 (2002)
2. T. Saraidarov, R. Reisfeld, A. Sashchiuk and E. Lifshitz, J. Sol-Gel Sci. Technol. **26**, 533 (2003)

PO-15

Sulphide Nanocrystals for Solar Cell Applications

P. Kulis, A. Petruhins, J. Butikova, B. Polyakov, I. Muzikante, I. Tale
Institute of Solid State Physics, University of Latvia, Latvia
e-mail: p.kulis@cfi.lu.lv

Several nanocrystal (NC) based solar cell architectures were demonstrated in recent time. Main architectures are Schottky type [1], blend of NC and polymer [2], blend of two different NC materials [3], and Gratzel type solar cell [4]. One of most significant advantage of NC based solar cell technology is synthesis from solution, which is much cheaper in comparison with conventional vacuum technologies used for silicon solar cells.

It is well known that band gap of nanocrystals may be tailored in wide range varying its size due to quantum confinement effect. Sulphide materials have rather large Bohr radius (18 nm for PbS and 2.4 nm for CdS). Another important material characteristic for solar cell engineering is work function. Ability to modify work function of NC is essential for increasing solar cell efficiency.

In this study we report Kelvin probe measurements of work function of chemically synthesized PbS and CdS nanocrystal thin films.

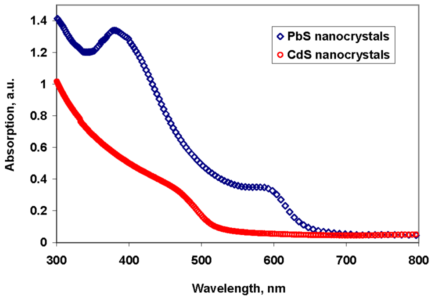

Fig. 1.Optical absorption of PbS and CdS nanocrystals

References

1. J. Luther, M. Law, M. Beard, Q. Song, M.Randy, J. Ellingson, A. Nozik, *Nanoletters* **8**, 2008, 3488-3492
2. J. Choi, Y. Lim, M. Santiago-Berrios, M. Oh, B. Hyun, L. Sun, A. Bartnik, A. Goedhart, G. Malliaras, H. Abruna, F. Wise, T. Hanrath, *Nanoletters* **9**, 2009, 3749-3755
3. Y. Wu, C. Wadia, W. Ma, B. Sadtler, A. Alivisatos, *Nanoletters* **8**, 2008, 2551-2555
4. B. Hyun, Y. Zhong, A. Bartnik, L. Sun, H. Abrun, F. Wise, J. Goodreau, J. Matthews, T. Leslie, N. Borrelli, *ASC NANO*, **2**, 2008, 2206-2212

P.K. and A.P. were supported by ESF Grant no. 2009/0202/1DP/1.1.1.2.0/09/APIA/VIAA/141

PO-16

Optical Properties of Original Metal Complex with Cr Atoms

S. Popova[1], A. Vembris[1], I. Muzikante[1], E. Kirilova[2]
[1]Institute of Solid State Physics, University of Latvia, Latvia
[2]University of Daugavpils, Latvia
e-mail: aivars.vembris@cfi.lu.lv

Most of the organic compounds emit light from singlet state. Electrically exited molecules can be in singlet and in triplet states. From spin statistics follows that only 25% of exited states will be singlet, other 75% triplet states. It means that quantum efficiency of organic light emitting diode (OLED) in the best case could be only 25%. Metal complex emit light also from triplet state due to the singlet – triplet coupling. That is why such materials could be more promising in (OLED) devices.

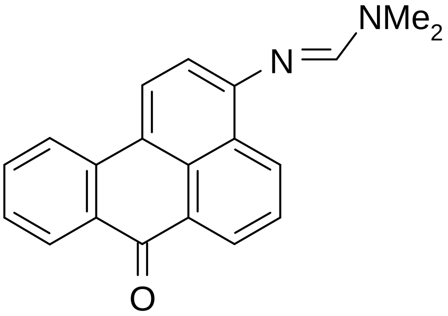

Fig.1 3-N-(N’,N’-Dimethylformamidino)benzanthrone

In this presentation we will show optical properties of solution and thin films of 3-N-(N’,N’-dimethylformamidino)benzanthrone (see Fig.1) [1] ligand which contains Cr atoms.

References

1. Kirilova E. M, Belyakov S. V, Kalnina I., Topics in Chemistry & Materials Science, Sofia: Heron Press (ed: G. Vayssilov, R. Nikolova); 3, 19-28. (2009)

PO-17

Fluorescence Characteristics of Styryl-4H-Pyran-4-ylidene Fragment Containing Derivatives

A. Vembris[1], I. Muzikante[1], R. Karpicz[2], V. Gulbinas[2]

[1]Institute of Solid State Physics, University of Latvia, Latvia

[2]Institute of Physics, Center for Physical Sciences and Technology, Lithuania

e-mail: aivars.vembris@cfi.lu.lv

Organic molecules become more popular in electro-optical devices, like organic light emitting diodes (OLED). Glass forming low molecular organic compounds could be perspective due to easier synthesis and thin film processing from solution. Fluorescence decay time constants and quantum yield are important parameters to estimate application possibility of organic compound in OLED device.

In the work we were measured fluorescence kinetics for six glass forming styryl-4H-pyran-4-ylidene fragment containing derivatives in solution and thin films. Dichloromethane was used as a solvent for preparation of solutions and thin films. The concentration of molecules was between 10^{-6} to 10^{-5} mol/l for solutions. Thin solid samples were prepared by spin coating method. The thickness was from 400 to 600 nm. Picoseconds diode laser with wavelength 375nm was used as excitation source.

Fluorescence kinetics in solution consists of one exponential decay but in thin solid films at least of two exponential decays. The slowest process time constant is 1 to 2 nanoseconds and fastest one is several hundreds of picoseconds.

PO-18

Polarization Holographic Recording in Disperse Red1 Doped Polyurethane Polymer Film

J. Aleksejeva, A. Gerbreders, U. Gertners, M. Reinfelde, J. Teteris
Institute of Solid State Physics, University of Latvia, Latvia
e-mail: aleksejeva.jelena@gmail.com

In this report holographic recording of polarisation and surface relief gratings in Disperse Red 1 (DR1) doped polyurethane polymer films was studied. In this material DR1 is chemically bounded to polyurethane polymer main chain. Polarization holographic recording was performed by orthogonally linearly and circularly polarized two beams. Lasers with 532 nm and 632.8nm were used for that purpose. Photoinduced birefringence is a precondition for polarization holograms recording, therefore a detailed study of a photoinduced birefringence and changes of optical properties was performed. The lasers with wavelengths of 375nm, 448nm, 532 nm and 632.8 nm were used as pumping beam for sample excitation. The photoinduced birefringence Δn was measured at 532 nm and 632.8 nm wavelengths. The sign and numeral values of photoinduced birefringence and their dependence on the pumping beam wavelength and intensity were evaluated. The relaxation of photoinduced birefringence in a dark and under light illumination was studied. Surface relief grating (SRG) formation was observed during polarization holographic recording process. A profile of SRG was studied by AFM. A relationship between SRG formation and photoinduced birefringence has been discussed.

References:

1. Dong Hoon Choi, Suk Hoon Kang, *Chem. Soc*. Vol. **20**, No. 10, 1186 (1999)
2. L. Pan, Q. Yang, M. Jin, G. Sun, Z. Jiang, J. Phys. D: Appl. Phys. **37** 1002, (2004)

PO-19

FTIR and Raman Spectroscopy Studies of Polyisoprene-Nanostructured Carbon Composites

K. Ozols[1], L. Dolgov[2], M. Knite[1]
[1]Riga Technical University, Institute of Technical Physics, Latvia
[2]University of Tartu, Institute of Physics, Estonia
e-mail: kozols@ktf.rtu.lv

Polyisoprene-nanostructured carbon composites (PNCC) are known for their potential use as piezoresistive and volatile organic compound sensors. For better theoretical understanding of physical and chemical processes taking place at different manufacturing stages of PNCC as well as for practical development of sensors with higher sensitivity, studies on optical properties of the composites were conducted. The goal of this study was to find out how the concentration of nanoparticles and vulcanization duration of polyisoprene – nanostructured carbon composites influence their optical properties.

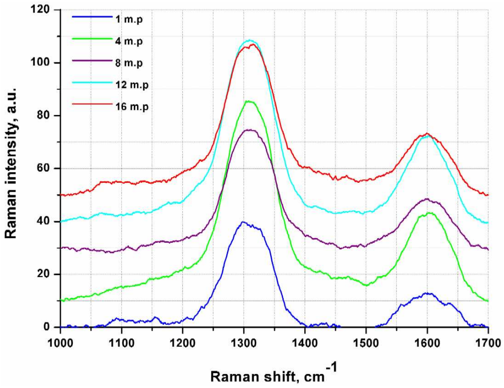

Fig.1 Raman spectra of composites with different concentration (m.p. – mass parts) of multi-walled carbon nanotubes.

FTIR spectroscopy was used to investigate the development of molecular bonds in PNCC samples with different vulcanization duration. These measurements have confirmed that, during vulcanization phase, chemical breaking and linking of molecular bonds takes place. The conducted measurements indicate a possible change of FTIR spectral peak height as aging process of PNCC samples takes place. In addition Raman spectroscopy measurements were made. Analysis of different peaks in FTIR and Raman spectra is carried out. Further optical studies are in progress.

PO-20

Photo-Induced Mass Transfer in Chalcogenides

U. Gertners, J. Teteris
Institute of Solid State Physics, 8 Kengaraga Str., Riga, LV-1063, Latvia

This work is devoted to the topical issue – photo-induced formation of relief in thin layers of chalcogenide vitreous semiconductors (ChVS) without following complicated chemical processing. Direct holographic recording technique is on of the advanced methods for surface relief structuring in light sensitive materials. Because of the high light and electric field gradient it is possible to obtain structures directly in time with illumination. In this report the study of direct mass transfer on ChVS like As-S, As-S-Se has been presented. Experiments was performed by 532nm wavelength. Also the mechanism of the direct recording of surface-relief on amorphous chalcogenide films based on the photo-induced plasticity has been discussed.

PO-21

Contribution of Electron-Hole Processes to Luminescence of $CaSO_4$ doped with RE^{3+} Ions

I. Kudryavtseva[1], A. Lushchik[1], A. Maaroos[1], Z. Salikhoja[2], A. Shugai[1]

[1]Institute of Physics, University of Tartu, Estonia

[2]L.N. Gumilyov Eurasian National University, Astana, Kazakhstan

e-mail: irina@fi.tartu.ee

Three main mechanisms of impurity emission excitation were revealed earlier for harmless luminescent materials based on $CaSO_4$ doped with RE^{3+} ions. A RE^{3+} ion could be excited via direct photoexcitation and due to the energy either transferred from an excited oxyanion $(SO_4^{2-})^*$ [1, 2] or released at the recombination between electrons and holes formed by photons of $h\nu > E_g \cong 9.5$ eV [2]. There is a need to perform a further comprehensive investigation of the recombination mechanisms. A series of $CaSO_4$:RE^{3+},Na^+ ($RE^{3+} \equiv Tb^{3+}$, Gd^{3+}, Eu^{3+} and Na^+ ions were used for charge compensation) and $CaSO_4$:RE^{3+},F^- ($RE^{3+} \equiv Tb^{3+}$ or Gd^{3+}) phosphors have been synthesized (see also [2]). The excitation spectra for different emission lines and bands as well as for phosphorescence have been measured in the region of 3.5-12 eV at 80-400 K. Photo- and thermally stimulated luminescence (PSL and TSL) have been measured at a sample heating from 80 to 500 K. The shape of the stimulation spectra (2.2-3.0 eV) for PSL of RE^{3+} in the phosphors preirradiated by photons of $h\nu > E_g$ is similar to that for binary metal oxides. The PSL arises at least in part due to transfer of the energy, released at the recombination between optically delocalized holes with some electron centres, to RE^{3+}. Gd^{3+} ions serve as electron traps and Gd^{2+} centres formed in the preirradiated samples are stable up to ~200 K. The TSL peaks at 110 and 160 K are connected with the thermal release of holes. A role of a compensator (Na^+ or F^-) on the luminescence and TSL of $CaSO_4$:RE^{3+} is analyzed. The contribution of electron-hole and hole-electron recombination (i.e. either an electron or a hole acts as a mobile participant) to the energy transfer to RE^{3+} ions is discussed.

References

1. E. van der Kolk, P. Dorenbos, A. P. Vink, R. C. Perego, C. W. E. van Eijk, A. R. Lakshmanan, Phys. Rev. B **64**, 195129 (2001)

2. I. Kudryavtseva, P. Liblik, A. Lushchik, A. Maaroos, E. Vasil'chenko, Z. Azmaganbetova, T. Nurakhmetov and B. Toxanbayev, J. Lumin. **129**, 1890 (2009)

PO-22

The Prospects of Modifications of Glass Properties on the Base of Constant Stoichiometry Grouping Concept

O. Yanush, I. Apakova, T. Markova
St. Petersburg State Technological University of Plant Polymers, Russia
e-mail: O.V.Yanush@inbox.ru

Earlier it was shown that vibrational spectroscopy can serve for detection of structural units of oxide glasses (as of inorganic polymers) that was called constant stoichiometry groupings (CSGs) [1]. Vibrational spectra of glasses are interpreted as a superposition of relatively small number of unchangeable spectral forms (principal spectral components (PSCs)) belonging to CSGs. The composition dependences of the concentrations of the CSGs afford an opportunity to explain, calculate and predict new crystalline compounds [2], dependences of refractive index, density, the fraction of atoms in different coordination, Kerr coefficient and other properties of glasses and even in the case of glass forming systems characterized by so-called “anomalous” property-composition dependences. It is found that CSG concept made it possible to determine composition of glasses built from CSGs of a single type only (“pseudo single component” glasses) characterized by minimum Rayleigh scattering losses which can be lower than those of silica glass. The latter seems valuable for elaboration of communication fibers and effective Raman amplifiers. Expected correlation between values of Rayleigh scattering losses and band widths of vibrational spectra has been demonstrated for glass formers and multicomponent sodium borate, phosphate, silicate and germanate glasses enriched in CSGs of a single type.

Analysis of Raman scattering spectra of sodium-potassium “disilicate glasses” doped with niobium oxide evidenced that the intensity of the vibration band at 600 cm^{-1} related to the Nb–O–Nb bridging bonds in CSG $Na_2O{\cdot}Nb_2O_5$ clusters correlates to Kerr coefficient of the glasses. This result may be used for designing novel glasses with the record of Kerr coefficient and for manufacturing of electrooptical fibers and glass ceramics [3].

This work was supported by grants from the RFBR (Projects N09-03-00755-a, N10-03-00323-a).

References

1. O. V. Yanush, T. S. Markova “New interpretation of oxide glasses properties on the basis of constant stoichiometry groupings (CSG) concept” in the book "Properties and Structure of Oxide Glasses" (Editors: Valentin P. Klyuev and B.Z. Pevzner), Resarch Signpost, 2010. P. 1 – 44.
2. I. E. Apakova, V. K. Goncharuk, I. G. Maslennikova, I. G. Polyakova, A. V. Anan’ev, L. V. Maksimov, T. S. Markova, O. V. Yanush. Glass Phys. and Chem. **36,** 637 (2010).
3. A. A. Lipovskii, Yu. Kaganovskii, V. G. Melehin, D. K. Tagantsev, O. V. Yanush, J. Non-Cryst. Sol. **354**, 1245 (2008).

PO-23

The Nature of the Color Centers in KDP Crystals

Baltabekov A.S., Tagaeva B.S., Koketajtegi T.A., Kim L.M.

Karaganda State University, Kazakhstan

The KDP (KH_2PO_4) crystals obtain color after irradiation by UV-radiation or X-rays. This is due to the formation of defects. Currently in KDP crystals the following radiation defects are established to form: the self-trapped holes (B-radicals, $H_2PO_4^0$), holes with hydrogen vacancy (A-radicals, HPO_4^-), interstitial atoms of hydrogen (H_i^0) and PO_3^{2-} ions [1]. The radiation induced absorption bands at temperature of liquid nitrogen have maxima at 230 nm, 390 nm and 550 nm (5.39 eV, 3.18 eV, 2.25 eV). In [2] it is suggested that absorption bands at 3.18 eV, 2.25 eV are associated with B-radicals. The nature of the absorption band at 5.39 eV was not established.

We obtained absorption spectra for pure KDP monocrystals at 80K before and after irradiation by X-rays. The results agree well with the data in [2]. In the figure the thermodiscoloration curves for all radiation induced absorption bands are shown.

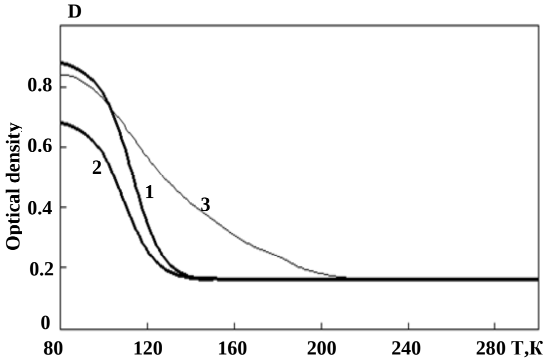

Fig. 1.The curves of thermodecolouration absorption bands with maxima at 2.26 эВ (1), 3.17 эВ (2) and 5.75 эВ (3)

It is clear that the radiation induced absorption bands with maxima at 2.26 эВ and 3.17 эВ are annealed in 110-130K range of temperatures, and with a maximum at 5.75 эВ – at about 200K. Comparison of these curves to the data on EPR [1] allows to establish that absorption bands at 2.26 эВ and 3.17 эВ are caused by B-radicals, and 5.75 эВ – by interstitial atoms of hydrogen. Thermoannealing of absorption bands at 140K allows to reveal an additional absorption band with a maximum at 2.8 эВ. We assume that it is associated with PO_3^{2-} ions. We also suggest the mechanisms of recombination of radiation defects.

References

1. Chirila M. M., Garces N. Y., Halliburton L. E., Demos S. G., Land T. A., Radousky H. B. Production and thermal decay of radiation-induced point defects in KD_2PO_4 crystals// J. Appl. Phys. – 2003. - Vol.94, № 10.- P. 6456-6462.
2. Dieguez E., Cabrera J.M., Agullo-Lopez F. Radiation-induced absorption in KDP crystals///J. Chem. Phys. – 1984. – Vol.81, №8. – P. 3369-3373.

PO-24

Temperature Dependent Raman Study of $NiWO_4$

N. Mironova-Ulmane[1], A. Kuzmin[1], I. Sildos[2]

[1]Institute of Solid State Physics, University of Latvia, Latvia

[2]Institute of Physics, University of Tartu, Tartu, Estonia

e-mail: nina@cfi.lu.lv

$NiWO_4$ belongs to a group of the isomorphous series of tungstates MWO_4 (M=Mg, Cd, Mn, Fe, Co, and Zn) with the monoclinic wolframite structure [1]. Below 67 K, $NiWO_4$ undergoes cooperative transition to antiferromagnetically ordered state [2]. The lattice dynamics of $NiWO_4$ has been studied in the past by Raman spectroscopy at room temperature [3] and interpreted using the first principles calculations [4].

In this work we have performed the Raman scattering study (excitation by 830 nm) of polycrystalline $NiWO_4$ from 10 K to 300 K. It was found for the first time that a set of new peaks at about 570, 790, 1030, and 1090 cm^{-1} appears in the Raman signal below 90 K. The origin of new peaks and their relationship to the magnetic structure in $NiWO_4$ will be discussed.

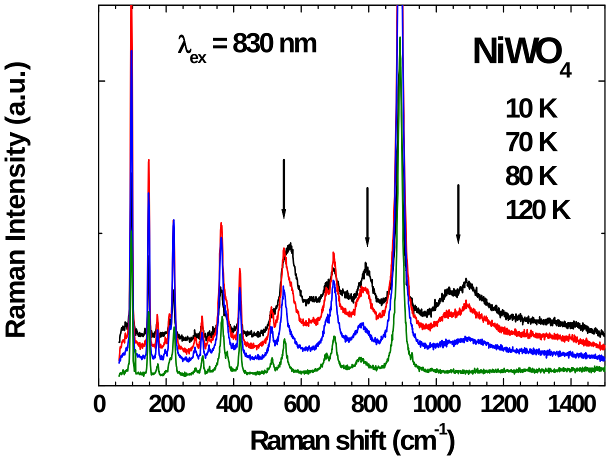

Fig. 1. Temperature dependent Raman spectra of polycrystalline $NiWO_4$

References

1. A. W. Sleight, Acta Crystallogr. B 28, 2899 (1972).
2. H. Weitzel, Solid State Commun. 8, 2071 (1970).
3. A. Kuzmin, J. Purans, R. Kalendarev, Ferroelectrics 258, 21 (2001).
4. A. Kuzmin, A. Kalinko, R.A. Evarestov, Cent. Eur. J. Phys. (2011).

PO-25

Study of Iron Proteins in Blood of Chernobyl Clean-Up Workers by EPR

M. Polakovs[1], N. Mironova-Ulmane[1], A. Pavlenko[1], T. Zvagule[2], N. Kurjane[2], N. Gabrusheva[2]

[1]Institute of Solid State Physics, University of Latvia, Latvia

[2]Centre of Occupational and Radiological Medicine of P.Stradins Clinical University Hospital, Latvia

e-mail: nina@cfi.lu.lv

In the present work we report results of investigations of iron proteins (methemoglobin, transferring) in blood of Chernobyl clean-up workers by EPR (Electron paramagnetic resonance) spectroscopy. EPR can detect the concentration of methaemoglobin and transferrin ions of more accurately than any other technique [1]. The samples of venous blood were received from the Center of Occupational and Radiological medicine of P.Stradins Clinical hospital of Latvia, where Chernobyl “liquidators” are examined. Retrospective dosimetry was performed for all Chernobyl clean-up workers donated blood for our study as well [2,3].

The EPR spectra of frozen blood were measured on a BRUKER EMX-6/1 spectrometer equipped with an Aspect 2000 data system. The EPR signal intensities in blood were measured against fixed standard signals using the standard crystal MgO (Cr^{3+}) placed in resonant cavity.

These processed data show that methemoglobin and transferrin levels in the blood of Chernobyl clean-up workers is above normal. Methemoglobin or (ferric form of hemoglobin) is the form of hemoglobin, when iron Fe^{2+} in the heme is oxidized to the Fe^{3+} ferric state and this form of hemoglobin is not able to bind oxygen. We assume that ion Fe^{2+} heme hemoglobin is oxidized to the Fe^{3+} in heme by radiation.

References

1. M.K. Pulatova, V.L. Sharygin, T.G. Shlyakova, etc., Biofizika, 2009, Vol. 54, No. 2, pp. 323–333.
2. N. Mironova-Ulmane, M. Polakovs, A. Pavlenko, D.Riekstina, T. Zvagule, etc. Proc. Of the 5th International Conference on Medical Physics 2007, KTU, pp. 55-59. ISNN 1822-5721
3. Mironova-Ulmane N, Pavlenko A, Zvagule T etc al. (2001) Radiat. Prot. Dosim. 96:237-240

PO-26

The Luminescence of BiI_3 Nanoclusters Embedded in CdI_2 Layered Crystals

I.D. Karbovnyk[1], V.M. Lesivtsiv[1], I.M. Bolesta[1], S.R. Velgosh[1], I.M. Rovetsky[1], V. Pankratov[2], A.I. Popov[2]

[1]Ivan Franko National University of Lviv, Department of Electronics, 107 Tarnavskogo str., Lviv, 79017, Ukraine
[2]Institute of Solid State Physics, University of Latvia, Kengaraga 8, 1063 Riga, Latvia
e-mail: popov@ill.fr

Cadmium iodide single crystals, CdI_2, belong to the class of compounds having layered structure. These crystals can be considered as two-dimensional systems and their investigations are important for the physics of low-dimensional structures. Besides that, CdI_2 also has relevance from the practical point of view as a prospective scintillator with subnanosecond luminescence decay time for use in electromagnetic calorimeters. Cadmium clusters in CdI_2 layered crystals and their influence on the optical properties were recently reported in [1,2].

Here, we will present the results of the comprehensive study of BiI_3 nano-inclusions in cadmium iodide layered crystals. AFM, SEM and spectroscopic investigation were performed in order to analyze cluster morphology and the effect of nanoclusters on the luminescent properties of the host crystal. Obtained CdI_2:BiI_3 crystals contain 1 mol. percent of BiI_3 phase which is inhomogeneously distributed over the sample volume. Samples, where BiI_3 content is higher, are dark red while those with less BiI_3 phase content are yellow. Microphotographs of the obtained crystals confirmed the luminescence from small areas (clusters) with linear dimensions of several microns. Optical absorption study indicated that several absorption peaks are present in the spectra of dark red crystals and yellow crystals do not exhibit such absorption bands. Absorption bands in crystals with higher BiI_3 concentration exhibit slight dependence on temperature. We have also observed two emission peaks at 2.1 eV and 3.1 eV in the luminescence spectra of CdI_2:BiI_3 crystals. Their origion will be discussed. In conclusion, both direct observations and spectroscopic studies show the influence of embedded clusters on light emission and absorption processes in BiI_3 doped CdI_2.

References

1. S. Bellucci, I. Bolesta, M. Cestelli Guidi, I. Karbovnyk, V. Lesivtsiv, F. Micciulla, R. Pastore, A.I. Popov, and S. Velgosh, Cadmium clusters in CdI_2 layered crystals: the influence on the optical properties. - J. Phys.: Cond. Matter, 2007, **19**, 395015 (p. 1-9).
1. Bolesta, S. Velgosh, Yu. Datsiuk, I. Karbovnyk, V. Lesivtsiv, T. Kulay, A.I. Popov, S. Bellucci, M. Cestelli Guidi, A. Marcelli, and M. Piccinini, Optical, infrared and electron-microscopy studies of metallic clusters $(Cd_i)_n$ in layered CdI_2 crystals. - Radiation Measurements, 2007, **42**, p. 851-854.

PO-27

Luminescence Properties of $BaZrO_3$ Perovskites under Synchrotron Radiation

A.I. Popov[1], V. Pankratov[1], D. Jakimovicha[1], E. Klotins[1], L. Shirmane, A. Kotlov[2]

[1]Institute of Solid State Physics, University of Latvia, 8 Kengaraga, LV-1063 Riga, Latvia

[2]HASYLAB, DESY, Notkestrasse 85, D-22761 Hamburg, Germany

e-mail: popov@ill.fr

The perovskite-type ternary oxide $BaZrO_3$ is materials of relevance in various fields of technology. Its refractory properties are of importance for high temperature applications, such as in the form of thermal barrier coatings. When it is appropriately doped, it has gained attention as potential high temperature proton conductors with applicabilities in fuel cells or hydrogen sensors. Zirconates in particular are used as insulators in the electroceramic industry and are gaining importance for heterocatalysis.

The purpose of this talk is to report new data of the luminescence properties of $BaZrO_3$ under synchrotron radiation.

Luminescence of $BaZrO_3$ were studied under vacuum ultraviolet (VUV) and ultraviolet (UV) synchrotron radiation (3.6 – 25 eV) emitted from DORIS III storage ring at SUPERLUMI station [2], HASYLAB DESY, Hamburg, in the wide temperature range of 10–293 K.

As it is well known, $BaZrO_3$ experimentally determined band gap energy is Eg= 5.3 eV, and thus use of synchrotron radiation provides ideal conditions for the multiplication of electronic excitations, when each absorbed photon produces two or more electronic excitations. To study this effect, we have measured the appropriate excitation spectra of the complex luminescence band (2.15-2.90 eV). In particular, a prominent threshold for excitation multiplication at about 13.5 eV (as high as 2.5 Eg) was discovered. The luminescence results obtained are compared with that obtained under electron irradiation

The experiments at DESY leading to these results have received funding from the European Community’s Seventh Framework Programme (FP7/2007–2013) under Grant agreement #226716.

PO-28

Electronic Excitation and Luminescence of 3C-SiC Pure and Neutron-Irradiated Silicon Carbide

A.I. Popov[1], V. Pankratov[1], V. Bratus[2], A. Kotlov[4]
[1]Institute of Solid State Physics, University of Latvia, 8 Kengaraga, LV-1063 Riga, Latvia
[2]V. Lashkaryov Institute of Semiconductor Physics NASU, Prospect Nauky, 45, 03028 Kyiv, Ukraine
[3]HASYLAB, DESY, Notkestrasse 85, D-22761 Hamburg, Germany
e-mail: popov@ill.fr

Silicon carbide (SiC) is a wide band gap semiconductor suitable for high-voltage, high-power, and high-temperature devices from dc to microwave frequencies. However, elementary processes of multiplication of electronic excitations under irradiation by synchrotron radiation have not been studied yet in these type of the materials. The aim of the present talk is to report on the investigation of multiplication of electronic excitations processes and luminescence in cubic 3C-SiC crystals with theoretically well-studied electronic structure. For these reason the luminescence and excitation spectra of as grown and neutron 3C-SiC as well as the appropriate reflection spectra were studied under vacuum ultraviolet (VUV) and ultraviolet (UV) synchrotron radiation (3.6 – 25 eV) emitted from DORIS III storage ring at SUPERLUMI station, HASYLAB DESY, Hamburg at 10 K.

Results obtained demonstrate that there is clear difference between as grown and neutron-irradiated crystals. Luminescence mechanisms and the appropriate role of neutron-induced defects will be discussed in details. The results obtained are compared with the reflectivity and valence electron-energy loss spectroscopical data. A comparison with the results of electronic structure calculations is also presented.

The experiments at DESY leading to these results have received funding from the European Community’s Seventh Framework Programme (FP7/2007–2013) under Grant agreement #226716.

PO-29

Comparative Study of the Luminescence Properties of Macro and Nanocrystalline Mgo Using Synchrotron Radiation

A.I. Popov[1], V. Pankratov[1], A. Lushchik[2], E. Klotins[1], L. Shirmane[1], V.E. Serga[3], L.D. Kulikova[3], A. Kotlov[4]

[1]Institute of Solid State Physics, University of Latvia, 8 Kengaraga, LV-1063 Riga, Latvia
[2]Institute of Physics, University of Tartu, Riia 142, Tartu 51014, Estonia
[3]Institute of Inorganic Chemistry, Riga Technical University, Salaspils, Latvia
[4]HASYLAB, DESY, Notkestrasse 85, D-22761 Hamburg, Germany
e-mail: popov@ill.fr

Comparative analysis of the luminescent properties of nanocrystalline MgO with macrocrystalline powder analogues and a single crystal has been performed under excitation by pulsed VUV synchrotron radiation. Special attention was paid to VUV spectral range, which is not reachable with commonly used lamp and laser sources.

The nanopowder of magnesium oxide (MgO) was prepared by the extractive-pyrolytic method at the Institute of Inorganic Chemistry, Salaspils. The X-ray diffraction measurements have been performed in order to investigate the crystalline structure and to provide an average crystallite size of nanoparticles (10-15 nm). Single crystals of MgO were grown by the arc-fusion method at the Institute of Physics, Tartu.

Luminescence spectra and the excitation spectra for different emissions have been studied at the SUPERLUMI station of HASYLAB at DESY using synchrotron radiation of 3.6-25 eV from the DORIS III storage ring in a wide temperature range of 10-293 K.

Results obtained show clearly a distinct difference in the excitation spectra for nano- and macrocrystalline samples, especially at the energies exceeding the energy gap E_g .

Differences in the spectral region related to the multiplication of electronic excitations are also demonstrated and discussed.

The experiments at DESY leading to these results have received funding from the European Community’s Seventh Framework Programme (FP7/2007–2013) under Grant agreement #226716.

PO-30

Size Effect and Intrinsic Luminescence of $LaPO_4$ Nanoparticles

V. Vistovskyy[1], A. Voloshinovskii[1], A. Gektin[2], G. Stryganyuk[2], E. Mitina[3], A. Shapoval[3], A. Zaichenko[3]

[1]Ivan Franko National University of Lviv, Ukraine

[2]Institute for Scintillation Materials NAS of Ukraine

[3]National University “Lvivs’ka Politechnika”, Ukraine

e-mail: vistovskii@physics.wups.lviv.ua

The size effects for free excitons which are revealed in the form of quantum confinement, interference of coherent excitons, etc. are well studied for the quantum dots in semiconductors. The conditions for quantum confinement effect manifestation for self-trapped excitons with radius commensurable with cell parameters (≤10 Å) in wide bandgap particles of nanoscale size (5-10 nm) are not satisfied. In a case of wide bandgap insulator particles the size effects connected with relationship between the free path of band charge carriers and nanoparticles size can considerably influence on self-trapped excitons, which are responsible for fundamental absorption edge and intrinsic luminescence of materials [1].

In our work we present low-temperature (10 K) luminescent properties of pure $LaPO_4$ nanoparticles with different size (8-50 nm) studied under vacuum ultraviolet and ultraviolet synchrotron radiation (3.6 – 20 eV) emitted from DORIS III storage ring at SUPERLUMI station, HASYLAB (DESY, Hamburg).

The significant dependence of intrinsic luminescence intensity of $LaPO_4$ nanoparticles on their size and the energy of exciting quanta is observed. Upon the excitation in the range of optical creation of self-trapped excitons the luminescence intensity decreases at the decrease of the nanoparticle size, however this decrease is not so sharp as upon the excitation in the range of recombinational creation of excitons. Practically, the luminescence of self-trapped excitons is not excited by quanta with energies $E_g < E < 2E_g$ for nanoparticles of 8-16 nm size; in the same time the self-trapped exciton emission of low intensity upon the excitation in the range of photon multiplication onset ($E > 2E_g$) is remained yet. The luminescence peculiarities are discussed in the terms of the electron excitation radius, the free path of electrons (holes) and the nanoparticle size.

References

1. V. N. Makhov, Ch. Lushchik, A. Lushchik, M. Kirm, Zhi-Fang Wang, Wei-Ping Zhang, Min Yin, Jing-Tai Zhao. Journal of Luminescence 129 (2009) 1711–1714.

PO-32

Luminescence of Eu^{2+} Doped $LaCl_3$ Microcrystals Embedded into NaCl Host

P.V. Savchyn[1], V.V. Vistovskyy [1], A.S. Voloshinovskii[1], V. Pankratov[2], A. Kotlov[3], A.I. Popov[2]
[1]Physics Department, Ivan Franko National University of Lviv, Ukraine
[2]Institute of Solid State Physics, University of Latvia, Latvia
[3] HASYLAB, DESY, Hamburg, Germany
e-mail: savchynp@gmail.com

In recent years among scintillation materials much research efforts have focused on cerium doped crystals of UCl_3 structure due to their outstanding scintillation properties such as light yield, energy resolution etc. Eu^{2+} doped single crystals also show very high values of light yield (above 100,000 photons per MeV for $SrCl_2$ and SrI_2 hosts) [1].

In our work we present low-temperature (10 K) luminescent properties of $LaCl_3$ microcrystals activated by divalent europium ions embedded in NaCl host, which were studied under vacuum ultraviolet (VUV) and ultraviolet (UV) synchrotron radiation (3.6 – 25 eV) emitted from DORIS III storage ring at SUPERLUMI station, HASYLAB (DESY, Hamburg).

Single crystal of NaCl–$LaCl_3$(1 mol%)–$EuCl_3$(0.1 mol%) composition was grown and annealed by means of technique described in [2]. In that work the feasibility of the formation of $LaCl_3$ microcrystals doped by cerium ions embedded into a NaCl host has also been shown on NaCl–$LaCl_3$–$CeCl_3$ system.

In our case the luminescent spectrum reveals intensive narrow band peaked at 410 nm typical to 5d–4f emission of Eu^{2+} centers in $LaCl_3$ host [3]. At the same time, the absence of the 428 nm photoluminescence band, which is typical to Eu^{2+} centers in NaCl:Eu system, indicates that most of europium ions are entered into $LaCl_3$ microcrystals. The possibility of the determination of divalent europium level location is discussed. Excitation energy transfer mechanisms to Eu^{2+} centers will be explained as well.

References

1. N. J. Cherepy, IEEE Trans. Nucl. Sci. **56**, 873 (2009)
2. V. V. Vistovskyy, J. Phys.: Condens. Matter **20**, 325218 (2008)
3. D. M. Gruen, J. Chem. Phys. **25**, 1102 (1956)

PO-33

Synthesis of Perovskite Photocatalysts by Solid State Reaction Method

L. Grinberga

Institute of Solid State Physics, University of Latvia, Latvia

e-mail: Liga.Grinberga@cfi.lu.lv

Photocatalytic water splitting using solar energy could be one of solutions of environmentally friendly and clean ways of hydrogen production. The basic material for the production of ‘solar hydrogen’ is water that is a renewable resource and on the earth it is enough and easy to access.

However, there are many problems that must be solved before this technology become economically feasible. The choice and synthesis of a photocatalyst material plays a key role in the effective photocatalytic H_2 production. It should be corrosion resistant, chemically stable, visible light harvesting.

Nanoscience and nanotechnology opens different opportunities in the development of highly active, nanostructured photocatalysts with large surface areas and other positive properties. Multi-component metal oxides with perovskite structures like have suitable band structures for visible light water splitting, since more metal elements can contribute to the construction of valence and/or conduction band.

Different additives and synthesis methods allow adjusting bandgap and band positions. There are several ways of band engineering where the most common ones are: cation doping, valence band modification and solid solution formation.

In this work solid state reaction method for nanosized phtocatalyst Ni/$KNbO_3$ is reviewed and the optimisation of the process is discussed.

Acknowledgement: Thanks to European Social Fund project Nr. 2009/0202/1DP/1.1.1.2.0/09/APIA/VIAA/141 for financial support.

PO-34

Photo-Activity Research of Nano-Structured TiO_2 Layers: Influence of Plasmon Light Absorption on Hydrogen Evolution Intensity

J. Kleperis[1], J. Linitis[2], A. Kalis[3], L. Grinberga[1]
[1]Institute of Solid State Physics, University of Latvia, Latvia
[2]Faculty of Chemistry of University of Latvia, Latvia
[3]Faculty of Physics and Mathematics of University of Latvia, Latvia
e-mail: kleperis@latnet.lv

The photocatalytic process is based oh hydrogen/oxygen evolution on oxide electrodes in the water cell under the light of Sun. So far the photocatalytic water splitting has been criticized as being uneconomical compared with other hydrogen production systems, due to its inherently low efficiency [1]. In order to resolve these problems and make photocatalytic hydrogen production feasible, continuous efforts have been made to improve the activity of the photocatalysts employed: growing up TiO_2 nanotube layers; their activation with catalysts etc [2]. Recently Tatsuma et all [3] found the plasmon absorption effect on photocurrent and photopotential of Au25-modified TiO_2 electrodes with related sensitivity shift to visible and NIR region.

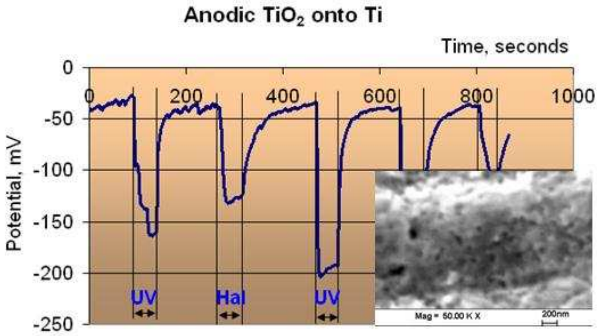

Fig.1 Surface morphology and light sensitivity of anodic TiO2 film.

We obtained nano-structured thin TiO_2 in anodic oxidation process using Ti foil as anode and platinum coated Ti foil as cathode. The electrolyte was composed of 0.14M NaF and 0.5M H_3PO_4 and anodic oxidation was carried out at 20V for 30min with following annealing at 500 ^oC in air. Very thin film of Au was evaporated onto annealed TiO_2 film using thermal vacuum evaporation method and used as plasmon light absorption initiator. Influence of surface plasmon light absorption on hydrogen evolution intensity in cell was studied.

Acknowledgements: Authors acknowledge National Research Program in Energy for support.

LG thanks European social fund project Nr. 2009/0202/1DP/1.1.1.2.0/09/APIA/VIAA/141

References:

1. C. A. Grimes, G.K. Mor, TiO2 Nanotube Arrays. Springer (2009), 379 pages.
2. S. Caramori, V. Cristino, R. Argazzi, L. Meda and C.A. Bignozzi, Inorg. Chem. **49,** 3320 (2010).
3. K. Yu, N. Sakai, and T. Tatsuma, Electrochemistry, **76**, 161 (2008)

PO-35

Catalyst Activation of Silica Based Nano-Pore Structure Material for Hydrogen Storage

L. Grinberga[1], A. Sivars[1], L. Kulikova[2], V. Serga[2], J. Kleperis[1]
[1]Institute of Solid State Physics, University of Latvia, Latvia
[2]Institute of Inorganic Chemistry of Riga Technical University, Latvia
e-mail: ligagr@cfi.lu.lv

Efficient hydrogen storage for on-board automotive applications is not solved yet and much effort has been dedicated to investigate different possibilities for hydrogen storage. Molecular hydrogen can be stored as physisorbed on low weight materials with a large specific surface area, such as: carbon nanotubes, activated carbons, carbide-derived carbons and other carbon nanostructures, alkali-doped carbon nanotubes and nanostructures and metal-organic frameworks [1].

In our experiments we used on SiO_2 based materials – Pyrex and high surface silicate gel. Using extractive pyrolytic method both type samples were coated with 10 wt% of nanosized Pd.

This research presents the results obtained from the study on hydrogen sorption experiments on raw and activated samples. The experiments where made using Sievert’s type *Hy-Energy PCTPro 2000* apparatus at the constant pressure and temperature.

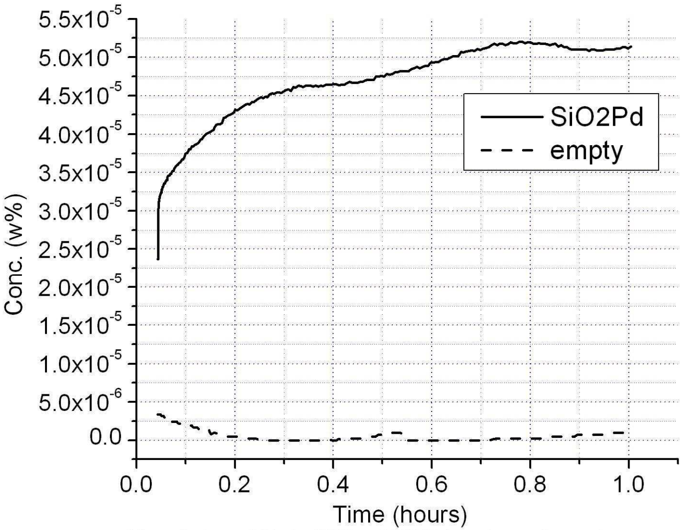

Absorbrion of H_2 in SiO_2 +10%Pd and empty system

Acknowledgements:

Thanks to the State Research Program in Energetics and Research project 09.1553 of Latvian Council of Science for financial support.

References:

1. M. Jordá-Beneyto, F. Suárez-García, D. Lozano-Castelló, D. Cazorla-Amorós and A. Linares-Solano, Carbon **45,** 293 (2007)
2. M. Sprynskyy , R. Golembiewski, G. Trykowski and B. Buszewski, J. Phys. Chem. Solids, **71**, 1269 (2010)

PO-36

Nano-Pore Structure Zeolite Material as Potential Storage Media for Hydrogen Gas

A. Sivars[1], J. Fricsons[2], J. Kleperis[1], L. Grinberga[1]
[1]Institute of Solid State Physics, University of Latvia, Latvia
[2]AdviserUnion Ltd., Latvia
e-mail: ligagr@cfi.lu.lv

Expressed gas adsorption, ion–exchanging capability and catalytic behaviour of different zeolites have made them as an interesting material for different life science, environmental and industrial applications [1]. Zeolites are crystalline aluminosilicate materials with ordered nanometer-scale pores built in network from AlO_4 and SiO_4 tetrahedra network and exchangeable alkaline and alkaline earth metal cations (normally Na^+, K^+, Ca^{2+}, and Mg^{2+}) in addition to water in their structural framework. The physical structure is porous, containing interconnected cavities in which the metal ions and water molecules are contained. Clinoptilolite is one of the natural zeolites used to remove cations such as heavy metals and ammonium ions from aqueous solutions.

Our idea is to test clinoptilolite as potential media for storage the hydrogen and hydrogen-rich gases (ammonia, methane). The loading of molecules into the zeolitic channels were performed in two different ways – using high pressure sorption/desorption equipment PCT Pro2000 and electronic balance Kern. Pore diameter and distribution as well pore volume was determined with nitrogen adsorption method using sorptiometer BET 202A. SEM analysis revealed that clinoptilolite is with lamellar structure. Generally two types of porosities such as primary porosity and secondary one are observed. The primary porosity may be defined as microporosity presented by nanotube system of the clinoptilolite 3-dimensional aluminosilicate framework. The secondary porosity is formed by meso- and macropores, where the first ones are presented by slot pores determined mainly by cleavability of the zeolite crystallites [2]. This research presents the results obtained from the study on dynamic adsorption experiments on raw and acivated zeolite.

Acknowledgements: Thanks to research project 09.1553 of Latvian Council of Science for financial support.

References

1. R.M. Barrer, Zeolites and clay minerals as sorbents and molecular sieves. Academic Press. London. pp. 103-223 (1978)
2. M. Sprynskyy , R. Golembiewski, G. Trykowski and B. Buszewski, J. Phys. Chem. Solids, **71**, 1269 (2010).

PO-39

Material Engineering to Increase the Eddy Currents

I. Dirba[1], J. Kleperis[2]

[1]Faculty of Physics and Mathematics of University of Latvia, Latvia

[2]Institute of Solid State Physics, University of Latvia, Latvia

e-mail: kleperis@latnet.lv

When a conductive material is subjected to a time-varying magnetic flux, Eddy (Foucault) currents are generated in it and generate a magnetic field of opposite polarity as the applied magnetic field. The interaction of the two magnetic fields causes a force that resists the change in magnetic flux. However, due to the internal resistance of the conductive material, the Eddy currents will be dissipated into heat (Joule heating). Conventional domestic water heaters utilize gas burners or electric resistance heating elements to heat the water in the tank and substantial part of the heat that is generated is wasted. The use of electromagnetic induction heating of a liquid could be used to heat water. Another way to use Eddy current is in instruments for the measurement of electrical conductivity. The value of the electrical conductivity of a metal depends on several factors, such as its chemical composition and the stress state of its crystalline structure. Therefore, electrical conductivity information can be used for sorting metals, checking for proper heat treatment, and inspecting for heat damage.

Our idea is to use wind mechanical energy to generate heat. Wind turbine rotor with rotating strong ($B_r \approx 1{,}4T$) NdFeB permanent magnets creates a time-varying magnetic flux inducing Eddy currents in heat exchange camera connected with water boiler. Generated heat power dependence on parameters such as changing magnetic field frequency ω, magnetic field induction B, electrical conductivity of the material σ, charasteristic size of the material are analyzed. Specific material is needed to allow generating of high Eddy currents and quick heat removal. Material evaluation is performed using mathematical modelling. 2 dimensional finite element model is made to compare analytical and numerical results.

Acknowledgements: Authors acknowledge National Research Program in Energy for support. ID acknowledge European Social Fund for financial support.

References

1. J.H. Bell. US Patent 6011245 (2000).
2. S. Caramori, V. Cristino, R. Argazzi, L. Meda and C.A. Bignozzi, Inorg. Chem. **49,** 3320 (2010).
3. K. Yu, N. Sakai, and T. Tatsuma, Electrochemistry, **76**, 161 (2008)

PO-40

Behaviour of Tritium in Carbon Fibre Composites under Action of JET's Plasma

M. Haļitovs[1], G. Ķizāne[1], A. Vītiņš[1], E. Pajuste[1], L. Avotiņa[1], G. Ivanov[1], J. Gabrusenoks[2]

[1]Institute of Chemical Physics, University of Latvia, Riga, Latvia

[2]Institute of Solid State Physics, University of Latvia, Riga, Latvia

e-mail: gunta.kizane@lu.lv

Carbon based materials, such as carbon based fibre composites, are planed as plasma facing materials for future fusion power reactors. Important issues are related to plasma wall interaction processes. The main disadvantage of carbon based materials is its chemical erosion under fuel particle bombardment and accordingly with this the ability to accumulate large quantities of tritium and deuterium also. It is well known that accumulation of plasma fuel components tritium and deuterium is going on a surface and in a volume of divertor tiles. Tritium retention in the divertor tiles is an important issue not only from ecological point of view but also from view of economics. Determination of tritium retention in plasma facing components of the divertor is of high priority in order to understand the mechanisms of fuel retention. Plasma facing components Concept I used as divertor materials of JET are manufactured by Dunlop Ltd and in this study we represented investigations on changes of a fibres of the divertor tile and tritium accumulation in the CFC tile 14 BWG 4B of the MkII-SRP (septum replace plate) divertor of JET exploited in the period 2001-2004. In this period D +D plasma campaign had been realized and tritium had been pushed in the vacuum vessel of JET. Structural changes analysed by SEM have been observed in CFC tile both in toroidal and poloidal directions. A diameter of fibres increases from the middle part of the tile to backside of it up to 30 %. Changes of graphite structure had been observed after exploitation of the tile in vacuum vessel of JET. The characteristic lines of graphite at 1588 cm^{-1} and 1355 cm^{-1} in the Raman spectra change their position and width, a Fourier-transform infrared spectra had been analysed in this study. The highest retention of tritium had been observed on the shadowed part of the tile. Important part (98 – 99 %) of accumulated tritium is located on plasma facing layer (~ 1 mm thickness) of the tile (tritium activity 10^{6} – 10^{8} Bq/g). Relatively small quantities of tritium penetrate deep in the tile. Tritium mass activity in the middle part is ~10^{4} Bq/g and is rather even in poloidal and toroidal direction of tile. A higher tritium activity had been detected on the backside part of the tile (tritium activity 10^{5} – 10^{6} Bq/g), which is caused by erosion material transport beneath tiles through gaps between tiles and technical boreholes within. Observed that thermo-desorption of tritium starts approximately at temperature 473 K, a maximum of release rate are at 923-973K, but tritium release rate decreases very sharply at temperatures above 950 K.

PO-41

Accumulation of Radiolysis Products and Defects in Nanopowders of Lithium Orthosilicate

A. Zarins[1], A. Supe[1], G. Kizane[1], Br. Lescinskis[1], L. Baumane[2], I. Steins[3], A. Berzins

[1]Institute of Chemical Physics, University of Latvia, Riga, Latvia

[2]Institute of Organic Synthesis, Latvia, Riga, Latvia

[3]Institute of Inorganic Chemistry, Riga Technical University, Riga, Latvia

[4]Department of Chemistry, University of Latvia, Latvia

e-mail: gunta.kizane@lu.lv

Lithium orthosilicate has more physico-chemical properties widely used for resolution of some today's technical and future problems. Lithium orthosilicate is foreseen as tritium breeder material for the helium cooled pebble bed (HCPB) blanket being developed in the EU. One of the key parameters of lithium orthosilicate for future fusion reactors is relatively high tritium breeding ratio as lithium density, 0.56 g.cm-^{3}, is good compare with others lithium containing compounds. The second advantage of lithium oprthosilicate is a relatively high possibility to absorb CO_2 (up to 36.7%) from different temperature medium and a selective reaction with CO_2 which is reversible at temperatures higher then 450°C. In this study physico-chemical properties of lithium orthosilicate nanopowders had been investigated under action of moisture. Nanopowders of lithium orthosilicate with particle size 100±10 nm and specific area 24 $m^2 \cdot g^{-1}$ were synthesized in high temperature plasma of nitrogen. Changes of composition of high temperature plasma-synthesized stoichiometric and nonstoichiometric lithium orthosilicate nanopowders depending on heat treatment and air humidity on the basis of thermogravimetric (TG), differential thermal analysis (DTA) and powder x-ray diffractometry (XRD) results are observed. In high temperature plasma synthesized stoichiometric and nonstoichiometric nanopowders of lithium orthosilicate main phase is lithium orthosilicate, but minor phase is lithium metasilicate. Formation of lithium metasilicate in "stoichiometric" nanopowder could be explained by producing of lithium metasilicate as by - product of plasma stage synthesis: Thermally treated (600°C for 2 hours) stoichiometric and nonstoichiometric nanopowders of lithium orthosilicate atmosphere with a reduced (10.5%) and elevated (77.6%) humidity in isothermal condition 19^{o}C up to 10.75 days gradually sorb airborne atmospheric gases - H_2O and CO_2. Absorbed gases in nanopowders of lithium orthosilicate facilitated formation of monohydrate of lithium hydroxide, lithium metasilicate and lithium carbonate. Characteristic reflexes of main phase – lithium orthosilicate and little reflexes of minor phase – lithium metasilicate had been observed in the XRD difractogramms after thermal treatment.

PO-42

Investigations of copper doped thin TiO2 films

U. Joost[1, 2], A. Kikas[1], I. Kink[1, 2], L. Matisen[1], A. Saar[1], V. Kisand[1]

[1]Institute of Physics, University of Tartu, Riia 142, 51014, Tartu, Estonia

[2]Estonian Nanotechnology Competence Center, Riia 142, 51014, Tartu, Estonia

e-mail: urmas.joost@ut.ee

TiO2 has shown great potential as a photocatalyst [1, 2] in various environmental applications. TiO2 also finds use as coating on “self-cleaning” and anti-fogging glasses [3]. The greatest challenge connected with using TiO2 as a photocatalyst is the bandgap, which is 3.2 eV for anatase and 3.0 eV for rutile. This inhibits greatly applications using sunlight, because solar irradiance intensity in this region is relatively low. Therefore great efforts have been made to narrow the band-gap of TiO2, to make use of its good photocatalytic and light induced superhydrophilic properties under visible region more effectively.

In present work copper doping was employed to shift the absorption edge of titanium dioxide to lower energies. The films were prepared using similar sol-gel method as described in our previous work about nickel doped titania films [4].

Hydrophilicity of the films was investigated without additional UV irradiation, in normal laboratory conditions. Good hydrophilic properties (contact angles as low as 5°) were achieved without any additional UV irradiation. Photocatalytic activity of films was estimated using degradation of rhodamine 6G under UV irradiation. Photodegradation experiments showed that pure titania films degrade rhodamine 6G 3-6 times faster than copper doped titania films.

In conclusion it can be stated that copper as a dopant adds an additional absorbance structure prior to the optical absorption edge of anatase and increases hydrophilic properties of titania films, but does not help to improve photocatalytic properties of titania films under UV irradiation.

References

1. Jean-Marie Herrmann, Heterogeneous photocatalysis: fundamentals and applications to the removal of various types of aqueous pollutants, Catalysis Today 53, 115-129, (1999).
2. K . Osunada, Y. Kikuchi, K. Hashimoto, A. Fujishima, Bactericidal and detoxification effects of TiO2 thin film photocatalysts, Environmental Science & Technology 32, 726-728, (1998).
3. T. Watanabea, A. Nakajimaa, R. Wanga, M. Minabea, S. Koizumia, A. Fujishima, K. Hashimotoa, Photocatalytic activity and photoinduced hydrophilicity of titanium dioxide coated glass, Thin Solid Films 351, 260-263, (1999).
4. V. Kisand, U. Joost, V. Reedo, R. Pärna, T. Tätte, J. Shulga, A. Saar, L. Matisen, A. Kikas, I. Kink, Influence of the heating temperature on the properties of nickel doped TiO2 films prepared by sol–gel method, Applied Surface Science 256, 4538–4542, (2010).

PO-43

Preparation and Photocatalytic Activity of Modified TiO_2 Nanotubes

R. Drunka, J .Grabis, Dz. Jankoviča, A. Patmalnieks
Institute of Inorganic Chemistry of Riga Technical University, Latvia
e-mail: reinis_drunka@inbox.lv

Titanium dioxide is very promising material for photocatalysts, decomposition of organic compounds, splitting of water, for manufacturing self-cleaning materials and dye- sensitized solar cells. It is generally concluded that the photocatalytic activity depends on the specific surface area, degree of crystallization of the titania particles, phase composition and presence of dopants, which promotes absorption of visible light. In recent years considerable efforts was directed forwards preparation of TiO_2 nanotubes. Despite the considerable number of papers, there is lack of investigation about photoactivity of TiO_2 nanotubes, especially in the presence of dopants.

In this paper the characteristics of TiO_2 nanotubes and their photocatalytic activity were studied by varying conditions of anodization of Ti foil and introduction made of N_2 and WO_3 dopant.

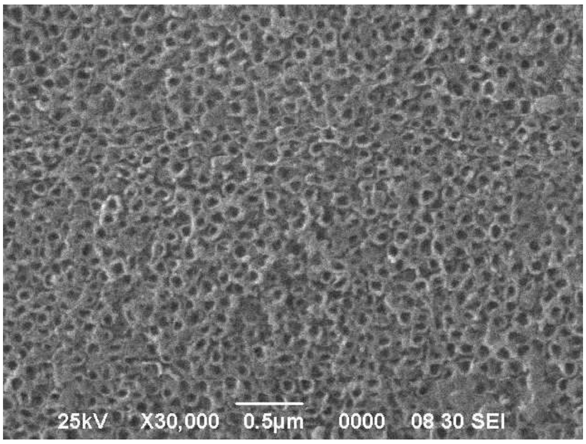

Fig1. Micrograph of TiO_2 nanotubes layer

Self-organized TiO_2 nanotube-layers were formed by electrochemical anodization of titania foil in a $(NH_4)_2SO_4$/HF electrolyte. The prepared by anodization TiO_2 nanotubes were fully X-ray amorphous. The crystalic anatase nanotubes with diameter about 30-250 nm and length about 7–9 μm (*Fig.1*) were obtained after additional calcination at 500 ^oC during 2 h.

Doped with WO_3 nanotubes were prepared by additional anodization in peroxotungstic acid sol and ethanol-water electrolyte or by anodization of Ti foil rubbed with W powder in $(NH_4)_2SO_4$/HF electrolyte. The doped with nitrogen nanotubes were obtained by their treatment at 500 ^oC per 2h in NH_3or N_2 flow.

The catalytic activity was determined by degradation of MB solution under UV and visible light illumination.

References

1. A. Benoit, I. Paramasivam, Y.-C. Nah, P. Roy, P. Schmuki, Electrochemistry Communications 11 (2009) 728–732
2. Yan Wang, Caixia Feng, Zhensheng Jin , Jiwei Zhang, Jianjun Yang, Shunli Zhang, Journal of Molecular Catalysis A: Chemical 260 (2006) 1–3

PO-44

Examination of Different Approaches to LiFePo4 Thin Film Laser Annealing

J. Smits, A. Sarakovskis, G. Bajars, L. Grinberga, J. Kleperis

Institute of Solid State Physics, University of Latvia, Latvia

e-mail: smitsjanis@gmail.com

As electronic appliances increase in functionality and decrease in size, the energy storage systems that power them must follow suite. LiFePO4 batteries are becoming increasingly popular due to the material's high charge/discharge capability and excellent electrochemical properties. Recently a lot of attention has been directed to the properties of material when deposited in thin layers either by magnetron sputtering [1] or laser ablation [2], and the texture effects of said material. One of the chief issues of LiFePO4 thin layers which still remains to be solved is the poor electrochemical performance of as-deposited layers due to low crystallinity.

In this research laser crystallization has been examined as a perspective alternative to thermal annealing. LiFePO4 thin films with varying carbon content deposited via magnetron sputtering were annealed with UV/visible laser light using varying power density and scan speed. To increase the visible light absorption of the thin films attempts were made to exploit surface plasmon resonance by depositing a 20 nm Ag layer obtained via thermal evaporation [3].

The structure and morphology of the thin films were examined with SEM and XRD analysis. Electrochemical analysis of the annealed thin layers was performed in a LiFePO4/LiClO4/Li cell with a Li reference electrode, voltampere and charge/discharge curves were analyzed.

Acknowledgements: Thanks to National Research Program in Materialscience and Informatics for financial support.

References

1. K.-F. Chiu, P.Y. Chen, Surface & Coatings Technology 203 (2008) 872–875
2. C. Legranda, L. Duponta, K. Tang, H. Li, X.J. Huang and E. Baudrin, Thin Solid Films 518 (2010) 5447–5451
3. Kuang-Che Lee, Su-Jien Lin, Chih-Hong Lin, Chih-Song Tsai and Yu-Jen Lu, Surface & Coatings Technology 202 (2008) 5339–5342

PO-45

Lithium-Ion Intercalation Rate Dependence on Preparation Conditions of $LiFePO_4$ Thin Films

G. Bajars, G. Kucinskis, J. Smits, J. Kleperis
Institute of Solid State Physics, University of Latvia, Latvia
e-mail: gunars.bajars@gmail.com

To modify the properties of $LiFePO_4$/C thin films they have been deposited on Si and stainless-steel substrates by radio frequency magnetron sputtering using different sputtering conditions (residual pressure, bias voltage, discharge power) and subsequent annealing in argon atomsphere (500–700 °C). It is known that suitable preparation conditions resulted in films with finer grains and pure olivine phase [1]. Obtained results showed that $LiFePO_4$/C thin films deposited at higher power exhibited reduced crystallization, grain sizes and conductivity as compared with films deposited at lower power. Higher sputtering power lead to dense-packed film structure composed from granular crystals (Figure 1). Film cracking was observed after annealing in argon atmosphere at 700 ^{o}C, but lower annealing temperatures don`t revealed improved crystallinity. Charge-discharge and cyclic voltammetry curves were measured in three electrode cell. The films with higher crystallinity displayed higher initial charge capacity than those without annealing or annealed at temperatures around 500 °C. However, the cycling stability is greatly improved for denser films. This probably indicates on the importance of the mechanical strains at the substrate - $LiFePO_4$/C thin film interface on the film structural modifications and cycling stability [2].

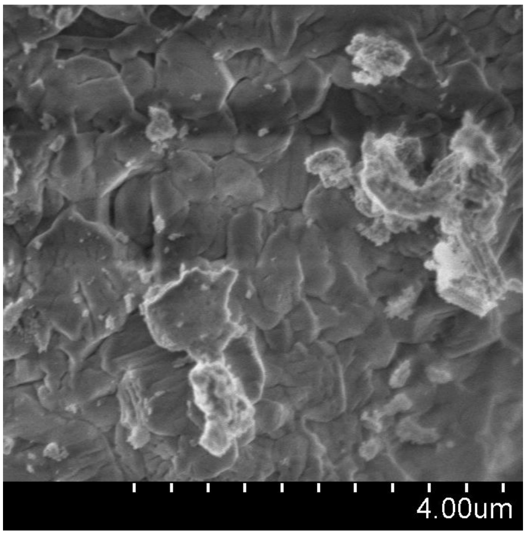

Fig.1 SEM image from $LiFePO_4$ thin film with characteristic granular structure.

References

1. J. Sun, K. Tang, X. Yu, H. Li and X. Huang. Thin Solid Films **517**, 2618 (2009)
2. F. Sauvage, L. Laffont, J.-M. Tarascon and E.Baudrin. J. Power Sources **175**, 495 (2008)

PO-46

Epitaxial CVD Growth of Hexagonal Boron Nitride Using Aluminum Nitride as a Buffer Layer

M. Chubarov, H. Pedersen, H. Högberg, A. Henry
Department of Physics, Chemistry and Biology, Linköping University, Sweden
e-mail: mihails.cubarovs@liu.se

Boron nitride (BN) is a promising material for various applications, such as optical devices in the UV–range, surface acoustic wave devices and insulating coatings. Hexagonal boron nitride (hBN) has interesting properties such as good electrical resistance, wide band gap (~ 6 eV) [1, 2], low dielectric constant, piezoelectricity and good stability at high temperatures [3]. Further, hBN can easily be doped p- and n-type for electronic applications. However, hBN is, perhaps, the less investigated material of the group III nitrides. In this study growth of hBN using CVD (without plasma or other enhancements besides heat) with the precursor gases NH_3 and triethyl boron (TEB), using (0001) sapphire as substrate is presented. The typical growth pressure was 100 mbar, the temperature in the range 1300 – 1500 °C and the N/B-ratio between 600 – 1000 by applying an AlN buffer layer. An AlN buffer layer was formed by nitridization [4] of the sapphire surface by introducing NH_3 into the reaction chamber at growth temperature and 10 minutes before introducing TEB. The AlN buffer layer circumvents the formation of less ordered hBN, so called turbostratic BN (tBN). The characterization of the grown films was done by X-Ray diffraction (XRD), high resolution XRD (HR XRD), Raman spectroscopy, photoluminescence (PL) and Elastic Recoil Detection Analysis (ERDA). XRD measurements in the θ – 2θ configuration showed (0001) oriented hBN (Fig. 1) and HR XRD confirmed epitaxial growth. High growth temperatures (1600 °C) lead to polycrystalline AlN, which prevents growth of hBN.

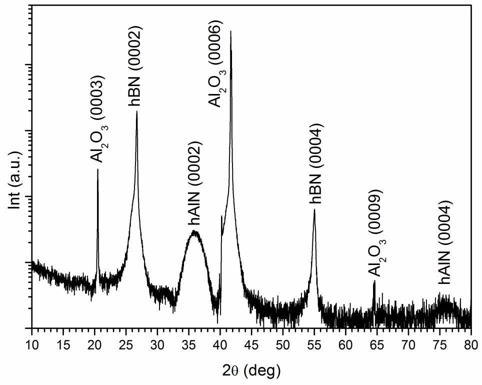

Fig. 1 XRD of hBN sample grown on the sapphire with AlN buffer layer

References

1. M. G. Silly *et al.*, Phys. Rev. B 75, 085205 (2007)
2. Y. Kobayashi *et al.*, J. Crystal Growth 298, 325 – 327 (2007)
3. S. Zhang *et al.*, J. Crystal Growth 223, 545–549 (2001)
4. K. Akiyama *et al.*, J. Crystal Growth 311, 3110–3113 (2009)

PO-47

Characterization of the Phase Composition and Structure of Electrodeposited Nanostructured Magnetic Ni-Fe Alloys for Different Electrodeposition Processes

I. Vītiņa, A. Krūmiņa, M. Lubāne, V. Belmane
Institute of Inorganic Chemistry, Riga Technical University, Latvia
e-mail: nki@nki.lv

Sputtered Ni-Fe (81±0.5) alloy layers do not have uniform nonporous structure. Therefore, a topical issue is electrodeposition of these alloy layers. Using simple-salt electrolyte (E1) and complex potassium pyrophosphate electrolyte (E2) in the presence of an inorganic reducer, which prevents oxidation of Fe^{2+}. Ni-Fe alloy layers (thickness 0.5-1.5 μm) containing 75-85 wt.% Ni were electrodeposited. From electrolyte E1 at pH 1.5-1.75 and the cathode current density j - 1.2 A/dm^2, the Ni content in the Ni-Fe alloy was 79.7-81.1 wt.%. From electrolyte E2 at pH 7.4-7.6 and j - 0.6-0.8 A/dm^2, the Ni content in the Ni-Fe alloy was 79.4-80.5 wt.%. X-ray diffraction studies with a Bruker D8 ADVANCE diffractometer with DIFFRAC Plus Evaluation software (Package Release 2007-EVA V13) determined the fact that the Ni-Fe alloys electrodeposited from both electrolytes E1 and E2 approximately correspond to $FeNi_3$ compound with the crystal size 10-15 nm. Structural studies with a JOEL 100S transmission electron microscope showed that the Ni-Fe layers containing 76.4-85.1 wt.% Ni had a globular structure, which is characteristic of amorphous layers. The relief of the globular structure depends on the electrolyte composition and the cathode current density.

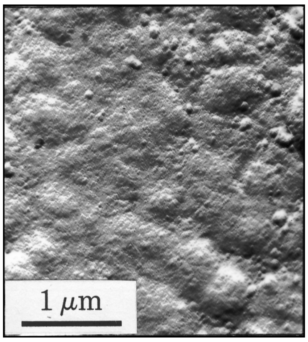

a) E1 Fe-Ni (80.9) pH 1.6; j-1.0 A/dm^2

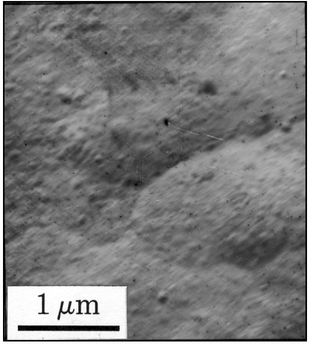

b) E2 Fe-Ni (80.9) pH 7.5; j-1.7 A/dm^2

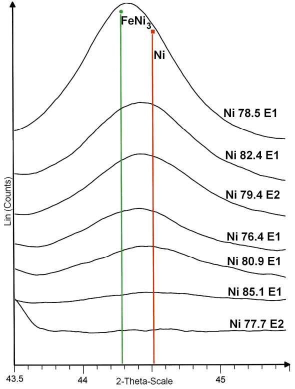

c)

Fig.1 Fe-Ni structures (a, b) and XRD patterns (c)

PO-48

Studies of Radiation Defect EPR Hyperfine Structure in Oxyfluoride Glass Ceramics

Dz. Berzins, A. Fedotovs, U. Rogulis
Institute of Solid State Physics, University of Latvia, Latvia
e-mail: dzb@inbox.lv

This work presents electron paramagnetic resonance (EPR) studies of the oxyfluoride composites based on alkaline silicate glasses with nanostructured fluoride compounds, obtained at the Institute of Solid State Physics of University of Latvia. Glass ceramics exhibit interesting properties as host materials for up-conversion processes related effects [1, 2] and also could be used as storage phosphors [3].

The aim of the work was to study radiation induced defects in nanocrystals embedded in the oxyfluoride glass matrixes. Radiation defects produced in nanocrystals could potentially affect optical performance of these materials. We used EPR techniques to investigate structure of these defects and location in particular crystalline structures. EPR spectra were measured prior and after X-ray irradiation at room temperature and at 77 K.

There are obvious differences between EPR signal in oxyfluoride glass material and in the glass-ceramics. Radiation induced defects in oxyfluoride glass ceramics, in which crystallites have not been yet created, show no explicit EPR hyperfine (*hf*) interaction related spectra. However, in glass ceramics, which already contains fluoride crystallites, the *hf* structure characteristic to fluorine nuclei appears in the EPR spectra. The preliminary analysis of the experimental spectra left several questions unanswered [4]. In the present work observed EPR spectra have been analysed in more details, and their further interpretation will be discussed.

References

1. M. J. Dejneka, MRS Bulletin **23,** 57 (1998)
2. D. Chen, Y. Wang, Y. Yu, E. Ma, F. Bao, Z. Hu and Y. Cheng, Mater. Chem. Phys. **95,** 264 (2006)
3. A. Edgar, G.V.M. Williams, P.K.D. Sagar, M. Secu, S. Schweizer, J.-M. Spaeth, J. Hu, P.J. Newmann and D.R. MacFarlane, J. Non-Cryst. Sol. **326&327,** 489 (2003)
4. A. Fedotovs, U. Rogulis, A. Sarakovskis and L. Dimitrocenko, J. Phys.: Conf. Ser. **249**, 012019 (2010)

PO-49

Low Temperature Measurements by Infrared Spectroscopy in $CoFe_2O_4$ Ceramic

R. Bujakiewicz-Korońska[1], Ł. Hetmańczyk[2], B. Garbarz-Glos[1], A. Budziak[3], A. Kalvane[4], K. Bormanis[4]

[1]Pedagogical University, Institute of Physics, Podchorążych 2, 30-084 Cracow, Poland
[2]Jagiellonian University, Faculty of Chemistry, Ingardena 3, 30-060 Cracow, Poland
[3]The H. Niewodniczański Institute of Nuclear Physics PAN, 31-342 Cracow, Poland
[4]Institute of Solid State Physics, University of Latvia, Kengeraga 8, LV-1063, Riga, Latvia
e-mail: rbk@up.krakow.pl

Spinel cobalt ferrite $CoFe_2O_4$ (CFO) ceramic belongs to class of magnetic materials. This kind of materials attract attention due to its possible wide applications in the future. CFO sample was obtained by a conventional method from high purity reagents. The performed EDS study revealed that the sample was perfectly sintered and chemically homogeneous. The EPMA investigations confirmed its high quality. It hardly contains glassy phase and its grains are well shaped. The average values of grain size (measured by the linear intercept method) is 0.8 μm. X-ray studies were carried out using an X'Pert PRO (PANalytical) diffractometer with the CuK_α radiation and a graphite monochromator.

The sample CFO persists the cubic structure (sg. Fd-3m) in the temperature range 85- 360 K without any traces of distortion. Lattice parameter grows from 8.3757 Å at 85 K up to 8.3901 Å at 360 K, which corresponds to the change of the unit cell volume ~ 0.5%.

There was employed the infrared spectroscopy (wavenumber range of 4000 –400cm^{-1}) in order to investigate low temperature phase transitions in CFO ceramic sample. The middle infrared spectra collected in the temperature range of 300 ÷ 8 K were measured with Bruker VERTEX 70v vacuum Fourier Transform spectrometer. The powder sample was prepared as KBr pellet. CFO was cooled from 300 K at the constant rate of 3 K/min to desired temperature and then stabilized for ca. 3 minutes at this chosen temperature before the spectrum was measured. The band positions and its shape are the same in the wide temperature range. On the current level of knowledge the polycrystalline CFO does not exhibit phase transition in the temperature range from 300 to 8 K.

Acknowledgements

The research (FT-MIR) was carried out with the equipment purchased thanks to the financial support of the European Regional Development Fund in the framework of the Polish Innovation Economy Operational Program (contract no. POIG.02.01.00-12-023/08).

PO-50

The Effect of Radiation Modification and Uniform Magnetic Field on Deformation Properties of Polymer Composite Blends

I. Reinholds[1], V. Kalkis[1], R.D. Maksimovs[2], J. Zicans[3], R.M. Meri[3], T. Ivanova[3]
[1]Faculty of Chemistry, University of Latvia, Latvia
[2]Institute of Polymer Mechanics, University of Latvia, Latvia
[3]Institute of Polymer Materials, Riga Technical University, Latvia
e-mail: Valdis.Kalkis@lu.lv

An experimental study of radiation-modified blends of high-density polyethylene (PE) and chlorinated polyethylene (CPE) exposed at constant magnetic field with induction B equal to 0.7, 1.0, 1.4 and 1.8 T is presented. Preliminary irradiation has been done using γ-radiation absorbed doses equal to 50, 100 and 200 kGy. The main focus of this research is devoted on deformation (elastic and viscoelastic) properties of the material. The gained data show the effect of the absorbed dose of γ-radiation and magnetic field induction on the modulus of elasticity E and creep ε of the investigated polymer composite PE/CPE with m.% ratio 80:20 under the influence of constant tension. It is shown that at the induction B=1.8 T the value of E decreases 1.25 times for the non-irradiated composite. Increasing the absorbed dose of γ-radiation up to 200 kGy the value of E remains almost constant, in contrast to the non-irradiated samples, at induction in the range of 0.5 to 1.8 T. A significant effect of the magnetic field on the creep of non-irradiated material is determined and is in accordance with several investigations [1, 2]. Pre-radiation modification minimizes the effect of the magnetic field on the creep.

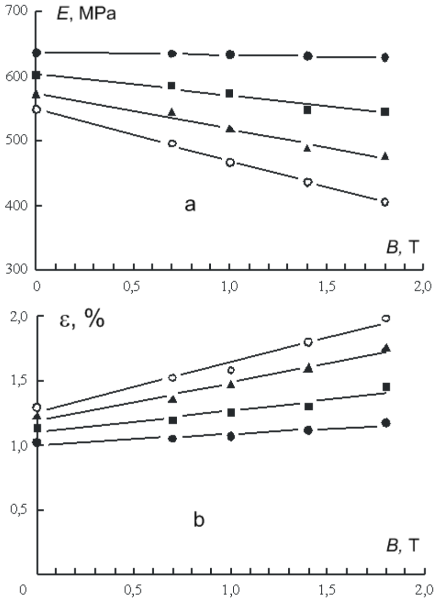

Fig.1. Dependence of the modulus of elasticity E (a) and creep ε (b) on the magnitude of induction of uniform magnetic field B for non-irradiated (o) and γ-irradiated samples (absorbed doses: 50 (▲), 100 (■) and 200 (•) kGy) of polymer blends PE/CPE

References

1. J. P. Rodin, Mechanics of Composite Materials, **3**, 490 (1991)
2. N. N. Peschanskaya, A. B. Sinani, Physics of the Solid State, **50** (1), 182 (2008)

PO-51

NMR Investigations of Hydrogen Intercalates of GaSe and InSe Layered Crystals

Y.I. Zhirko[1], Z.D. Kovalyuk[2], V.V. Trachevskii[3]
[1]Institute of Physics, National Academy of Sciences of Ukraine, Ukraine,
[2]Chernivtsi Department of Institute for Materials Science Problems, NAS of Ukraine, Ukraine,
[3]Institute for Physics of Metals, NAS of Ukraine, Ukraine
e-mail: zhirko@nas.gov.ua

Temperature (295÷380K), polarized ($\boldsymbol{B}\perp\boldsymbol{C}$, $\boldsymbol{B}\parallel\boldsymbol{C}$, where orientation of magnetic field $\boldsymbol{B}$ according to optical $\boldsymbol{C}$-axis) as well as concentration ($\boldsymbol{x}$=0÷4.0, where $\boldsymbol{x}$ means amount of hydrogen atoms in one formula unit of the crystal) NMR investigations (NMR spectrometer Bruker Avance***TM*** 400) of H_XGaSe and H_XInSe hydrogen intercalated GaSe and InSe single crystals and their powder enabled us to confirm the model developed in [1] that describes presence of hydrogen in these layered compounds as interlayer and intralayer particles being predominantly in the H_2 molecular state. There are two clearly pronounced bands in H_XGaSe powder spectra [2], which are split by slightly polarized pair of doublets in the case of H_XGaSe single crystals. With increasing the temperature up to 380K (at temperatures under 390K and permanent pumping down hydrogen is really deintercalated from InSe layered crystals [1]), one can observe a reverse proportion in the temperature dependence both of the energy shift and band splitting, which is indicative of the increased mobility of H_2 molecules inside intralayer and interlayer spaces of GaSe crystal. And vice versa, growth of the hydrogen concentration $\boldsymbol{x}$ results in the increased energy shift and band splitting, which testifies the growing influence of crystalline field on hydrogen molecules and preservation of their rigid orientation relatively to magnetic field $\boldsymbol{B}$.

The increase of a lattice parameter and interlayer space that take place in InSe according to GaSe single crystals resulted in increasing of a half-width of H_2 bands in NMR spectra and to reduction of their chemical shift and splitting. It is also indicative that compare to GaSe crystal reduction of a crystal field influence on H_2 molecules in InSe crystal increased their mobility inside intralayer and interlayer spaces.

References

1. Yu. I. Zhirko, Z. D. Kovalyuk, M. M. Pyrlja, V. B. Boledzyuk// in book "Hydrogen Materials Science and Chemistry of Carbon Nano-materials", P. 325, © 2007 Springer.
2. Yu. I. Zhirko et all// Proc. of the 15-th Int. Conf. "Hydrogen Economy and Hydrogen Treatment of Materials",Donetsk, May 21-25, V.2, P. 606, 2007.

PO-52

Gradient Composite Metal-Ceramic Foams with Controllable Physical Properties as Supportive Component for SOFCs and MIEC Membranes

O. Smorygo[1], V. Mikutski[1], A. Marukovich[1], V. Sadykov[2], V. Usoltsev[2], N. Mezentseva[2],
A. Borodinecs[3]
[1]Powder Metallurgy Institute, Minsk, Belarus
[2]Boreskov Institute of Catalysis, Novosibirsk, Russia
[3]Institute of Heat, Gas and Water Technology, Riga Technical University, Latvia
e-mail: anatolijs.borodinecs@rtu.lv

Planar intermediate temperature solid oxide fuel cells (SOFC) or membranes with mixed ionic-electronic conductivity (MIEC) should be preferably designed as laminated thin-layer composites to decrease their internal electric resistance and, hence, their performance. In this case, a supportive component is necessary to ensure reasonable stiffness and stability. A concept with a porous metal support brings many additional benefits, including the thermal shock resistance and elimination of the temperature gradients.

A novel substrate concept described in the presentation implies the following. The substrate consists of two layers. A thick stiff supportive layer (2-3 mm) is made from open cell foam with the composite strut structure (ceramic core and metallic shell). This composite microstructure structure ensures a combination of high electric conductivity, thermal conductivity, structural stiffness and eliminates the corrugation when heating. The substrate thermal expansion can be adjusted via the control of the metal/ceramic ratio. Analytical equations to control main substrate properties were derived from simple models. Another (thin, ~500 μm) layer with the pore size of about tens of microns facilitates the deposition of functional layers. This thin layer can be manufactured via the plastic deformation of conventional metal foams and sintered to the thick one.

The substrates (in a form of bi-layer structures and single-layer compressed foams) were studied in different processes as catalyst substrates for the hydrocarbon steam reforming to syngas, substrates for the intermediate temperature SOFCs, substrates for the high-temperature multilayer MIEC membranes. Their corrosive resistance in the reaction media was found to be satisfactory, and no remarkable effect upon the contacting active catalytic layers was found.

PO-53

Relief, Phase and Surface Potential Investigations of Composite Polymer Membranes Using AFM

J. Hodakovska, J. Kleperis
Institute of Solid State Physics, University of Latvia, Latvia
e-mail: julia_h_lv@yahoo.co.uk

Composite membrane consisting from two different polymers – SPEKK and PVDF was used as two-phase sample for investigations with atomic force microscope (AMF). Three AFM modes were used for analysis – scanning of relief, phase and surface potential. Theoretical advantage of all three methods used for same sample is possibility to provide more detailed information on different material phases. AFM results of surface investigation for pure SPEKK showed small fluctuation in height and phase (only difference about 5º) what means that material is homogeneous. For composite membrane sample with PVDF addition the changes in both diagrams are much more significant: for height it reaches 600 nm, but for phase – 20º (Fig. 1). Surface potential from this region of composite polymer sample clearly identifies some areas as SPEKK polymer while in relief and phase images these places are identified as PVDF polymer. This can be explained with the fact that polymers dissipate charge not only from surface but also little in depth. Even with such small potential contrast the surface potential mode of AFM can be used to determine polymer structure not only on surface but also in a layer under the surface.

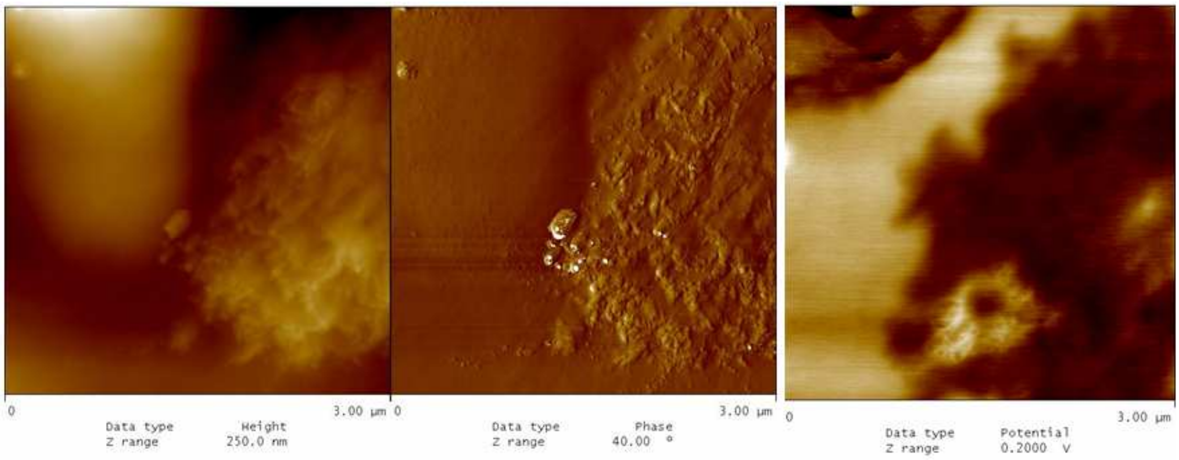

Fig.1 AFM images of SPEKK with 20 w% of PVDF composite membrane: surface profile (left), phase (middle) and surface potential distribution (right).

Acknowledgements: Author (JH) acknowledges European Social Fund and DBU for financial support and GKSS Polymer Institute for possibility to make experimental part.

PO-54

Water Uptake and Proton Conductivity in the Hpa-Pva Composite Membrane

A.I. Chikin[1], A.E. Ukshe[1], Y.A. Dobrovolsky[1]

[1]Institute of Problems of Physical Chemistry, RAS, Russia

e-mail: chikinai@gmail.com

Proton-conducting hybrid membranes composed of poly(vinyl alcohol) (PVA) and phosphotungstic heteropoly acid (HPA) were prepared by solution-blending. The effect of HPA doping on the membrane proton conductivity and water uptake was investigated.

Using Fisher titration method we showed, that composite membrane under unhumidified conditions was able to contain from 7 to 30 molecules of water per HPA molecule, depending on HPA concentration in polymer matrix. Fig.1 shows the dependence of water uptake and proton conductivity of the composite membrane on volume ratio of HPA under 43% relative humidity. One can see, that maintenance of water per single HPA molecule in region from 40 to 60 vol. % of HPA in membrane is close to 12 molecules and constant. This value is in agreement with composition of HPA hydrate under the same conditions, so we suppose, that all these water molecules form a water shell of HPA molecules, which organize continuous conducting network. Increase of conductivity is due to rising concentration of protons in this region.

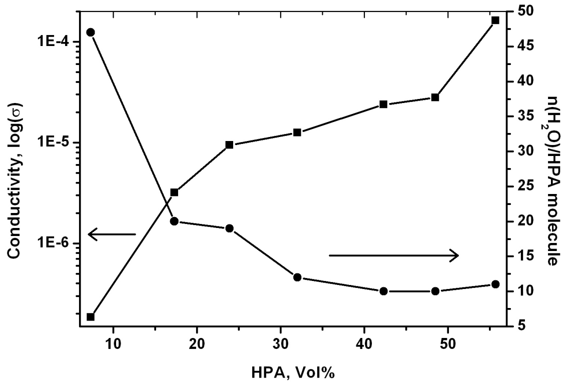

Fig.1 Dependence of proton conductivity and maintenance of water on system composition under RH=43% and T=30 ^{0}C.

While the HPA concentration decreases, conducting network collapses despite the increase of water amount per HPA molecule, so there is drastic reduction in conductivity of the system when volume ratio of HPA is about 25%.

Under high relative humidity (RH=75%) proton conductivity of composite membranes, synthesized in this study, comes up to $1*10^{-3}$ Sm/cm at room temperature.

PO-55

Different Formats of Monolithic Polymer Materials and Examples of their Application

S. Abele[1, 2], O. Yavorska[1], P. Smejkal[3], F. Foret[3], A. Viksna[2], M. Macka[1*]

[1]National Centre for Sensor Research and School of Chemical Sciences, Dublin City University, Dublin 9, Ireland
[2]Faculty of Chemistry, University of Latvia, Riga
[3]Institute of Analytical Chemistry, ASCR, v.v.i., 60200 Brno, Czech Republic
e-mail: silvija.abele@lu.lv

Different formats of monolithic polymer materials are shown - classical polymer monoliths obtained using thermal polymerisation and porous-layer open tubular (PLOT) capillary columns obtained by photopolymerisation. Such monolithic columns can be used in chromatography and other separation methods. Quite often monolithic surface is coated with polymeric nano-particles with the aim to increase the surface area and the efficiency of monolithic columns in separations.

In 1992 Svec and co-workers has pioneered the use of porous polymer monoliths as alternative column materials for chromatography [1]. Monolithic materials as stationary phases offer several advantages in comparison to particle packed columns (better mechanical stability, range of different pore size and different surface chemistries available).

PLOT columns are a form of open tubular capillary column where the wall is coated with porous polymer. PLOT columns often replace packed columns in gas chromatography. PLOT capillary columns could be used as capillary micro-reactors. Enzymatic reactor function is shown as an application example for the obtained methacrylic PLOT columns. Pepsine A was grafted on the monolith column surface and digestion of myoglobin was conducted with subsequent on-line ESI-TOF MS analysis of the protein digest [2]. Digestion efficiency of obtained PLOT columns is comparable with that of full monolithic columns [3].

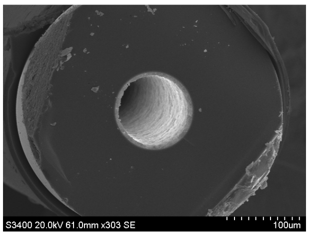

Fig.1 SEM image of PLOT column in fused silica capillary, i.d.100 μm

[*] Current address: Australian Centre for Research on Separation Science (ACROSS) and School of Chemistry, University of Tasmania, Hobart 7001, Australia

References

1. F. Svec, J. M. J. Fréchet, Anal. Chem. **64**, 7, 1992
2. J. Krenkova, K. Kleparnik, F. Foret, J. Chrom. A, **1159**, 110-118, 2007
3. S. Abele, P. Smejkal, O. Yavorska, F. Foret, M. Macka, The Analyst, **135**, 477-481, 2010

PO-56

Synthesis And Properties Of Red Luminescent 2-(3-Styryl)-5,5-Dimethylcyclohex-2-Enylidene)Malononitrile Fragment Containing Material For Organic Light-Emitting Diodes

E. Zarins[1], V. Kokars[1], M. Utinans[1]
[1]Institute of Applied Chemistry, Riga Technical University, 14/24 Azenes Str., Riga LV-1048, Latvia
e-mail: Elmix2003@inbox.lv

Small organic molecules with electron transfer in an excited state are widely adopted in such fields of photonics as materials for creating molecular electronics elements, organic magnets, solar cells and organic light emitting diodes (OLEDs) for full display panels. However, the production of light-emitting layer is still complicated and expensive due to the technological film-forming process as OLED systems are mostly made by thermal evaporation of small organic molecules in vacuum [1-2].

In this work we present new organic glass-forming 2-(3-styryl)-5,5-dimethylcyclohex-2-enylidene) malononitrile fragment containing material IWK capable of forming a thin solid amorphous film from volatile organic solvents (chloroform and DCM).

The synthesized glassy material IWK have VIS absorption in the region between 400 nm to 600 nm. It absorption maximums show batochromic shift going from less polar to polar solvents. Material IWK is also characterized with intensive photoluminescence, which maximum is dependant on solvent and is between 600 nm to 675 nm. Properties of IWK make them perspective in technological processes constructing electroluminescent devices by laying OLED emission layer with simple "spin-coating" method.

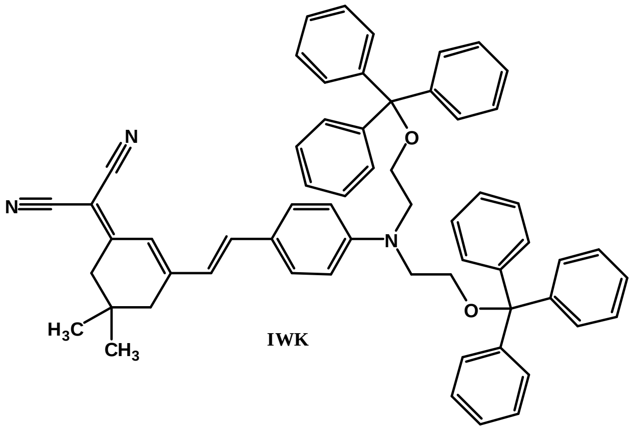

IWK

References

1. L. S. Hung, C. H. Chen, J. Mater. Sci. Eng: R. **39**, 143-222 (2002)
2. P. Strohriegel, J. V. Grazulevicius, Adv. Mater., **14**, 1439-52 (2002)

PO-57

Optical Study of Thin Solid Films with Azobenzene Molecules Containing Carboxyl Groups

E. Laizane[1], D. Gustina[2], I. Muzikante[1], M. Narels[1]

[1]Institute of Solid State Physics, University of Latvia Latvia

[2]Latvian Institute of Organic Synthesis, Latvia

e-mail: elina.laizane@gmail.com

In the design of a new molecular structure of the azobenzene (Fig.1) derivatives we have developed our investigations in the field of modified azobenzene derivatives showing high reversible cis/trans photoisomerization. We have focused our attention on the dependence of the photosensitivity of azobenzene carboxylic acids to variations of the substituents in the sulfonamide moiety.

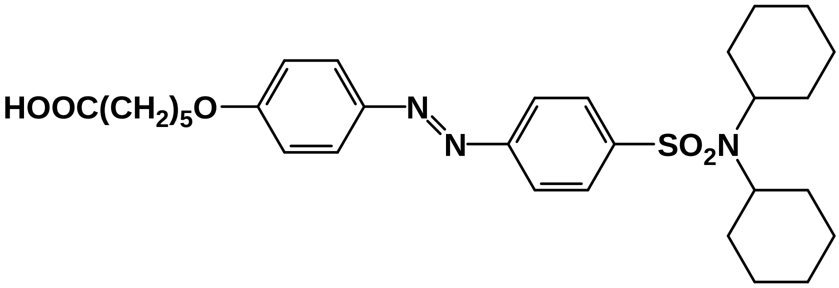

A-45

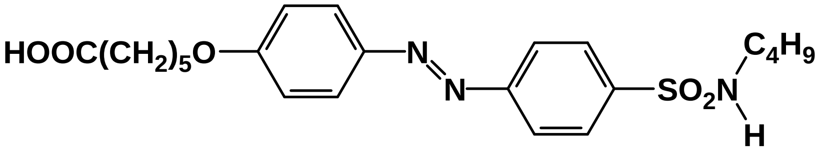

A-46

Fig.1 Azobenzene molecules

Several azobenzene derivatives with bulky cyclohexyl, phenyl and butyl groups were chosen to investigate its influence on photoisomerization process. The samples with 1 to 10 wt% azobenzene molecules in polymer matrix were made by spin – coating technique. The efficiency of photoizomerisation process was studied by the response time and changes of optical absorption of trans band due to the irradiation of different wavelengths.

PO-58

Small Molecular Azobenzene and Indanedione Based Chromophores as Potential Non Linear Optics Materials

K. Traskovskis[1], I. Mihailovs[1, 2], A. Tokmakovs[2], V. Kokars[1], M. Rutkis[2]

[1]Institute of Applied Chemistry, Riga Technical University, Latvia

[2]Institute of Solid State Physics, University of Latvia, Latvia

e-mail: kaspars.traskovskis@rtu.lv

Research towards potential applications of small molecular organic materials (molecular glasses) as non linear optical (NLO) components in optoelectronic devices face certain unsolved problems: unsatisfactory thermoplastic properties and excessive dipole-dipole interactions diminishing molecular order achieved by external electric field polling. Introduction of bulky substitutes into small organic molecules creates steric forces between chromophores inhibiting unwanted interactions between them. This results in increased amorphous phase stability and reduced dipole interactions.

We present novel design of molecular glasses - triphenylmethyl and triphenylsilyl substituted small molecular N,N-dihydroxyethyl derivatives. As chromophores series of azobenzenes **Azo(1-4)** and benzylidene 1,3-indandione **Ind(1-2)** were synthesized (Fig. 1). Compounds show good solubility and amorphous phase forming abilities.

Results of quantum chemical calculations, synthesis, chemical characterization and experimentally obtained linear and nonlinear optical properties of materials will be presented.

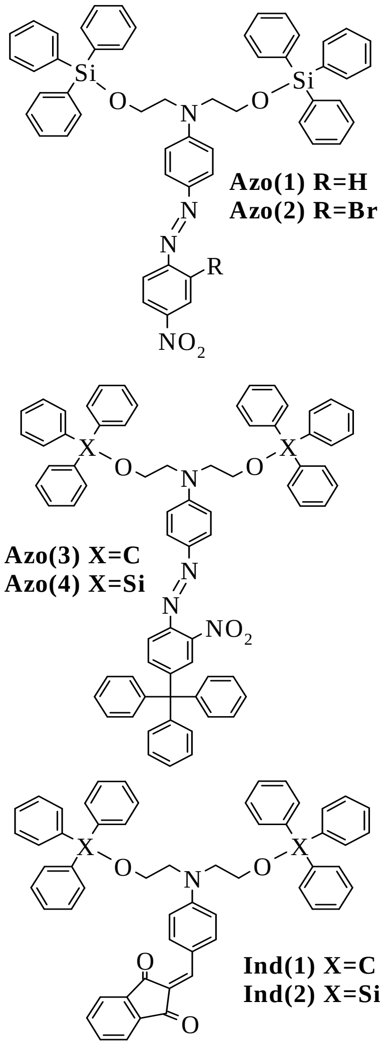

Fig. 1. Chemical structures of synthesized N,N-dihydroxyethyl derivatives

PO-59

Studies of Energy Structure of Organic Films with Metal Electrodes

K. Pudzs, I. Muzikante

Institute of Solid State Physics, University of Latvia

Study of charge carrier transport in organic photovoltaic (OPV) devices, and organic field-effect transistors is one of the most important points. Many organic materials with high charge carrier mobility both for electrons and holes are under investigation. Among them derivatives of carbazole became the subject of numerous investigations.

In this work, we have studied electrical properties and energy structure of carbazole oligomers with different electrodes. We used “sandwich” type samples *(see Fig.1.)* consisting of derivative of carbosole oligomer as an active layer sandwiched between top contacts of different metals and gold bottom contacts.The organic films were prepared by vacuum evaporating method with the thickness of order of 0.5 to 0.9 µm. It allows applying space charge limited current method to characterise charge carrier injection and energy distribution of traps in the thin films. The electrodes (Au, Pd, Al, Cu) were chosen in order to inject electrons or holes in carbazole films. It is known that from Au, Pd, Cu electrodes in JS100 layer the holes can be injected, but from Al - electrons. The work functions of metal layers and surface potential of oligomers films were obtained by Kelvin probe technique. The thermal dependences of electrical conductivity were investigated in space charge limited current regime. The dependence of activation energy on voltage allows to characterisize energetical structure of local trapping states.

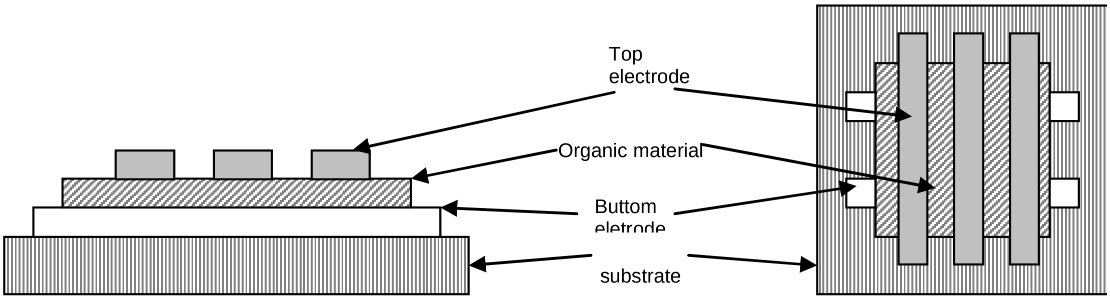

Fig. 1. “sandwich” type sample

This work is supported by the ERAF Project No. 2010/0252/2DP/2.1.1.1.0/10/APIA/VIAA/009

PO-60

Evaluation of Polymer-Nanostructured Carbon Composites Response to Chemical Stimuli

G. Sakale[1], S. Stepina[1], V. Tupureina[2], M. Knite[1]

[1]Institute of Technical physics, Riga Technical University, Latvia

[2]Institute of Polymer materials, Riga Technical University, Latvia

e-mail: sssvvj@inbox.lv

The task of this work is to design, elaborate and investigate polymer nanostructured carbon composite (NCC) for polar organic solvent (ethanol) vapour detection. Both polyethylene glycol (PEG) with molecular weight 40000 and ethylene-vinyl acetate (EVA) with different vinyl acetate content (29,7%, 25% and 11,6%) were used as matrixes for composite production. Carbon black nanoparticles (CB; PRINTEX XE-2; mean size of nanoparticle: 30 nm; specific surface: 950 m2/g; DBP absorption: 380 ml/100 g) were used as conductive ingredients for composite material. Ethanol was chosen as less hazardous solvent from the polar organic solvent class for vapour sensing effect testing. When sensor material senses the ethanol vapour the electric resistance rises in 30 seconds and exponentially returns. The change of the electrical resistance has been observed at different values of ethanol concentration.

PEG-NCC and EVA (29.7%)-NCC samples with different thickness were produced. It was found that PEG-NCC and EVA(29.7%)-NCC ethanol vapour sensitivity increases with decreasing thickness. Ethanol vapour sensing effect of EVA-NCC with different vinyl acetate content 29,7%, 25% and 11,6% has been determined. EVA-NCC ethanol vapour sensitivity increases with increasing vinyl acetate -content in the copolymer. As copolymer consists of two repeating units ethylene (non-polar) and vinyl acetate (more polar like), ethanol vapour sensitivity would be observed better for composition with larger vinyl acetate content The PEG-NCC shows better ethanol sensing effect than EVA(29,7%)-NCC with the same content of CB and similar thickness.

PO-61

Polyvinylacetate-Nanostructured Carbon Composite Ethanol Vapour Sensitivity

G. Sakale[1], E. Liepa[1], V. Tupureina[2], M. Knite[1]
[1]Institute of Technical Physics, Riga Technical University, Latvia
[2]Institute of Polymer materials, Riga Technical University, Latvia
e-mail: elinaLiepa@gmail.com

There is need for new sensor materials, because global technological development is increasing. For this reason we search for compact sensor material, which could be produced with minimal expenses. Here we present polyvinylacatate – nanostructured carbon composite (PVAc-NCC) as a sensor material for ethanol vapour detection. When the composite senses the ethanol vapour the composite electrical resistance increases in short time (30s) and relaxes fully, when the composite is removed from vapour. This composite material was made from PVAc matrix and defined mass parts of carbon black (CB) nanoparticle filler. Samples with varying thickness have been produced and ethanol sensor effect has been determined (see Fig.1.). As thinner is the sample of PVAc-NCC, as better sensor effect it has.

Various content of plasticizer was added to PVAc-NCC to improve the sensitivity of PVAc – NCC. When 1% of plasticizer di-n-octyl sebacate (DOS) was added to PVAc-NCC, an improvement in ethanol sensitivity has been noticed. But the best sensitivity have been determined for PVAc – NCC with 15% DOS.

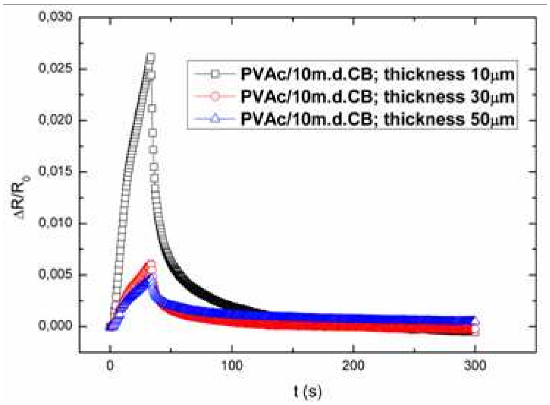

Fig. 1.Relative electrical resistance change in time for PVAc-NCC with various thickness

We also tried to make composite material with polyethylene glycol with molecular weight 6000 (PEG6000), but a smooth coating of PEG6000 did not form. So we used matrix of both PVAc and 20% PEG6000 and another composite with the same materials with inverse proportional content of matrix components. In this case better sensitivity for PEG 6000 with 20% PVAc has been determined.

PO-62

The Synthesis of Different Azo-Polyurethane Polymers for Optical Record

A. Gerbreders, J. Aleksejeva, J. Teteris
Institute of Solid State Physics, University of Latvia, Latvia
e-mail: andrejmah@gmail.com

The new polyurethane azo-polymers based on polyol, toluene diisocyanate and Disperse Red 1 (DR1) azo dye were synthesized through step-by-step method. The difference between the present described method and previously described nonlinear optic azo-polymers is in chemical bonding of DR1 molecules through toluene diisocyanate to the main polyurethane chain. Thin films of the polymer were obtained by casting from solutions in organic solvents on glass substrate. The thickness of dry films was in the range of 3.0 – 7.0 μm. The optical absorption spectra and photo-induced birefringence of the films were studied. The polarization holographic recording and direct surface patterning were realized on the synthesised samples.

PO-63

Time-Dependent Cytokine Expression in Bone of Experimental Animals after Hydroxyapatite (Hap) Implantation

M. Pilmane, G. Salms[1], I. Salma[1], A. Skagers[1]
Riga Stradins University, Institute of Anatomy and Anthropology
[1]Department of Oral and Maxillofacial Surgery
e-mail: pilmane@latnet.lv

Proinflammatory cytokines are known to increase in crevicular fluid from patients with periimplant disease and mediate bone loss [1, 2]. However, there are no complete data about the expression of cytokines into the tissue around the implant in bone. The aim of our work was to research on the distribution and appearance of inflammatory cytokines and anti-inflammatory proteins in the bone of jaw of experimental rabbits after Hap implantation in different time periods.

Material was obtained from 5 rabbits in lower jaw 6 and 8 months after Hap implants. The control consisted of bone tissue of other side jaw with just drilled hole in the bone without implant. Tissues were proceeded for immunohistochemical detection of IL 1, IL, 6, IL 8, IL10, and defensin 2.

Results demonstrated practically unchanged expression of ILs between both – experimental and control side 6 month after implantation. However, individual variation could affect IL8 and Il 10 expression only into the experimental side. IL1 and IL 8 notably decreased 8 months after implantation in experimental side, while Il 10 decreased in both sides, but expression of IL 6 was similar to such in 6 month. Defensin 2 was detected only in control side.

Conclusions. Bone with Hap implants mainly expresses IL 10, moderately – IL1 and Il6, while IL8 shows scarce expression independently on implantation time that proves local anti-inflammatory (IL10) and anti-resorbtion (IL1,6,8) actions of bone around the implants realized on basis of almost absence of antimicrobial proteins.

References

1. V. O. Severino, M. H. Napimoga, S. A. deLima Pereira. Arch. Oral. Biol. In press (2011)
2. S. M. Dai, L. Nishioka, K. Yudoh. Chin. Med. J (Engl). **115**, 46 (2002)

Acknowledgements. The European Social Fund within the project “Multidisciplinary Research in Biomaterials Technology of New Scientist Group”, No.2009/0199/1DP/1.1.1.2.0/09/APIA/VIAA/090.

PO-64

Photoelectrical Properties of Thin Films of DMABI Derivatives

R. Grzibovskis[1], J. Latvels[1], I. Muzikante[1], M. Rutkis[1]

[1]Institute of Solid State Physics, University of Latvia, Latvia

e-mail: raitis1898@gmail.com

Organic thin films with semiconducting properties have been intensively studied in nowadays due to very promising applications in organic electronics, for example, organic photovoltaic. Among organic semiconductors, group of indandiones with their electrical properties, thermal and chemical stability are good candidates for use in design of novel molecular electronic devices.

Goal of the work is based on design of heterojunction between two different dimetilaminobenziliden-1,3-indandion (DMABI) derivatives which may be realized due to the occurrence of an energy barrier between both molecular materials with shifted highest occupied molecular level (HOMO) and lowest unoccupied molecular level (LUMO).

We have investigated photoconductivity quantum efficiency and its spectral dependence of several DMABI derivatives. Value of the threshold energy E_{th} from spectral dependence of quantum efficiency of photoconductivity is obtained. The values of the surface potential of thin films of DMABI derivatives are compared with oxidation potentials and HOMO values according to the RHF *ab initio* calculations.

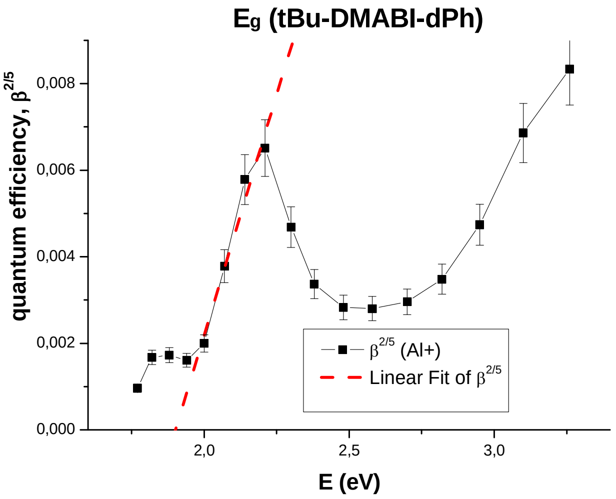

Fig.1 The band gap determination

This work is supported by the
ERAF Project No. 2010/0252/2DP/2.1.1.1.0/10/APIA/ VIAA/009

PO-65

Open Circuit Voltage Dependence on Electrode Material for P3HT Based Organic Solar Cells

I. Kaulachs, I. Muzikante[2], L. Gerca[2], G. Shlihta[1], M. Roze[3], G. Rozite[1]

[1]Institute of Physical Energetics, Aizkraukles 21, Riga, Latvia

[2]Institute of Solid State Physics, University of Latvia, Kengaraga str.8, Riga, Latvia

[3]Riga Technical University, Azenes 14, Riga, Latvia

e-mail: kaulacs@edi.lv

For production organic bulk heterojunction polymer solar cell one of the best materials is regioregular poly-3-hexylthiophene (P3HT), which is widely used as a donor molecule and a hole transporter, with soluble fullerene derivative (PCBM) as acceptor and electron transporter. To extend the spectral range of the cell up to 850 nm hydroxygallium phthalocyanine GaOHPc and PCBM blend was used as additional layer because GaOHPc has strong and wide intermolecular charge transfer (CT) absorption band around 830-850 nm.

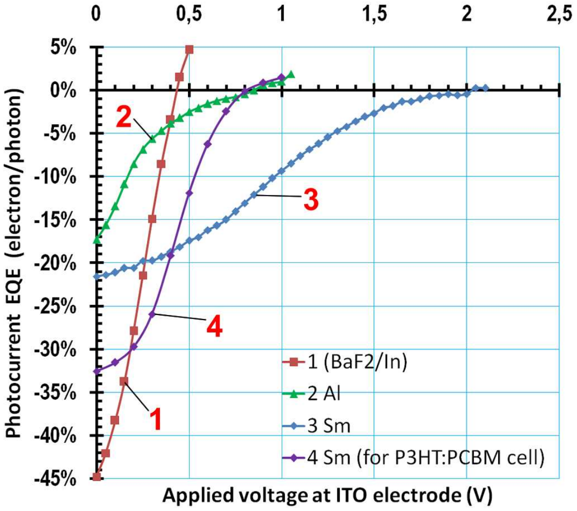

Fig.1 Photocurrent EQE dependences on the applied external voltages for bi-layer bulk heterojunction cell ITO/PEDOT:PSS/GaOHPc:PCBM/P3HT:PCBM/(BaF2/In or Al or Sm) (curves 1-3) and for ITO/PEDOT:PSS/P3HT:PCBM/Sm (curve 4).

The highest photocurrent EQE values have been obtained by BaF_2/In top electrode (curve 1), but the cell exhibited low open circuit voltage (Voc) and Voc≤0.48V. Therefore we look for more appropriate top electrode. The cells with Al top electrode exhibited higher Voc value ~0.8-0.9V, but very low fill factor as seen in curve 2. The best Voc values have been obtained by samarium top electrode, where Voc exceeded 2 volts (curve 3), very close to value expected from MIM model. But quite different Voc value was observed for monolayer P3HT:PCBM bulk heterojunction cell, where Voc was ~0.8V (curve 4), practically the same as for Al top electrode.

PO-66

Magnetoelectric effect in Metglas/MFC 2-2 composites

R. Grechishkin[1], I. Kaplunov[1], G. Lebedev[2], O. Malyshkina[1], N. Mamkina[1], A. Zalyotov[3]
[1]Tver State University, Tver, Russia
[2]CEA, LETI, MINATEC Campus, Grenoble, France
[3]Tver State Medical Academy, Tver, Russia
e-mail: rostislav.grechishkin@tversu.ru

The direct magnetoelectric effect (ME) is an electric polarization response of a material to an applied external magnetic field, $\delta P = \alpha \delta H$, where α is the magnetoelectric coefficient [1]. In composite materials comprising piezoelectric and magnetostrictive components, the ME effect is generated through the magnetic field-induced strain of the magnetostrictive phase which is mechanically coupled to the piezoelectric component subjected to stress changes which are transduced to a voltage. Thus, the ME is described as a product property since neither magnetostrictive nor piezolectric phase is magnetoelectric.

In an effort to maximize sensitivity, typically Terfenol-D alloys with giant magnetostriction are chosen as the magnetostrictive material [2]. In the present work we used an alternative method to maximize sensitivity with the aid of a Metglas-type magnetically soft rapidly quenched and thermomagnetically annealed ribbons 35 μm thick with a modest magnetostriction (35 vs 1500 ppm of Terfenol-D), but a very large magnetic permeability (up to 400,000 vs ~10 of Terfenol-D). Flexible macrofiber composites (MFC) with piezoelectric constant d_{33} ~75 ppm/V (Smart Material Corp.) were chosen to serve as a piezoelectric component of the composite. In this way flexible ME laminated structures were prepared (Fig. 1). Very high (down to nanotesla range) sensitivities are achieved when exploiting these structures as magnetic sensors. Other possible applications include micropower energy harvesting devices, mechanical strain sensors, etc.

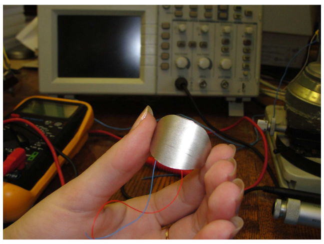

Fig. 1 Flexible magnetoelectric Metglas/MFC 3-layer sandwich sensor.

This work was performed within the Federal Target Program "Research and Research-Pedagogical Personnel of Innovation Russia for 2009-2013".

References

1. M. Fiebig, Revival of the magnetoelectric effect, J. Phys. D: Appl. Phys. **38**. R123–R152. (2005).
2. J. Ryu, S. Priya, K. Uchino, H.E. Kim, Magnetoelectric effect in composites of magnetostrictive and piezoelectric materials. J. Electroceramics. **8.** 107–119 (2002).

PO-67

Structural and Electrical Investigations of $(Ag_3AsS_3)_x(As_2S_3)_{1-x}$ Superionic Glasses

I. Studenyak[1], Y. Neimet[1], C. Cserháti[2], S. Kökényesi[2], E. Kazakevicius[3], T. Salkus[3], A. Kezionis[3], A. Orliukas[3]

[1]Faculty of Physics, Uzhhorod National University, Ukraine

[2]Faculty of Physics, University of Debrecen, Hungary

[3]Faculty of Physics, Vilnius University, Lithuania

Ag_3AsS_3–As_2S_3 chalcogenide glasses differ among the other by high conductivity, making them promising materials for solid state ionic. Synthesis of compounds in Ag_3AsS_3–As_2S_3 glassy system were carried out at a temperature of 700 ^{0}C during 24 h with following melt homogenization during 72 h. Melt tempering was held at cooling on the air (at room temperature).

Structural studies were performed using scanning electron microscopy (SEM) technique (Hitachi S-4300). Optical transmission spectra were studied in the interval of temperatures 293–500 K by an MDR-3 grating monochromator. The measurements of complex electrical conductivity were carried out in the range of frequencies 10 Hz – 3 GHz in a temperature interval 300–400 K by a coaxial impedance spectrometer set-up.

Temperature measurements of the transmission coefficient at fixed 850 nm wavelength show that transparency of $(Ag_3AsS_3)_x(As_2S_3)_{1-x}$ glasses with x=0.3-0.6 decreases sharply down to zero at T>440-450 K. During the subsequent cooling of the glasses transparency do not recovers and glasses keep opaque for the optical radiation of this wavelength. Thereby, the structural studies of heated to more than T>450 K and cooled to 293 K glasses were carried out. Investigations, carried out by the SEM technique, helped to reveal a nanostructural formation on the glass surface that leads to a sharp decrease of a transparency.

Compositional studies have shown that the electrical conductivity of $(Ag_3AsS_3)_x(As_2S_3)_{1-x}$ superionic glasses with increasing of Ag_3AsS_3 content nonlinearly increases with maximum at x=0.5. It should be noted that the activation energy at x value increasing nonlinearly decreases, besides the most noticeable change of activation energy (decreasing more than 24%) is observed at transition from $(Ag_3AsS_3)_{0.4}(As_2S_3)_{0.6}$ to $(Ag_3AsS_3)_{0.5}(As_2S_3)_{0.5}$.

PO-68

Ab initio Calculations of Bulk and Surface F Centers in MgF_2

A.F. Vassilyeva[1], R.I. Eglitis[2], E.A. Kotomin[2, 3], A.K. Dauletbekova[1], F.U. Abuova[1]

[1]L. N. Gumilyov Eurasian National University, 3Munaitpasova, Astana, Kazakhstan

[2]Institute of Solid State Physics, 8 Kengaraga str., University of Latvia, Riga

[3]Max Planck Institute for Solid State Research, Heisenbergstr.1, Stuttgart, Germany

e-mail: annavassilyeva1228@gmail.com

MgF_2 is important wide-gap optical material with numerous applications. We present and discuss the results of calculations of *F* centers in its bulk and at surface. These calculations are based on the *ab initio* Hartree-Fock (HF) method with the electron correlation corrections and on density-functional theory (DFT) calculations with different exchange-correlation functionals, including DFT-HF hybrid techniques. Both approaches use the localized Gaussian basis set and allow us to obtain the MgF_2 bulk band gap of 9.5 eV [1] in good agreement with experimental value. In order to understand the behaviour of the material with respect its optical properties, we performed *ab initio* calculations of the electronic structure, atomic geometry, and formation energy of the *F* center in MgF_2. For the bulk *F* center we used several supercells, with lattice vector extensions 1x1x1 and 2x2x2, thus containing 6 and 48 atoms, respectively. We performed also surface *F* center calculations in MgF_2 located on the neutral (001) surface.

Reference

1. A. F. Vassilyeva, R. I. Eglitis, E. A. Kotomin, and A. K. Dauletbekova, *Physica B*., 2010.

PO-69

The Electronic Structure Calculations of Hole Centers in MgF_2

F. Abuova[1], E.A. Kotomin[2], A.K. Dauletbekova[1]

[1]L. N. Gumilyov Eurasian National University, 3Munaitpasova, Astana, Kazakhstan

[2]Institute of Solid State Physics, 8 Kengaraga str., University of Latvia, Riga

e-mail: Fatika_82@mail.ru

Magnium fluotire (MgF_2) is unique optical material with high radiation stability. It is believed that this occurs due to unusually high mobility of hole (*H*) centers and efficint recombination with the complementary *F* centers.

To shed some light on this problem, we present and discuss the results of calculations of *H* centers in MgF_2. The calculations are based on the so-called hybrid of Hartree-Fock (HF) method with the electron correlation corrections and the density-functional theory (DFT). The results of these first-principles calculations of the electronic structure, atomic geometry, migration barrier and formation energy of the *H* center in MgF_2 are analysed and discussed. We have used several supercells, with lattice vector extensions 1x1x1 and 2x2x2, thus containing 6 and 48 atoms, respectively.

PO-70

Ab initio Calculations of Surface H Centers in BaF_2

R.I. Eglitis[1], H. Shi[2], R. Jia[3]

[1]Institute of Solid State Physics, University of Latvia, Latvia

[2]School of Science, Beijing Institute of Technology, 100081 Beijing, Peoples Republic of China

[3]Bergische Universitat Wuppertal, D-42097 Wuppertal, Germany

e-mail: reglitis@yahoo.com

H center, a hole trapped at an interstitial anion site, placed on the (111) surface of BaF_2 has been studied by means of density functional theory with hybrid exchange potentials B3PW [1]. Two different configurations of surface H center are investigated. Both surface H center systems have strong relaxations because of the surface effect. In the configuration that the interstitial fluorine atom is within the surface, named case 1 in this paper [1], the unpaired electron is almost equally distributed onto the two atoms of the H center, which is quite different from the bulk H center case. The other configuration with one of the F atoms of the H center located above the BaF_2 (111) surface (case 0) has a more polarized charge distribution as compared to that obtained in the bulk case and case 1. The calculation on total energies of different surface F center configurations implies that H centers have a trend to locate near the surface. The creation of a surface H center in BaF_2 results in a new β-hole band located at the Γ point 3.99 and 2.70 eV, for the cases 0 and 1, respectively, above the top of valence bands. According to our calculations on density of states, the constituents of the defect bands are cleared and the β-hole band is primarily composed of p_z orbitals localized on the H center.

References

1. H. Shi, R. Jia, and R. I. Eglitis, Phys. Rev. B **81**, 195101 (2010)

PO-71

First-Principles Calculations for the H Center in SrF_2 Crystals

R.I. Eglitis[1], L. Yue[2], R. Jia[3], X. He[3], H. Shi[4]

[1]Institute of Solid State Physics, University of Latvia, Latvia

[2]University of Osnabruck, D-49069 Osnabruck, Germany

[3]Bergische Universitat Wuppertal, D-42097 Wuppertal, Germany

[4]School of Science, Beijing Institute of Technology, 100081 Beijing, Peoples Republic of China

e-mail: reglitis@yahoo.com

The ground state of H-center systems for the SrF_2 crystal is simulated with two different arrangements, which are oriented along either [100] or [111] axes. The calculations are based on hybrid Hartree-Fock and density functional theory exchange functionals by using Beckes three-parameter method combined with the nonlocal correlation functionals of Perdew and Wang. The energy difference between H centers with different orientations shows that the H center oriented in the [111] direction in alkali earth fluorides is the most stable configuration [1]. The geometric relaxations of the neighboring atoms surrounding the H centers are presented. The combination energy of an H center and the formation energy of the related F-H pair in both alkaline earth fluorides are discussed. We report also the electronic structure of the H center systems. The effective charges and spins of the substitutional and interstitial fluorine atoms show that the hole is located at the interstitial fluorine in the system with the [111] orientation of the H center. The band structures are illustrated. With the help of studying the total and partial density of states, the constituents of the defect bands are clarified.

References

1. L. Yue, R. Jia, H. Shi, X. He and R. I. Eglitis, J. Phys. Chem. A **114**, 8444 (2010).

PO-72

Semiempirical Hartree-Fock Calculations for Pure and Li-doped $KTaO_3$

R.I. Eglitis[1]

[1]Institute of Solid State Physics, University of Latvia, Latvia

e-mail: reglitis@yahoo.com

I present total-energy results for nonferroelectric $KTaO_3$ as a pure crystal (concentrating on the frozen phonon calculations) and that with Li impurities. The magnitudes of off-center Li displacements and the relaxation energies related to reorientation of Li are calculated and compared with experimental estimates and earlier calculation results [1]. The spatial extent of lattice relaxation around Li impurities and contribution from different neighbors to the relaxation energy are discussed.

References

1. R. I. Eglitis, A. V. Postnikov and G. Borstel, Phys. Rev. B **55**, 12976 (1997).

PO-73

Temperature Dependence of the Dielectric Constant in Quantum Paraelectrics

P. Konsin[1], B. Sorkin[1]

[1]Institute of Physics, University of Tartu, Estonia

e-mail: konsin@fi.tartu.ee

In [1-7] the electron-lattice theory of displacive ferroelectrics with an order-disorder component in perovskite oxides is developed. In the present work the electron-lattice (vibronic) theory of quantum paraelectrics is developed. The vibronic interaction induces paraelectricity. According to the present theory the ferroelectric phase transition temperature T_0 in quantum paraelectrics is imaginary, i.e. $T_0^2 < 0$. The dielectric susceptibility in quantum paraelectrics in our approach has the form $\chi = \frac{C_0}{T^2 + T_o^2}$, where C_0 is the constant. Such temperature dependence is caused by the electron-lattice coupling between oxygen 2p states and empty 3d titanium states (in $KTaO_3$ the Ta electronic states are actual) and the anharmonic phonon-phonon interaction between TO critical soft branch and TA acoustical vibrations. The ionic masses also determine the paraelectric state of oxides ($CaTiO_3$, $KTaO_3$, $SrTiO_3$ and TiO_2). The oxygen isotope effect in these compounds is caused by the electron-lattice interaction and the quantum fluctuations (zero-point motion). In $KTaO_3$ the oxygen isotope effect [8] is absent because of the masses of K and Ta. We have calculated the temperature dependence of dielectric susceptibility of $SrTiO_3$, $KTaO_3$, $CaTiO_3$ and TiO_2 and it correlates with the obtained in [9]. The Barrett type formulae are also obtained if the coupling between the TO optical branch and TA acoustical vibrations is weak and the vertex electron-phonon corrections are taken into account. The photoinduced effects in quantum paraelectrics are considered. The change of the population of electronic states induced by light supports paraelectricity. In the strong laser field the renormalization of the vibronic hybridization constants leads to dielectricity.

This work is supported by the Estonian Science Foundation grant No 7389.

References

1. P. Konsin and N. Kristoffel, Ferroelectrics **226**, 95 (1999)
2. P. Konsin and B. Sorkin, Ferroelectrics **270**, 399 (2002)
3. P. Konsin and B. Sorkin, Ferroelectrics **283**, 23 (2003)
4. P. Konsin and B. Sorkin, Ferroelectrics **353**, 63 (2007); Ferroelectrics **379**, 318 (2009)
5. I. B. Bersuker, The Jahn-Teller Effect. Cambridge: Cambridge University Press; (2006)
6. P. Konsin and B. Sorkin, Integrated Ferroelectrics **109**, 81 (2009)
7. N. Kristoffel and P. Konsin, Phys. Status Solidi (b) **149**, 11 (1988)
8. V. V. Lemanov et al., Solid State Commun,**110**, 611 (1999)
9. M. Itoh et al., Phys.Rev. Lett. **82**, 3540 (1999)

PO-74

Influence of Al and Ga Dopants on Electronic Properties of ZnO: *Ab Initio* Simulations

A. Sorokin[1], Yu.F. Zhukovskii[2], J. Purans[2], E.A. Kotomin[2]
[1]Faculty of Physics and Mathematics, University of Latvia, Latvia
[2]Institute of Solid State Physics, University of Latvia, Latvia
e-mail: as08504@lu.lv

Substantial attention is paid nowadays to production of transparent electroconducting materials that can be used, for example, in relatively cheap solar cells. Zinc oxide doped with a few different metallic elements may be considered as a suitable candidate for this role: in visible spectrum range it keeps a low light absorption index while its resistivity ($10^{-3}\ \Omega$ cm) is found to be quite small as compared to pure ZnO, a wide-gap insulator (E_{gap} = 3.68 eV) [1].

The current study aims to investigate influence of Al and Ga dopants on the structural and electronic properties of ZnO as well as to show trends of those properties with respect to the defect concentration. For this purpose, large-scale *ab initio* calculations based on the density functional theory (DFT) have been performed, to study both the structural lattice relaxation and electronic charge redistribution in fully-optimized structures of ZnO doped with Al and Ga atoms, which substitute Zn lattice sites with concentrations $^1/_8$ and $^1/_{27}$ *per* super cell. For these calculations, the hybrid Kohn-Sham&Hartree-Fock exchange-correlation Perdew-Burke-Ernzerhof functional (PBE0) has been used as implemented in *CRYSTAL-09* computational package [2] within approach of the localized atomic basis sets (LCAO).

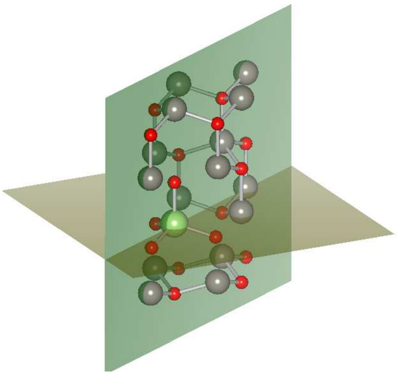

Fig. 2: Horizontal and vertical sections of Ga-doped ZnO lattice.

Our results qualitatively confirm earlier published data for perfect ZnO single crystal on the lattice parameters, bulk modulus, cohesion energy as well as energy gap. Substitution of Zn by either Al or Ga atoms in different concentrations results in noticeable electronic charge transfer from the impurity towards the nearest oxygen atom (0.3–0.4 *e per* point defect) reducing both Al–O and Ga–O bond lengths. This is also confirmed by corresponding plots of the electronic charge redistributions in Al- and Ga-doped ZnO.

References

1. A.A. Sokol, S.A. French, S.T. Bromley, C.R.A. Catlow, H.J.J. van Dam, P. Sherwood, *Faraday Discussions* 2007, **134**, 267-282.
2. R. Dovesi, V.R. Saunders, C. Roetti, *et al. CRYSTAL-2009 User Manual*: University of Torino: Turin, 2009.

PO-75

Ab Initio Calculations of Pairwise Interactions Betweem Defects for Ods Steels

A. Gopejenko[1], Yu.F. Zhukovskii[1], P.V. Vladimirov[2], E.A. Kotomin[1], A. Möslang[2]
[1]Institute of Solid State Physics, University of Latvia, LV-1063 Riga, Latvia
[2]Forschungszentrum Karlsruhe, Institut für Materialforschung-I, Karlsruhe, Germany
e-mail: agopejen@inbox.lv

Oxide dispersion strengthened (ODS) structures of reduced activation ferritic-martensitic (RAFM) steels are considered as promising construction materials for further applications in fusion reactors.

Large-scale first principles calculations have been performed on the γ-Fe lattice containing pairs of Y impurity atom with either Fe vacancy or Y atom and different configurations of three-atom clusters Y-O-Y. Results calculated for *fcc* Fe lattice clearly demonstrate a certain attraction between the Y substituted atom and Fe vacancy whereas no binding has been found between the two Y atoms [1]. Results of calculations for different Y-O-Y cluster configurations show that not only a presence of oxygen atom favors a certain binding between the impurity atoms inside the γ-Fe lattice but also the increased concentration of Fe vacancies is required for the growth of the Y_2O_3 precipitates within the iron crystalline matrix [2].

The found significant influence of Fe-vacancies on the binding energies resulted in the interest in studying the interactions between two Fe-vacancies in Fe lattice as well as in performing the calculations of two Y substitute atoms with Fe-vacancy.

In order to start the LKMC calculations it is necessary to perform the modeling of all possible combinations of pair defects. Currently these calculations include the modeling of Y-O, O-O and V-V (two Fe-vacancies) interactions.

References

1. A. Gopejenko, Yu.F. Zhukovskii, P.V. Vladimirov, E.A. Kotomin, and A. Möslang, *Ab initio* simulation of yttrium oxide nanocluster formation on *fcc* Fe lattice. - *J. Nucl. Mater.*, 2010, **406**, pp. 345–350.
2. A. Gopejenko, Yu.F. Zhukovskii, P.V. Vladimirov, E.A. Kotomin, and A. Möslang, Modeling of yttrium, oxygen atoms and vacancies in γ-iron lattice, *J. Nucl. Mater.*, 2011, *in press (corrected proof, available online since 13 December 2010).*

PO-76

UN (110) Surface Properties: *ab initio* Calculations

D. Bocharov[1, 2, 3], Y.F. Zhukovskii[1], D. Gryaznov[1], E.A. Kotomin[1]
[1]Institute for Solid State Physics, University of Latvia, Kengaraga 8, Riga LV-1063, Latvia
[2]Faculty of Computing, University of Latvia, Raina blvd. 19, Riga LV-1586, Latvia
[3]Faculty of Physics and Mathematics, University of Latvia, Zellu 8, Riga LV-1002, Latvia
e-mail: bocharov@latnet.lv

Application of actinide nitrides as a fuel in the fast transmutation reactor offers potentially enhanced performance as compared to conventional actinide oxide fuels [1, 2]. These fuels are receiving renewed attention across the world since the commencement of the Generation IV initiative. Unfortunately, one of the problems with actinide nitrides is their interaction with the oxygen which results in an effective fuel oxidation and degradation. Therefore, it is significant to know more about chemical properties, reactivity and oxidation mechanism of UN surfaces as well as processes on grain boundaries in polycrystalline UN.

In this study, we present results of UN(110) surface calculations performed within the DFT plane-wave formalism as implemented in VASP code [3]. Slab model and ultra-soft pseudopotentials combined with the Projector-Augmented-Wave (PAW) method have been used for this aim. The non-local exchange-correlation functional within the Perdew-Wang-91 Generalized Gradient Approximation (PW91 GGA) has been applied.

We perform spin density and full geometry optimization within the supercell of fixed linear dimensions. The effective atomic charges, atomic displacements, average magnetic moments μ_{av} of U atoms, surface energies E_{surf} for defect-free slabs of different thicknesses as well as formation energies of surface nitrogen vacancies E_{form} have been obtained.

Comparison of both UN(001) [4] and UN(110) surfaces shows that the former is energetically more favorable. Depending on slab thickness, the surface energies equal to 1.22-1.44 $\mathrm{J{\cdot}m^{-1}}$ for UN(001) *vs.* 1.83-1.98 $\mathrm{J{\cdot}m^{-1}}$ for UN(110) surface. Energies of the nitrogen vacancy formation on the uranium mononitride surface are close for both (110) and (001) faces although E_{form} is ~0.5-0.7 eV smaller for (110) face. Possibility of the $\mathrm{UN}(110)/(\bar{1}10)$ interface formation used as a simplest sigma-model of grain boundary is discussed too.

References

1. Hj. Matzke, Science of Advanced LMFBR Fuels (North Holland, Amsterdam, 1986).
2. The Nuclear Fuel Cycle, Ed. P.D. Wilson (University Press, Oxford, 1996).
3. G. Kresse and J. Hafner, VASP the Guide (University of Vienna, 2007).
4. D. Bocharov, D. Gryaznov, Yu.F. Zhukovskii, and E.A. Kotomin, *Surf. Sci.*, 2011, **605**, 396-400.

PO-77

Density Functional Theory Calculations on Magnetic Properties of Actinide Compounds

D. Gryaznov, E. Heifets, E. Kotomin
Institute of Solid State Physics, University of Latvia, Latvia
e-mail: gryaznov@mail.com

We have performed a detailed analysis of the magnetic (collinear and noncollinear) ordering as well as the atomic and electronic structure of UO2, PuO2 and UN on the basis of density functional theory with the Hubbard electron correlation correction (DFT+U). It is shown that the 3-k magnetic structure of UO2 is stabilized for U = 4.6 eV (Ueff = U – J is 4.1 eV), consistent with experiments, when Dudarev's formalism for exchange-correlation functional is used. UO2 retains a cubic shape in this structure. Neither UN nor PuO2 show the energetical prevelence for the rhombohedral distortion, in contrast to UO2, and, thus, complex 3-k magnetic structure does not occurs in these materials having the AFM tetragonal <001> structure. A number of properties were analyzed for UN varying the Hubbard U-parameter: the lattice parameters, the spin and total magnetic moments, and the density of states. The metastable states typical for actinide compounds were carefully analyzed, in order to reproduce properly the UN magnetic and structural behavior. The metastable states appear in the range of U-values between 1.5 and 2.5 eV (at fixed J = 0.125 eV). The material is characterized by several U atom magnetic moments and lattice parameters at each U within this range of energies (fig. 1a). We have demonstrated the crucial role of spin-orbit interactions for reproducing the magnetic moment of UN. The optimized value of the effective Hubbard Ueff = U – J is 1.875 eV (fig. 1b). This value allows proper description of both the magnetic moments and the antiferromagnetic ordering in UN. A comparison with the previous DFT+U calculations for UN is also given.

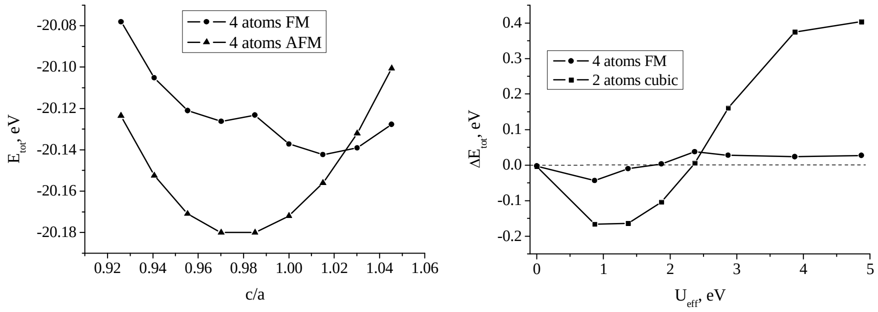

Fig. 1. a) The total energy as a function of lattice parameter ratio c/a for the FM and AFM 4 atoms unit cells and U_{eff} = 2.37 eV b) The total energy difference with respect to the AFM unit cell with spin orbit interactions included as a function of U_{eff} parameter.

References

1. S. L. Dudarev, G. A. Botton, S. Y. Savrasov, Z. Szotek, W. M. Temmerman, A. P. Sutton, Phys. Status Solidi A 166, 429 (1998).
2 B. Dorado, B. Amadon, M. Freyss, M. Bertolus, Phys. Rev. B 79, 235125 (2009).
3 Y. Lu, B.-T. Wang, R.-W. Li, H. Shi, P. Zhang, J. Nucl. Mater. 406, 218 (2010).

PO-78

Density Functional Theory beyond Translational Invariance: Discrete Variable Representation

E. Klotins[1], A.I. Popov[2], V. Pankratov[1]
[1]Institute of Solid State Physics, University of Latvia, Latvia
[2]Institute Laue-Langevin, Grenoble, France
e-mail: klotins@cfi.lu.lv

The study is addressed to the extension of conventional density functional theory (DFT) toward systems other than translationally invariant condensed phases.

Formally the single-electron self-consistent eigenvalue problem for Kohn-Sham equation is preceded within the discrete variable representations (DVR) defined by integrable functions that satisfy the Kronecker, orthogonality and completeness properties on appropriate selected spatial grid addapted to realistic types of boundary conditions [1].

Unique feature of this DVR approach is the unified real-space treatment of system-size effects and the potential for advancements toward the electronic and spectroscopic properties.

How and to which extent the DVR is possible in the practice is demonstrated by algorithmic and software details for the self-consistent Kohn-Sham eigenvalue problem with special emphasis on the Laplacian operators for kinetic energy of electrons, the Hartree potential for direct Coulomb energy and solutions of Kohn-Sham equations.

Expected applications of DVR for condensed state include nanostructures, violated disorder in complex oxides [2] and other long-standing problems of atomic ordering.

This work was supported by the Latvian State research program, Project #2 and ESF project Nr. 2009/0202/1DP/1.1.1.2.0/09/APIA/VIAA/141.

References

1. Yi Liu, D.A. Yarne, M.E. Tuckerman, Phys. Rev. B 68, 125110 (2003)
2. E. Klotins et al, Cent. Eur. J. Phys. • 9(2) • 2011 • 438-445

PO-79

Cluster Embedding Method for Theoretical Study of Processes in Nanosystems

E.K. Shidlovskaya[1, 2]
[1]Information Systems Management Institute, Latvia
[2]Institute of Chemical Physics, University of Latvia, Latvia
e-mail: shidlovska@inbox.lv

When we theoretically study nanosize system we have to treat the whole quantum system as two subsystems: small finite fragment of nanowire or nanotube and the remaining part of it. There is another problem of this kind in the solid state theory - cluster with a point defect and the rest of crystal. This problem is successfully resolved in the frameworks of embedded molecular cluster (EMC) model [1] with *orthogonal* wave functions. We have treated cluster embedding problem in the frameworks of one-electron approximation with *non-orthogonal* wave functions. We have developed modified cluster embedding scheme and have demonstrated that this scheme may radically reduce boundary effects in EMC model [2].

To use our cluster embedding method for theoretical treatment of processes in nanosystems, we should overcome limitations of one-electron approximation. It may be done by configurations interaction (CI) and perturbation theory (PT) methods or in the frameworks of DFT Kohn-Sham approach. For this purpose we need occupied and vacant cluster states of the same localization. Our initial embedding equations [2] are established to give localized in the cluster region occupied states and delocalized vacant ones [3]. To get the same localization degree for the both states, modified equations are proposed [3]. Our embedding equations are compared with the equations obtained in the frameworks of the theory of pseudopotentials [4]. As the result, after some modification our embedding scheme became compatible with DFT and CI or PT. It gives us possibility to use this scheme for theoretical treatment of electron transitions and excited states. We demonstrate that our embedding scheme may be applied for theoretical study of transport phenomena and propose approach combining this scheme with the methods for calculation of electric current in nanodevices.

References

1. L.N. Kantorovich, *J. Phys. C: Solid State Phys.* **21**, 5041 (1988).
2. E.K. Shidlovskaya, *Int. J. Quantum Chem.* **89**, 349 (2002).
3. E.K. Shidlovskaya, *Computer Modelling and New Technologies* **10,** No 4, 17 (2006).
4. E.K. Shidlovskaya, *Computer Modelling and New Technologies* **13,** No 1, 17 (2009).

PO-80

First-Principles Simulations on Double-Wall Bn and TiO_2 Nanotubes with Hexagonal Morphology

R.A. Evarestov[1], Yu.F. Zhukovskii[2], S. Piskunov[3, 4], M.V. Losev[1]

[1]Department of Quantum Chemistry, St. Petersburg State University, Petrodvorets, Russia

[2]Institute of Solid State Physics, University of Latvia, Riga, Latvia

[3]Faculty of Computing, University of Latvia, Riga, Latvia

[4]Faculty of Physics and Mathematics, University of Latvia, Riga, Latvia

e-mail: quantzh@latnet.lv

The line symmetry groups for one-periodic (1D) nanostructures with rotohelical symmetry have been applied for symmetry analysis of double-wall boron nitride and titania nanotubes (DW BN and TiO_2 NTs) formed by rolling up the two stoichiometric two-periodic (2D) slabs of hexagonal structure with the same or opposite orientation of translation and chiral vectors in both single-wall (SW) constituents (direct or inversed morphology, respectively). We have considered the two sets of commensurate DW NTs with either $(n,n)@(m,m)$ (armchair-type) or $(n,0)@(m,0)$ (zigzag-type) chiralities. To establish the equilibrium inter-wall distances corresponding to the formation energy minima, we have varied chiral indices m and n of the constituent SW nanotubes [1]. To analyze the properties of DW NTs, we have performed their *ab initio* LCAO calculations using the hybrid Hartree-Fock/Kohn-Sham exchange-correlation functional PBE0 as implemented in *CRYSTAL-09* code [2].

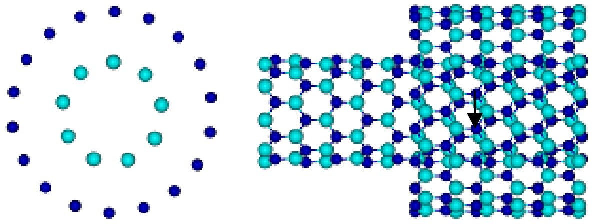

Fig. 1. Cross-section and aside images of hexagonal DW BN NTs (9,0)@(18,0) with optimized diameters for inversed morphology of zigzag chirality

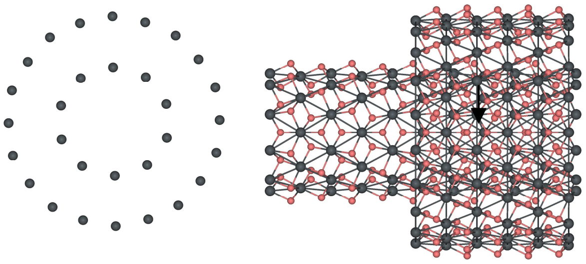

Fig. 2. Cross-section and aside images of hexagonal DW TiO_2 NTs (10,0)@(20,0) with optimized diameters for direct morphology of zigzag chirality.

Stability of DW NTs depends mainly on the inter-wall distance (ΔD_{NT}) and the diameter of the internal shell. To estimate an influence of ΔD_{NT} on the nanotube stability, its formation energy (E_{form}) has been chosen as a criterion. The Morse-type potential curves $E_{form}(\Delta D_{\mathrm{NT}})$ for double-wall nanotubes of both chiralities permit to estimate their equilibrium configurations.

References

1. R.A. Evarestov, Yu.F. Zhukovskii, A.V. Bandura, S. Piskunov *J. Phys. Chem. C,* 2010, **114**, 21061-21069.
2. R. Dovesi, V.R. Saunders, C. Roetti, *et al. CRYSTAL-2009 User Manual*: University of Torino: Turin, 2009.

PO-81

The Quantum-Chemical Simulation of the Self-Trapped Exciton in $LiYF_4$ Crystal

Y. Bikhert, A. Dauletbekova, F. Abuova
L.N. Gumilyov Eurasian national university, Astana, the Republic of Kazakhstan
e-mail: bihertevgenij@rambler.ru

The pulse cathodluminescence spectrum of $LiYF_4$ crystals lying in the range of 3,8 - 5 eV. This is the spectrum of self-exciton luminescence. It consists of two bands with maxima at 4,2 and 4,75 eV, half-width of 0,49 and 0,57 eV, respectively. Kinetic characteristics of luminescence are equalized.

In his article [1] W. Hayes pointed out the feasibility of four possible V_k centers, suggesting the possibility of localization and migration of excitons in four possible directions. However, from experiments on a puls spectrometer was found that not all configurations are realized, and one of these directions is perhaps the most probable. To test this hypothesis, we resorted to computer quantum-chemical simulation using the software package CAChe Workspace, CAChe Worksystem Pro Version 6.1.12.33, Software licensed to L.N. Gumiljov Eurasian National University, Customer Serial #: 1503000354, Copyright 2000 Fujitsu Limited, 1989-2000 Oxford Molecular Ltd. A model of the crystal $LiYF_4$ was constructed. Because of the inability of the free electron model, we resorted to simulation of the hole-type component of the exciton. The first step was the simulation of localized on the fluorine atom hole in the crystal volume. Energy of this system is E = -1486, 1 a.u. The following models are the two related fluorine atom, one of which is localized hole that is very similar to the V_k center. These V_k centers were located in three possible ways: a (100), b (010) and c (001). The results are shown in Table 1, where d – is the direction of the V_k center, E_{Vk} – is the system energy, ΔE – is the difference $\Delta E = E_{Vk} - E$.

Table 1. The results of the computer quantum-chemical simulation.

d	E_{Vk}, a.u.	ΔE, a.u.
a (100)	-515,56	970,54
b (010)	-815,355	670,745
c (001)	-950,287	535,843

As it seen from the represented data V_k center is localized and migrate along the axis c (001) with the highest probability.

References:

1. W. Hayes, M. Yamaga, D.J. Robbins and B. Cockayne., J. Phys. C: Solid st. Phys., 13 (1980) L1011-5.
2. Crystal chemistry of fluoride/ Babel P.? Tressaud A.// Inorganic Solid Fluorides/ Academic press. -1985. - P.

PO-82

Modeling Of Decay Kinetics of Self-Trapped Exciton Luminescence in $CdWO_4$ under Femtosecond Laser Excitation in Absorption Saturation Conditions

S. Markov[1, 2], V. Nagirnyi[1], A. Vasil'ev[3], V. Makhov[2], R. Laasner[1], S. Vielhauer[1], R. Grigonis[4], V. Sirutkaitis[4]

[1]Institute of Physics, University of Tartu, Tartu, Estonia

[2]P.N. Lebedev Physical Institute, Moscow, Russia

[3]Skobeltsyn Institute of Nuclear Physics, Lomonosov Moscow State University, Moscow, Russia

[4]Laser Research Centre of Vilnius University, Vilnius, Lithuania

e-mail: gls.markov@gmail.com

Non-proportional response of scintillators is one of the key factors restricting their efficiency and energy resolution. In scintillators like $CdWO_4$, $CaWO_4$ or $PbWO_4$, whose operation is based on luminescence of self-trapped excitons (STE), the effect of non-proportional response originates from quenching of STE luminescence due to the mutual interaction of excitons created at high densities in particle tracks [1]. Modeling studies of STE interaction under high-density excitation conditions were performed for $CdWO_4$ using high-power pulsed femtosecond lasers for excitation. The model of Förster's dipole-dipole interaction of excitons was used for a quantitative description of experimental data on STE luminescence decay kinetics [1, 2]. However, under the conditions of extremely high-density excitation the interaction model has to be modified to account for the possible saturation effect in absorption, which can cause a non-exponential decrease of intensity with penetration depth [3].

In the present study, the three-dimensional spatial distribution of excitons was calculated taking into account the saturation effect for absorption near the center of the incident laser beam with Gaussian transversal profile. Self-focusing effects are not considered in this approximation. The model was verified experimentally for exciton creation in $CdWO_4$ by 80 fs laser pulses in the region of weak excitonic absorption of the order of 10^2-10^3 cm^{-1}, where the saturation effects are explicitly well pronounced.

References

1. M. Kirm, V. Nagirnyi, E.Feldbach, et al., Phys. Rev. B **79**, 233103 (2009)
2. V. Nagirnyi, S. Dolgov, R. Grigonis et al., IEEE Trans. Nucl. Sci. **5**(3), 1182 (2010)
3. R. T. Williams, J.Q. Grim, Qi Li et al., Phys. Stat. Sol. (b) (Feb. 2011, in press), DOI:10.102/pssb.201000610

PO-83

Creation of Defects and Self-localized Vibrations in Crystals: Effects of Long-range Forces in Nonlinear Dynamics

M. Haas[1], V. Hizhnyakov[1], M. Klopov[2], A. Shelkan[1]
[1]Institute of Physics, University of Tartu, Riia 142, 51014, Tartu, Estonia
[2]Institute of Physics, Tallinn University of Technology, Ehitajate tee 5, 19086, Tallinn, Estonia
e-mail: haas@fi.tartu.ee

Nonlinear vibration interactions are well localized; as a consequence, intrinsic localized modes (ILMs) and other types of nonlinear excitations can exist in perfect crystal lattices. On the contrary, linear interactions in 3D systems strongly depend on long range forces (LRF), which make unsatisfactory MD simulations based on a cluster consideration of nonpolarizable ions. In [1-3], an analytical theory of ILMs was developed, which takes LRF into account. Here we present a method of MD simulations, which allows include both nonlinearity and LRF. The method is based on the nonlinear equations of motion in the site representation, the harmonic (long-range) forces included via the phonon Greene functions.

The proposed method was used for the investigation of the formation of radiation defects, following the recoil of scattered neutrons and X-rays. It was established that in alkali-halide crystals the threshold recoil energy of the defect formation does not exceed 1 eV. LRF can also qualitatively change ILM properties: instead of ILMs with the frequency in the gap of the phonon spectrum, one may obtain self-localized modes with the frequency above the phonon spectrum. Such an effect was found to exist in simple metals where electronic screening together with Friedel oscillations can cause a remarkable reduction of the odd anharmonicities. Our MD simulations in Ni and Nb crystals allow to conclude that the nonlinearity-induced localization of vibrational energy may exist more widely than it was believed to take place on the basis of theories neglecting LRF.

References

1. V. Hizhnyakov et al, Phys. Rev. B **73**, 224302-1 (2006).
2. V. Hizhnyakov, A. Shelkan, M. Klopov, Physics Letters A, **357**, 393 (2006).
3. M. Haas et al, IOP Conference Series, Material Science and Engineering **15**, 012045 (2010).

PO-84

Simulation of Phase Stability of Pb_2ScTaO_6

J. Gabrusenoks

Institute of Solid State Physics, University of Latvia, Latvia

e-mail: gabrusen@latnet.lv

Lead scandium tantalate single crystals (PST) belong to perovskite structure with general formula $AB_xB^1_{1-x}O_3$. This work present ab initio calculations of structural and dynamical properties of PST ordered crystal. To perform the first-principle DFT-B3PW calculations the CRYSTAL06 computer code was used.

Calculated phonon frequencies show instability of Fm3m lattice for F1g and F1u phonon modes, phonon mode F2g is also close to instability. Possible crystal R-3m, R-3 and R3 lattices in connection with these unstable modes are analysed.

PO-85

Effect of Surface Methylation on the Stability of Silicon Nanoparticles

A. Mukhtarov[1], A. Normurodov[1], S. Khudayberganov[1], I. Zaitov[2]

[1]Institute of Nuclear Physics of Uzbekistan Academy of Science, Uzbekistan

[2]National University of Uzbekistan, Uzbekistan

e-mail: ofm@inp.uz

Nanosized silicon cluster have attracted a big interest due to the photoluminescence effect revealed in these materials. The origin and characteristics of their luminescence is related not only with the size of the nanoparticle, but also its shape and surface. Hydrogenation of the cluster surface allows you to save the configuration and the basic properties of nanosilicons, but it can not prevent the oxidation of silicon nanoparticles in the air. Effective way to stabilize the surface of particles and their photo luminescent properties is an implantation of the organic monolayer on a hydrogen saturated surface of the nanoparticles by the hydrosylilation reaction. However, in general it has not previously been possible for blue-emitting silicon nanoparticles (1 nm in diameter). Organic functional groups on the cluster surface reduce meeting the surface atoms with oxygen molecules. Nevertheless, at present there is no microscopic model of such saturation, the degree of saturation and its influence on the stability of the cluster and band performance. In this report we present the results on silicon nanoparticles containing 29 atoms which surface dangling bonds are saturated with hydrogen in various combinations. To calculate the spatial and electronic structure of the clusters, we used a nonconventional tight-binding method, recently developed by Khakimov [1]. Also Si_{29} cluster with the surface covered partially or fully with methyl groups have been considered. In the case of partial saturation of the surface atoms with methyl groups, the rest of the dangling bonds are saturated with hydrogen atoms. Hydrogenated silicon cluster with 1, 2, 4 and 24 methyl groups on the surface have been computed. Note that an increase of the number of hydrocarbons on the surface lead to the cluster becomes stable in positively charged state. In the case of full coverage of the Si29 cluster by methyl groups ((Si_{29} $(CH_3)_{24}$), double positively charged state is prevailed.

References

1. Z.M. Khakimov, et al., Phys. Rev. B **72**, 115 335 (2005)

PO-86

Possibility Analysis of Mathematical Modeling for the Process of SOG-Si Production from MG-Si by Using Electron Beam Melting and Directional Solidification

A. Muiznieks[1], A. Sabanskis[1], M. Plate[1], G. Chikvaidze[2]

[1]Department of Physics, University of Latvia, Latvia

[2]Institute of Solid State Physics, University of Latvia, Latvia

e-mail: andris.muiznieks@lu.lv

The mathematical modeling is now widely established as one of development instruments for the industrial silicon single crystal growth methods (Czochralski (CZ) and floating zone (FZ)) for electronic needs. The models include temperature and velocity fields in the melt, the mass transport of impurities and dopants, heat exchange via radiation in the system, the usage of electromagnetic fields for silicon melting and for the influencing the melt motion, the segregation process at the crystallization front etc., see e.g. [1], [2] and Fig. 1.

Because of needs of photovoltaic power industry, nowadays intensive research is carried out for the development of economical mass production methods for the producing of solar grade silicon (SOG-Si) from metallurgical grade silicon (MG-Si). The present paper analyses the possibility of application of previously developed mathematical models (for CZ and FZ) for the process of production of SOG-Si from MG-Si by using electron beam melting and directional solidification, see e.g. [3] and Fig. 2.

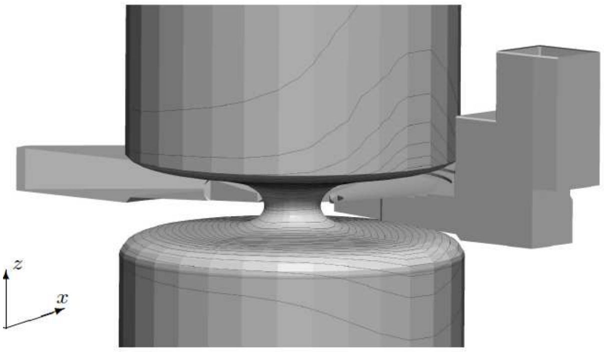

Fig.1 Example of the modeling of FZ process.

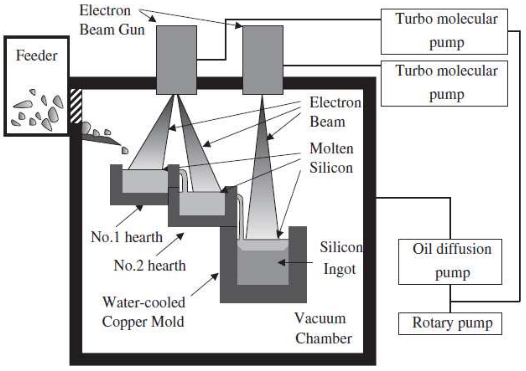

Fig. 2 Continuous melting by electron beam, [3]

References

1. A. Krauze, N. Jēkabsons, A. Muižnieks, A. Sabanskis, U. Lācis, Journal of Crystal Growth, Volume 312, Issue 21, 15 October 2010, Pages 3225-3234.
2. K. Lācis, A. Muiżnieks, A. Rudeviċs,, A. Sabanskis, Magnetohydrodynamics, Vol. 46, No. 2, 199-218, 2010.
3. K. Hanazawa, N. Yuge, Y. Kato, Materials Transactions, Vol. 45, No. 3 (2004), 844-849

PO-87

Reverse Monte Carlo Modelling of Structural and Thermal Disorder in Crystalline Materials

J. Timoshenko, A. Kuzmin, J. Purans

Institute of Solid State Physics, University of Latvia, Latvia

e-mail: janis.timoshenko@gmail.com

Reverse Monte Carlo (RMC) simulation method allows one to determine a 3D model of the compound atomic structure by minimizing the difference between its structure-related experimental and calculated properties, e.g., extended x-ray absorption fine structure (EXAFS) [1]. In this work we present the RMC modelling scheme, designed to probe the local structural and thermal disorder in crystalline materials by fitting the wavelet transform (WT) of the EXAFS signal [2], thus accounting for the signal behaviour in both energy (*k*) and real (*R*) space. We believe that the proposed method will improve the efficiency and accuracy of currently available data analysis approaches.

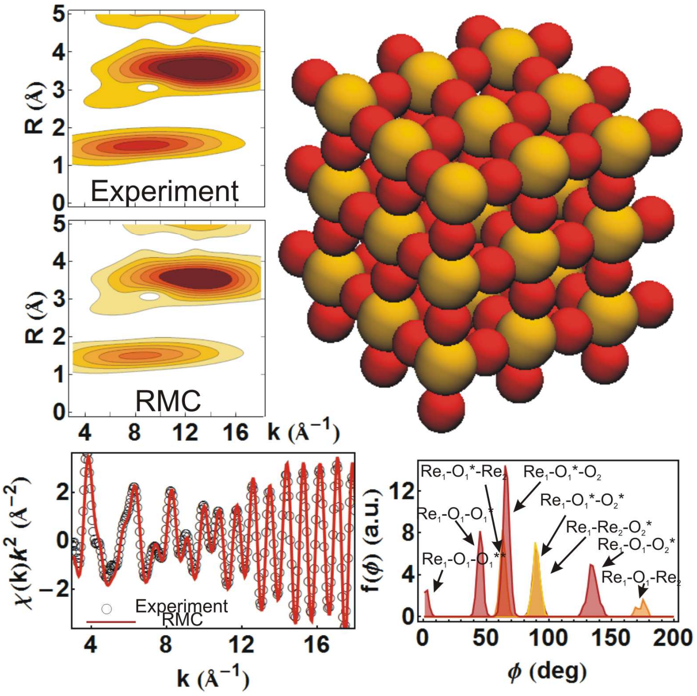

Fig.1 Example of the RMC modeling for ReO_3: the WTs of the experimental and calculated Re L_3-edge EXAFS signals (*top left panels*); the atomic configuration, obtained by the simulations (*top right panel*); experimental and simulated EXAFS spectra (*bottom left panel*); calculated bond angle distributions in ReO_3 *(bottom right panel).*

Application of the method to the interpretation of the Ge K-edge [3] and Re L_3-edge [4] EXAFS signals in crystalline germanium (Ge) and rhenium trioxide (ReO_3), respectively, will be addressed with special attention to the problem of thermal disorder and related phenomena. The obtained results will be compared with those from previous molecular dynamics simulations [5, 6].

References

1. S.J. Gurman and R.L. McGreevy, J. Phys.: Condens. Matter **2**, 9463 (1990)
2. J. Timoshenko and A. Kuzmin, Comp. Phys. Commun. **180**, 920 (2009)
3. J. Purans et al., Phys. Rev. Lett. **100**, 055901 (2008)
4. J. Purans et al., AIP Conf. Proc. **882**, 422 (2007)
5. J. Timoshenko, A. Kuzmin, and J. Purans, Cent. Eur. J. Phys. (2011), doi: 10.2478/s11534-010-0074-0
6. A. Kalinko, R.A. Evarestov, A. Kuzmin, and J. Purans, J. Phys.: Conf. Series **190**, 012080 (2009)

PO-89

Simulation of SVHF Electromagnetic Properties of Carbon Nanotubes

V.I. Gopeyenko[1], Y.N. Shunin[1, 2]
[1]Information Systems Management Institute, Riga, Latvia
[2]Institute of Solid State Physics, University of Latvia, Riga, Latvia
e-mail: viktors.gopejenko@isma.lv, shunin@isma.lv

Super-Very-High-Frequency (SVHF) electromagnetic properties of 1D nanosystems are presented. Frequency properties in the range from *dc* to THz have been considered.

The main goal of the work is the implementation of the circuit model (Fig.1) for the study of CNT's electromagnetic properties taking into account possible interconnects in novel nanodevices [2].

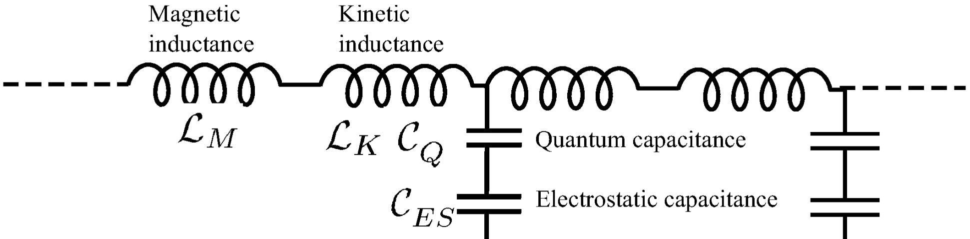

Fig. 1. SW CNT circuit model [1]

It is shown that for *ac* circuit model in the range of up to GHz, kinetic inductance and quantum capacitance can be neglected. For the THz frequency electronic quantum effects become significant. The resistance of SW CNT is too high and for interconnects it is technologically reasonable to use CNT bundles. A parallel connection of CNT gives an essential decrease of kinetic inductance and quantum capacitance, which can be neglected.

Wide-scale simulations of *ac* CNT electric properties have been carried out.

References

1. P.J. Burke. IEEE Trans. Nanotechnology, vol. 1, no.3, 129-144 (2002)
2. Yu. N. Shunin, Yu. F. Zhukovskii, V.I. Gopeyenko, N. Burlutskaya, S. Bellucci. Nanoscience and Nanotechnology Letters (2011) (in print)

PO-90

Theoretical Study of Nb/α-Al_2O_3 Interfaces

V.V. Melnikov[1, 2], S.V. Eremeev[1, 2], S.E. Kulkova[1, 2]
[1]Institute of Strength Physics and Materials Science of the Siberian Branch of RAS, Tomsk, Russia
[2]Tomsk State University, Russia
e-mail: melnikov@phys.tsu.ru

Aluminum oxide being high-temperature structural ceramics owing to its mechanical characteristics, heat resistance and chemical inertness is used in many practical applications, such as microelectronics, instrument engineering, catalysis, corrosion protection, etc. Interfaces between metals and ceramics play a vital role in many processes and have been studied rather intensively in recent decades. To control processes at interfaces and their behavior under different conditions, including deformation, and understand adhesion on the microscopic level it is necessary to know the electronic structure of α-Al_2O_3 low-index surfaces. The Nb/α-Al_2O_3 interface can be described by the following orientational relationships: $[0001]\|[111]$, $[\bar{1}100]\|[11\bar{2}]$ и $[11\bar{2}0]\|[1\bar{1}0]$, and according to available experimental data Nb grows on the oxide surfaces almost strain free and forms a highly ordered crystal structures. Atomic and electronic structures of the α-Al_2O_3(0001) have been studied rather intensively using *ab initio* methods but the surfaces $(\bar{1}100)$ and $(11\bar{2}0)$ were devoted considerably less attention. In our work the atomic and electron structures of (0001), $(\bar{1}100)$ and $(11\bar{2}0)$ α-Al_2O_3 surfaces were calculated within the density functional theory. The interaction between ions and electrons was described by ultra-soft Vanderbilt pseudopotentials implemented in VASP package [1-2]. The structural and electronic properties of the oxide surfaces and the chemical bonding of the niobium films on different metal/oxide interfaces are discussed. A relationship between electronic, geometrical factors and mechanical properties of three Nb/ Al_2O_3 interfaces was studied. It is shown that the niobium films adhesion strongly depends on the type of the oxide surface.

Financial support was provided by the Russian foundation for basic research under grant No. 09-03-00523. Computational resources for this research were provided by the Interregional computational centre of the Tomsk State University (SKIF-Cyberia).

References

1. G. Kresse, J. Hafner, Phys. Rev. B **47**, 558 (1993)
2. G. Kresse, J. Furthmuller, Comput. Mater. Sci. **6**, 15 (1996)

Nanoobject Sizes of Defects in Porous Systems and Defective Materials According ADAP Method

V.I. Grafutin[1], E.P. Prokopev[1], S.P. Timoshenkov[2]
[1]A.I.Alikhanov Institute for theoretical and experimental physics (ITEP), Moscow, Russia
[2]Moscow state institute of electronic technology (MIET), Zelenograd, Russia

It is known [1], that positrons effectively probe free nanoobject volumes (basically vacancies, divacancies and pores) with the sizes ≤ 1-100 nanometer both in metals and alloys, and in semiconductors and porous systems. We receive on the basis of model of movement of a particle in a plane limited by round cylindrical absolutely impenetrable wall, more correct formulas for definition of radiuses R_c cylindrical (symbol) c and the specified formulas of radiuses spherical (symbol) sp of nanopores in the width a component of angular distribution of annihilation photons (ADAP) $\theta_{1/2}$ and energies E_{1c} and E_{sp} of the basic parapositronium state, annihilated in pores in porous silicon and aluminium dioxyde

$$R_c[\overset{0}{A}] = \frac{21{,}1}{\theta_{1/2}[mrad]}, R_c[\overset{0}{A}] = \left(\frac{30{,}58}{E_{1c}(eV)}\right)^{1/2}, \tag{1}$$

$$R_{sp}[\overset{0}{A}] = \frac{16{,}6}{(\theta_{1/2})[mrad]}, R_{sp}[\overset{0}{A}] = \left(\frac{18{,}85}{E_{1sp}(eV)}\right)^{1/2}, \tag{2}$$

where R and $\theta_{1/2}$ are expressed in Å and $mrad$ accordingly. Let's note, that in formulas (1), (2) and further in (5), (6) numbers 16,6, 18,85, etc. have dimensions [Å] while value $\theta_{1/2}$ in $[mrad]$ actually is size dimensionless.

For experimental value in porous silicon $\theta_{1/2} = 0{,}8$ мрад [1], have received average value of radius of cylindrical times $R \approx 26{,}4$ Å ≈ 3 nanometer. Their concentration in a porous layer has appeared equal ~ $5{,}6 \cdot 10^{13}$ cm^{-3}. Approach of spherical pores gives size $R_{sp} \approx 20{,}75$ Å ≈ 2 nanometer and $N_{sp} \sim 1{,}3 \cdot 10^{14}$ sm^{-3}.

Reference

В.И.Графутин, Е.П.Прокопьев, Ю.В.Фунтиков. Научная Онлайн-Библиотека: http://www.portalus.ru/modules/science/data/files/prokopiev/Prokopev-pos-Report.doc

PO-92

Iron Oxide Based Magnetic Nanoparticles Loaded With Oleic Acid/Amphiphilic Choline Analogs

I. Segal[1], A. Zablotskaya[1], A. Mishnev[1], A. Svarinskis[1], M. Maiorov[2]

[1]Latvian Institute of Organic Synthesis, Latvia

[2]Institute of Physics, University of Latvia, Latvia

e-mail: seg@osi.lv

Recently we have reported on preparation of magnetic nanoparticles bearing model organosilicon choline molecules. These molecules contain hydrophilic head and long lipophilic tails, which are able to deepen inside the first surfactant shell (oleic acid), forming bilayer membrane like structures. The influence of the silyl group nature and the hydrophobic alkyl chain length on the sorption process and on the properties of the desired nanoparticles has been examined [1-2]. Here, using the developed methodological approach, we present the preparation of the same type nanostructures for biomedical application, functionalized with more complex silyl pro-drugs – N-(2-dimethylalkylsiloxyethyl)-1,2,3,4-tetrahydro-isoquinolines. The oleic acid has been used as inter-mediator for covering of iron oxide nanoparticles with biologically active compound.

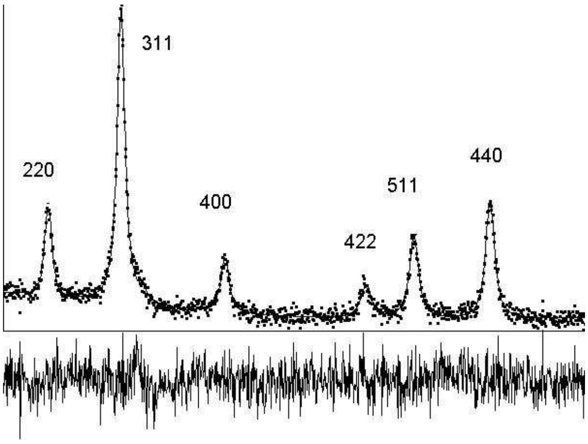

Fig.1. X-ray powder diffraction pattern with Miller indexes and profile fitting results of the initial Fe_3O_4 nanoparticles

Structural conclusions and size determination for synthesized nanoparticles are drawn based upon methods of magnetogranulometry, DLS and X-ray diffraction analysis (Fig.1). Average domain size of the particles was107Å.

Acknowledgments

We acknowledge support from Latvian Council of Sciences in the form of grant funding (Project no. 09.1321).

References

1. I. Segal, A. Zablotskaya, E. Lukevics, M. Maiorov, D. Zablotsky, E. Blums, I. Shestakova, I. Domracheva, Appl. Organometal. Chem. **22**, 82 (2008).
2. A. Zablotskaya, I. Segal, E. Lukevics, M. Maiorov, D. Zablotsky, E. Blums, I. Shestakova, I. Domracheva, J. Magn. Magn. Mater. **321**, 1428 (2009).

PO-93

Methods of Obtaining Nanodisperse Ni Ferrite, Their Structure and Magnetic Properties

N. Zaporina[1], J. Grabis[1], A. Krumina[1], M. Maiorov[2], G. Heidemane[1], D. Bocharov[3]

[1]Institute of Inorganic Chemistry, Riga Technical University, Latvia

[2]Institute of Physics, University of Latvia, Latvia

[3]Institute of Solid State Physics, University of Latvia, Latvia

e-mail: naz@latnet.lv

Nickel ferrite as typical soft ferromagnetic material has a large number of application in high frequency transformers, recording tapes, inductors, heterogeneous catalysis and gas sensors [1]. However the physical characteristics of ferrite strongly depend on the particle size and shape [2].

The aim of the present work is to study structure and morphology of nickel ferrite nanopowders by analytical electron microscopy and X-ray diffraction methods in dependence on preparation procedure and to establish connection between their structure and magnetic characteristics. The last are performed employing the vibration sample magnetometer at room temperature in the magnetic field from –10 to +10 kOe.

Three kinds of nickel ferrite nanopowders have been prepared: 1 – NiFe2O4 obtained by combustion synthesis; 2 – powder (1) covered with copper; 3 – NiFe2O4 powders, obtained by plasma chemical technique. Detailed examination of particles allows get information about the dependence of morphology and structure of powders on the conditions of their preparation. The investigation of magnetic properties of the obtained ferrite powders shows that the plasma powders have larger magnetization but its coercivity is far less then that one obtained by the chemical method.

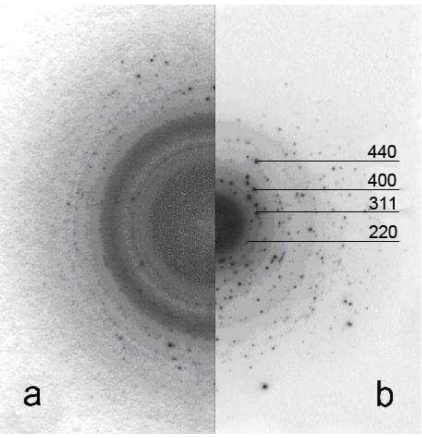

Fig. 1. Microdiffraction patterns from powders obtained by chemical (a) and plasma (b) routes.

References

1. N. Iftimie, E. Rezlescu , P. D. Popa , N. Rezlescu, J.Optoelectronics and Advanced Mater. 8, 1016, (2006).
2. X .Huang , Z. J. Chen, Magnet. and Magn. Mater. 280, 37, (2004).

PO-94

Fractionation and Size Determination of the Ferrite Nanoparticles

M. Maiorov[1], G. Kronkalns[1], M. Kodols[2], M. Lubane[2], E. Blums[1]
[1]Institute of Physics, University of Latvia, Latvia
[2]Institute of Inorganic Chemistry, Riga Technical University, Latvia
e-mail: maiorov@sal.lv

The ferrite nanoparticles obtained by wet method of chemical coprecipitation are investigated. This method is prevalent for synthetic magnetic fluid [1], but particle size distribution in the samples is not enough narrow for some applications. To obtain narrow particle distribution the nanoparticle set may be transformed to stabilized colloidal solution in liquid matrix. Then it may be fractionated by centrifugation or by gradient magnetic field.

In this work the centrifugation at acceleration 7000g were used for separation narrow fractions from colloidal solution of nanoparticles. The alternative way was a separation on thin ferromagnetic wire in external magnetic field well-known as High Gradient Magnetic Separation. The solution under investigation was a colloidal solution nanoparticles of maghemite and magnetite in hydrocarbon, which was stabilized by oleic acid.

The particles sizes of obtained fraction were determined by different methods. These are magnetization curve analysis (magnetogranulometry), X-ray diffraction line broadening, electronic microscopy, Dynamic Light Scattering. On Fig. 1 the sizes distributions from magnetogranulometry are shown for original sample and for different fractions after centrifugation.

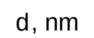

Fig.1. Ferrite particles magnetic sizes distribution: 1 – original sample, 2 and 3 - light and dark part after centrifugation.

References

1. E. Blums, A. Cebers, M. M. Maiorov, Magnetic Fluids, Walter de Gruyter & Co., Berlin -- New-York, 1997, 416 p.

PO-95

Conductive and Photoconductive Properties of V-VI Group Semiconductor Nanowires

G. Kunakova[1], P. Birjukovs[1], J. Prikulis[1], Z. Alute[1], J. Varghese[2], J.D. Holmes[2], D. Erts[1]

[1]Institute of Chemical Physics, University of Latvia

[2]National University of Ireland, Cork, Ireland

e-mail: Pavels.Birjukovs@lu.lv

V-VI group semiconductor nanowires grown in ordered anodized aluminium oxide (AAO) membrane are perspective for applications in energy conversation, sensors, and nanoelectronics. Bi_2S_3 and Sb_2S_3 nanowire arrays used in our experiments were grown inside AAO pores with diameter 20-200 nm.

In the work, we have combined various techniques for investigation of conductive and photoconductive properties of encapsulated nanowires inside AAO. Macroscopic contacts were used for characterization of groups of nanowires inside AAO. Optically transparent conductive electrode was deposited on the top surface and thick Au film on bottom side of nanowire arrays.

In-situ Adapted SmarAct GmbH 13D-manipulation and probing system inside a Scanning Electron Microscope (SEM) Hitachi S-4800 and atomic force microscope with conductive probe were used for characterization of individual nanowires. Electron beam lithography also was used for fabrication of Ti/Au contacts on individual nanowires deposited on the surface. Individual Bi2S3 nanowires were obtained by dissolution of AAO matrix while freestanding Sb2S3 nanowires were used for characterization.

Resistivity of individual nanowires was determined from I(V) characteristics. Samples were illuminated with different wavelengths and intensities to induce optoelectronic processes. Photoconductivity, kinetic components, response time, on-off ratio and stability were measured using all above methods.

PO-96

Electrical Impedance Spectroscopy of Bi_2S_3 and Gold Nanowire Arrays

J. Katkevics[1], A. Viksna[1], G. Kunakova[2], A. Pastare[2], J.D. Holmes[3], D. Erts[2]

[1]Department of Chemistry of University of Latvia, Latvia

[2]Institute of Chemical Physics, University of Latvia, Latvia

[3]Department of Chemistry, Materials Section and Supercritical Fluid Center, University College Cork, Ireland

e-mail: Arturs.Viksna@lu.lv

Characterization of conductive properties and filling quality of nanowires incorporated inside anodized aluminum oxide (AAO) membranes is important for applications in nano, optoelectronics and sensors. The main aim of the current study is electrochemical characterization of nanowire arrays by Electrochemical Impedance Spectroscopy (EIS).

In order to measure the fragile samples of XX nm thick AAO, a special electrochemical cell using the total volume of electrolyte up to several droplets was developed (Fig. 1). Various parameters of EIS spectra were investigated for filled and empty AAO membranes with different pore sizes (50-200 nm).

The complex electrochemical impedance and double layer capacitance were calculated for the whole area of investigated membrane electrode, as well as for individual nanopores or nanowires. Additionally for the characterization of nanopores and nanowires electron microscopy mapping was used. Nanowire resistivity was calculated using Levi method.

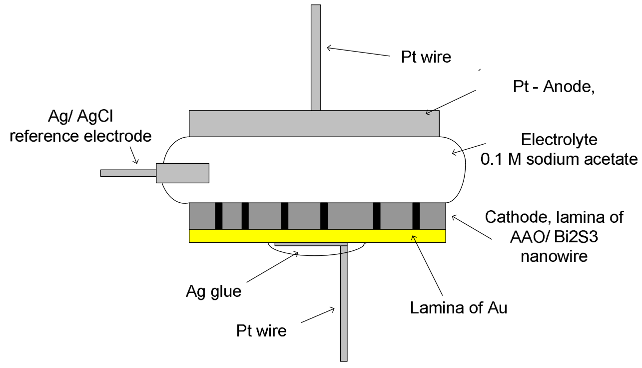

Fig. 1 Schematic drawing of a drop electrochemical cell

The experimental results show that the EIS parameters of cell with AAO membrane can be interpreted in terms of equivalent circuit denoted as R(RQ)((CR)(RQ)), but with sintered Au and Bi_2S_3 nanowires as R(RQ)(RQ). We show that EIS method can be applied not only for measurements of electrochemical impedance parameters of nanomaterials, but also for the conductivity calculation of individual nanowire in an array.

PO-97

Electrochemical Impedance Spectra of Particulate Matter and Nanosmoke Particles

A. Osite, J. Katkevics, A. Viksna, G. Vaivars
Faculty of Chemistry, University of Latvia
e-mail: agnese.osite@lu.lv

The ambient atmosphere contains millions of tonnes of solid matter and smoke aerosols of different size and content. Aerosols from internal combustion engines, coal fly ash originated from combustion, dust from mineral formation, metallic and smoke nanoparticles containing different metallic elements belong to such particulate matter that is complex chemical mixture. Commonly fine $PM_{2.5}$ and coarse PM_{10} airborne particles are fractionated, and lately an increased attention is being paid to ultra fine particles $PM_{1.0}$ [1, 2].

Black carbon, which is considered as important component of nanosmoke and airborne particles, is investigated relatively for a long time, but only a few papers are describing the investigation of impedance spectra of atmospheric particles [3]. The investigation of electrochemical impedance spectra would help to acquire competence regarding electro stationary and electro dynamical properties of particulate matter. The methodology of particle sampling and the sample preparation was developed to obtain electrochemical impedance spectra of aerosol particles. The principles of the electrochemical cell's structure and the relationship between parameters obtained from impedance spectra and black carbon mass concentration present work describes (Fig.1).

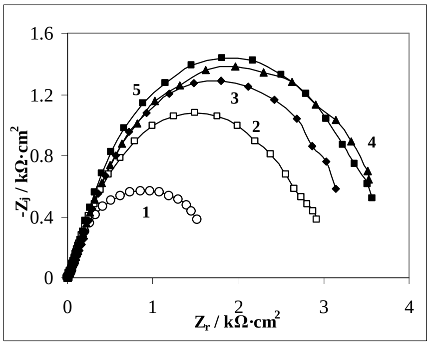

Fig.1. Impedance data for airborne aerosol particle samples with black carbon (BC) concentration as a parameter after 30 min of immersion under statistic conditions in a 0.1 M K_2SO_4 solution (using Pt plate electrodes): applied polarization potential -0.35 V; 1 – filter with PM, BC 0.7 $\mu g \cdot cm^{-2}$; 2 – filter with PM, BC 1.8 $\mu g \cdot cm^{-2}$; 3 – filter with PM, BC 2.4 $\mu g \cdot cm^{-2}$; 4 – filter with PM, BC 3.2 $\mu g \cdot cm^{-2}$; 5 – filter with PM, BC 6.1 $\mu g \cdot cm^{-2}$.

References

1. T. A. Pakkanen, V. M. Kerminen, *et.al.* Atmos. Environ. **35**, 4593-4607 (2001)
2. B. Nowack, T. D. Bucheli. Environ. Pollut **150**, 5-22 (2007)
3. I. Salma, R. Ocskay, G. Lang. Atmos. Chem. Phys. Discuss. **8**, 1981 – 2011 (2008)

PO-100

Non-Destructive Characterisation of Nanocomposite Material Properties

P. Akishin, M. Wesolowski, E. Barkanov
Institute of Materials and Structures, Riga Technical University
e-mail: pavels.akisins@rtu.lv

Carbon nanotubes (CNT) and their mechanical properties have been investigated from 1990s. CNT have the Young's modulus of 1 TPa, making them ideal reinforcement for different composite materials. Nowadays CNT-reinforced aluminium alloys have promising perspectives for an application in many industrial sectors such as aerospace, marine and land transport. Unfortunately the material data provided by manufacturers very often do not contain all necessary information to predict the behaviour of nanocomposite materials using different analyses tools. Additionally, due to high costs of nanocomposites, their experimental testing with conventional fracture methods suffers from high expenses too. On this reason non-destructive techniques for the material properties characterisation have been adapted for testing of nanocomposite samples with small dimensions.

Static approach using three-point-bending test and two dynamic methods, namely, impulse excitation method and inverse technique based on the planning of experiments and response surface methodology have been applied to study strength and dissipative material properties of aluminium alloys with different CNT volume content. Three-point-bending test allows to determinate the elastic modulus of the material in terms of the measured centre deflection δ, the applied load P and the geometry of a beam. In order to keep this approach non-destructive, this technique is only applicable for the elastic behaviour of composite beams which can be obtained usually for a strain less than 0.5%. Vibration test based on the impulse excitation is adopted for the determination of elastic properties of nanocomposite beams. In this method the main requirement is to establish dimensions, material density, and experimental fundamental flexural and torsion frequencies of a beam with free-free boundary conditions. The inverse technique based on vibration tests is applied to estimate storage and loss moduli of nanocomposite materials. This approach consists of the experimental set-up, the numerical model and the material parameters identification procedure developed by applying a non-direct optimisation method based on the planning of the experiments and a response surface method in order to considerably decrease the computational efforts.

PO-101

Synthesis and Characterization of Inorganic Nanotubes and Fullerenes-like Nanoparticles

A.C. Peterlevitz, H.J. Ceragioli, H.G. Zanin, V. Baranauskas
Faculdade de Engenharia Elétrica e de Computação Departamento de Semicondutores, Instrumentos e Fotônica
Universidade Estadual de Campinas
e-mail: apeterlevitz@gmail.com

In recent years, inorganic fullerenes-like structures (IF) and nanotubes have been made using numerous compounds with two layers dimensional structures, such as MoS_2, which are unstable in planar form [1]. The purpose of the present work was to investigate a method of synthesize inorganic nanotubes and fullerenes-like nanoparticles in a reactor of hot filament assisted chemical vapor deposition (HF-CVD).This process used mineral oil and camphor diluted in acetone, hydrogen and high concentration of nitrogen. The oil was comercial MolykoteA2 that is a stable suspension of particles of molybdenum disulfide (MoS_2) tiny in neutral mineral oil. Silicon substrates have been used. After cleaning, the substrates have been coated with MolykoteA2. In the sequence, the samples were immersed in the CVD system reaction chamber and fed with a mixture of camphor and acetone diluted in hydrogen (15 % vol.) and nitrogen (85 % vol.). A total flow rate of about 100 sccm, regulated by precision flow meters, and a total pressure of about 30 mbar were maintained throughout. The deposition temperature, measured by a thermocouple positioned at the reverse side of the substrate, was set at 773 K [2]. The produced samples are evaluated in relation to the morphological data obtained by Field emission scanning electron microscopy (FESEM), High resolution transmission electron microscopy (HRTEM), Energy dispersion x-ray spectroscopy (EDS) and Raman spectroscopy.

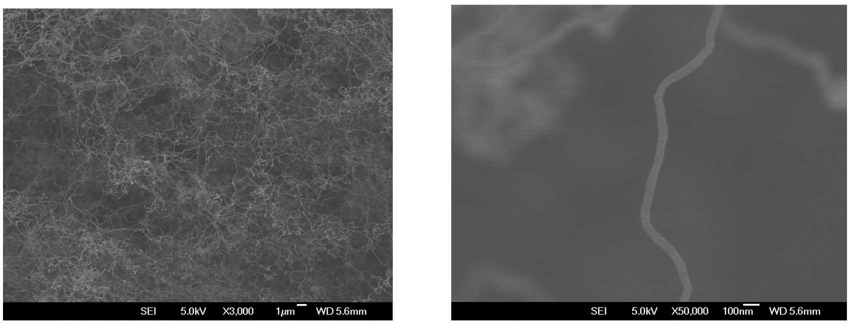

Fig.1 FESEM images of inorganic nanotubes with different magnifications

References

1. R. Tenne and C.N.R. Rao, Phil. Trans. R. Soc. Lond. A, **362**, 2099-2155 (2004).
2. H. J. Ceragioli, A. C. Peterlevitz, J. C. R. Quispe, A. Larena, M. P. Pasquetto, M. A. Sampaio and V. Baranauskas, Journal of Physics: Conference Series **100**, 1-4 (2008).

PO-102

Growth Temperature Influence on the GaN Nanowires Grown by MOVPE Technique

L. Dimitrocenko, K. Kundzins, A. Mishnev, I. Tale, A. Voitkans, P. Kulis
Institute of Solid State Physics, University of Latvia, Latvia
e-mail: lauris@cfi.lu.lv

One-dimensional gallium nitride (GaN) nanostructures are promising material for nanoscale optoelectronic of blue and ultraviolet nanodevices due to its wide direct bandgap [1]. In the present work GaN nanowires (NWs) were successfully grown by Vapor-Liquid-Solid (VLS) growth mechanism on GaN template using metal-organic vapor phase epitaxy (MOVPE) technique (Fig.1). High purity trimthylgallium and ammonia used as gallium and nitrogen sources respectively. Hydrogen is used as a carier gas. The diameter of NWs ranges from 100 to 200 nm and their length is up to few microns. Fabricated NWs were characterized by scanning electron microscopy (SEM) and X-ray diffraction (XRD) where XRD reveals that the GaN NWs is of single-phase wurtzite structure. We investigated the temperature influence on the NWs growth and found that growth conditions are strongly dependent on the substrate temperature.

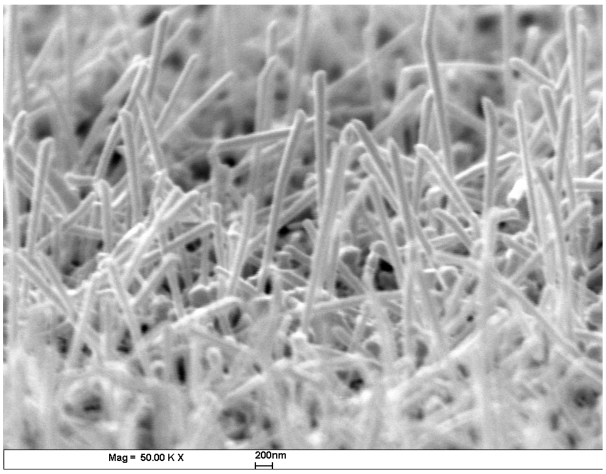

Fig.1 GaN nanowires grown on GaN template using MOCVD technique

References

1. Haraguchi K, Katsuyama T, Hiruma K and Ogawa K, *Appl. Phys. Lett.* **60**, 745 (1992)

PO-103

Ex Situ Investigations of MOCVD-Grown Gallium Nitride Nanowires Using Reflection High Energy Electron Diffraction

A. Voitkans[1], L. Dimitrocenko[1], S. Bartlin[2], P. Kulis[1], I. Tale[1]

[1]Institute of Solid State Physics, University of Latvia, Latvia

[2]University of Rostock, Germany

e-mail: andris.voitkans@lais.lv

Vertically oriented nanowires (NWs) of single-crystalline wurtzite GaN have been fabricated on sapphire substrate, via metal organic chemical vapor deposition (MOCVD) process at 800 °C using trimethylgallium and ammonia as source materials. Large and small GaN NWs (~100 nm in diameter) are formed by a vapor-liquid-solid growth mechanism where tapering tips of larger NWs are attributed to the simultaneous epitaxial growth.

Herebay we present *ex situ* investigations on the orientation and structure of grown GaN nanowires on GaN(0001) surface using reflection high energy electron diffraction (RHEED). Compared to X-ray based techniques RHEED has several advantages: high surface sensitivity, the de-Broglie wavelength can be easily adjusted and electrons have a much higher cross section. Also the relative low cost of the experimental setup makes it suitable for daily work in laboratory conditions. While RHEED is a standard tool for *in situ* investigations on crystal and thin film growth it has been scarcely used for *ex situ* nanostructure investigations, although it gives simultaneous information on properties of surface and supported nanostructures [1].

References

1. A. Klaibert, A. Voitkans and K.-H. Meiwes-Broer, Phys. Rev. B **81**, 073412 (2010)

PO-104

Structure, Morphology and Dynamics of Ni_{1-X} O Thin Films

A. Anspoks, R. Kalendarev, A. Kuzmin
Institute of Solid State Physics, University of Latvia, Latvia
e-mail: andris.anspoks@cfi.lu.lv

Nickel oxide thin films find a variety of applications, for example, in electrochromic and memory devices, gas and spin-valve giant magnetoresistance (GMR) sensors, and p-type transparent conducting electrodes. In this work we present the results for nanocrystalline $Ni_{1-x}O$ thin films, produced using reactive dc-magnetron sputtering for different Ar/O_2 gas ratios on three different substrates (silicon, glass, and polyimide tape).

X-ray diffraction patterns for all films consist of a single broad peak indicating a prefered NiO(200) growth orientation with the nanocrystallites size of ~20 nm, ~15 nm, and ~6 nm, according to the Scherer’s analysis. The morphology of the films depends on the substrate type (Fig. 1 (a,a′)) and sputtering conditions (Fig. 1(a,b,c)).

The local structure around nickel atoms in nanocrystallites was studied by the Ni K-edge x-ray absorption spectroscopy using synchrotron radiation from the HASYLAB DESY C1 bending-magnet beamline in the temperature range of 10-300 K. The experimental EXAFS signals were interpreted using (i) conventional approach, based on the single-scattering approximation, and (ii) molecular-dynamics simulations taking into account multiple-scattering effects [1]. The obtained results indicate nanocrystallites volume expansion and the presence of large static disorder.

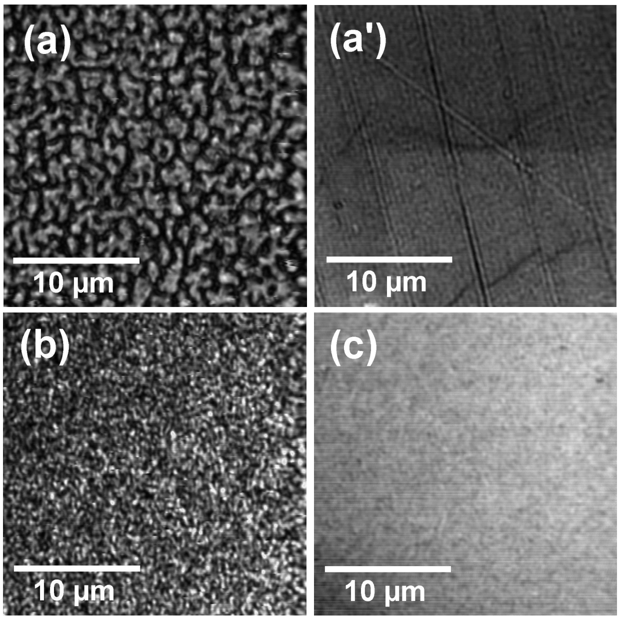

Fig.1 Confocal images of NiO_{1-x} thin films sputtered on glass (a,b,c) and polyimide film (a′) with the nanocrystallites size of (a) ~20 nm, (b) ~15 nm, (c) ~6 nm.

References

1. A. Anspoks, A. Kuzmin, A. Kalinko, and J. Timoshenko, Solid State Commun. **150**, 2270 (2010).

PO-105

Local Structure Relaxation and Lattice Dynamics in Polycrystalline and Nanocrystalline NiO

A. Anspoks, A. Kalinko, A. Kuzmin
Institute of Solid State Physics, University of Latvia, Latvia
e-mail: andris.anspoks@cfi.lu.lv

An abnormal magnetic crossover, closely related to the lattice expansion, has been observed recently in NiO nanocrystals at room temperature for particle sizes smaller than 50 nm [1]. To clarify the mehanism of structure change in nanoparticles, we performed an accurate comparative study of local atomic structure and lattice dynamics in polycrystalline and nanocrystalline NiO in the temperature range from 6 K to 300 K using the Ni K-edge EXAFS spectroscopy.

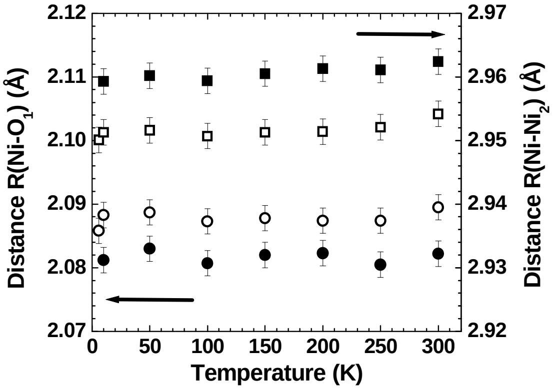

Fig. 1. Temperature dependence of the first shell Ni-O_1 and second shell Ni-Ni_2 distances in polycrystalline and nanocrystalline NiO.

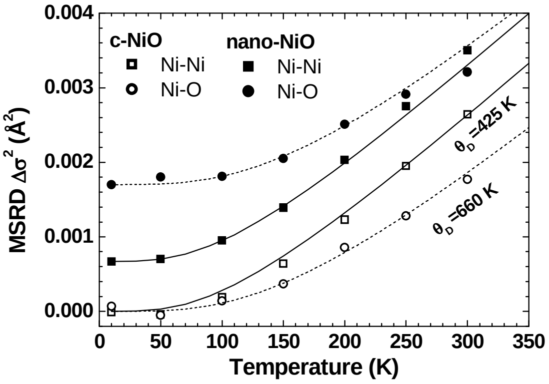

Fig. 2. Temperature dependence of the relative MSRD $\Delta\sigma^2=\sigma^2(T)-\sigma^2(0\ K)$ for Ni-O and Ni-Ni atom pairs in polycrystalline and nanocrystalline NiO. Debye model (θ_D) approximation is shown by solid and dashed lines.

Our results unambiguously indicate that (i) the average first shell Ni-O_1 distance in nanocrystalline NiO shrinks compared with polycrystalline NiO (Fig. 1); (ii) the average second shell Ni-Ni_2 distance expands in nanocrystalline NiO compared with polycrystalline NiO, in agreement with overall unit cell volume expansion observed by diffraction (Fig. 1); (iii) the thermal contribution into the mean-square relative displacement (MSRD) σ^2 is close in both polycrystalline and nanocrystalline NiO and can be described by the Debye models (Fig. 2); (iv) the static disorder is additionally present in nanocrystalline NiO in both Ni-O_1 and Ni-Ni_2 shells due to the structure relaxation (Fig. 2).

References

1. L. Li, L. Chen, R. Qihe, G. Li, Appl. Phys. Lett. **89**, 134102 (2006).

PO-106

Effect of Nano-Powder Morphology on the Properties of ZnO Sintered Ceramics

R. Zabels, F. Muktepāvela, L. Grigorjeva, K. Kundziņš

Institute of Solid State Physics, University of Latvia, Latvia

e-mail: rzabels@gmail.com

In this work a simple method of Zn vapor condensation and oxidation in a tube furnace was utilized to obtain ZnO powders with grained (d=100-300 nm) and multipod-like (whiskers) (d=50-100 nm, l=3-10 µm) morphology. Powders were compacted at identical conditions and a following sintering performed at temperature of 1200 ^{o}C. Research included structural investigations using optical, AFM and SEM microscopies, a photoluminescence investigation for an evaluation of present defects and a nanoindentation to characterize a mechanical behavior and stability of obtained ceramics.

Ceramics sintered from the grained powder have large grains – in diameter ranging from 3 to 20 µm with an average size of about 10 µm. The surface of the ceramic is covered with large ZnO spheres which are a product of a rapid oxidation of an escaped excess Zn vapor. The porosity is high – polishing revealed that large voids with a size 10-80 µm are present throughout the volume of ceramics. Micropores are located not only at grain boundaries but inside grains as well. At 12 K besides an excitonic peak this ceramic exhibited a broad green luminescence band attributed to defect states (particularly oxygen vacancies or interstitial Zn) which is in an agreement with the SEM micrographs.

For the ceramic from the multipod-like powder grain sizes range from 1 to 10 µm with an average grain size of 4 µm. In this case micropores are present only in triple junctions of grain boundaries. No pores were detected inside the volume of grains. Luminescence at 12 K revealed a narrow excitonic band with a probable satellite peak and an almost non-existent green luminescent band which is an evidence of a high quality of ceramic sintered from whiskers powders. Mechanical properties (hardness is 3 GPa and Young's modulus 120 GPa.) of these ceramics are high and comparable to high pressure ceramics and a single crystal ZnO. Indentation tests have shown the specific role of the grain boundaries in the deformation behavior of ceramics. The effect of the powder morphology on the properties of sintered ceramics may be explained from the standpoint of contacts phenomena during the sintering.

Acknowledgments

This work has been supported by the European Social Fund within the project «Support for Doctoral Studies at University of Latvia».

PO-107

Swift-Ion-Induced Nanostructuring of Lif Crystals: Comparison between Heavy and Light Projectiles

J. Maniks[1], I. Manika[1], R. Zabels[1], R. Grants[1], E. Tamanis[2], K. Schwartz[3]
[1]ISSP, University of Latvia, 8 Kengaraga Str., LV 1063 Riga, Latvia
[2]University of Daugavpils, 1 Parades Str. LV5400 Daugavpils, Latvia
[3]GSI, Darmstadt, 1 Planckstrasse, D-64219 Darmstadt, Germany
e-mail: manik@latnet.lv

Modifications of the structure of LiF crystals irradiated with swift heavy (^{238}U, ^{208}Au) and lighter (^{50}Ti, ^{12}C) ions of the specific energy of 11.1 MeV/u at fluences in the range of 10^{11} to 10^{13} cm^{-2} have been studied using the AFM, SEM, High-resolution XRD and nanoindentation methods. The structure was revealed by a chemical etching. The AFM and SEM studies on samples irradiated with heavy ions (^{238}U, ^{197}Au) showed a nanostructuring of the irradiated layer. The nanostructure consists of columnar grains with a width of about 50-100 nm. In the case of the lightest ions (^{12}C), the irradiation resulted in the formation of dislocation-reach structure. No bulk nanostructures were observed even at the highest fluence of 5×10^{12} cm^{-2}. For ions with an intermediate atomic mass (^{50}Ti), either a dislocation-reach structure or a nanostructure was formed in relation to the fluence and the energy loss.

In the nanostructured layer, the rocking curves obtained by a high-resolution X-ray diffraction expose the formation of a mosaic structure with low-angle boundaries between blocks.

Nanoindentation tests show a strong ion-induced increase of hardness (up to 150-200%) confirming the high volume concentration of strong obstacles for dislocations, such as defect aggregates, dislocations and grain boundaries. The results show that strong modifications of the structure and mechanical properties occur under conditions of a track overlapping that leads to a saturation and an aggregation of single defects.

PO-108

Aggregation Processes and Nanostructuring in LiF Crystals Irradiated with 150 MeV ^{84}Kr Ions

A. Dauletbekova[1], I. Manika[2], R. Zabels[2], R. Grants[2], A. Akilbekov[1], M. Zdorovets[3]

[1]Eurasian National University, Astana, the Republic of Kazakhstan

[2]Institute of Solid State Physics, University of Latvia, Latvia

[3]Institute of Nuclear Physics, accelerator DC-60, Astana, the Republic of Kazakhstan,

e-mail: alma_dauletbek@mail.ru

Beams of swift heavy ions with the MeV-GeV energy have increasingly gained an interest for their application in the structuring of materials on the micro- and nanometre scale. Generally, heavy ions (e.g. U, Pb and Au) cause more substantial modifications of the structure and properties compared to lighter projectiles. However, the irradiation with swift heavy ions is accompanied by undesirable effects of swelling and a generation of long-range stresses. The results of the present study show that the nanostructuring in LiF crystals can be ensured also under the irradiation with lighter Kr ions. With this aim, we used 150 MeV Kr ions, the energy loss of which in the surface layer exceeds the threshold for the track core damage (10 keV/nm). Irradiations were performed at the fluence 10^{12} cm^{-2} ensuring the overlapping of tracks. Methods of optical absorption spectroscopy, AFM, SEM and nanoindentation in the present study were used.

The optical absorption measurements show the saturation of F centers (~ 10^{19}cm^{-3}) at the fluence of 10^{12} ions/cm^2 in LiF irradiated with 150 MeV Kr ions with a decrease of the F center concentration at higher fluence. In LiF crystals irradiated with Kr ions an enhancement of F and F_n (F-aggregates) absorption bands via flux was observed. This demonstrates the increase of the mutual interaction between H centers leading to the enhancement of F and F_n centers.

The AFM and SEM results show the formation of bulk nanostructures in the surface layer where the energy loss of ions surpasses the threshold of 10 keV/nm. The nanostructure consists of columnar grains with nanoscale dimensions (~100 nm). At a lower energy loss the structure enriched with defect aggregates (e.g. prismatic diclocation loops, colloids, bubbles of molecular fluorine) was found to appear. The nanoindentation tests show a strong ion-induced increase of hardness that confirms a high volume concentration of strong obstacles for dislocations e.g. defect aggregates, dislocations and grain boundaries.

PO-109

Elaboration of Polymer/Nanostructured Carbon Composite for Humidity Sensor Application

M. Novada[1], K. Ozols[1], M. Knite[1], V. Tupureina[2]
[1]Institute of Technical physics, Riga Technical University, Latvia
[2]Institute of Polymer materials, Riga Technical University, Latvia
e-mail: marika.novada@gmail.com

Humidity detection in the surrounding atmosphere is of great interest for industrial, scientific and environmental application. Our main goal is to create humidity sensor, which is small in dimensions, flexible and which is able to measure moisture inside different materials. Interaction of polyvinyl alcohol – high structure carbon black (PVA-CB) nanoparticle composite with water vapor has been investigated in this work. It was found that under influence of water vapour the electrical resistance of the composite changes and the change depends on exposition time. The humidity sensing effect of PVA-CB composite can be explained as fallows: water vapour induces composite matrix swelling, distance between carbon aggregates is increased and tunneling currents in thin layers of matrix are changed. Samples containing 9 w.% of nanostructured carbon black showed more stable initial resistance and were found to be more sensitive showing 33 % resistance change in 10 min. in humid environment (relative humidity 99%). The effect is reversible, necessary time for relaxation has been found to be equal to 60 min. Comparing results obtained from simultaneous measurements of the electrical resistance and the sample length with theory of charge tunneling in conductor-polymer composite, we can conclude that current tunneling exists in thin layers of PVA-CB composite among carbon nanoparticles (Fig.1). In our opinion, the existence of tunneling currents in the composite directly enhances the sensitivity of the composite to water vapour.

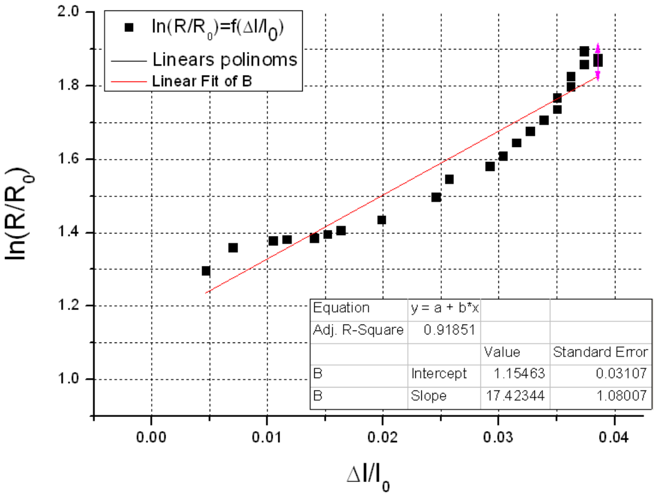

Equation	y = a + b*x		
Adj. R-Square	0.91851		
		Value	Standard Error
B	Intercept	1.15463	0.03107
B	Slope	17.42344	1.08007

Fig. 1. The change of electrical resistance of PVA-CB9 composite versus relative elongation induced by composite swelling in water vapour.

PO-110

Polyisoprene – Nanostructured Carbon Black Composite for Pressure Sensing

J. Zavickis, A. Kjapsņa, A. Linarts, M. Knite
Institute of Technical Physics, Riga Technical University, Latvia
e-mail: juriszavickis@inbox.lv

Recent studies show, that elastomer composites containing nanostructured conductive fillers can be used as pressure sensing materials [1], and theoretically they could outcompete certain pressure sensing materials, which are used at the moment.

In this work the polyisoprene-nanostructured carbon black composite has been studied, possessing both: piezoresistive and hyper-elastic properties. The primary goal was to investigate electrical properties of the composite, depending on concentration of conductive filler.

The percolation threshold (Fig.1) and its critical parameters have been determined at first, as it is crucial for further investigation. This has been done according to W.Bauhofer [2]. The obtained percolation threshold has been compared with similar thresholds, acquired for composites using different dispersing techniques and fillers. The time dependence of composites electrical resistivity has been experimentally studied and evaluated at constant strain (mechanical loading) as well as directly after switching out the loading.

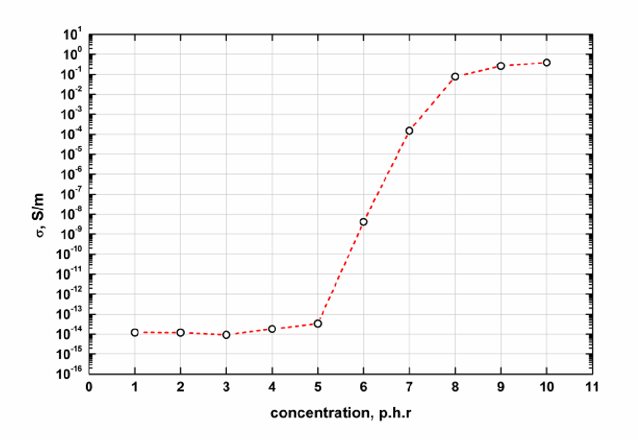

Fig.1 The dependence of the electrical conductivity of polyisoprene-nanostructured carbon black composite on the concentration of conductive filler.

References

1. M.Knite, V.Teteris, A.Kiploka, J.Kaupuzs, Sensor. Actuat. A **110**, 142 (2004)
2. W. Bauhofer, J.Z.Kovacs, Compos. Sci. Technol. **69**, 1486 (2009)

PO-111

Thermodiffusion Motion of Electrically Charged Nanoparticles

A. Mezulis, O. Petrichenko

Institute of Physics, University of Latvia

e-mail: ansis@sal.lv

Nanoparticles are of great interest not only in solid physics but also as colloidal nanocarriers. Colloidal systems offer a lot of applications, a particular part of that is related to the particle migration at concentration and temperature gradient conditions. Generally, if the dielectrophoretic effect is negligible, the nanoparticle flux is described as $j = -D_M\left(\nabla c + S_T c\nabla T\right)$, where the Soret (i.e. thermodifussion) coefficient S_T can be either positive or negative. The sign of the Soret coefficient governs the nanoparticle flux along the temperature gradient or opposite it. Experimental and theoretical investigations in last 15 years with hard particles of diameter 10...20 nm prove that the sign of thermodiffusion coefficient is determined by applied method of particle stabilization.

Principal theoretical investigations [1] predict that electrically charged nanoparticles may have both signs of S_T. It depends on non-dimensional particle surface potential $\zeta = e\varphi_R/kT$, which usually is 5...10 after stabilization by Massart method [2], and on the ratio λ between double layer thickness and particle radius. By different concentration of ions in electrolyte λ can be varied in rather wide range 0.01...0.2. Actual values of ζ and λ may result both signs of theoretically calculated velocity of thermodiffusion motion u, which is linked with the Soret coefficient:

$$S_T = -\frac{3}{4}\frac{R_H}{L_B}\frac{c}{T}u(\lambda,\zeta), \qquad (1)$$

where RH is the hydrodynamic radius of a particle and LB is Bjerrum length.

In the present work some electrically stabilized colloidal nanoparticle samples with different parameters are examined. Experimental work provides the values of ζ, λ, R_H and S_T that allows to make a comparision between measured and theoretically calculated thermodiffusion coefficient by Eq. (1). The accordance within 30% must be taken as rather good, since in the present model the behaviour of electric double layer is considerably simplified.

References:

1. K. Morozov, Thermal Nonequilibrium Phenomena in Fluid Mixtures, Lect. notes in Phys. **584**, p.38 (2002)
2. R. Massart, IEEE Trans. on Magn. MAG-**17**, p.1247 (1981)

PO-112

Microconvection in Optically Induced 3D Structures of Magnetic Nanoparticles

D. Zablotsky, E. Blums

Institute of Physics of University of Latvia, Salaspils, Latvia

e-mail: Dmitrijs.Zablockis@gmail.com

Ferrofluids are colloidal suspensions of magnetic nanoparticles and as such they possess superparamagnetic properties. We will consider a periodic concentration grating induced in a thin layer of ferrofluid by interfering laser beams under the action of the externally applied uniform magnetic field (Fig.1). As soon as the optical grating is focused within the layer, the corresponding concentration grating starts to develop due to the strong Soret effect of the colloidal solution. When the diffusion and thermodiffusion reach equilibrium, the beams are switched off and the gratings are allowed to relax. It is suspected ([1-2]) that microconvective instability driven by the internal demagnetizing fields may develop at this stage causing enhanced mixing and significant increase of the effective diffusion coefficient.

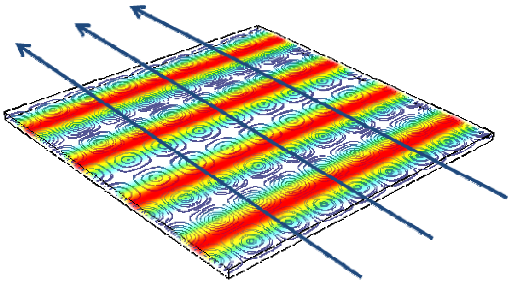

Fig.1. Problem setup

We will consider the equilibrium distribution of temperature and concentration and the time-dependent base state describing the relaxation of the grating for different orientations of the applied magnetic field. We pay special attention to the role of the transversal boundary and the corresponding gradients violating the uniformity of the induced grating. We determine the role of the microconvection in the relaxation of the grating by means of the numerical simulations and nonlinear Galerkin model.

References

1. M. Igonin, Magnetohydrodynamics 40 (1) (2004) 53–64.
2. A. Mezulis, E. Blums, Magnetohydrodynamics 41 (4) (2005) 341–348

PO-113

The Effects of Zr on Temperature Ranges of Hydrogen Desorption in Mg-Zr composition

I. Neklyudov, N. Lomino, O. Morozov, V. Kulish, V. Zhurba, V. Ovcharenko, O. Kuprin
National Science Center “Kharkov Institute of Physics and Technology”, Kharkov, Ukraine
e-mail: morozov@kipt.kharkov.ua

One of materials production method in nanocrystalline state is introduction nanoforming addition. To nanoforming elements it is necessary to carry of chemical elements which do not form binary phases with components alloy and show negligible solubility. At the present stage of solubility studying of chemical compounds in system Mg-Zr is not revealed. Production magnesium-zirconium of composites was carried out by a method of plasma evaporation - sputtering a component on molybdenum. Deuterium saturation of Mg-Zr composites was realized through 24 keV D_2^+ ion implantation at temperatures of ~110 K to doses ranging between 1×10^{17} and 5×10^{18} D/cm^2. After implantation of the preset deuterium dose, the temperature ranges of deuterium desorption in zirconium were determined by the thermal desorption spectroscopy technique.

Contents of the zirconium below 30 at.% lead to significant downturn of temperature desorption deuterium. At the same time excess of this concentration is accompanied by slight increase of temperature desorption deuterium in comparison with allocation from pure Mg.

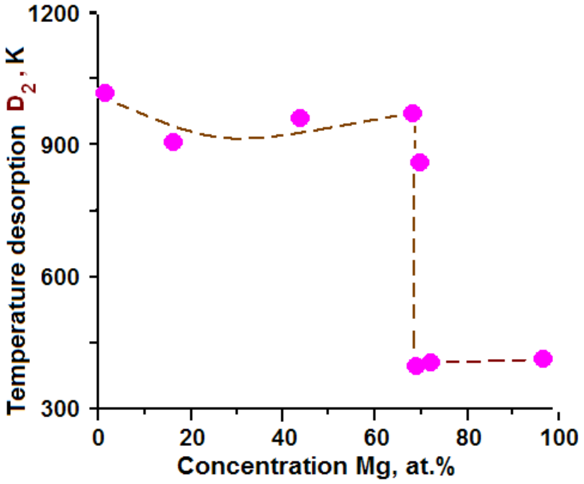

Fig.1. Dependence of maxima temperature desorption deuterium peak from component Mg-Zr composites A deuterium dose ~7.3×10^{17}D/см^2

Dependence of maxima temperature desorption deuterium peak from composition a component magnesium - titanic composites (see fig. 1) evidently shows quantum character of temperature allocation of the same doses implanted deuterium depending on component magnesium - zirconium composite elements. On the basis of the received data on десорбции hydrogen on an example of compositions Mg-Zr it is drawn a conclusion on perspectives of search of materials of hydrogen storage which have nanoforming.

PO-114

Band Gap Tuning and Improved Optical Properties of ZrO_2-SnO_2 Nanocomposite Thin Films Prepared by Sol-Gel Route

J.S. Lakshmi, K. Joy, I.J. Berlin, J.K. Thomas, P.V. Thomas

Thin film Lab, Post Graduate and Research Department of Physics, Mar Ivanios College, Thiruvananthapuram 695015, India

e-mail: lakshmi.sunny@gmail.com

Transparent nanocomposite ZrO_2-SnO_2 thin films(various molar ratio) with grain size < 100nm are of significant scientific and technological importance due to several advantages such as tailoring of grain size and band gap for applications in optical devices[1]. Such mixed-composition thin-film systems often exhibits improved optical and physical properties against the participating component films [2]. XRD pattern of ZrO_2-SnO_2 (0.5/0.5) thin film prepared by sol-gel dip-coating technique annealed at 773K shows that the films are crystalline with a particle size of 10.98 nm (tetragonal ZrO_2), 8.04 nm (tetragonal SnO_2) and 14.26 nm (orthorhombic $ZrSnO_4$). SEM shows that microstructure of the 0.5/0.5 composite consists of isolated SnO_2 particles dispersed in ZrO_2 matrix. Maximum transmittance in UV-VIS region (> 80%) was observed for the composite film with ZrO_2/SnO_2 molar ratio 0.5/0.5 suggesting a better densification and homogeneity of the thin film. ZrO_2/SnO_2 nanocomposite thin film with molar ratio of 0.9/0.1 has one direct band to band transition with a band gap at 5.25eV. This band gap decreases to 3.95eV with 0.1/0.9 ratio substantiating tailoring of band gap by varying molar ratio. The nanocomposite thin film exhibit improved photoluminescence (PL) emission peak at 426 nm for excitation wavelength of 373 nm. The high density of oxygen vacancies present in the nanocomposite film interact with interfacial atoms of zirconium and tin and leads to formation of a considerable amount of trapped states within the band gap giving rise to PL. The changes in the grain size as well as band gap , accompanied by modification of structure, makes ZrO_2-SnO_2 thin film ideal for gas sensor applications.

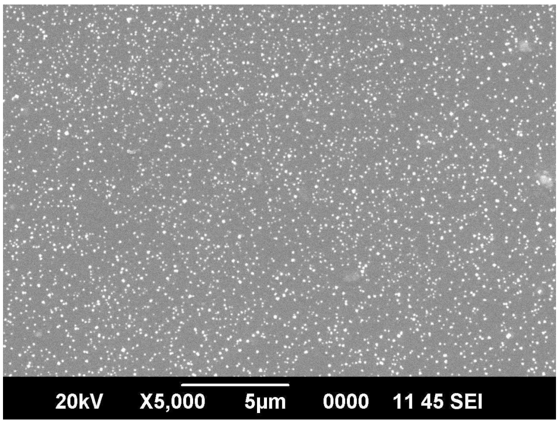

Fig.1 SEM micrograph of ZrO_2-SnO_2 thin film(0.5/0.5) on corning glass (5 coatings) annealed at 773K

References

1. J.S. Chen, S. Chao, J.S. Kao, H. Niu, C.H. Chen, Appl. Opt. **35**, 90 (1996)
2. N.K. Sahoo, A.P. Shapiro, Appl. Opt. **37**, 8043 (1998)

PO-115

Nanostructure of Metaphosphate Glasses

L. Maksimov[1], A. Anan'ev[1], V. Bogdanov[2]
[1]Research and Technological Institute of Optical Material Science, Russia
[2]Saint Petersburg State University, Russia
e-mail: maksimov@interglass.spb.su

The study is aimed at estimation of nano-scaled inhomogeneities in glassy metaphosphates of alkali, alkali-earth, barium, lead, rare-earth and some other metals and their influence on glass parameters significant for their applications in fiber optics, optoelectronics, photonics, etc. Measure of glass inhomogeneity is the Landau-Placzek ratio which is determined from Rayleigh and Mandel'shtam-Brilllouin scattering (RMBS) spectra of glasses. It includes contributions from density, concentration and anisotropy fluctuations “frozen-in” at glass melt cooling. These contributions can be determined separately via the Schroeder-Macedo formalism [1] if the high temperature acoustic data for glass melts is known. Pure and mixed glassy metaphosphates of alkali, alkali-earth, rare-earth metals have been studied by means of RMBS spectroscopy and their melts – by the measurement of temperature and frequency dependencies of ultrasonic wave propagation.

Comparison of the data obtained with results of X-ray scattering data [2, 3] demonstrates that glassy metaphosphates cannot be considered as highly chemically homogeneous pseudo single component glasses characterized by the “frozen-in” isobaric density fluctuations only. It was found that concentration fluctuations were poorly developed in glassy sodium metaphosphate while increase in atomic mass and polarizability of a metal ion led to non monotonous growth of concentration fluctuations in glasses.

Obtained systematic data on fluctuation inhomogeneities in glassy metaphosphates opens the opportunity to design multicomponent phosphate glasses with extremely low Rayleigh scattering losses for fiber optic communication lines, effective laser glasses, glasses for electooptical fiber drawing, etc.

The study was partially supported by RFBR (Grant # 10-03-00323).

References

1. J. Schroeder, Light Scattering of Glass. Treatise on Material Science and Technology, 12, Glass 1, − New York, N.Y. Academic Press (1977)
2. G. Walter, R. Kranold, W.Gocke, N. Enenke. J.Appl.Cryst. 24, 616 (1991)
3. R. Kranold, G. Walter, D.Stachel. A.Barz. Glastech. Ber. Glass Sci. Technol. 71C, 512 (1998)

PO-116

The Polarization Profile in PZT Based Piezoelectric Ceramics

O. Malyshkina[1], A. Movchikova[1], E. Barabanova[1], O. Kalugina[1], I. Embil[2], S. Pugachev[2]

[1]Tver State University, Tver, Russia

[2]State Marine Technical University of St. Petersburg, St.- Peterburg, Russia

e-mail: Olga.Malyskina@mail.ru

The bulk PZT based piezoceramic samples find the wide application for medical instruments, hydroacoustics and other ultrasonic devices. To improve the electromechanical properties of piezoelectric ceramics in the main chemical composition is added various oxides [1-4]. At the same time in the literature are widely covered only a question of the dielectric parameter of these materials. Information on chemical composition effect to the polarization profile of the piezoelectric ceramics is absent.

In the present work the polarization distribution of PZT based ceramics with following composition: of lead zirconate titanate (**PZT**), PZT (75%) and barium zirconate titanate (25%) (**PBZT**), PZT (86%) and sodium bismuth zirconate titanate (14%) (**PNBZT**) has been studied. The polarization profile was examined with the TSW method [5].

It is shown the differences between the polarization profiles were measured on the samples with and without vacuum deposition of silver black layer (AgO). For ceramics with silver black layer were poled less than 2 months to measurement time near surface was observed space charge, which induces an additional polarization (Fig.1). It should be noted that deposition of silver black layer on the samples were poled more then a few months before measuring this effect is not observed. A similar effect may mean that the relaxation of free charge at the grain boundaries after the poled process is quite a long time.

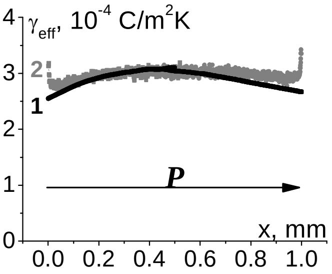

Fig.1 Polarization profiles of PZT ceramic. Sample without (cover 1) and with (cover 2) silver black. Arrow shows the direction of spontaneous polarization vector.

This work was performed within the Federal Target Program "Research and Research-Pedagogical Personnel of Innovation Russia for 2009-2013".

References

1. Electronic catalog "Morgan Matroc", USA: http: //www.morganmatroc-ecd.com/catalog/propert.htm
2. Sensor Technology Limited (BM Hi-tech Division). Piezoelectric ceramics. Product catalogue. Application notes. 1995.
3. Electronic catalog "APC International Ltd.", USA: http://www.thomasregiser.com/olc/apc/apcpiez.htm
4. Electronic catalog "SPK Electronics Co. , Ltd.", Taiwan: http: //spkecl.com/chapte8b.htm
5. O. V. Malyshkina, A.A. Movchikova, R.M. Grechishkin, O.N. Kalugina. Ferroelectrics. **400**, 63-75 (2010).

PO-117

The Pyroelectric Properties of SBN Crystals of Different Composition

O. Malyshkina[1], V. Lisitsin[1], A. Movchikova[1], J. Dec[2], T. Lukasiewicz[3]

[1]Tver State University, Tver, Russia

[2]University of Silesia, Institute of Materials Science, Katowice

[3]Institute of Electronic Materials Technology, Warsaw

e-mail: Olga.Malyskina@mail.ru

In solid solutions of strontium barium niobate $Sr_xBa_{1-x}Nb_2O_6$ (SBN) barium oxide BaO is replaced by strontium oxide SrO. In this connection it is interesting to study the effect of the percentage of Sr - Ba on the pyroelectric properties and the state of polarization in these materials. The SBN crystals with x<0.5 are not relaxor, whereas with x>0.5 have the relaxor properties. It was investigated the SBN crystals with nominal concentrations of strontium in the solution 26%, 35%, 50%, 61% and 75 %. The crystals were grown by the Czochralski method [1]. The real composition, was determined using the Inductively Coupled Plasma – Optical Emission Spectroscopy (ICP-OES) method, are $Sr_{0.35}Ba_{0.69}Nb_2O_{6.04}$ (SBN35) $Sr_{0.40}Ba_{0.60}Nb_2O_{6.0}$ (SBN40), $Sr_{0.51}Ba_{0.48}Nb_2O_{5.98}$ (SBN50) $Sr_{0.59}Ba_{0.38}Nb_2O_{5.97}$ (SBN61), and $Sr_{0.72}Ba_{0.25}Nb_2O_{5.97}$ (SBN75) respectively.

The pyroelectric effect and influence of thermocycling on the polarization state in the SBN crystals was examined by several methods: the dynamic pyroelectric measurement and TSW method [2]. In particular it is shown that at room temperature in SBN crystals without relaxor properties the value of the pyroelectric coefficient is less than that of relaxor SBN (Fig. 1). At the same time, the question of whether it is connected with the increase of the Curie point in SBN crystals with smaller *x* or due to a lower value of polarization in SBN crystals without relaxor properties is the subject to further study.

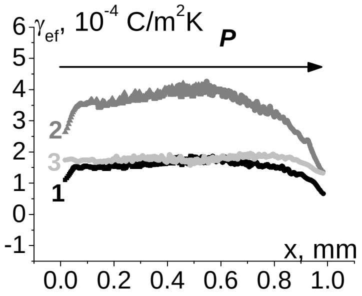

Fig. 1 The distribution of the effective value of the pyroelectric coefficient on thickness for the SBN40 (1), SBN61 (2) and SBN35 (3) crystals. The polarization direction in the sample is shown by an arrow

This work was performed within the Federal Target Program "Research and Research-Pedagogical Personnel of Innovation Russia for 2009-2013".

References

1. T. Lukasiewicz, M.A. Swirkowicz, J. Dec, W. Hofman, W. Szyrski. J. of Crystal Growth. **310**. 1464-1469 (2008).
2. O. V. Malyshkina, A.A. Movchikova, R.M. Grechishkin, O.N. Kalugina. Ferroelectrics. **400**, 63-75 (2010).

PO-118

Dielectric Properties of Nanograin PSN Ceramics

M. Ivanov[1], M. Kinka[1], S. Rudys[1], J. Banys[1], C. Bogicevic[2], J.M. Kiat[2, 3]

[1]Laboratory of Phase Transitions Dielectric Spectroscopy, Faculty of Physics, Vilnius University, Sauletekio str. 9 III 817, LT-10222, Vilnius, Lithuania

[2]Laboratoire Structures, Propriétés, Modélisation des Solides (UMR 8580) Ecole Centrale Paris, Grande Voie des Vignes 92295 Châtenay-Malabry Cedex

[3]Laboratoire Léon Brillouin, CE Saclay CNRS-UMR 12, 91991 Gif-Sur-Yvette Cedex, France

e-mail: maksim.ivanov@ff.stud.vu.lt

Ferroelectric materials are of high interest for both researchers and engineers due to their remarkable properties, which makes them great targets of fundamental research for scientists and materials of choice for a variety of devices [1]. As a result, nanoscale size effects became of interest in both scientific and technological fields.

Size has clear influence on dielectric properties of the material, as can be seen from figure 1. Firstly, maximum of dielectric permittivity diminishes and dispersion region shifts to lower temperatures with smaller grain sizes. Furthermore, no relaxor-normal ferroelectric phase transition at 370 K is observed, which is typical for bulk ceramics [2]. However, this graph shows remnant anomaly in imaginary part around 370 K for grains bigger than 60 nm. This must mean that in this case some weak interaction between polar nanoregions still takes place.

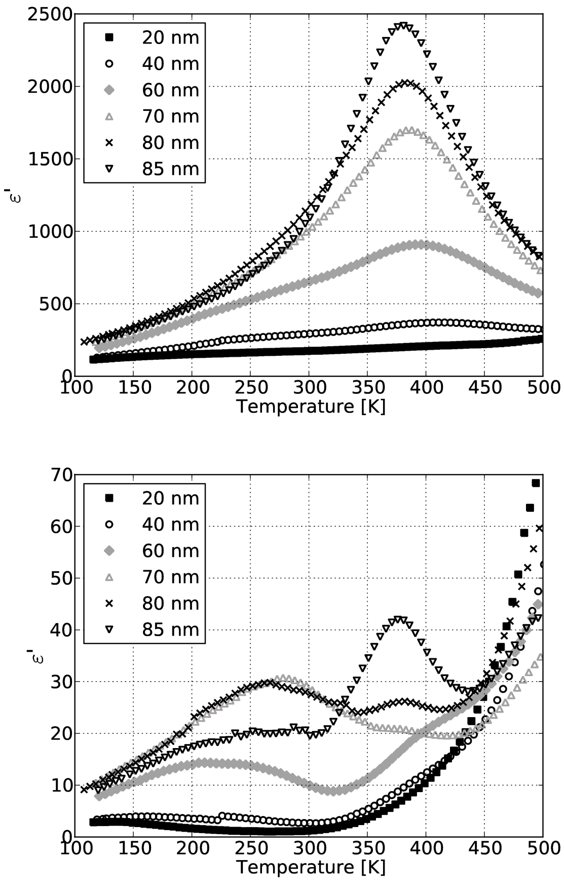

Fig.1 Temperature dependencies of the real part (top) and imaginary part (bottom) of complex dielectric constant for different grain sizes at 1.21 kHz frequency.

References

1. C. H. Ahn, K. M. Rabe, and. J.-M, Triscone, Science **303**, 488 (2004).
2. F. Chu, I. M. Reaney, and N. Setter, J. Appl. Phys. **77**, 1671 (1995).

PO-119

The Electrical Properties of $BaZr_xTi_{1-x}O_3$ Solid Solution

B. Garbarz-Glos[1], K. Bormanis[2], M. Antonova[2]

[1]Institute of Physics, Pedagogical University, Podchorążych 2, 30-084 Krakow, Poland

[2]Institute of Solid State Physics, University of Latvia, Kengeraga 8, LV-1063, Riga, Latvia

e-mail: barbaraglos@gmail.com

Ferroelectric ceramics are the materials most frequently used in practice as sensors, transducers, memory cell, tunable microwave devices (filter and phase shifter), multilayer ceramic capacitors, microelectromechanical systems and actuators. Among a number of well-known ferroelectric materials a barium titanate (BT) and its some solid solutions are the most interesting due to excelent dielectric properties. One of them is a barium titanate-barium zirconate solid solution ($BaTiO_3$-$BaZrO_3$). Zr-substitution at Ti-site is an effective way to improve the electrical properties of the material. Moreover, $BaTi_{1-x}Zr_xO_3$ (BZT) solid solutions are lead-free compounds and enviroment-friendly dielectrics with similar performances as many Pb-based electroceramics. In present paper the structural and electric properties of zirconium-doped barium titanate $BaZr_xTi_{1-x}O_3$ ceramics prepared by conventional sintering process were investigated. Powder X-ray measurements were used for structure and phase analysis. A single-phase perovskite structure of the materials has been identified. X-ray diffraction indicate clearly the structural changes and confirm the effective diffusion of zirconium to form BZT. Scanning electron microscopy investigations reveals a fine grain and dense microstructure. No significant impurities were detected in an EDS spectrum and the samples are in good stoichiometric ratio. Electric properties as a function of temperature and frequency were measured. All measurements were performed under normal atmospheric conditions. For $x>0.20$ the obtained dielectric data suggest a relaxor character of phase transformation and indicate the existence of only one phase transformation. Two different activation energy values corresponding to two different regions were observed in the Arrhenius plot, which was attributed to two different types of trap levels present in the BZT ceramics.

PO-120

Dielectric Properties Of 0.4Na$_{1/2}$Bi$_{1/2}$Tio$_3$ – (0.6 – X)SrTio$_3$ - XPbTio$_3$ Solid Solutions

Š. Svirskas[1], M. Ivanov[1], Š. Bagdzevičius[1], J. Banys[1], M. Dunce[2], M. Antonova[2], E. Birks[2], A. Sternberg[2], V. Zauls[2]

[1]Vilnius University, Faculty of Physics, Saulėtekio av. 9, III b., LT-10222 Vilnius, Lithuania

[2]Institute of Solid State Physics, University of Latvia, Kengaraga street 8, LV-1063 Riga, Latvia

e-mail: sarunas.svirskas@stud.ff.vu.lt

Many solid solutions based on Na$_{1/2}$Bi$_{1/2}$TiO$_3$ (NBT) were brought to the daylight of ferroelectric society in order to find low-lead compositions suitable for practical applications. Barium titanate (BT), strontium titanate (ST) and lead titanate (PT) were used as secondary materials for NBT solid solutions [1, 3]. The only report on such solid solutions as NBT-ST-PT is published in [2]. It is known that PT and ST influence phase transition of NBT differently. PT induces ferroelectric phase transition, while ST enhances relaxor properties [1]. So the main interest is to find out how these materials interact with each other in NBT solid solutions.

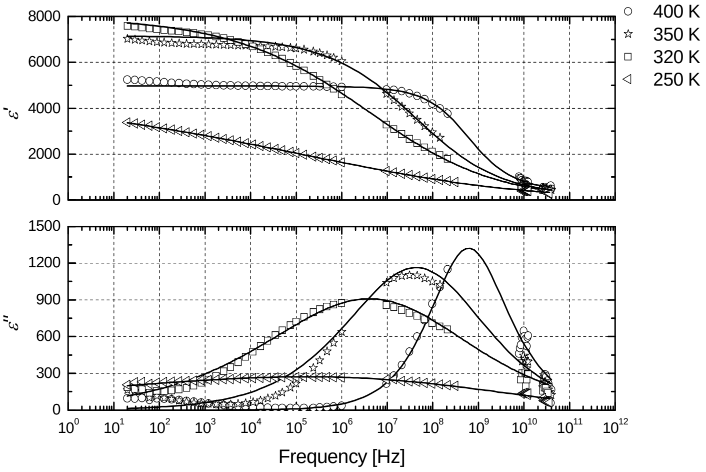

Fig. 2 Frequency dependence of complex dielectric permittivity for x = 0.1 at different temperatures, solid lines are fits with Havriliak-Negami formula

Fig. 1 shows frequency dependence of complex dielectric permittivity for x = 0.1. The purpose of the report is to investigate dynamic dielectric properties of 0.4NBT-(0.6-x)ST-xPT for x = 0.1 and 0.15.

References

1. Lee, J.K.; Hong, K.S.; Kim, Ch.K.; Park, S.E.; Phase transitions and dielectric properties in A-site ion substituted (Na$_{1/2}$Bi$_{1/2}$)TiO$_3$ ceramics (A=Pb and Sr), *Journal of Applied Physics*, vol. 91, No.7 (2002)
2. Birks, E., Dunce, M., Antonova, M. and Sternberg, A., Phase transitions in modified Na$_{1/2}$Bi$_{1/2}$TiO$_3$-SrTiO$_3$ solid solutions, *Physica Status Solidi C*, vol.6, No.12 (2009)
3. Gomah-Pettry, J.R.; Said, S.; Marchet, P.; Mercurio, J.P.; Sodium-bismuth titanate based lead-free ferroelectric materials, *Journal of the European Ceramic Society*, vol. 24, Issue 6, Electroceramics VIII (2004)

PO-121

Dielectric Properties of $Ba_2Pr_xNd_{1-x}FeNb_4O_{15}$ Relaxor Materials

M. Kinka[1], S. Bagdzevicius[1], R. Grigalaitis[1], E. Castel[2], M. Josse[2], M. Maglione[2]

[1]Faculty of Physics, Vilnius University, Sauletekio 9, LT-10222, Vilnius, Lithuania

[2]ICMCB-CNRS, 87 avenue du Docteur Schweitzer, F-33608 Pessac Cedex, France

e-mail: martynas.kinka@delfi.lt

Most relaxor materials, under nowaday investigation, belong to the perovskite family and a lot of them contain lead ions. It has been reported that lead-free perovskites are more flexible than lead-containing ones because a continuous crossover from ferroelectric to relaxor is observed in many solid solutions [1]. Another interesting issue in these structures is the coexistence of relaxor and ferroelectric behavior in the same material.

Here we present our results of dielectric investigation of novel lead-free $Ba_2Pr_xNd_{1-x}FeNb_4O_{15}$ materials with a more open (compared with perovskites) crystalline network, the so-called tetragonal tungsten bronze structure. $Ba_2NdFeNb_4O_{15}$ is a ferroelectric (T_C=323 K) whereas $Ba_2PrFeNb_4O_{15}$ is a relaxor below 170 K. The flexibility of the open TTB network allows the ferroelectric to relaxor crossover on scanning the composition from Nd to Pr in these solid solutions. We have obtained a continuous crossover between these end member behaviors with a coexistence of ferroelectricity and relaxor in the intermediate range. Phase transition temperatures are only slightly affected by Pr amount, but also a huge cooling-heating hysteresis was observed, which origin is under discussion yet.

References

1. A. Simon, J. Phys.: Condens. Matter **16**, 963 (2004)

PO-122

Dielectric Spectroscopy of 7 % Sb Doped ($K_{0.5}Na_{0.5}$)NbO_3 Ceramic

S. Bagdzevicius[1], R. Grigalaitis[1], J. Banys[1], A. Sternberg[2], K. Bormanis[2], V. Zauls[2]

[1]Faculty of Physic, Vilnius University, Sauletekis str. 9/3, 10222 Vilnius, Lithuania

[2]Institute of Solid State Physic, University of Latvia, Kengaraga str. 8, 1063 Riga, Latvia

e-mail: sarunas.bagdzevicius@ff.stud.vu.lt

Over last decades electroceramics like PZT ($Pb(Zr_xTi_{1-x})O_3$), PMN ($Pb(Mg_{1/3}Nb_{2/3})O_3$) or PSN ($Pb(Sc_{1/2}Nb_{1/2})O_3$ attracted great technological and scientific interest because of excellent piezoelectric properties[1]. These ceramics are widely used in sensors, transducers and other micro and macro electromechanical devices. However, the toxicity of lead oxide led to a demand for safer materials[2]. One of such ceramic potentially could be sodium potassium niobate $K_xNa_{1-x}NbO_3$ (KNN) near one of its morphotropic phase boundary (MPB) which is at about 50% K and 50% Na for KNN[1]. The main problem with KNN is sintering: it is difficult to obtain well-sintered KNN ceramic using an ordinary sintering process because of the high volatility of alkaline elements at high temperatures[3].

In this work we present obtained dielectric permittivity and conductivity results of KNN ceramics doped antimony $(K_{0.5}Na_{0.5})(Nb_{0.93}Sb_{0.07})O_3$ with sintering aid MnO_2 (0.5 mol. % MnO_2). Its dielectric properties was investigated in broad frequency (from 1 Hz to 54 GHz) and temperature (from 130 K to 800 K) range.

Above room temperature obtained results shows two phase transitions at T=560 K and T=425 K. Partial substitution of Nb^{+5} ions with Sb^{+5} lowers both of these phase transitions temperatures compared to undoped KNN ceramics[4]. Below room temperature investigation revealed one more dielectric permittivity dispersion, which could be attributed to diffused phase transition corresponding to phase transition in pure KNN from orthorhombic into rhombohedral ferroelectric state at $T_{O\text{-}R}$=165 K[4].

References

1. J. Rodel, W. Jo, K. T. P. Seifer, E. M. Anton, T. Granzow and D. Damjanovic, *J. Am. Ceram. Soc.*, 92 [6] 1153–1177 (2009).
2. Council Epat, Directive 2002/95/EC of the European parliament and of the council of January 2003 on the restriction of the use of hazardous substances in electrical and electronic equipment. *Eur. J.*, 37**,** 19 (2003).
3. M. Dambekalne, M. Antonova, M. Livinsh, A. Kalvane, A. Mishnov, I. Smeltere, R. Krutokhvostov, K. Bormanis, A. Sternberg, *Integrated Ferroelectrics* 102 (1) 52-61 (2008).
4. E. Buixaderas, V. Bovtun, M. Kempa, M. Savinov, D. Nuzhnyy, F. Kadlec, P. Vanek, J. Petzelt, M. Eriksson and Z. Shen, *J. Appl. Phys.* 107, 014111 (2010).

PO-123

Thermal Characterization of Dielectric Properties and Ferroelectric Phase Transition in $(Ba_{0.8}Sr_{0.2})(Ti_{0.75}Zr_{0.25})O_3$ Solid Solution

D. Sitko[1], W. Śmiga[1], B. Garbarz-Glos[1], K. Bormanis[2], A. Kalvane[2]

[1]Institute of Physics, Pedagogical University, Podchorążych 2, 30-084 Krakow, Poland

[2]Institute of Solid State Physics, University of Latvia, Kengeraga 8, LV-1063, Riga, Latvia

e-mail: dsitko@up.krakow.pl

The present work concerns the dielectric characteristic of $(Ba_{0.8}Sr_{0.2})(Ti_{0.75}Zr_{0.25})O_3$ (BSTZ) for the future application. A lead-free solid solution $(Ba_{0.8}Sr_{0.2})(Ti_{0.75}Zr_{0.25})O_3$ was prepared by a two-stage hot-pressing technology. The structure and morphology of BSTZ were characterised by X-ray diffraction (XRD) and scanning electron microscopy (SEM).

The studies of electric permittivity were performed depending on frequency of electric measuring field in heating and cooling processes in wide range of temperature (150K -500K). The thermal bahaviour of BSTZ was studied using the Differential Scanning Calorimetry.

The results obtained showed diffuse of the phase transition in investigate temperature region. The same evidence we obtained from the electric permittivity measurements. Furthermore the electric permittivity clearly depends on frequency. The maximum values of ε_m show decrease with increasing of frequency. However, the loss tangent of $(Ba_{0.8}Sr_{0.2})(Ti_{0.75}Zr_{0.25})O_3$ ceramics reveal inverse trends.

PO-124

Effect of Electromechanical and Temperature Loading on Dielectric Properties of PLZT−x/65/35 Ceramics (x=8 and 8.5)

J. Suchanicz[1], K. Pytel[2], K. Konieczny[1], A. Finder[3], M. Livinsh[4], A. Sternberg[4]

[1]Institute of Physics, Pedagogical University, ul. Podchorążych 2, 30-084 Kraków, Poland
[2]Institute of Technics, Pedagogical University, ul. Podchorążych 2, 30-084 Kraków, Poland
[3]High National School, ul.Mickiewicza 21, 38-500 Sanok, Poland
[4]Institute of Solid State Physics, University of Latvia, Kengaraga 8, LV-1063 Riga, Latvia
e-mail: sfsuchan@gmail.com

Influence of uniaxial pressure (0-1000 bars) applied parallel to the *ac* electric field on dielectric properties of La–modified lead–zirconate–titanate ceramics with Zr/Ti ratio of 65/35 was investigated. Applying uniaxial pressure leads to a reduction of the peak intensity of the electric permittivity (ε), of the frequency dispersion as well as of the dielectric hysteresis. The peak intensity of ε becomes diffuse and shifts to a higher temperature with increasing the pressure. Our results show that applying uniaxial pressure induces similar effects as increasing the Ti–ion concentration in PZT system. We interpreted our results based on the Cochran soft-mode and domain switching processes under action of combined electromechanical loading. These studies clearly showed that the applied stress has significant influence on the dielectric properties of perovskite ceramics.

PO-125

Dielectric and Ferroelectric Froperties of Lead-Free NKN and NKN-Based Ceramics

J. Suchanicz[1], I. Smeltere[2], A. Finder[3], K. Konieczny[1], B. Garbarz-Glos[1], M. Antonova[2],
A. Sternberg[2]

[1]Institute of Physics, Pedagogical University, ul. Podchorążych 2, 30-084 Kraków, Poland
[2]Institute of Solid State Physics, University of Latvia, Kengaraga 8, LV-1063 Riga, Latvia
[3]High National School, ul.Mickiewicza 21, 38-500 Sanok, Poland
e-mail: sfsuchan@gmail.com

Lead-free ceramics of $Na_{0.5}K_{0.5}NbO_3$ (KNN), $Na_{0.5}K_{0.5}(Nb_{0.94}Sb_{0.06})O_3$ (KNNS6) and $Na_{0.5}K_{0.5}(Nb_{0.94}Sb_{0.06})O_3$ +0.5%MnO_2 (KNNS6+0.5%MnO_2) have been produced by a solid phase hot pressing sintering process. The ceramics have been sintered at 1120-1145°C.

The results of the X-ray diffraction measurements show that obtained samples possess perovskite structure. The micrograph of the fractured surface showed a dense structure ceramics, which was in good agreement with 91-95% relative density determined by the Archimedes method. An average grain size decreases after Sb and Mn doping (from about 15 μm for KNN to about 5 and 2 μm for KNNS6 and KNNS6+0.5%MnO_2, respectively). Low frequency (100Hz-200kHz) investigations revealed the diffuse phase transitions. It was found that Mn or Sb doping influence dielectric and ferroelectric properties.

The pyroelectric and hysteresis loops measurements show that obtained ceramics possess ferroelectric behaviour with the relatively large remanent polarization (18-22 μC/cm^2) and the low coercive field (7-9 kV/cm). The obtained results are discussed in the framework of foreign ions/lattice imperfections, which create local electric and elastic fields. The obtained materials are expected to be promising candidates for lead-free electronic ceramics.

PO-126

The Structural, Microstructural, Mechanical and Dielectric Properties of the $Li_{0.1}Na_{0.9}NbO_3$ Ceramic

W. Śmiga[1], M. Livinsh[2]

[1]Institute of Physics, Pedagogical University, Podchorążych 2, 30-084 Krakow, Poland

[2]Institute of Solid State Physics, University of Latvia, Kengeraga 8, LV-1063, Riga, Latvia

e-mail: w.smiga@gmail.com

For the ABO_3 ferroelectrics substituting A or B cation sit by izo- or heterovalent ions can alter electric properties of the investigated material. One of these popular composition is lithium sodium niobate (LNN), in which the ferroelectric and dielectric properties are significantly dependent on the Li content. In the present paper structural, mechanical and dielectric behavior in perovskite LNN ceramics were studied. Polycrystalline samples of $Li_{0.1}Na_{0.9}NbO_3$ were obtained by means of conventional ceramic technology. X-ray diffraction (XRD) measurements followed by Reitveld analysis showed the formation of single perovskite phase with an orthorhombic structure at room temperature. Calculated lattice parameters a, b, c, and the volume of the unit cell V for $Li_{0,1}Na_{0,9}NbO_3$ decreased in comparison with pure $NaNbO_3$. This is in an accordance with the fact, that the ionic radius of Li^+ is much smaller than the ionic radius of Na^+, which causes the decrease of lattice parameters. The microstructure and EDS measurements have been performed by means of scanning electron microscope (SEM). The examined sample is good quality, the grains are well shared and there is a very small amount of a glassy phase. The EDS analysis shows the fairly homogenous distribution of all elements throughout grains. The EPMA was applied to the analysis of the distribution of elements at the sample surface. Youngs′s modules E, shear modules G and Poisson ratio ν were determined using an ultrasonic method. The performed investigations of mechanical properties show that the lead-free material based on sodium niobate solid solution (***LNN***) posses better mechanical parameters than pure $NaNbO_3$. The dielectric measurements were performed in heating and cooling processes for temperatures from 300 to 800 K in the range of frequencies 100 Hz – 200 kHz. Local minima electrical conductivity appearing is associated with a polaronic transport mechanism. The minimum values of this electrical conductivity can be a results of the change in the nature of the conduction mechanism: from the tunnel into the hopping mechanism, that is the short-range into the long-range mechanism. At high temperatures at all frequencies the value of a.c. conductivity differs little from the value of d.c. conductivity. The activation energy was calculated from the Arrhenius plots.

PO-127

Influence of BaTio$_3$ on Synthesis and Structure of Lead-Free Ceramics Based on KNN

I. Smeltere[1, 2], M. Antonova[2], M. Livinsh[2], B. Garbarz-Glos[3]

[1]Biomaterials Innovation and development centre, Riga Technical University, 3/3 Pulka Str., Riga, LV-1007, Latvia

[2]Institute of Solid State Physics University of Latvia, 8 Kengaraga Str., Riga, LV-1063, Latvia

[3]Institute of Physics, Pedagogical University, ul.Podchorażych 2, 30-084 Krakov, Poland

e-mail: ilze.smeltere@cfi.lu.lv

In the present work processing and characterization of lead free KNN based ceramics have been studied. Compositions with a stoichiometric formula $(1\text{-}x)(K_{0.5}Na_{0.5})Nb_{1\text{-}y}Sb_yO_3\text{-}xBaTiO_3$ (x=0.01, 0.02, 0.04; y=0.04, 0.07) were produced by solid state sintering method. Manganese oxide MnO_2 was added after synthesis in order to promote the sintering of ceramic samples. Presence of MnO_2 in the composition lowers the optimal sintering temperatures. The influence of $BaTiO_3$ on the microstructure, density and electrical properties was investigated. X-ray diffraction analysis confirmed that obtained samples had a pure perovskite structure with no traces of secondary phase. However with increasing content of $BaTiO_3$ the cell changed from monoclinic to tetragonal at room temperature. Microstructural investigation reveals that ceramic samples have homogenous structure with cubical grain shape; the smaller ones ~0.5µm are slightly rounded. The grain sizes (0.4-2 µm) are quite similar for different compositions however MnO_2 addition suppresses the grain growth. Phase transition point T_c is shifted to lower temperatures in comparison to Sb-substituted KNN ceramics. Phase transition peak at T_c is broad indicating the diffuse phase transition.

PO-128

Dielectric Properties of Hot-Pressed Modified Lead Free Ceramics Based on Alkaline Niobates

I. Smeltere[1], M. Livinsh[1], M. Antonova[1], A. Kalvane[1], B. Garbarz-Glos[2]

[1]Institute of Solid State Physics, University of Latvia, Latvia

[2]Institute of Physics, Pedagogical University of Krakow, Poland

e-mail: ilze.smeltere@cfi.lu.lv

Lead-free piezoelectric ceramics $(K_{0.5}Na_{0.5})(Nb_{1-x}Sb_x)O_3$+0.5mol.%$MnO_2$, where $x=0 \div 0.10$, with single phase structure and orthorhombic symmetry at room temperature were prepared by conventional ceramic sintering and hot-pressing technology. The optimal hot-pressing temperatures of compositions were within 1120^o – 1150^{o}C for 2-4 h with 20 MPa pressure. It has been found that sintering densification occurs within a narrow temperature range, and the density decreases apparently when the sintering temperature slightly exceeds the optimal one. The same tendency was observed in the case of dielectric and piezoelectric properties. MnO_2 functions as a sintering aid and effectively improves the densification. The samples reached density from 4.26g/cm^3 (94.0% of theoretical density) for undoped $(K_{0.5}Na_{0.5})NbO_3$ to 4.41 g/cm^3 (97% of TD) for Mn/Sb^{5+} co-doped hot-pressed ceramics.

Compared with undoped $(K_{0.5}Na_{0.5})NbO_3$, the co-effects of MnO_2 doping and Sb^{5+} substitution for Nb^{5+} lead to significant improvement in the dielectric properties: ε at the T_c increased from 6000 to 12400 (conventional ceramic method) and from 11000 to 16400 (hot-pressing method).

PO-129

Thermal Expansion, Burns Temperature and Electromechanical Properties in $Na_{1/2}Bi_{1/2}TiO_3$-$SrTiO_3$-$PbTiO_3$ Solid Solutions

M. Dunce[1], R. Taukulis[1], E. Birks[1], I. Aulika[2], A. Fuith[3], M. Antonova[1], A. Sternberg[1]
[1]Institute of Solid State Physics, University of Latvia, Latvia
[2]Italian Institute of Technology-IIT@PoliTO, Italy
[3]Institute of Experimental Physics of University of Vienna, Austria
e-mail: marija.dunce@cfi.lu.lv

The thermal expansion and electromechanical properties are presented in $Na_{1/2}Bi_{1/2}TiO_3$-$SrTiO_3$-$PbTiO_3$ solid solutions, possessing different stages of relaxor behaviour in dependence of $PbTiO_3$ concentration. Absence of clear declining of thermal expansion from paraelectric behaviour at high temperatures, which could be used to determine Burns temperature, is found. Instead Burns temperature is determined by comparing behaviour of thermal expansion of compositions with various levels of relaxor properties (different $PbTiO_3$ concentrations). The jump of thermal expansion above certain concentration of $PbTiO_3$ corresponds to a spontaneous 1st order phase transition between relaxor and ferroelectric state. Piezoelectric coefficients d_{33} and d_{31} are determined in the concentration range, where ferroelectric phase exists without applying external electric field.

PO-130

Relation of Dielectric Permittivity and Electric Field Dependence of Polarization in Some Relaxors with Perovskite Structure

M. Dunce, E. Birks, M. Antonova, M. Kundzinsh, A. Sternberg
Institute of Solid State Physics, University of Latvia, Latvia
e-mail: marija.dunce@cfi.lu.lv

Quasi-static electric field dependence of polarization P(E) in relaxors with perovskite structure (1-x)$PbMg_{1/3}Nb_{2/3}O_3$-x$PbTiO_3$, $Pb_{1-x}La_x(Zr_{0.65}Ti_{0.35})O_3$ and 0.4$Na_{1/2}Bi_{1/2}TiO_3$-(0.6-x)$SrTiO_3$-x$PbTiO_3$ is compared with dielectric permittivity in low frequency range. The results show that two electric field ranges can be distinguished in the temperature region below the maximum of dielectric permittivity. The slope of P(E), observed at low electric fields, decreases with decreasing temperature. While the slope, observed at higher electric fields, increases, if temperature is decreased, following the trend of linear P(E), which exists at temperatures above the maximum of dielectric permittivity. The values of dielectric permittivity, calculated from P(E) dependences at different temperatures, are compared with the measurements of temperature-frequency dependences of dielectric permittivity. The influence of the bias on the distribution function of relaxation times is discussed, using dependence of dielectric permittivity on the bias electric field.

PO-131

Behaviour of the Reverse Dielectric Permeability in SBN-75 Ceramics

K. Bormanis[1], A.I. Burkhanov[2], S.V. Mednikov[3], L.T. Njan[3]
[1]Institute of Solid State Physics, University of Latvia, Riga, Latvia
[2]Volgograd State Architectural and Engineering University, Volgograd, Russia
[3]Volgograd State Technical University, Volgograd, Russia
e-mail: bormanis@cfi.lu.lv

The dielectric nonlinearity observed in SBN-75 ceramics is reported. Earlier studies of polarisation switching in SBN-75 single crystals [1, 2] had shown essential decrease (as compared with ordinary ferroelectrics) of polarisation with each cycle in the thermal range of the relaxor phase, which had been related to “freezing” processes in disordered ferroelectrics.

Manifestations of similar processes were of interest in SBN-75 ceramics taking into account that dielectric permittivity ε' and dielectric loss ε'' are smaller compared with single crystal by more than order of magnitude if measured along the polar axis.

Behaviour of reverse $\varepsilon'(E_=)$ at $T < T_m$ and at $T \geq T_m$ in SBN-75 ceramics is presented in Fig. 1. a and b, respectively. Behaviour of dielectric nonlinearity at $T < T_m$, different from single crystal, is similar to that of ordinary ferroelectrics – the $\varepsilon'(E_=)$ curve is closed while at $T \geq T_m$ the magnitude of ε' practically does not depend on the bias field $E_=$.

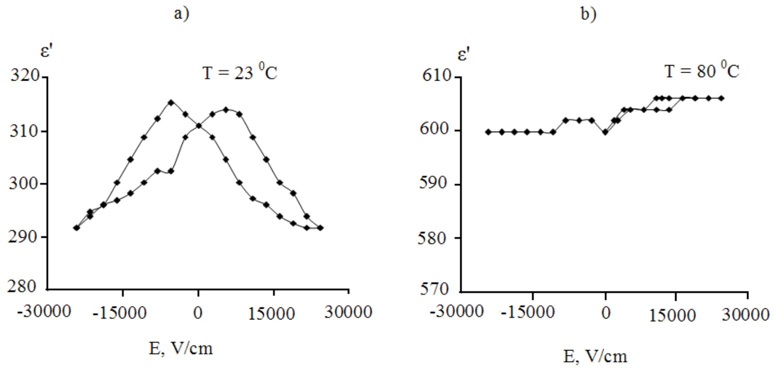

Fig. 1. Field dependence of dielectric permittivity at different temperatures for SBN-75.

Possible effects of mechanical tension on features of dielectric nonlinearity in ceramics are discussed, suppression of relaxor properties in case of ceramic materials, in particular.

References

1. A.I. Burkhanov, A.V. Shil′nikov, and R.E. Uzakov, Crystallography, **42**, 1069 (1997).
2. V.V. Gladky, V.A. Kirikov, E.V. Pronina, T.R. Volk, R. Pancrat, M. Vĕleke, Solid State Physics, **43,** 2052 (2001).

PO-132-a

Physical and Chemical Principles of Designing Containers for Thermo-Chemical Treatment of High Purity Compounds of Niobium and Tantalum

M. Palatnikov[1], A. Frolov[2], E. Voinich[2], E. Kirkova[2], O. Shcherbina[1], N. Sidorov[1], K. Bormanis[3]

[1]Institute of Chemistry, Kola Science Centre RAS, Apatity, Murmansk Region, Russia

[2]Frantsevich Institute for Problems of Materials Science of NASU

[3]Institute of Solid State Physics, University of Latvia, Latvia

e-mail: bormanis@cfi.lu.lv

Mathematical modelling of the distribution of strain in layered quartz ceramics with protective coating of niobium pentoxide from two sides is reported. It is found that fragmentation of the basic layer (decreasing the area of the continuous boarder between layers) and smoothing of sharp edges of the base fragments should reduce the strains on the boundary between the substrate and coating and, correspondingly, enhance the thermal resistance of the samples.

Treatment of the niobium pentoxide coating by concentrated light flow (CLF) induces a network of fractal micro- and nano-size fractures that compensates the difference of thermal expansion between the layers. The absolute value of the negative coefficient of linear thermal expansion (CLTE) of Nb_2O_5 treated by CLF decreases while the curve of relative thermal expansion becomes more symmetric. Due to the fractal micro- and nano-size structures forming at treatment by CLF in optical oven the CLTE of tantalum pentoxide samples exhibits a region of negative or close to zero values. The fraction of nanometre-size fractures in case of Ta_2O_5 treatment by CLF is likely considerably larger as compared with Nb_2O_5.

The studies have demonstrated that possible control of bulk expansion of the material and fragmentation of the basic layer allow to obtain layered ceramics and products thereof possessing enhanced thermal resistance to withstand thermal cycling.

Experimental acoustic emission studies have confirmed the increase of thermal resistance of the samples by factor ~1.5. Smoothing the edges of the fragments of the ceramic substrate provides additional increase of thermal resistance by ≈15 %. Containers for calcination of high purity grade niobium hydroxide made of fragmented ceramic substrate and coated by CLF-processed Nb_2O_5 have shown improved thermal resistance. Such containers withstand thousands of fast thermal cycles $T_{room} \leftrightarrow 1000\ ^{o}C$.

PO-132-b

Ceramic Coatings of Crucibles for Thermo-Chemical Treatment of High Purity Niobium Composites

K. Bormanis[1], M. Palatnikov[2], A. Frolov[3], O. Shcherbina[2], N. Sidorov[2], V. Kalinnikov[2]

[1]Institute of Solid State Physics, University of Latvia, Latvia

[2]Institute of Chemistry, Kola Science Centre RAS, Apatity, Murmansk Region, Russia

[3]Frantsevich Institute for Problems of Materials Science of NASU

e-mail: bormanis@cfi.lu.lv

Safeguard from admixtures emitted by the walls of technological crucibles deserves particular attention at production of high purity grade materials. Thermo-chemical processing of high purity substances in crucibles provided with a protective liner or made of the material obtained in the process is one of the ways of protection. Designing crucibles for heating cycles in a wide range of temperature is a complex problem of material science. Composition of the protective layer is pre-determined by the substance to be synthesized. Besides, high thermal resistivity of the coating is necessary.

Complex calcitrant oxides of low thermal expansion comprise the basis of materials for designing ceramics able to withstand sharp high-temperature thermal cycles. A study of the effect of concentrated light flow (CLF) on thermal expansion of ceramic niobium pentoxide (Nb_2O_5) is presented.

Compounds of Nb_2O_5 submitted to treatment by CLF are found to exhibit a region of negative or close to zero coefficients of thermal expansion and fractal nano-structures suppressing the latter. CLF-treated Nb_2O_5 ceramics of low and negative thermal expansion coefficients have been used constructing ceramic crucibles for calcination of high purity grade niobium hydroxide. Such crucibles withstand thousands of fast thermal cycles $T_{room} \leftrightarrow 1000\ ^{o}C$.

PO-133-a

Structure of Ferroelectric Lithium Niobate Single Crystals

N.V. Sidorov[1], M.N. Palatnikov[1], P.G. Chufyrev[1], V.T. Kalinnikov[1], K. Bormanis[2]

[1]Institute of Chemistry, Kola Science Centre RAS, Apatity, Russia

[2]Institute of Solid State Physics, University of Latvia, Latvia

e-mail: bormanis@cfi.lu.lv

A wide region of homogeneity on the phase diagram is an essential feature of ferroelectric $LiNbO_3$ crystals the existence of which allows growing ostensibly pure and modified by admixtures single crystals of diverse compositions the composition of congruent melt being different from stoichiometric. Such structures usually are spatially heterogeneous comprising a variety of point and extended defects as well as defects represented by micro- and nano-scale structures and fractals.

Raman studies of ordering details of structural units and formation of defects in various $LiNbO_3$ single crystals are presently reported. The weak Raman bands not related to fundamental lattice vibration modes are found to be most sensitive to changes of composition. Anomalous narrowing of bandwidths and decrease of frequency of the weak Raman bands of 309, 349, and 693 cm^{-1} is observed as the composition changes from congruent to stoichiometric. The change of bandwidths suggests of anomalously delicate ordering of structural units of the cation sub-lattice at disordering of it on the whole. The anomalous behaviour of the bandwidths is shown to be related to supra-structures of micro- and nano-size clustered defects in the cation sub-lattice of the $LiNbO_3$ crystal. It seems reasonable to assume the clusters being distributed as ordered sub-lattices of the size of a few translation periods around intrinsic Nb_{Li} defects, it is – as nano-size objects. The change of the kind and ordering of the cluster defects can be presumed to affect parameters of the related weak Raman bands of $LiNbO_3$ crystals.

Further experimental precision studies of similar anomalous ordering of structural units and computer modelling of the cluster structures are of practical interest. New information on forming of the defected structure of $LiNbO_3$ opens opportunities for more refined control of the quality of real single crystals and for improvement of production technologies of high quality lithium niobate materials, for optical applications in the first place.

PO-133-b

Computer Modelling of Cluster Formation in Ferroelectric Lithium Niobate Crystals

V. Voskresensky[1], O. Starodub[1], N. Sidorov[1], M. Palatnikov[1], K. Bormanis[2], V. Kalinnikov[1],
E. Fedorova[3], L. Aleshina[3]

[1]Institute of Chemistry, Kola Science Centre RAS, Apatity, Murmansk Region, Russia
[2]Institute of Solid State Physics, University of Latvia, Latvia
[3]Petrozavodsk State University, Petrozavodsk, Russia
e-mail: bormanis@cfi.lu.lv

Within the vacancy models, the paper reports results of X-ray and Raman studies of structural disorder and cluster formation in the cation sub-lattice of congruent and stoichiometric lithium niobate crystals including crystals containing yttrium and gadolinium admixtures. The features of cluster formation in the crystal are theoretically studied within the semi-classical atomistic model. Disordering of the crystal structure at introducing yttrium, as detected by X-ray diffraction and Raman spectra, is shown to be related to penetration of yttrium into the cation sub-lattice of the congruent crystal. When Y^{3+} substitutes Nb^{5+} located in the niobium site (Nb_{Nb}) the Nb^{5+} ion is forced into vacant octahedrons increasing disorder of cations and vacancies along the polar axis and distorting the octahedrons since the ion radius of Y^{3+} is larger compared with ion radius of Nb^{5+}.

The modelling was made employing software for minimising the energy of clusters of the lithium niobate structures by moving or taking away the “critical” atoms. Parameters used by the software included the kind of element, formal charge values, and coordinates according to space group symmetry obtained from X-ray analysis. The energy of clusters was calculated using the Coulomb attraction and Born-Mayer potentials. The step-by-step optimisation of the critical atoms was used to minimise the energy of clusters comprised of up to 20 hexagonal unit cells. Resulting data were applied to analyse the structures of clusters before and after minimisation of energy. The lithium atoms being found this way as the most “critical” is in good agreement with other data. However, increasing the size of a cluster by translations of the elementary cell along the crystallographic axes the structure becomes more complicated and critical niobium and oxygen atoms appears in addition to lithium.

Structures of clusters of different size were studied. By minimisation of energy of the structures the dipoles and energies of clusters were found as functions of the number of unit cells along the crystallographic axes. Computer experiment revealed non-zero dipole moments along the X and Y directions in small clusters gradually vanishing as the cluster grows bigger.

PO-134-a

Phase Transitions in the $Li_{0.12}Na_{0.88}Ta_yNb_{1-y}O_3$ Solid Solution System

N.V. Sidorov[1], M.N. Palatnikov[1], N.A. Tepljakova[1], V.T. Kalinnikov[1], K. Bormanis[2]

[1]Institute of Chemistry, Kola Science Centre RAS, Russia

[2]Institute of Solid State Physics, University of Latvia, Latvia

e-mail: bormanis@cfi.lu.lv

Results of comprehensive studies of thermal and concentration-induced phase transitions (PT) in the $Li_{0.12}Na_{0.88}Ta_yNb_{1-y}O_3$ ferroelectric solid solution (SS) system in the 293-450 ˚C range are reported. The $Li_{0.12}Na_{0.88}Ta_yNb_{1-y}O_3$ compound at $y = 0.1 – 0.9$ is of interest due to a sharp increase of Li ion conductivity at $T = 400 – 450$ ˚C and transfer to super-ionic (SI) state at temperatures above the temperature of anti-ferroelectric phase transition. The ferroelectric (FE) to anti-ferroelectric (AFE) transition at 350 ˚C precedes the SI PT manifested by disappearance of the strong Raman band at 875 cm^{-1} related to stretch of oxygen atoms bridging the BO_6 (B = Nb, Ta) octahedrons. The Raman bands broaden considerably approaching the PT temperature from below. The groups of vibration bands related to oxygen octahedrons and cations located in voids of the octahedral structures merge into broad Raman bands retaining in the spectrum of the SI phase. Frequencies of the bands do not show any anomalous behaviour at rising the temperature suggesting that change of the quasi-elastic constants is negligible. The 875 cm^{-1} band is shown to be suitable to evaluate the dipole ordering in ferroelectric structures of oxygen octahedrons. The band absent in the AFE phase is distinctly pronounced in spectra of the FE phase. The absence of the 875 cm^{-1} band unambiguously indicates the absence of ferroelectricity.

The $Li_{0.12}Na_{0.88}Ta_yNb_{1-y}O_3$ SS of low tantalum concentrations ($y < 0.25$) are strong ferroelectrics and do not exhibit any anti-ferroelectric features at room temperatures while SS compounds of $y > 0.3$ may occur in both the ferroelectric and the anti-ferroelectric states. A considerable disordering proceeds in the niobium and tantalum sub-lattice (due to decrease of the long-range order) of the SS at increasing y from 0 to 0.5 by which the spatial (geometric) conditions for Li ion transport are enhanced. At growing disorder in the niobium and tantalum sub-lattice the structural transformations at heating become less distinctive the FE-AFE phase transition point considerably shifting to lower temperatures. The FE-AFE PT is also preceded by growing disorder of the orientation of the BO_6 octahedrons at increasing the temperature. The latter is reflected in Raman spectrum by decrease of the intensity and broadening of the 80 cm^{-1} band into the Rayleigh wing. Frequency of this band decreasing monotonously points to softening and supports relating the 80 cm^{-1} band to symmetric librations of the BO_6 octahedrons: the soft mode belongs to the most symmetric and lowest frequency vibration.

PO-134-b

Dielectric Properties and Conductivity of Ferroelectric $Li_{0.07}Na_{0.93}Ta_{0.1}Nb_{0.9}O_3$ and $Li_{0.07}Na_{0.93}Ta_{0.111}Nb_{0.889}O_3$ Solid Solutions

M.N. Palatnikov[1], V.V. Efremov[1], N.V. Sidorov[1], K. Bormanis[2], I.N. Efremov[1]

[1]I.V. Tananaev Institute of Chemistry, Kola Science Centre RAS, Apatity, Russia

[2]Institute of Solid State Physics, University of Latvia, Riga, Latvia

e-mail: bormanis@cfi.lu.lv

The ABO_3 ferroelectric (FE) solid solutions (SS) of perovskite structure on the basis of sodium niobate exhibit a number of properties interesting for application: relatively low values of density and dielectric permittivity, high ultrasonic velocity and good piezoelectric performance, and a wide range of mechanical Q-factor. Presently results of dielectric and conductance studies over the thermal range of 290 – 700 K and frequency range of 25 - 10^6 Hz in $Li_{0.07}Na_{0.93}Ta_{0.1}Nb_{0.9}O_3$ and $Li_{0.07}Na_{0.93}Ta_{0.111}Nb_{0.889}O_3$ perovskite FESS are reported. Electric properties and phase transition parameters of $Li_{0.07}Na_{0.93}Ta_{0.1}Nb_{0.9}O_3$ and $Li_{0.07}Na_{0.93}Ta_{0.111}Nb_{0.889}O_3$ FESS are found to depend substantially on the way the initial mixture is synthesised. A first-order FE phase transition proceeds in the $Li_{0.07}Na_{0.93}Ta_{0.1}Nb_{0.9}O_3$ and $Li_{0.07}Na_{0.93}Ta_{0.111}Nb_{0.889}O_3$ FESS within the observed range of temperature. The co-precipitated $Ta_{2y}Nb_{2(1-y)}O_5$ pentoxides being used for synthesis of the $Li_{0.07}Na_{0.93}Ta_{0.111}Nb_{0.889}O_3$ FESS it is possible to achieve rather high values of dielectric permittivity at high frequencies while the Curie point shifts by ~ 75 K to a lower temperature as compared with $Li_{0.07}Na_{0.93}Ta_{0.1}Nb_{0.9}O_3$, synthesised from mechanical mixture of the Ta_2O_5 and Nb_2O_5 oxides, which cannot be explained by the minor difference in proportions of the ingredients in the final SS. Techniques of obtaining the initial oxides has also a substantial effect on the ion conductivity of the $Li_{0.07}Na_{0.93}Ta_{0.1}Nb_{0.9}O_3$ and $Li_{0.07}Na_{0.93}Ta_{0.111}Nb_{0.889}O_3$ FESS. The activation energy of ion conductivity in the $Li_{0.07}Na_{0.93}Ta_{0.111}Nb_{0.889}O_3$ FESS is lower while its value – considerably higher compared with $Li_{0.07}Na_{0.93}Ta_{0.1}Nb_{0.9}O_3$. The different thermal behaviour of the real part of dielectric permittivity and conductivity between the $Li_{0.07}Na_{0.93}Ta_{0.1}Nb_{0.9}O_3$ and the $Li_{0.07}Na_{0.93}Ta_{0.111}Nb_{0.889}O_3$ FESS are obviously related to the way of obtaining the initial oxides Ta_2O_5 - Nb_2O_5 and $Ta_{2y}Nb_{2(1-y)}O_5$.

PO-135

Wet Chemical Synthesis of Cobalt Nanostructures in Non-Aqueous Solvents

L. Claudio[1], A. Reverberi[1], P. Nanni[1, 2]

[1]Department of Chemical and Process Engineering, University of Genoa, P.le Kennedy 1, Genoa I-16129, Italy

[2]Institute for Energetics and Interphases-CNR, Via de Marini 6, Genoa I-16149, Italy

e-mail: claudiolaros@virgilio.it

Cobalt nanoparticles have long been used in many fields of research for their attractive magnetic, catalytic and biochemical properties [1-3]. The usually adopted chemical methods to realize nano-particles dispersion are generally based on the reduction of a precursor containing the cation in question by means of an organic or inorganic electron donator in aqueous medium.

In the field of hydrometallurgy, cobalt precipitation from zinc salts solution with a cementation method by more electropositive elements was thoroughly investigated and it was found that the kinetics of the relevant electrochemical reaction are strongly enhanced by the presence of host cations as Ni, Pd, Cu, in the precursor. In his pioneering works [4-5], McKinnon pointed out that the aforementioned kinetics of cementation are extremely slow when the cobalt is present alone in the liquid solvent or in the presence of organic impurities, a finding that represents a crucial limitation in the use of a cementation technique in the synthesis of cobalt nanoparticles.

To circumvent this drawback, we have analyzed a cementation process when a cobalt salt is dissolved in an organic solvent (ethanol) with a small water content (less of 10%) and we have checked the role of several surfactants according to their chemical structure. In particular, the use of cationic surfactants proved to be particularly useful as they have an unexpected enhancing effect on the cementation kinetics. The yield in metallic cobalt, the geometries of the metal nanostructures and their relevant scale length have been investigated with respect to the main parameters of the process such as temperature, the energy dissipated in mechanical stirring and the concentration of surfactant and precursor. The obtained nanostructures were characterized by means of X-ray diffraction (XRD), scanning electron microscopy (SEM) and transmission electron microscopy (TEM).

References

1. V.F. Puntes, K. Krishnan, A.P. Alivisatos, Science, 291, 2115 (2001)
2. V. Skumryev, S. Stoyanov, Y. Zhang, G. Hadjipanayis, D. Givord, J. Nogues, Nature, 423, 850 (2003)
3. J. Waddella, S. Inderheesa, M.C. Aronsona, S.B. Dierkera, J. Magn. Magn. Mater. 297, **54** (2006)
4. O. Bckman, Hydrometallurgy 54, 65 (2000)
5. D.J. MacKinnon, Can. Mines Branch Res., Res. Rep. 259, **20** (1973).

PO-136

Synthesis of Bi_2WO_6 Photocatalyst Nanopowders with Wet Chemical Methods

M. Kodols[1], S. Didrihsone[1], J. Grabis[1]

[1]Institute of Inorganic Chemistry, Riga Technical University, Latvia

e-mail: maris.kodols@gmail.com

Over the past decade Bi_2WO_6 photocatalytic activity has been extensively studied due to the potential application for photo-degradation of organic compounds and water splitting under visible light irradiation. At present bismuth tungstate has been prepared by solid-state of oxides at high temperature or by hydrothermal synthesis. It is well known that activity of photoctalysts depend strongly on particle size and crystallinity. From this viewpoint development of it preparation methods of nanosized Bi_2WO_6 is actual task.

Due to the development of green chemistry there are different materials needed which ensures sustainability of used materials. One of such material is bismuth tungstate Bi_2WO_6 nanopowders and it ceramic materials. Bismuth tungstate Bi_2WO_6 is commonly known as mineral called Russelite had it has showed several good practical properties. For example high potocatalytic activity not only under UV irradiation but also under visible light and the good success for water splitting for future energy, also it has been used in semiconductors as most of tungstate materials.

Bi_2WO_6 nanopowders for photocatalytic usage have been prepared with wet chemical methods – modified sol-gel self combustion method and with microwave assisted sol-gel synthesis. In both methods the commercial salt solutions are mixed together with organic fuel (ethanol, glycine, ethylene glycol) and nitric acid and synthesized by varying heating techniques. The XRD patterns shows that obtained material is high crystalline but during synthesis some impurity phases can occur – WO_3, $Bi_2W_2O_9$, $Bi_{14}WO_{24}$, which can be avoid by further calcinations process at temperature 650 - 800 ^oC temperature. The calcinated bismuth tungstate nanopowders have high crystallinity and specific surface area (BET) in range of 12 – 22 m^2/g depending on used fuel and calcinations temperature.

PO-137

Description of Model and Verification Experiments for Hydrogen Evolution Reaction: Dependence on Electrode Material

M. Vanags, J. Kleperis, G. Bajars, A. Lusis
Institute of Solid State Physics, University of Latvia, Latvia
e-mail: kleperis@latnet.lv

Hydrogen has high demand in industry as a general purpose chemical in production of ammonia, hydrogenation processes and also as fuel in fuel cells for generation of electricity. On commercial scale it is produced by steam reforming of hydrocarbons, but in case of sustainable productin hydrogen can be produced from water electrolysis using electricity from renewables. The economics of this process can be improved only by efficient electrocatalysis so as to minimize the overpotentials and Coulombic heat (IR), see equation for applied voltage: $E_{appl} = E_e + |\eta_c| + \eta_a + IR$. Considering the overpotentials and the IR drop, the operating cell voltage is about 2.0 V for steel and Ni electrodes in the cell, although the equilibrium cell voltage for decomposition of water is 1.23 V. Overpotential for O_2 evolution on nickel is ~0.5 V, what is a major cause for excessive consumption of electrical energy. If we can replace Ni anode or modify it with an electro-catalytic nano-material so as to reduce the overpotential even by 0.1 volt, the current produced will be more than 10 times the initial value and will cause large overall savings during production of both hydrogen and oxygen from water.

In our studies we have proved that pulse voltage power supply increases the efficiency of water electrolysis comparing with commercial available alkali electrolysers. Using short time and high voltage pulses (1-3 μs, 500 V), the current behavior is investigated using water electrolytes. It is observed that current pulse changes polarity with increasing water dissociation degree (concentration of electrolyte). This effect is explained with assumption that electrons are tunneling from cathode to an electrolyte under influence of high voltage pulse. Emitted electrons can be discharged with ions in an electric double layer, but if the number of ions is too low, electrons can diffuse back to the cathode. Results are described about the dependence of this effect from material and his surface roughness. Nanostructuring of the surface is improving the efficiency of electrolysis.

Acknowledgements: MV acknowledges European Social Fund for support; all authors acknowledge National Research Program in Energy for support and V. Nemcevs for technical assistance.

PO-138

Crystallization Processes of Amorphous Si by Pulsed Laser Processing

I. Tale, J. Butikova, G. Marcins, A. Muhins, B. Polyakov, A. Voitkans
Institute of Solid State Physics, University Latvia

In order to investigate crystallization kinetics of a-Si layers, sets of programmed YAG laser pulse exposures have been applied. Amorphous Si thin films sputtered on sapphire and SiO_2-coated Si wafers have been used in this study. It has been proposed that the heating rate and heat diffusion in a-Si layer can be controlled during annealing process using sets of short single pulses of programmed frequency and set-to-set delay. Depending on single pulse energy and pulse set duration both the initial sample surface layer temperature and the depth of exposed layer can be controlled.

Crystallinity and surface modification of a-Si layer have been investigated by Raman spectroscopy and atomic force microscopy respectively. To determine crystallization depth profile of Si layer after laser processing, chemical etching and Raman measurements have been performed.

It has been stated that increase of the laser pulse energy and decrease of pulse set duration accelerates growth rate of nanocrystals sufficiently. Thus, the probability for Si atoms to penetrate the nucleation energy barrier is governed by the local temperature. Increase of pulse repetition rate during processing results in increased size of nanocrystals.

At an initial stage, a pulsed laser processing results in nucleation of Si nanocrystals inside the amorphous Si matrix. Nanocrystals are settled near the a-Si layer surface. The size of nanocrystals depends on the pulse energy significantly. Si nanocrystals obtained during the pulsed laser processing can be used as seed particles for the following laser stimulated processing to produce poly-Si layer.

I.T, J.B., A.M., B.P., A.V. supported by ERAF Nr.2010/0252/2DP/2.1.1.1.0/10/APIA/VIAA/009

PO-139

Methodology Development for Optimum Placement of Piezoelectric Actuators

A. Kovalovs, S. Gluhihs, E. Barkanov
Institute of Materials and Structures, Riga Technical University, Latvia
e-mail: kovalovs@bf.rtu.lv

The purpose of present investigations is development of optimisation methodology for an active vibration control to obtain composite structures with maximum damping and minimum actuator quantity and energy applied, extending by this way the structural life and reducing operation costs. In the first stage the parametric analysis is carried out for a one-dimensional problem to study an optimal placement of piezoelectric actuators for the vibration reduction. It is well known that an active control is more effective in application to operate with lower structural modes.

Vibration control of a clamped-free beam under variable harmonic pressure is realized through piezoelectric actuators bonded on the panel. Simulations of an active control are performed in ANSYS environment. The shell elements (SHELL99) are used for the modelling of piezoelectric actuators and beam. Since an investigated panel is thin, the thermal analogy is applied, where piezoelectric coefficients characterising actuator are examined as thermal expansion coefficients.

Using results of a parametric study (Fig. 1), a problem for the optimum placement of piezoelectric actuators has been formulated for the two-dimensional case presenting an active control of laminated composite plate.

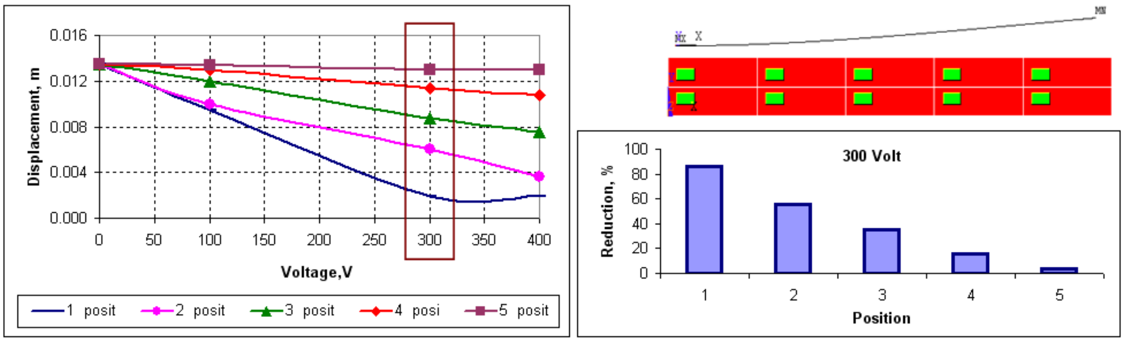

Fig. 1. PZT location for the 1st mode (bending)

PO-140

Identification of Elastic Properties of Composite Plate

A. Kovalovs, S. Rucevskis
Institute of Materials and Structures, Riga Technical University, Latvia
e-mail: kovalovs@bf.rtu.lv

Composite laminates are used extensively in the aerospace industry, especially for the fabrication of high-performance structures. The determination of stiffness parameters for complex materials, such as fibre-reinforced composites, is much more complicated than for isotropic materials. A conventional way is testing the coupon specimens, which are manufactured by technology similar to that used for the real, large structures. When such a method is used, the question arises of whether the material properties obtained from the coupon tests are the same as those in the large structure. Therefore, the determination of actual material properties for composite laminates using non-destructive evaluation techniques has been widely investigated.

A number of various non-destructive evaluation techniques have been proposed for determining the material properties of composite laminates. In the present study, attention is focused on the identification of the elastic properties of laminated plate using vibration test data. The problem associated with vibration testing is converting the measured modal frequencies to elastic constants. A standard method for solving this problem is the use of a numerical-experimental model and optimization techniques. The identification functional represents the gap between the numerical model response and the experimental one. This gap should be minimized, taking into account the side constraints on the design variables (elastic constants). The minimization problem is solved by using non-linear mathematical programming techniques and sensitivity analysis.

The results obtained were verified by comparing the experimentally measured eigenfrequencies with the numerical ones obtained by FEM at the point of optima

PO-141

Applicability of Cylindrical Thin-Walled Polymer Specimen Deformability Test for Instrumentation of “Single Sample” Principle

E. Auzins[1], M. Kalnins[1]

[1]Institute of Polymer Materials, Riga Technical University, Latvia

e-mail: erns@inbox.lv

Method of evaluation of deformational characteristics by compression or tension of thin polymer films shaped as cylindrical shell was recently proposed [1-2].

The aim of present work was to approve the suitability of this method for the repeated multiple assessment of changes of deformational characteristics caused by certain structural transformations in a single sample. An expectation to reach this goal was based on the fact that values of actual relative tensile deformation reached in test are small (< 0,03) and for large majority of polymer materials practically reversible.

The dependence of elastic modulus of polyvinyl alcohol films prepared by casting (containing different amount of plasticizer – diethylene glycol) on absorbed water content was studied. Sample in flat shape (30 x 110 mm, thickness 160 .± 5 μm) was kept in desiccator (providing relative humidity of ~ 55 %) for certain time to reach definite water content c_w (weighing), then gently fixed in specially designed test bench as cylindrical shell (diameter - 35 mm) and tested. The value of elastic modulus E was calculated according [1]; accuracy of measurements: force ± 0,01 g, displacement ± 0,02 mm. Then sample was returned in desiccator (again in flat shape) to reach higher water content and the cycle repeated once again.

Series of curves E versus c_w of acceptable acuracy and reproducibility were obtained. E values of dry samples were in the range 5 – 10 Gpa (lesser at higher plasticizer content). As expected, significant drop of E values with increase of water content was observed. At the equilibrium water content E values were even more then an order of magnitude lower.

Multiple measurements (including repeated fixation and relief) for the same sample kept in constant conditions (no changes in structure) coincide well.

References

1. S. Gluhih, A. Kovalov, A. Tishkunov, D. Cerpakovska, M. Kalnins, Scientific Proceedings of RTU, Material Science and Applied Chemistry. **21**, 84 (2010)
2. S. Gluhih, A. Kovalov, A. Tishkunov, P. Akishin, A. Chate, E. Auzins, M. Kalnins, Mechanics of Composite Materials. In print

PO-142

Nanoporous Carbon Materials for Supercondensers

G. Dobele[1], T. Dizhbite[1], V. Jurkjane[1], N. Mironova-Ulmane[2], I. Sildos[3], T. Centeno[4]

[1]Latvian State Institute of Wood Chemistry, Latvia

[2]Institute of Solid State Physics, University of Latvia, Latvia

[3]Institute of Physics, University of Tartu, Tartu, Estonia

[4]Instituto Nacional del Carbon-CSIC, Oviedo, Spain

e-mail: gdobele@edi.lv

The processing of lignocellulose (LC) residues attracts increasing attention, first of all, due to the solution of ecological safety issues and the elaboration of new principles of the complex utilisation of all components of renewable plant biomass, and the creation of novel materials. The approach, incorporating the use of lignocellulose materials for producing low-cost high-efficient nanoporous carbon materials (NCM) by the method of thermochemical activation, using sodium hydroxide as the activation agent, is attractive. When developing fuel elements, supercapacitors (EDLCs) are regarded as especially promising. Depending on the treatment conditions and the LC properties, NCM with a great specific surface (more than 2000 m^2/g according to the BET theory) and low oxygen content (below 10%) will be obtained for investigating electrochemical processes. The retaining of charging was tested by the galvanostatic charge-discharge voltage cycle (potentiostat-galvanostat Autolab-Ecochimie PGSTAT 30) at the current density 1 and 100 $mAcm^{-2}$.

The obtained results have shown that the capacity increased with increasing NCM surface. Besides, the uniformity of nanoporous sizes (1-3 nm) and the oxygen content are the necessary and decisive indices. It is shown in the experiments that the cyclic voltagrams for the carbons have a right angle form over wide regions of the investigated ranges. It is observed that the holding of the obtained carbons at a high current density is similar to the case of other commercially activated carbons, which are used for the production of supercapacitors The NCM obtained in the present work were investigated using the Raman scattering study (excitation by 514 nm).

References

1. V.Torne-Fernandez, J.Maria Mateo-Sanz, D.Montane, V.Fierro, J.Chem.Eng.Data 54, 2216 (2009)

PO-143

Evaluation of Analyte Vapour Diffusion in Polymer-Nanostructured Carbon Composite

G. Sakale, M. Knite, V. Teteris
Institute of Technical Physics, Riga Technical University, Latvia
e-mail: gitasakale@inbox.lv

Previously polymer-nanostructured carbon composite (PNCC) electrical resistance response, when the composite is exposed to different volatile organic compounds (VOC), has been investigated and determined. As PNCC electrical resistance change is a result of VOC molecule diffusion in the composite and subsequent swelling, then analyte diffusion behaviour evaluation is essentially important.

According to classical analyte diffusion theory into polymers, diffusion behaviour can vary from Fickian to non-Fickian type diffusion depending on the structure of the polymer (amorphous-rubbery, amorphous-glassy or crystalline). Diffusion type indirectly characterizes mobility of polymer segmental unit. Rapid PNCC response to VOC and fast electrical resistance recovery can be enabled by choosing polymer matrix with high segmental unit mobility. To determine analyte diffusion type into the composite and correlate diffusion characteristics with PNCC electrical resistance change, experimental setup has been build with possibility to register simultaneously the PNCC sample mass, length and electrical resistance change.

VOC diffusion characteristics (diffusion velocity and type) into the composite sample depending on used nanostructured filler material (carbon black nanoparticles or carbon nanotubes), filler content, matrix material structural state as well as type of analyte have been evaluated.

PO-144

Synthesis of Microporous Carbon Templated by Zeolite 13x

V. Grehov, J. Kalnacs, A. Murashov, A. Vilken

State Research Institute “Institute of Physical Energetics”, Latvia

e-mail: jkalnacs@edi.lv

Creation of adsorbents with the large specific volume of pores and relatively identical pore size will allow solution such problems, as H2 storage [1], or separation certain carbon nanostructures from graphite arc discharge soot [2].

One of methods for production such adsorbents are pyrolitic carbonization of organic precursor in micro channels of porous templates, such as zeolites or silica gels. This kind of carbon structures are termed as templated carbon or TC [1].

As a porous template we used zeolite 13X (Na_{86} [$(AlO_2)_{86}$ $(SiO_2)_{106}$] *H_2O), with the size of pores ~8Å. As carbon precursor served Furfural ($C_5H_4O_2$). Carbonization was done in controllable conditions on TG device Setsys Evolution 1750. The common zeolite/carbon composite materials where divided from zeolite by etching in fluoric acid. The phase composition of the acquired TC was checked by a method of the temperature-programmed oxidation.

For pore size distribution (PSD) determination, the adsorption of nitrogen at 77K by TC samples, using device Autosorb-1, is studied.

TC samples possess porosity of 0.9 cc/g and PSD is shifted towards the smaller sizes of the pores in comparison with a usual activated coal AC [2] (Fig1).

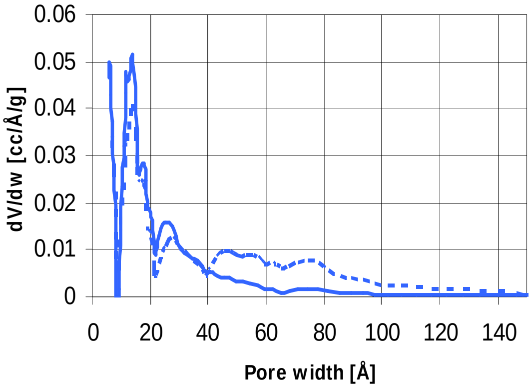

Fig. 1. The pore size distribution according to the DFT method for the TC and AC samples.

References

1. C. Guan, K. Wang, C. Yang, X.S. Zhao. Micropor. Mesopor. Mater.118, 503 (2009).
2. V. Grehov, J. Kalnacs, A. Murashov, A. Vilken. Latvian Journ. of Phus. and Techn. Science, 47, No6, 59 (2010)

PO-145

Universality of the Inverse Technique for the Viscoelastic Material Properties Characterisation

E. Skukis, E. Barkanov

Institute of Materials and Structures, Riga Technical University

e-mail: edskukis@bf.rtu.lv

Due to great importance to define performance, reliability and safety requirements for advanced viscoelastic adhesives, polymers and foams a considerable effort has been devoted to the study of their mechanical material properties and a lot of different identification methods based on vibration tests have been developed in the last three decades. However most of them do not give the possibility to characterise the viscoelastic material properties, when storage and loss moduli are frequency and temperature dependent values.

For this reason, a new inverse technique based on simple vibration tests has been developed to characterise the nonlinear mechanical properties of various viscoelastic materials. This novel approach allows to preserve the frequency dependence of the storage and loss moduli of viscoelastic materials in a wide range of frequencies and to analyse structures using high damping tests. The computational effort has been substantially reduced by using an optimisation based on the planning of the experiments and the response surface technique in order to minimize the error functional. In the present investigation a universality of the developed technique is demonstrated characterising the viscoelastic material properties (Fig. 1) of a 3M damping polymer (ISD-112) used as a core material in sandwich panels with different dimensions and boundary conditions. Fig. 1 shows that no special geometrical requirements are necessary for tested samples and even some structural components can be used for the unknown viscoelastic material properties characterisation.

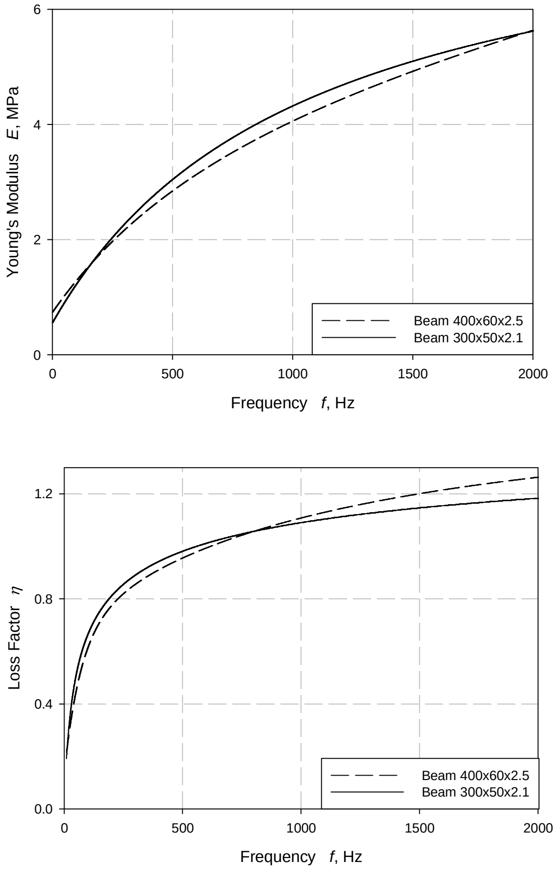

Fig. 1 Viscoelastic material properties identified from vibration tests

PO-146

Flexural Modulus Identification of Thin Polymer Sheets

S. Gluhihs, A. Kovalovs, A. Tiskunovs, A. Chate
Institute of Materials and Structures, Riga Technical University, Latvia
e-mail: kovalovs @bf.rtu.lv

The purpose of the present investigation is to elaborate a method for determining the flexural modulus of a polymer material based on the solution of compression and tension problems by using the finite-element method in the finite element program ANSYS.

To solve the nonlinear problem by the finite-element method, a macros-program was elaborated, which specifies the geometry, physical law, and properties of the material, boundary conditions, loading, division into finite elements, and the step scheme of the solution. The deformation of a thin polymer shell is characterized by great displacements and relatively low elastic deformations in a large range of movement of parallel planes. The solution obtained by finite element method allows making the universal loading diagram in dimensionless coordinates in the given range of thicknesses and elastic module. Equation of the universal loading diagram allows us to solve the inverse problem of determination of the elastic modulus according to experimental points on the loading diagram.

The method of determination of the flexural modulus of thin polymer shells discussed above was successfully approved on a series of various kinds of thin PVC specimens by tension test. Than specimens was tested for vibration (modal) test in order to measure the eigenfrequencies and the corresponding modes. The flexural modules received by compressing a circular cylindrical were verified by comparing the experimentally measured eigenfrequencies with numerical results from ANSYS program.

The method enables the use of a “single specimen principle”. For example, changes in the modulus caused by different processes affecting the structure and properties of polymer material, for example, different kinds of aging of polymer materials, absorption of liquids (water) and vapors by a certain material, and so on, can be studied on a solitary [on one and the same] specimen.

PO-147

The Influence of Surface Treatment by Hydrogenation on the Biocompatibility of Different Hydroxyapatite Materials

E. Palcevskis[1], A. Dindune[1], Y. Dekhtyar[2], N. Polyaka[2], Dj. Veljović[3], R.L. Sammons[4]
[1]Institute of Inorganic Chemistry, Riga Technical University, Latvia
[2]Riga Technical University, Biomedical Engineering and Nanotechnologies Institute, Latvia
[3]Faculty of Technology and Metallurgy, University of Belgrade, Serbia
[4]University of Birmingham School of Dentistry, UK
e-mail: eriksp@nki.lv

The synthesis of cationic and anionic substituted hydroxyapatite (HA) powders will be presented. The chemical interaction between calcium hydroxide and phosphoric acid was chosen as the basic reaction for synthesis of stoichiometric HA. The cationic substituted HA corresponds to the formula $Ca_{10-x}Me_x(PO_4)_6(OH)_2$, where Me is Mg, Mn, Sr and Ag. Only silicate was obtained as the anionic substituted HA and powder with the formula $Ca_{10}(PO_4)_{5,5}(SiO_4)_{0,5}(OH)_2$ was synthesized.

The aim of our work was to test the influence of surface hydrogenation on the biocompatibility of pure HA, substituted with manganese (Mn^{+2}) and with magnesium (Mg^{+2}) - all axially pressed and conventionally sintered for 2 h at a temperature 1200 ^oC, and pure HA isostatic pressed and sintered by the microwave technique for 15 min at 1200 ^oC.

Hydrogenation was performed by the treatment of HA materials in a hydrogen atmosphere at high pressure with the aim to increase the electron work function (EWF) and therefore also the bioactivity of the materials. Biocompatibility was compared by enumeration of the number of osteoblast-like cells to the materials before and after hydrogenation.

The results obtained demonstrate the greatest increase both of EWF and attached cells for manganese substituted HA after hydrogenation.

PO-148

Enrichment and Activation of Smectite-Poor Clay

J. Kostjukovs[1], I. Sarceviča[1], A. Actiņš[1]

[1]Department of Physical Chemistry, University of Latvia, Latvia

e-mail: inese.sarcevicha@gmail.com

Smectite clays are widely used as efficient sorbents, catalysts and matrixes for polymer materials. The quality of these materials depends on the smectite content in clay.

The smectite-poor clay deposits are found worldwide. The smectite content in this clay is lower than 40%, which is insufficient for industrial use. Venta basin Trias clay is an example of smectite-poor clay.

Evidently, the utilization of the smectite-poor clay for industrial production will be required. Therefore, the new effective and simple enrichment methods have to be developed.

We have developed a new simple method, which allows concentration of smectite minerals up to 70-80%. Simultaneously activation is performed by replacing calcium ions to sodium ions in the interlayer space.

The method is based on dispersing clay in a phosphate solution. Treatment with phosphates allows to separate smectite minerals from matrix. Quartz, calcium and magnesium carbonates are effectively removed from deposit clay. The solid material is separated from the suspension by coagulation.

The increase in sorption capacity from 0.3 mmol/g to 0.7 mmol/g was achieved for enriched clay. The smectite content in the product is high enough to allow efficient use of smectite clay as sorbents or catalysts.

PO-149

Separation of Magnetic Nanoparticles through Non-Isothermal Layer Between Permeable Walls in the Presence of Magnetic Field

V. Sints, A. Mezulis, G. Kronkalns, E. Blums

Institute of Physics, University of Latvia, Salaspils LV-2169

e-mail: viesturs.shints@gmail.com

Due to the promising applications of magnetic fluids in medicine (hyperthermia, drug targeting), it is becoming increasingly important to explore the transport properties of magnetic fluids within a capillary porous environment. In the present work we introduce recent experimental results on thermophoretic nanoparticle transport in nonisothermal ferrofluid layer between two permeable walls.

The setup consists of two symmetrical cylindrical volumes, separated by a thin layer formed by two permeable web-like sheets. The volumes are thermostated that allows creating and maintaining a given temperature in each of them during the experiment. Both the temperature and the concentration of magnetic phase are determined by measuring the ohmic resistance and the inductivity of electric coils embedded in the volumes. The layer is formed by two web-like sheets of porosity 40 %, separated by a distance of 1 mm.

During the experiment, a constant temperature difference is applied between both thermostated volumes, both of them considered isothermal, so that the gradient is perpendicular to the sheets. An external magnetic field is applied, so that its intensity is parallel to the gradient of temperature. Concentration of the magnetic nanoparticles in both volumes is measured throughout the experiment. The operation of the setup in running experimental mode can be ensured for a period of several days, as it is necessary for the experiment of slow particle separation.

Exponential trend of unsteady particle separation curves allows calculating both the mass diffusion coefficient and the thermodiffusion coefficient of nanoparticles. The obtained results agree relatively well with those calculated from dynamic curves of an optically induced thermal grating. The applied magnetic field causes strong reduction in the particle thermophoretic mobility and simultaneous growth of the mass diffusion coefficient. Both effects are significantly stronger than previously detected changes in optically measured transport coefficients in thermal grating experiments.

PO-150

Damage Detection in Composite Beams

S. Ručevskis, M. Wesolowski

Institute of Materials and Structures, Riga Technical University, Latvia

e-mail: sandris_r@bf.rtu.lv

Due to their advantages of stiffness and strength over conventional materials, composite materials are finding increasing use in a variety of engineering application. On the other hand, the mechanical properties in composites may degrade severely in the presence of damage. Damage in structure may cause failure leading to tragic consequences and therefore structural health monitoring and damage detection in civil, mechanical and aerospace engineering constructions has become one of the most important keys in maintaining the integrity and safety of a structure.

In the present paper a technique for damage detection which utilizes mode shape information obtained from vibration analysis of damaged laminated composite beams is proposed. The basic idea of the proposed vibration-based damage detection method is that a damage as a combination of different failure modes in the form of loss of local stiffness in the structure alters its dynamic characteristics, i.e., modal frequencies, mode shapes, and modal damping values. The phenomena used for the proposed damage detection method is that the following relation between mode shape curvature and flexural stiffness of a beam holds and allows exhibiting its local changes caused by the flexural stiffness reduction,

$$\frac{\partial^2 w}{\partial x^2} = \frac{M}{EI} \qquad (1)$$

where w is a transverse displacement, (EI) is a flexural stiffness of beam and M is an applied moment. The location and size of damage is estimated by application of the mode shape curvature square magnitude damage index expressed as follows

$$MSCSM = \frac{1}{N} \sum_{n=1}^{N} \left(\left(\frac{\partial^2 w}{\partial x^2} \right)^2_{(i,j)} \right)_n \qquad (2)$$

where N is a total number of mode shapes, i and j a number of measurement points in x and y direction, respectively.

Validity of proposed vibration-based damage detection method has been assessed by comparing it to results obtained by a pulse-echo ultrasonic inspection technique.

PO-151

Investigation of Spark-Plasma-Sintering (SPS) of Tungsten Carbide and Titanium Carbonitride Nanopowders

I. Zalite[1], P. Angerer[2]

[1]Institute of Inorganic Chemistry, Riga Technical University, Latvia

[2]CEST, Centre of Electrochemical Surface Technology, Austria

e-mail: ilmars@nki.lv

The main application of tungsten carbide (WC) is the use in high wear resistance parts (e.g. cutting tools), where an excellent hardness combined with good toughness is necessary. Titanium carbonitride (TiC_xN_{1-x}) has also acquired interest due to its properties. High hardness, good corrosion-resistance, and high cutting-edge stability make it suitable for cutting tools, wear parts, and corrosion-resistant gaskets. Titanium carbonitride can also be applied as an additive or as a coating to WC-Co cermets.

Most of these ceramics are made from powders and therefore their properties depend to a large extent on the quality of the starting materials. The powder determines the processing and sintering behaviour and the subsequent formation of the microstructure, which strongly influences many properties of the dense materials. The mechanical properties of materials are improving with the decrease of the grain size; therefore one of the possible ways for production of ceramic materials with a fine-grained structure is the application of nanosized raw powders. The nanosized samples have been synthesized by ultra-rapid condensation from the gas phase in high frequency plasma.

Two WC nanopowder samples with the total carbon content of 6,1 and 8,1 wt.% and a specific surface area of 37 - 38 m^2/g were used for the compacting experiments. The powder consists of particles of globular shape with a diameter in the range of 10 - 20 nm. Also two TiC_xN_{1-x} nanopowder samples with various chemical compositions ($TiC_{0,26}N_{0,74}$ and $TiC_{0,65}N_{0,35}$) were used for the compacting. TiC_xN_{1-x} samples consist mainly of idiomorphic cubic shaped particles with the size between 20 and 100 nm.

Aim of this study is the investigation of the sintering process of nanostructured tungsten carbide and titanium carbonitride samples by means of the spark-plasma-sintering method and to compare the results with the data from conventional hot pressing (HP).

The research was made due to financial support of the European Structural Funds (Project No. 2009/0215/1DP/1.1.1.2.0/09/APIA/VIAA/082)

PO-152

Investigation of the Pyrolysis of Organic Platinum Extracts To Produce Nanocrystalline Films by EPM

V. Serga[1], L. Kulikova[1], V. Grekhov[2], J. Kalnacs[2], A. Murashov[2], A. Vilken[2]

[1]Institute of Inorganic Chemistry, Riga Technical University, Latvia

[2]State Research Institute "Institute of Physical Energetics", Latvia

e-mail: vera_serga@inbox.lv

Investigation of the thermal decomposition of metal extracts is a significant part of the extractive-pyrolytic method (EPM) [1]. Noble metals, which exist as complex metal-containing anions ($PtCI_6^{2-}$, $PdCI_4^{2-}$, $AuCI_4^-$) in acid aqueous solutions, are extracted due to the anion-exchanging mechanism.

In the reported study, solutions of tri-n-octylamine ($(C_8H_{17})_3N$) in toluene were used to produce organic extracts of platinum. The thermal stability of tri-n-octylammonium hexachloroplatinate ($((C_8H_{17})_3NH)_2PtCI_6$) was studied after removal of the solvent. Pyrolysis was performed under controllable conditions alongside with thermogravimetric and thermal measurements. The gases emitted during heating were analyzed using infrared spectrometry.

It was found from the curves of mass losses, heat fluxes and evolved gas absorbance vs. Temperature, that the process of thermal decomposition had three stages at temperatures about 210, 230 and 270 ^{0}C. The decomposition at the first and second stages is accompanied by the emission of HCl, the second and third stages produce gaseous species with typical CH oscillation frequencies. The mass losses, vapour emissions and heat losses occur simultaneously at the above-mentioned temperatures. As soon as a temperature of 280 ^{0}C is achieved, no mass loss was observed, and if air is present in the gas carrier, ignition takes place with the release of heat, CO_2 and H_2O.

When producing platinum films, a thin layer of the metal extract was spread over glass substrates. After hot drying, the produced organic films were heated to 200^0, 250^0 or 300 ^{0}C, respectively ($V_{heating}$ = 10 ^{0}/min). The XRD phase analysis of first two samples has shown that, although the temperature of the complete decomposition of the organic phase (280 ^{0}C) is not achieved, platinum crystallites ($d \approx$ 5-6 nm) are present in the film. The temperature increase to 300 ^{0}C results in the formation of a nanocrystalline platinum film with the mean crystallite size about 15 nm. It is found that the variation of the pyrolysis temperature regime (the heating rate and treatment final temperature) allows to vary the size of platinum crystallites in the produced films.

References

1. A.I.Kholkin, T.N.Patrusheva. Extractive pyrolytic method. M., "Com Book", 2006.

PO-153

Tribological Properties of Aluminium Matrix Composite Al-W-B

A. Shishkin[1], V. Mironov[2], V. Lapkovsky[3]
[1]Faculty of Material Science and Applied Chemistry, Riga Technical University, Latvia
[2]Faculty of Civil Engineering, Riga Technical University, Latvia
e-mail: powder.al.b@gmail.com

Studies of tribological properties of Al-W-B composite material by use of pin-on-disk technique. The Al-W-B composite material has been studied by mean of TRB CSM Instruments with the following parameters applicable to all tests: linear test mode, linear speed 1 cm/s, normal load 5 N and total distance 10 m. The following coupled elements have been used Al_2O_3, steel 100Cr6 and WC.

Variation of friction coefficient and wear track characteristics have been studied. It was established that Al-W-B and Al_2O_3 have similar tribological properties. It was observed that in certain friction pairs an alternate seizure occurs. It was found that friction pair 'Al-W-B - 100Cr6' has the best conformability.

PO-156

Application of Electron-beam Technology for Electrical Contact Materials

V. Panibratskiy[1], V. Osokin[1], M. Gadzyra[2], G. Chikvaidze[3], V. Zauls[3]

[1]The State Scientific Research Institute “Helium”, Vinnitsa, Ukraine

[2]Institute of Problems for Material Sciences of the National Academy of Sciences of Ukraine

[3]Institute of Solid State Physics, University of Latvia

e-mail: panvaleriy@ukr.net

A new electron-beam technology to obtain materials for electrical contacts, which has no analogues in world practice has developed.

These materials, based on copper and molybdenum, with the addition of alloying elements can be produced by high-speed electron-beam evaporation of several substances simultaneously by mixing their steam flows at a certain program and by managing the subsequent condensation on the temperature-controlled surface (with a given substrate temperature). Separation of condensed layer from the substrate is carried out with help of pre-earlier caused separation layer.

On the operational life the new contacts superior to the known silver-containing ones (tungsten-silver, silver-cadmium oxide) in 1,5 ÷ 3 times, and at the same time they are in 2,2 ÷ 2,5 times cheaper. The developed materials are superior to the known contact materials on the radiation resistance, thermal stability, durability, and also has high thermal and electrical conductivity. They are well treated by cutting, grinding, drilling, easily soldered with standard silver-and-silver solders.

The most effective application of the materials|: electric transport (electrical contacts used in the city’s trams, trolley buses, subway trains, locomotives, trains, etc.), port cranes, mining equipment, passenger and freight elevators and other lifting mechanisms, electrodes for welding machines and other areas

PO-157

Aspects of Silicon Oxide Reduction by Nanoscale Stoichiometric Silicium Carbide

V. Panibratskiy[1], V. Osokin[1], M. Gadzyra[2], G. Chikvaidze[3], V. Zauls[3], V. Solonenko[4]
[1]The State Scientific Research Institute “Helium”, Vinnitsa, Ukraine
[2]Institute of Problems for Material Sciences of the National Academy of Sciences of Ukraine
[3]Institute of Solid State Physics University of Latvia
[4]State Pedagogical University of Vinnitsa, Ukraine
e-mail of presenting author: panvaleriy@ukr.net

The possibility of silicon reduction from kaolin mining waste using non-stoichiometric nanoscale silicon carbide and its subsequent post-treatment of electron-beam method to produce silicon solar grade was investigated in this work. The initial products for the experiments were: chemically purified quartzite of Kushtymsky deposit (the Urals), waste of kaolin production of Glukhovsky and Turbovsky deposits of Vinnytsa region, the natural graphite of Zavalevsky deposit in Kirovograd region. Formation of thermo expanded graphite based on natural graphite of grade GAK-2 was performed according to technique [1]. Synthesis of nano-sized non-stoichiometric silicon carbide was performed in accordance with technology [2]. The process of reduction of the waste of kaolin production (or quartzite) to free silicon was conducted in two stages. In the first stage liquid mixture of components was formed. A certain time of exposure was carried out to achieve complete wetting of nano-sized particles of non-stoichiometric silicon carbide by silicon oxide melt, and then the conditions for formation of free liquid silicon were achieved by a sharp rise in temperature of the melt up to 2000-2500°C. The process of electron-beam treatment was performed in a vacuum apparatus with a graphite intermediate tank and a water-cooled copper mold. It was established that the initial composition of the mixture of kaolin and quartzite does not affect on the process of nano-sized non-stoichiometric silicon carbide formation and also on the temperature regime of formation of free silicon. The use of treated waste of kaolin production leads to lower costs as the synthesis of non-stoichiometric silicon carbide, and finally leads to the price reduction of free silicon. Measured electro-physical characteristics of the silicon ingots corresponding requirements for silicon solar gradation,

References:

1. Махорин К.Е., Кожан А.П., Веселов В.В., Александров В.Н. Химическая технология. Научно-производственный сборник. – Киев: Наук. думка, 1987. № 2. С.43-49.
2. Гадзыра Н.Ф., Гнесин Г.Г., Михайлик А.А. Порошковая металлургия. – 2001. № 9-10. С.90-97.

PO-158

Elaboration of Method for Preparation of IVB Group Metal Carbides Nanocomposites

M. Umalas[1], V. Reedo[1], A. Lõhmus[1], I. Hussainova[2]

[1]Institute of Physics, University of Tartu, Estonia, Estonian Nanotechnology Competence Centre

[2]Department of Materials Engineering, Tallinn University of Technology, Estonia

e-mail: madis84@ut.ee

Recent studies have shown that TiC and ZrC ultra-fine powders can be produced at lower temperatures compared to traditional carbides synthesis methods by using sol-gel processing [1-4].

In the present study, we aimed at elaboration of mixed ZrC–TiC precursors of corresponding metal alkoksides using a sol – gel method to produce powders that would be suitable for fabrication of bulk specimens. For a successful sintering of a bulk composite, ZrC –TiC powder blend properties have to be clarified. The main advantage of the used sol-gel process is the reduction of the kinetic barriers between the formed metal oxide and the carbon particles created in pyrolysis of metal alkoxide polymer due to the homogeneous dispersion of reactants in the precursor material. The increased contact area of the nanograins results in a complete reaction between the metal oxide and carbon. The temperatures needed are lower than required for conventional powder processes and formation of small precipitates. Titanium and zirconium carbides were synthesized by carbothermal reduction at 1600 ^{o}C in an argon atmosphere (Carbon + Metal oxide → Metal carbide), as it is the most effective method for carbides preparation [2]. Characterization of the powders has been carried out by X-ray diffraction and scanning electron microscope measurements. The bulk and dense composite ceramic was formed by hot pressing at 1650 ^{o}C and an applied pressure of 18 MPa.

Metal carbide nano-powders have a great potential in technological applications as the precursors for preparation of nanocomposites with homogeneous phase distribution.

Acknowledgements This work was funded by Estonian Science Foundation grant No 8377, 8211.

References

1. Haijun Zhang, Faliang Li, Quanli Jia, Guotian Ye, , Sol-Gel Sci Technol (2008) 46:217–222.
2. Pierson HO. Handbook of refractory carbides and nitrides. Park Ridge, NJ: Noyes; 1996.
3. Yongjie Yan, Zhengren Huang, Xuejian Liu, Dongliang, Sol-Gel Sci Technol (2007) 44:81–85
4. Mickael Doll´e, Dominique Gosset, Christine Bogicevic, Fabienne Karolak, D. Simeone, G. Baldinozzi European Ceramic Society 27 (2007) 2061–2067.

PO-159

Formation of p-n Junction in ITO/P-Si/Al Structure by Laser Radiation for Solar Cells Applications

A. Medvid[1], P. Onufrievs[1], E. Dauksta[1], J. Barloti[1], I. Dmytruk[2], I. Pundyk[2]

[1]Riga Technical University, Latvia

[2]Physics Faculty, Ukraine

e-mail: Edvins.dauskta@rtu.lv

The research report is devoted to the development of a new method of nanostructures formation in ITO/p-Si/Al structure with powerful laser radiation and study of its optical and electrical properties for solar cells applications[1]. It was shown that after the structure irradiation by a Nd:YAG laser second harmonic, dark current voltage characteristics become diode-like. Increase of ITO/p-Si/Al solar cell efficiency after irradiation by the laser, using photocurrent voltage characteristic method, was shown.

Indium–tin-oxide (ITO) thin films are widely used as transparent conductive oxide in optoelectronics devices such as solar cells [2], liquid crystal displays (LCD) and plasma display panels.

In this report, we investigated the ITO/p-Si/Al structure irradiated by Nd:YAG laser with the aim to form a p-n junction and to grow nanocones on a interface of ITO/Si. It was shown that Quantum confinement effect (QCE) in nanocones with graded band gap has the main role in increase of solar cell efficiency.

In conclusion of the experiments possibility of p-n junction and Si nanocones formation by the laser irradiation in ITO/p-Si/Al structure was shown. The photoluminescence spectra from irradiated and non-irradiated ITO/p-Si/Al structure by the laser radiation have been found in visible part of spectra and is explained by presence of quantum confinement effect in nanocones with graded band gap. Study of dark I-V characteristics showed diode-like character with rectification coefficient K = 105 at 5 V caused by laser irradiation with intensity I = 2.83 MW/cm^2. After irradiation of ITO/p-Si/Al structure by the laser, the solar cell efficiency increased by two times comparison to the non-irradiated structure.

References

1. J.Zhua, Z. Yua, S. Fana and Y. Cui, Materials Science and Engineering, **70**, 330 (2010)
1. L. Bruk. V. Fedorov. D. Sherban. A. Simashkevich. I. Usatii. E. Bobeico and P. Morvillo: Materials Science and Engineering B, **160**, 282 (2009)

PO-160

Preparation of Metal Oxide Waveguiding Fibers and Microtubes by Sol-gel Technique

K. Utt, M. Part, T. Tätte, V. Kiisk, I. Sildos
Institute of Physics, University of Tartu, Estonia
e-mail: kathriin@ut.ee

Wide-gap metal oxide semiconductors (e.g. TiO_2, SnO_2) and insulators (e.g. ZrO_2, HfO_2) are attractive materials for optoelectronic and optical applications. Sol-gel method occurs to be a versatile and cost-effective technique for functional shaping of such oxides [1]. Moreover, this preparation method allows flexible doping of the hosts with optically active inclusions (e.g. rare earth ions) for luminescence applications [2].

The aim of this work was to develop sol-gel prepared fibrous waveguiding structures based on RE doped ZrO_2. The optical and structural properties of the samples were evaluated by using luminescence and Raman spectroscopies and XRD analysis.

ZrO_2(30%)-SiO_2(70%) fibers doped with 1 mol% of Sm^{3+} were pulled from sol precursor with suitable viscoelastic properties. Development of RE-doped ZrO_2 nanocrystals inside the amorphous silica matrix (i.e. transparent nanoceramics) was aimed by thermal treatment at temperatures reaching up to 1000^oC [3]. Structural analysis confirms the formation of zirconia nanocrystals while luminescence study suggests that most of the particular dopant ions were still located in silica surrounding.

Yttria-stabilized zirconia (YSZ) microtubes doped with 1 mol% of Eu^{3+} or Sm^{3+} ions were prepared by initially pulling the sol precursor into gel fibers which thereafter were left to self-hollow at specific conditions. The obtained microtubes were ~10 mm long and had an average diameter of ~40 µm and wall thickness of ~10 µm. The microtubes remained crack-free and transparent even after annealing at 1100^oC. Microtubes heated at 800-900°C exposed also excellent luminescent and light guiding properties.

References

1. V. Reedo et al., Physica Status Solidi (a) **205**, 1511 (2008)
2. C. Mignotte, J. Non-Cryst. Solids **291**, 56 (2001)
3. G. Brasse et al., Optical Materials **31**, 765 (2009)

PO-161

Synthesis and Characterization of Novel Composite Materials Prepared By Combining Metal Oxide and Ionic Liquid Micro– and Nanonetwork for Industrial Use

R. Välbe[1], V. Reedo[1], A. Lõhmus[1]
[1]Institute of Physics, University of Tartu
e-mail: raul005@ut.ee

The aim of current work is to study possibilities of mixing polar ionic liquids and non-polar metal alkoxides for elaboration of hybrid structures.

The great interest of ionic liquids is motivated by their unique combination of properties like non-flammability, negligible vapour pressure, high ionic conductivity and wide electrochemical stability. Some of ionic liquids are thermally stable up to temperatures 570 K [1].

Sol-gel method offers a flexible technology for preparing ceramic materials from a liquid metal-organic precursors. Among the other available techniques, the sol-gel process is one of the simplest and the cheapest [2].

In the current work we use water-in-ionic liquid microemulsion for preparation of metal oxide composite materials with nanoscopic ionic liquid networks. Various metal alkoxides $Zr(OBu)_4$, $Hf(OBu)_4$, $Ti(OBu)_4$, or $Sn(OBu)_4$ and ionic liquids e.g. [***EMIM***][***BF4***] in different concentrations have been tested for elaboration of hybrid metal oxide composites.

Thin sol-gel films with ionic liquid networks can be used as catalyst carrier medium, in optics as photon crystals and in electro-optical applications. We propose to cover textile fibers with sol-gel and ionic-liquid networks in it for improving electrical conductivity.

References

1. A. Vioux , L. Viau, S. Volland, J. L. Bideau “Use of ionic liquids in sol-gel; ionogels and applications"Académie des sciences, (2009)
2. M.Järvekülg, R. Välbe, K. Utt, M. Timusk, T. Tätte “Tailoring Sol-Gel Transition Processes for the Design of Novel Shape Metal Oxide Materials” Materials Research Society Spring Meeting, 2010

PO-162

Nanolevel Functionalization Problems of Natural Fiber Textiles

S. Vihodceva[1], S. Kukle[1], J. Barloti[3]

[1]Riga Technical university, Department of Design and Textile Products Technology

[3]Riga Technical university, Faculty of Electronics and Telecommunication

e-mail: sv85@inbox.lv

Having the ability to control the surfaces of a natural fiber offers great rewards that go far beyond pure economics as natural fibers are renewable and biodegradable resources.[1] The processes of vacuum evaporation and magnetron sputtering of ultra thin metal layers on natural fibers textile is carried out. Technologies comparison results show that metal layer on the surface of fabrics obtained by magnetron sputtering are more even, adhesion with surface are better than for the same textile by vacuum evaporation. It is hard to achieve even and stable metal coating of natural fiber textile surface, because they offer unique challenges as not only are their cross sections irregular, but their surfaces are chemically and physically heterogeneous, the ability of a particular construction textile fabric to hold treatment depends and on surface cleanness, so that's why it is necessary to develop textile pre-treatment technology. Research results show that: after immersing in 80 % acetone solution for 5 min and after surface modification by low pressure plasma surface adhesion increase twice.

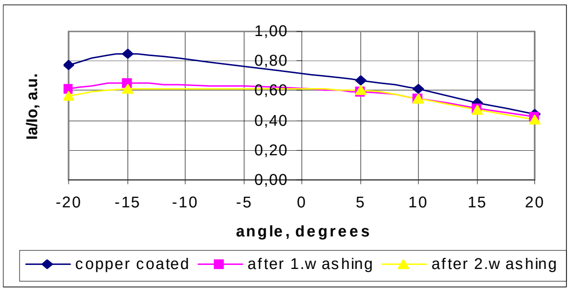

Fig.1 Comparison of reflected light of coated samples before and after washing.

To get a detailed insight into the changes of the textile surface properties and develop a tool for comparative analysis the surface of samples was examined with laboratory laser complex (indirect method of surface examination), by measuring reflected and passing light. From graph Fig.1. are seen that metal coating made by magnetron sputtering is influenced by first washing (necessary to continue investigation to find solution of this problem), second washing haven't influenced coating, reflected and passing light results show the same. It meets our expectations that indirect method can be used for surface examination during exploitation of textile.

References

1. Brown, P.J.; Stevens, K.. Nanofibres and nanotechnology in textiles, Woodhead Publishing Series in Textiles No.67., ISBN 1-84569-105-9, UK, 2007

PO-163

Evaluation Methods of Impedance for of Complex Al/Cu-Al_2O_3 Electrodes

J. Denisova[1], J. Katkevics[1], D. Erts[2], A. Viksna[1]
[1]Faculty of Chemistry, University of Latvia, Latvia
[2]Institute of Chemical Physics, University of Latvia, Latvia
e-mail: julija_denisova@inbox.lv

Noble metal nanoglobules on surfaces could be used as active sites for fixation of various nanostructures or biologically active substances.

The corrosion process of complex Al/Cu-Al_2O_3 electrodes in the form of aluminum alloy 2024 is investigated [1, 2].

The aim of the work is development of internal electrolyses deposition method for fabrication of Cu nanoglobules on Al/Al_2O_3 surfaces. We used Electrochemical Impedance Spectroscopy (EIS) measurement methodology and results for characterization of Al/Al_2O_3. Cu and Al/Cu-Al_2O_3 electrodes were evaluated. In EIS measurements following conditions were applied: 10^5–10^{-1} Hz AC frequency range and 10–15 mV amplitude of AC signal. We observed that electrolyte nature, electrode conditioning time in electrolyte before measurements and scanning potential affect EIS results.

0.1 M NaCl, CH_3COONa, K_2SO_4, mono- and diammonium citrate electrolytes are compared to evaluate its suitability for EIS method. Al/Al_2O_3, Cu and Al/Cu-Al_2O_3 electrodes are examined. The optimal conditions for measuring EIS spectra are following: 1) 0,1 M CH_3COONa electrolyte, 2) 30 min electrodes conditioning in electrolyte before measurements and 3) scanning potential range from -0,11 to -0,25 V. The investigation of the double layer shows that Al/Cu-Al_2O_3 electrode is the complex electrode (see Fig. 1.). It is shown that the Cu globules obtained by the internal electrolysis method are in direct contact with Al layer.

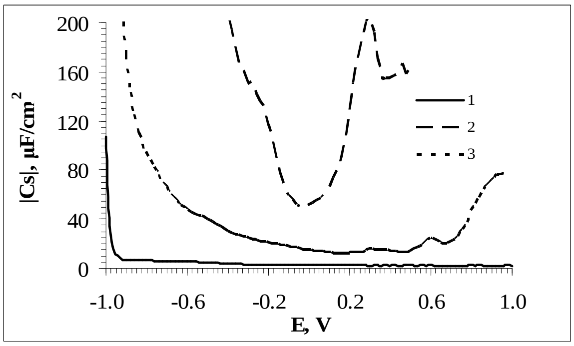

Fig.1. Dependence of double layer capacitance on the surface potential.
Labels: 1 - Al/Al_2O_3 , 2 - Cu, 3 - Al/Cu-Al_2O_3.

References

1. L. E. M. Palomino, J. F. W. de Castro, *et.al.*, J. Braz. Chem. Soc. **14**, 651 – 659 (2003)
2. R. Sabino, D. S. Azambuja and R. S. Goncalves, J. Solid State Electrochem. **14**, 1255 - 1260 (2010)

PO-164

Metallized Glass Fiber Fabric Characterization by Impedance Spectroscopy

A. Lusis, E. Pentjuss, G. Bajars, J. Balodis
Institute of Solid State Physics, University of Latvia, Latvia
Kengaraga Street 8, Riga, LV-1063
e-mail: lusis@latnet.lv

The metal coatings are widely used for functionalization of glass fiber fabrics for different technical applications. Metal-coated fabric characterization is an actual problem.

The fabrics of K-glass [composition: (18-22)Na_2O (3-5)Al_2O_3 (73-79)SiO_2] had been leached in water and dried at 220 ^{0}C [1]. Both sides of glass fiber fabrics (GF) are coated with known electrocatalysts – copper and nickel (Cu/GF/Ni) by DC magnetron sputtering of Cu and Ni in 100% Ar. The sheet resitances for metal coatings are 40-100 kOhm cm^2.

The electrical impedance spectroscopy (EIS) has been used for characterization of metal-coated fabrics. The leached glass fibers are porous. The porous media usually adsorbs some water from environment and content of moisture in fabrics have to be controlled. The impedance spectra of system Cu/GF/Ni are complicate due to the heterogeneous and nonhomogeneous constitution of system. There are problems with the interpretation of impedance data and the need for physical models. One of ways is to find relations between system Cu/GF/Ni constitution, pore and metal type and content of moisture.

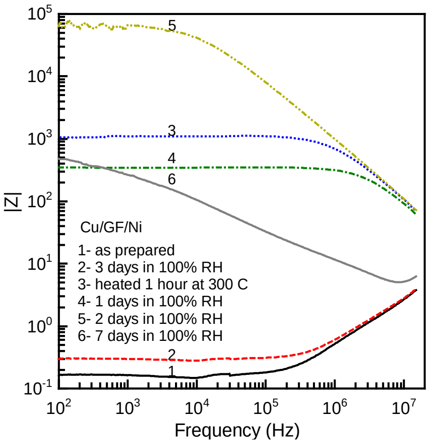

Fig.1. Impedance spectra of system Cu/GF/Ni

Impedance analyzer HP 4194A with dielectric test fixture HP 16451B (electrode area S = 11.3 cm^2) has been used for measurement of EIS. The impedance spectra of metal coated fabrics are senstive to moisture and depend on content of absorbed water (Fig.1).

The resistances of metal coated samples depend on amounts of deposited metal and adsorbed water and are in the range 10^{-1}-10^5 Ohm. The samples, which as prepared have $|Z| = 10^{-1} – 10^2$ Ohm, have metalic like conduction and changed to ionic like after adsorption of water. The deposited metal particles in porous surface are forming electronically conducting channels with some perculation threshold, which can be changed by concentration and size of metal particles and water content. H_2O molecules separate metal particles and provide ionic conductivity.

Functionalization of nanostructured technical glass fibers and fabrics with metal coatings requires deeper studies to explain how adsorbed H_2O change the impedance spectra.

References

1. G. Veveris, V.Eglitis, A. Lusis, E. Pentjuss. Leaching as method for surface nanostructuring of sodium alumosilicate glass fibres. Latvian Journal of Physics and Technical Sciences, 2006, No.4, p54-62.

PO-165

Impedance Spectroscopy Use of Flax and Hemp Fiber Functionalization Studies

A. Lusis, E. Pentjuss, J. Gabrusenoks, J. Balodis
Institute of Solid State Physics of University of Latvia Kengaraga Street 8, Riga, LV-1063, Latvia
e-mail: lusis@latnet.lv

Sustainable development of technical textiles is associated with natural fibers to replace the oil-producing fibers. In this context, it is necessary to carry out studies on the flax and hemp fiber and fabric functionalization for technical applications.The natural fibers (NF) as well as fabrics (FF) themselves are porous media. The porous media usually adsorbs some chemicals from environment. One of them is water and content of moisture in fabrics have to be controled. Metal coatings are widely used for functionalization of fabrics for different technical applications. To characterize the metal coating is a problem in itself. First of all, to functionalize fibers or fabrics is to examine the content of moisture and its role on mechanical and physical properties. In this regard, ongoing studies are on the moisture content determination methodology based on thermogravimetric analyses and impedance spectroscopy. The impedance spectroscopy (IS) has been used to study moisture in FF and metal coated fabrics (M/FF/M). The impedance spectra of such samples are complicate due to heterogeneous and nonhomogeneous constitution. The content of absorbed water in FF in box with 100% RH during 27 days is 7.5 wt % (Fig.1). The water content has strong influence on impedance modulus |Z| spectra (Fig.2). Analyses of |Z| spectra with simulation of equivalent circuit models, the best fit have been obtained with CPE and RC elements. The value of capacitance C depends on water content and can be used for controle of moisture content in flax and hemp fabrics.

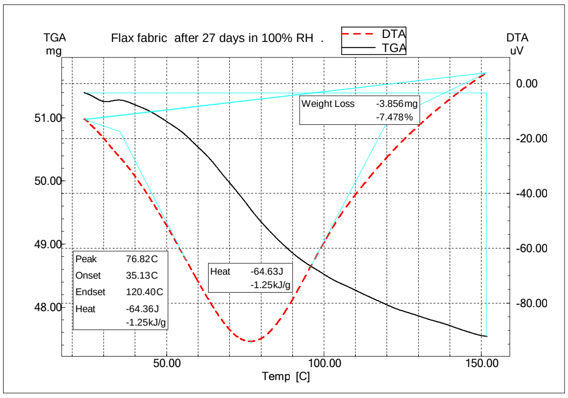

Fig.1. Thermal analysis result of flax fabric

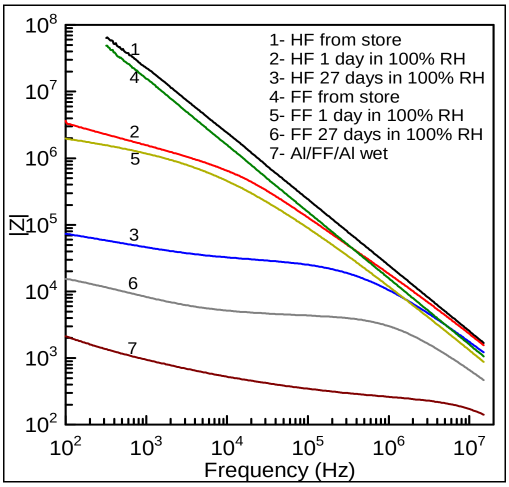

Fig.2. Impedance spectra of flax and hemp fabrics

PO-166

Use of Nanotechnologies for Obtaining Catalysts of Hydrocarbons Destruction

M.I. Rustamov, H.I. Abad-zade, G.S. Mukhtarova, G.F. Samedova, Ahmedov V.M., Huseynova R.I., Beshirova Sh.T.

Institute of Petrochemical Processes after Yu.H.Mammedaliyev of National Academy of Sciences of Azerbaijan, Baku
e-mail: gulermuxtarova@yahoo.com

At present, significant progress has been achieved in synthesis of catalysts of petroleum stock destruction using nanotechnologies.

With these purposes, in particular, for obtaining high-dispersity Re/Al_2O_3 catalyst with Re content 0,1 % mas. The method of vapour-phase synthesis was used that allows to uniformly fix tromsition metal atoms on the surface of solid carrier.

It is known that transition metals under the conditions of vapour-phase synthesis form complexes with aromatic hydrocarbons which, as a rule, are easily decomposed with formation of metallic and cluster nanoparticles exhibiting a high catalytic activity in a number of chemical reactions.

Cocondensation of transition metal atoms with aromatic hydrocarbons was carried out at the apparatus “VS-500” of “G.V.Planar Ltd” production equipped with an electron gun for vaporization of metal.

Low temperature destruction of model hydrocarbons-normal alkanes C_2-C_6, benzene and cyclohexane in the atmosphere of H_2 over the Re/Al_2O_3 has been carried out in the impulse mode in the catalytic microreactor connected to gas-liquid chromatograph. For each individual alkane C_2-C_6 temperature regime of complete destruction was established that varied from 260^{o}C for ethane to 180^{o}C for hexane. For benzene and cyclohexane temperature of complete conversion - 220^{o}C.

Thus, it has been established that the stable M/Al_2O_3 catalysts obtained by the method of vapour-phase synthesis and containing 0,1% of Re having nanometric dimensions catalyze destruction of alkanes, cycloalkanes and aromatic hydrocarbons in the atmosphere of H_2 at the temperature unusually low and atmospheric pressure.

PO-167

Novel Extractive-Pyrolytic Method for Heterogeneous Supported Palladium Catalyst Synthesis

S. Čornaja[1], L. Kuļikova[2], V. Serga[2], V. Kampars[1], K. Dubencovs[1], S. Žižkuna[1], O. Muravjova[1]
[1]Riga Technical University
[2]RTU Institute of Inorganic Chemistry
e-mail: Svetlana@ktf.rtu.lv

Glycerol is major by-product of bio-fuel production. A number of important products can be obtained in the process of glycerol oxidation. Glycerol liquid phase catalytic oxidation by molecular oxygen can substantially decrease the cost of oxidation products and makes possible to realize process in mild conditions in presence of green oxidizer. Usage of heterogeneous catalyst has several benefits from the technological perspective: simplified heterogeneous catalyst regeneration process and possibility of its reuse.

Influence of novel supported palladium catalysts synthesis parameters on the catalyst activity and selectivity for glycerol liquid phase catalytic oxidation is studied in this work. New extractive-pyrolytic method for catalysts synthesis, which makes it possible to obtain active palladium nanoparticles on various supports is proposed [1]. Palladium nanoparticles size, nature of support (Al2O3 (nanopowder or granules), Y2O3, C, SiO2), palladium load in catalyst (0,1-10%), number of palladium layers (from 1 to 12), precursor concentration [(C8H17)3NH]2PdCl4 (0,06-0,40 M) and catalyst pyrolysis temperature (473-673K) on its activity and selectivity is studied as well. The structure and specific surface area of catalysts is studied by mean of XRD and BET methods. There are optimal catalyst synthesis conditions and most active catalysts composition and their physical parameters are identified as the result of this study as following:

- Catalyst composition: 1,25 – 2,5%Pd/Al2O3(nanopowder)
- Number of palladium layers in catalyst: 1
- Specific surface area: 36 – 42 m2/g
- d(Pd crystallite) = 15 – 20 nm
- Concentration of precursor (by palladium) – 0,4 M
- Temperature of pyrolysis – 573 K

References

1. S. Čornaja, L. Kuļikova, V. Serga, V. Kampars, K. Dubencovs, S. Žižkuna, O. Muravjova. Glicerīnskābes selektīvās iegūšanas metode un katalizatori tās realizācijai. *Pat*. LV 14079 (20.05.2010).

PO-168

Lignin Oxidation Using Heteropolyanions of the Keggin's Type as Catalysts

T. Dizbite[1], G. Telysheva[1], L. Jashina[1], G. Dobele[1], A. Volperts[1], A. Andersone[1], J. Ponomarenko[1], N. Mironova-Ulmane[2], I. Sildos[3]

[1]Latvian State Institute of Wood Chemistry, Latvia

[2]Institute of Solid State Physics, University of Latvia, Latvia

[3]Institute of Physics, University of Tartu, Estonia

e-mail: ligno@edi.lv

It is widely recognized that advanced biorefinery of lignocellulosic non-food feedstocks, developing by analogy with oil refinery, constitute ecologically smart solutions for obtaining a series of high value green biofuels, materials, products and chemicals, which are of great demand today. Lignins separated as by-products in lignocellulosic chemical processing are considered as important renewable aromatic macro-monomers.

Development of the soft process for lignin oxidation enhancing its hydroxyl functionalities content without indicative deterioration of the solid polymer structure was the task of the present work. The organosolv lignin, obtained by the novel process of wheat straw consecutive fractionation, worked out by CIMV (France), was the object of the study.

Heteropolyanions of the Keggin's type $[PMo_{12}O_{40}]^{3-}$ and $[PMo_7V_5O_{40}]^{8-}$ were used as the catalysts for lignin oxidation, and influence of temperature, media pH, catalyst/lignin molecular ratio and the process duration on the efficiency of lignin modification was studied.

The oxidation products were examined using chemical analytical procedures, FTIR, Py-GC/MS, EPR and Raman spectroscopy. The highest increase in total content of hydroxyl groups (by 1.5 times) was achieved by treatment of CIMV lignin with $[PMo_{12}O_{40}]^{3-}$ (0.05 M). This effect was obtained due to COOH and OH aliphatic groups, whereas content of phenolic hydroxyl groups decreased, indicating the preferential attack of the catalyst on the phenolic lignin units. The antioxidant activity of oxidized lignin samples was estimated in $DPPH^{\bullet}$ and $ABTS^{\bullet+}$ assays.

Acknowledgement. The financial supports from the 7th FP Project BIOCORE, contract 241566 and Latvian Budget (Grant 1547) are gratefully acknowledged.

PO-169

How local is EXAFS spectroscopy?

A. Kuzmin, A. Anspoks, A. Kalinko
Institute of Solid State Physics, University of Latvia, Latvia
e-mail: a.kuzmin@cfi.lu.lv

Extended x-ray absorption fine structure (EXAFS) spectroscopy is commonly known as *the local structure probe* that provides information on the nearest coordination shells around absorbing atom [1]. Being atom type selective and independent on the presence of the long range order, EXAFS technique is particularly suitable to study non-crystalline and complex materials. Besides, it also complements successfully diffraction methods, when local distortions are present in a crystalline material.

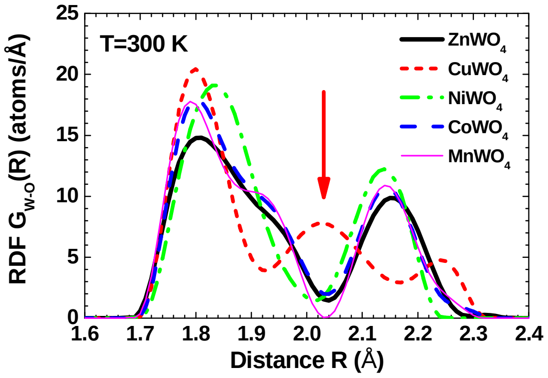

Fig. 1. Radial distribution functions (RDF) $G_{W\text{-}O}(R)$ for the first coordination shell of tungsten, reconstructed from the experimental W L_3-edge EXAFS spectra in MWO_4 (M=Mn, Co, Ni, Cu, Zn) compounds.

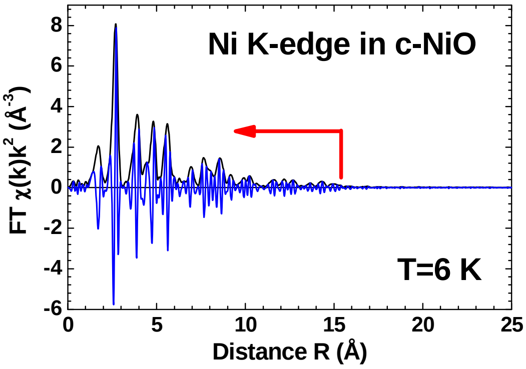

Fig. 2. Fourier transform of the experimental Ni K-edge EXAFS spectrum measured in NiO at T=6 K. The contribution from the structural peaks up to 15 Å is clearly visible.

In this report we will address two questions: how sensitive is EXAFS to strong local distortions? And how local is structural information contained in the EXAFS spectra? The answer will be given on the example of recent EXAFS studies of tungstates MWO_4 (M=Mn, Co, Ni, Cu, Zn) and nickel oxide NiO compounds.

References

1. S. J. L. Billinge, I. Levin, Science **316**, 561 (2007).

PO-170

Crystal Structure Determination Using EXAFS Total Scattering Phase

A. Kalinko, A. Kuzmin

Institute of Solid State Physics, University of Latvia, Latvia

e-mail: akalin@latnet.lv

The properties of any material are determined by its atomic structure, which can be probed by one of two direct methods – x-ray (neutron, electron) diffraction and x-ray absorption spectroscopy (XAS). Diffraction experiments require the presence of the long range order, i.e. the periodic structure, which is described in terms of the unit cell and symmetry operations. On the contrary, the short range order around an atom of a particular type is probed in the XAS experiment, which provides information on interatomic distances, coordination numbers, and relative atomic movements. Thus, the two methods are considered to be complementary.

In the present work we propose the method, which allows one to extract information on the long range crystal structure from the total scattering phase (TSP) of the extended x-ray absorption fine structure (EXAFS). The method is based on adjusting unit cell parameters (cell dimensions and fractional atomic coordinates), as in the diffraction data analysis, till the best agreement between the experimental and calculated TSPs is achieved.

On practice, the optimization procedure is realized using the simulated annealing method, and the TSPs are obtained by Fourier filtering procedure in a desired range of the *k* and *R*-space. The theoretical EXAFS signal $\chi(k)$ is calculated using the ab initio multiple-scattering formalism thus accounting for the many-body effects. Besides, the simultaneous analysis of several EXAFS signals, measured at different absorption edges in the same sample, can be performed to stabilize the solution.

The application of the method will be demonstrated on the Re L_3-edge in cubic perovskite-type ReO_3 and on the Ni K and W L_3 edges in monoclinic wolframite-type $NiWO_4$.

PO-171

DC Magnetron Deposition of Zn-Based TCo-S: Process Control by Plasma Optical Emission Spectroscopy

A. Azens, K. Vilnis, R. Kalendarev, J. Purans
Institute of Solid State Physics, University of Latvia, Latvia
e-mail: andris.azens@cf.lu.lv

Plasma optical emission spectroscopy (OES) has been used at the ISSP for thin film deposition process monitoring and control since the mid 1980-s, with the films of Indium Tin Oxide (ITO) being one of examples where the use of OES had helped to develop a well controlled deposition process. High deposition cost reduction have been obtained by deposition of doped aluminium zinc oxide films (AZO) - used as combined window and contact layer for thin film solar modules. However, commonly AZO films are DC sputtered from expensive ceramic AZO targets. Nowadays high deposition cost reduction can be expected by reactive sputtering of metallic alloy targets (Zn:Al) or dual magnetron sputtering. To deposit high quality AZO coatings special requirements are needed to stabilize the process.

In this study, transparent conducting oxide (TCO) layers have been deposited by DC magnetron sputtering of metallic Zn and ZnAl (2%Al) targets in an argon and oxygen atmosphere with the aim to develop a stable and reproducible process for production of TCO-s with optimized electrical and optical properties. Sputtering modes with constant power and constant current have been investigated from the process stability point of view. In both cases, the feedback based on plasma optical emission line intensities of zinc and oxygen has been highly valuable for improving the degree of process reproducibility.

PO-172

XAFS, Raman and EPR Studies of Fe-doped $SrTiO_3$ for Terabit Resistive Switching Memories

J. Purans[1], C. Lenser[2], R. Dittmann[2], K. Szot[2], E. Berzinš[1], A. Kalinko[1], A. Kuzmin[1], R. Waser[2, 3]

[1]Institute of Solid State Physics, University of Latvia, Latvia

[2]Institute of Solid State Research, Forschungszentrum Jülich, Jülich, Germany

[3]Institut für Werkstoffe der Elektrotechnik, RWTH Aachen, Aachen, Germany

e-mail: purans@cfi.lu.lv

Doped $SrTiO_3$ thin films are suitable functional materials for storage devices with a density in the terabit range since extended defects as dislocations or defect clusters with nanoscale dimensions are considered to be the single resistive switching units. Nevertheless, devices based on these materials are still in the early stage of development. Up to now, their performance does not fulfil the requirements for future resistive random access memory (RRAM) and the basic physical and chemical mechanisms are not completely understood.

XAFS measurements were performed at ESRF and HASYLAB on $SrFe_xTi_{1-x}O_{3-\sigma}$ thin films deposited via pulsed laser deposition (PLD) and Fe-doped $SrTiO_3$ single crystal. The thin films were deposited on Ti-free substrates ($NdGaO_3$) for Fe and Ti-K edge EXAFS and on a conducting Nb-doped $SrTiO_3$ substrate to do Fe-K edge EXAFS on a thin film resistive switching device. The single crystal was subjected to an electroforming treatment prior to the experiments, resulting in optically colored region at the cathodic part.

Fe-K edge EXAFS and XANES, as well as EPR and Raman measurements on the electroformed single crystal show a clear correlation between the sample color and the local structure (six-fold coordinated (octahedral) Fe^{3+} or Fe^{4+} and five-fold coordinated Fe^{3+}-V_O with oxygen vacancy). It was demonstrated that EXAFS spectroscopy measurements at the Fe-K edge are possible on the thin films as thin as 100 nm and containing as little as 1% iron. This fact becomes very important for further experiments on thin film structures for resistive switching, since it enables us to investigate thin metal-insulator-metal (MIM) structures. For these investigations, a micro-focused beam was used to reduce the beam size (5 μ) to the dimensions of the active electrode area of the MIM structure, which will improve the amount of signal detected from electrically active areas over that detected from non-active regions of the sample.

PO-173

Investigation of Glass Crystallization by X-ray Powder Diffraction

A. Stunda, L. Berzina-Cimdina

RTU Riga Biomaterials Innovation and Development Centre

e-mail: agnese.stunda@rtu.lv

X-ray powder diffraction (XRD) is a powerful tool for investigation crystalline phases. However at the very beginning of crystallization crystalline phase has low concentration and small size of crystallites. Thereby X-ray diffraction pattern in such cases has several features. Firstly, diffraction peaks of phases with smaller average size of crystallites are relatively wider and less intensive comparing to well crystalline substances. Secondly, nanocrystalline phases can be a transition state, non-stoichiometric phase that also can blur the typical diffraction pattern. And thirdly, the intensity of diffraction peaks is proportional to concentration of crystalline phase and at the beginning of crystallization the concentration of crystalline phase is low. To investigate crystalline phases qualitatively and quantitatively a resolution of diffraction patterns should be improved. One of solution is to increase the size of crystallites. But not always it is possible or desirable. Moreover at the early stages of crystallization metastable phases can form that disappear during further crystallization.

The aim of this study was to obtain an optimal set of XRD parameters to investigate the crystallization at an early stage. The studied material was glass in the system Na_2O-CaO-Nb_2O_5-P_2O_5. DTA showed several crystallization maximums, the glass was crystallized step by step accordingly to them. The parameters of XRD measurement was changed till pattern intensities was suitable for phase identification, although peaks were wide and overlapping. The metastable phases was supposed to be $Ca_3(PO_4)$ and $Ca_2P_2O_7$. The next phase was small amount of niobium containing phase. Further heating leads to relatively well crystalline $Na_4Nb_8P_4O_{32}$ and $Ca_2P_2O_7$.

The results showed that with choosing appropriate parameters the limits of conventional diffractometer can be significantly moved to the side of lower concentrations and smaller size of crystallites. The most effective way of increasing intensity of diffraction pattern is increasing time per step or decreasing measurement speed. There are also several other parameters that should be taken into account like increasing step size corresponding to peak width, optimal irradiated length and size of fixed and variable slits.

PO-174

Multi-Component Particle Analysis by Laser Particle Sizing

Z. Irbe[1], V. Lakevičs[1], V. Stepanova[1]

[1]Institute of General Chemical Engineering, Riga Technical University, Latvia

e-mail: zilgma.irbe@rtu.lv

Laser particle sizing is a method for determining particle size distribution. For submicron particles and particles in size of few microns refractive index and absorption index must be known to conduct necessary calculations [1-2]. There have been several attempts to analyze multi-component particles using laser particle sizing by adjusting optical constants for sample [3-4]. However the analysis in past works [3-4] was conducted on non-fractioned samples, i.e., larger particles (over 10 micron) were also present.

In this work it is investigated whether analysis of multi-component particles is feasible. Clay was chosen as model for multi-component particles. Other particle size analysis methods for clay are well developed (sedimentation methods, electron microscopy methods), but are time consuming. Fine fractions of clay were separated using sedimentation (pipette method) and analyzed by laser particle sizing.

Results show that is possible to use laser particle sizing for multi-component particle analysis. However it is of great importance to use additional particle sizing methods during adjustment of optical constants to confirm adequacy of analysis. Sedimentation analysis (pipette method) can overestimate particle size (if particles are smaller than 2 μm) in comparison to laser particle sizing.

References

1. A. Beekman, D. Shan, A. Ali, W. Dai, S. Ward-Smith and M. Goldenberg, Pharm. Res. **22**, 518 (2005)
2. C. M. Keck and R. H. Müller, Int. J. Pharm. **533**, 150 (2008)
3. C. Di Stefano, V. Ferro and S.Mirabile, Biosyst. Eng. **106**, 205 (2010)
4. G. Eshel, G. J. Levy, U. Mingelgrin, M. J. Singer, Soil Sci. S. Am. J. **68**, 736 (2004)

PO-175

Investigation of the Nanostructures Formation in the Irradiated by γ – Quanta Single-Crystal Silicon with Ultrasonic Method

T. Khaydarov, I.Kh. Abdukadirova, Yu. Karimov
Institute of Nuclear Physics of Academy Sciences of Uzbekistan, Uzbekistan
e-mail: izida@inp.uz

It’s determined that a phasic dynamics of deformation strengthening of single-crystal silicon irradiated by γ – quanta (with energy ~ 1,27 MeV) in the wide region of doses (from 10^2 up to 10^9 rad) by the internal friction measurement with widely known ultrasonic resonance method. We have detected appearance maximum on the dependence of internal friction (Q^{-1}) from dose at 10^5 rad in the samples p- Si with density of dislocations more then 10^3 cm^{-2}. Besides it the instability of nanodimensional dislocation structures has been established in the doses interval from 10^6 up to 10^9 rad, due to the formation and accumulation in the crystal lattice of the point like and continuous radiation defects (evolution of the dislocation densities in metals with rise of deformation were considered in [1-4]). On the temporal dependence $Q^{-1}(t)$ throughout 1,5 - 2 hours after irradiation the maximum has been established which position depends from ionizing dose. We suppose that such behavior of the $Q^{-1}(t)$ function is connected with manifestation of migration activity which coherent with annihilation of the dislocation loops in the first 1,5-2 hours when it’s growing in 2,5 times starting from the initial up to the maximum value. At the increasing of the observation time after stopping of the sample irradiation it is observed a monotonic decrease of $Q^{-1}(t)$ dependence, which is obviously connected with decreasing of the radiation defects densities in the result of their annihilation.

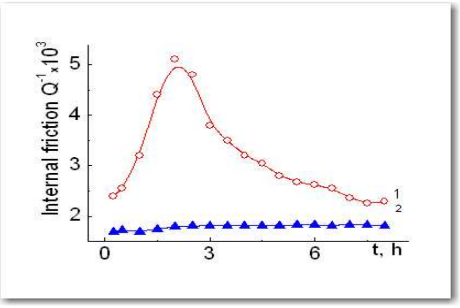

Fig.1 Time dependence of the single-crystal silicon internal friction after stop of the irradiation action.
(1) -10^8 rad, (2) – initial sample.

References

1. 1. Г. А.Малыгин. ФТТ **51**, 1709 (2009)
2. А. Малыгин. ФТТ **48**, 651(2006)
3. A.Godfrey, D.A. Hughes. Scripta Matter. **51**,8,831 (2004)
4. A.Godfrey, D.A. Hughes. Scripta Matter. **48**,8,1987 (2000)

PO-176

Analysis of Elastic Characteristics Stability Made from Sav-1 Alloys of Fuel Elements at the Wwr-Sm Reactor

I. Abdukadirova
Institute of Nuclear Physics Academy of Sciences Uzbekistan 100214, Tashkent. Uzbekistan. Ulugbek
e-mail: izida@inp.uz

At present work analysis were carried out on mechanical properties of some constructional materials, their stability under influence of external factors. Specifically for implementation of the problem put by acoustic methods were attracted. New information was received on stability of elasticity properties available for reactor technology of constructional materials type of aluminium alloys SAV-1, applied in manufacturing of fuel elements' shell for the WWR-SM reactor in thermal neutrons using ultrasonic methods. The experiment was carried out in 2008 at the WWR-SM reactor with power 10 Mt and active core fuel loading UO_2 –Al 36% enrichment on U with fuel assemblies IRT-3M type on series on prepared identical samples in the form of disks.

N	f(m,n)	E, 10^{10} Н/м^2	ΔE, 10^{10} Н/м^2
1	(0,2)	6,65	0,25
2	(1,0)	7,60	0,70
3	(0,3)	6,57	0,33
4	(0,2)	6,91	0,01
5	(1,1)	6,76	0,14

Table2. Value of elasticity of modules for samples #2, considered in function of resonance frequency

Data on elasticity properties were identified, dispersion dependence of main normal alloy modules before and after action of ionizing radiation on the basis of taken spectrums of bending vibration and their main characteristics: vibrational amplitude (A), resonance frequency (f), and also appropriate calculations. Based on data experimental value of resonance frequency f(m, n) were considered elastic parameter of samples (E - modulus of elasticity). As an example calculation results on modulus of elasticity of this sample are shown in the next table:

From this table we can obtain information on variation mode of the elastic characteristics of samples depending on vibration resonance frequency. It's necessary to conclude, that obtained by acoustic method dispersion dependence of the main modulus of elasticity E (f) long term constructional alloy indicates to insignificant of its fluctuations.

PO-177

Influence of Irradiation on the Some Electrofisicel Properties of Oxide Aluminium

I. Abdukadirova
Institute of Nuclear Physics Usbek Academy of Sciences. Taskent. Uzbekistan
e-mail: izida@inp.uz

The some oxides materials: Al_2O_3 – crystalline oxide aluminium (N 1) and oxide aluminium ceramics (N 2) is one of the prospective high-k electro-insulators und construction oxides materials. Besides, this oxide used widely as an active element or substrate at creation of laser, as a film coating and receiver of IR-radiation. From here this work aim at investigation of radiation stability of the electrophysical properties and a structure of this oxides after irradiated in the reactor and cource Co ^{60} canals of a high fluence. Features of dose and temperature dependencies of electric properties (the conductivity, dielectrical permittivity, dielectrical lose) were determined after influence of different doses of ionizing radiation. Increase of the dielectric permittivity and conductivity in samples N 1 and N 2 was found near temperatures (200-700 K) and high doses. Besides, at the dose of 10^3-10^5 Gy the electric conductivity and at T > 130 ^{o}C the dielectrical lose was decreased. The dose and temperature dependencies of the conductivity this plates in function $\sigma_1(1/T)$ и $\sigma_2(1/T)$, $\sigma_1(D)$ и $\sigma_2(D)$ was found to be nonmonotonic. The problems connected with the possible of causes was established of the peculiarities of kinetics in the position of the existence models is discussed on the base of these characteristics analysis. This paper presents the results of continue study of surface electric transfer of in a porous samples N 2 with a high humidity in the temperature interval of 200–450 K. Gamma-irradiation was applied for modification of the surface electric potential, the maximum current near 300-290 K and 250-230 K was study, which is absent in dry samples and hence is due to proton and hydrocsil transport. The activation energy and frequency factor were calculated from the experimental temperature dependence’s of the surface conductivity and both decreased after gamma-irradiation significantly. So it seems quite prospective to apply radiation for safe obtaining and accumulating hydrogen in samples N 2 oxide aluminium.

PO-178

The Obtaining and Clearing of Hydrogen on Nanokomposit Materials

S. Rustamova

Institute of Chemical Problems, named after acad. M.F.Nagiyev of NAS of Azerbaijan

e-mail: rsevil@rambler.ru

Attraction nanotechnologies opens possibilities for reception of highly effective catalysts of new generation in which structural and dimensional characteristics are regulated in area nanometres. Catalysts with application nanotechnologies can be used in structurally-sensitive reactions, which converting methane with carbon dioxide (the obtaining hydrogencontaning gas) and selective oxidation of carbon monooxide (clearing of hydrogen from carbon monooxide) concern also.

In the present thesis of the report it is informed on synthesis and research of nanokomposit systems with use molekull-sieve matrixes in reaction of methane conversion with carbon dioxide (MCD) and multicomponent catalytic systems in reaction of selective oxidation of carbon monooxide.

For reaction MCD nanoparticles are received by a method in-situ by matrix synthesis, and in the second case - an adhesive method.

The nickel catalyst is developed for reaction MCD on the basis of zeolite, connection between physical-chemical (the superficial acidic-basic, oxidation-reduction) and catalytic properties is established. It was determined, that the biggest correlation dependence (r=+0,65) between a hydrogen exit at 600^0C with electronoacceptor centers, but weaker correlation dependence (r=+0,58) is between strong basic centers.

For reaction of selective oxidation carbon monooxide from investigated $Mn_xFe_yCo_zO_4$ catalysts the best activity (100 % conversion of carbon monooxide) has shown $MnFe_{1,25}Co_{0,75}O_4$.

As a result of the spent researches for the reactions catalysts of the above-stated structure which huge advantage consists that they allow to refuse expensive active components (precious metals) are offered and provide high indicators of the important technical characteristics on process.

PO-179

Optical IR Transmission Spectra of Thin Epitaxial Lead Selenide Layers

Z.G. Akhvlediani[1, 2], L.P. Bychkova[1], O.I. Davarashvili[1], M.A. Dzagania[1], M.I. Enukashvili[1]

[1]Iv.Javakhishvili Tbilisi State University

[2]E.Andronikashvili Institute of Physics, Tbilisi, Georgia

e-mail: zairaak@yahoo.com

The nanotechnology of IV-VI semiconductor layers is topical not only for increasing the efficiency of IR optoelectronic devices, but also as an interesting opportunity of realization of efficient ”negative” pressure in the solid-state structure [1,2].

Actually, if a thin layer of, for instance, lead selenide grows on BaF2 or KCl substrates with much larger lattice constants, its tension takes place and, as a result, the width of the forbidden gap increases. At the same time, if the layers are doped with such dopants as Cr or In as well, the levels of these dopants shift deeply in the forbidden gap - the semiconductor transforms into a quasidielectric state.

The present work deals with the investigation of optical IR transmission spectra of thin layers of lead selenide of different thicknesses being grown on KCl substrates by the method of molecular epitaxy with “a hot wall” and its aim is optical characterization of the layers.

The refractive index, the reflection and absorption coefficients and their spectral dependencies were determined by the transmission spectra [3].

By straightening the α2 ~ hν ~ Eg relation typical for direct zone-zone transitions, the value of the width of the forbidden gap was determined for the layers with different degrees of residual deformations (different thicknesses). As the X-ray studies showed, the residual elastic deformations increased as the thickness of the layers decreased, and the “negative” pressure in the layers amounted up to 15 kbar.

The transmission spectra were recorded with the help of double-beam spectrophotometer “Specord-75 IR”. When analyzing the spectra, we paid special attention to the identification of spectral peaks and the calibration of the transmission scale. If the peaks were revealed in the spectrum (in the layers >0.5µm thick), the refractive index was determined from the relation 2Nd=mλ. In thinner layers, when there was not observed an interference pattern, we estimated the changes in the refractive index ΔN through the increase in the forbidden gap width in the stressed layer at known deformation ΔEg and refractive index derivative by energy dN/dE (from the dependence of the refractive index on the semiconductor composition): ΔN =dN/dE·ΔEg.

The reflection coefficients were determined with consideration for weak absorption in the layers beyond the absorption edge, whereas the absorption coefficients were determined by using the data of the transmission in the thin layer which was regarded as a Fabri-Perot interferometer.

The width of the forbidden gap, determined by the spectral dependence of the absorption coefficient, increased in accord with the increase of the “negative” pressure in the layers.

References

1. G.G.Gegiadze, K.B.Gelovani,O.I.Davarashvili, M.I.Enukashvili, N.P.Kekelidze, Georgian Chem. J. 5,265 (2005).
2. O.I.Davarashvili, L.P.Bychkova, M.I.Enukashvili, M.A.Dzagania, Proc.Georg.Nation.Acad., 35, 479 (2009).
3. Z.G.Akhvlediani, L.P.Bychkova, O.I.Davarashvili, M.A.Dzagania, M.I.Enukashvili, Proc.Georg. Nation. Acad., 36, 279 (2010).

PO-180

Use of Multi-Walled Metal-Containing Carbon Nanotubes as Catalyst for Oil Hydrocarbons Aerobic Oxidation

Aliyeva A.Z., Nuriyev L.H., Zeynalov E.B.
The Institute of Petrochemical Processes of NASA, Azerbaijan, Baku
e-mail:aykaza@inbox.ru

The process of synthetic petroleum acids (SPA) production by catalytic oxidation of oil fractions is one of the promising both in oil-refining and petrochemical industries. Main idea of the synthesis is to create alternative way to replace natural petroleum acids which well-known as products of broad application.

The catalytic oxidation of a naphthenic-paraffinic fraction of Balakhani oil in the presence of transition metals (Mn, Fe, Co, Ni) salts has shown that the end product yield does not exceed 16%. Moveover, along with SPA the oxy-acids as by product are formed in quantities of 10-12%. Thus there is substantial capacity to improve the process.

The present report describes use of metal-containing multi-walled carbon nanotube CNT- MW (1) containing Co in quantity of 1.5wt. % (Future Carbon GmbH) as new catalyst for the oxidation of naphthenic hydrocarbons fraction izolated from Baku Balakhani oil. The catalyst have demonstrated catalytic activity which 300 times more than that of for the metal-naphthenates. It is presumed that the effect observed is due to intensive charges shuttled transfer between the intercalated metal (M) and the CNT [1] leading to the forced decay of petroleum hydrocarbons (RH) hydroperoxides (ROOH) with concomitant and final obtaining SPA:

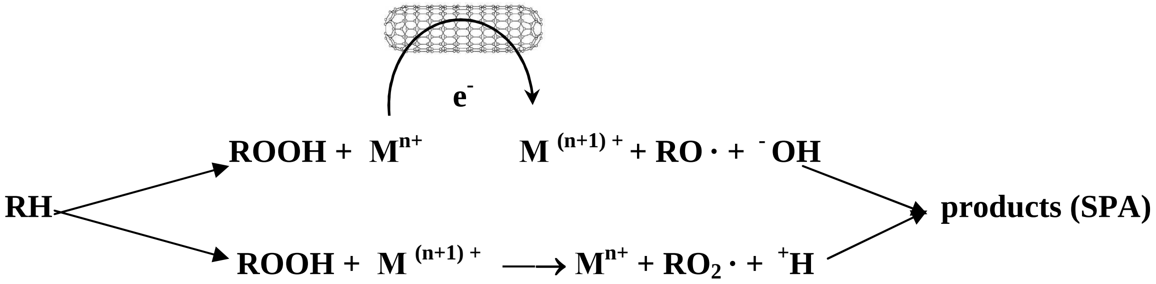

$$RH \rightarrow ROOH + M^{n+} \xrightarrow{e^-} M^{(n+1)+} + RO\cdot + {}^{-}OH \rightarrow \text{products (SPA)}$$

$$RH \rightarrow ROOH + M^{(n+1)+} \longrightarrow M^{n+} + RO_2\cdot + {}^{+}H \rightarrow \text{products (SPA)}$$

These results are basic for improvement of the process of SPA production according to the accepted modern industrial requirements.

References

1. M.Menon, A.N.Andriotis, G.E.Froudakis, Chem.Phys.letter. 320, 425 (2000)

PO-181

Raman Spectroscopy of $CoFe_2O_4$ Nanopowders

N. Mironova-Ulmane[1], M. Polakovs[1] J. Grabis[2], V. Serga[2], L.Kulikova[2],
D. Jakovlevs[3] I. Sildos[4]
[1]Institute of Solid State Physics, University of Latvia, Latvia
[2] Institute of Inorganic Chemistry, Riga Technical University, Latvia
[3]Biomaterials Innovation and development center, Riga Technical University, Latvia
[4]Institute of Physics, University of Tartu, Estonia
e-mail: nina@cfi.lu.lv

$CoFe_2O_4$ has an inverse spinel crystal structure. In the case of an inverse spinel such as $CoFe_2O_4$, the Co cation occupies one half of the octahedral coordination sites. Half the Fe^{3+} cations occupy the other half of the octahedral coordination sites as well as all of the tetrahedral coordination sites. Magnetic fine particles of cobalt ferrite have been prepared by method of pyrolytic [1] and the plasma synthesis. X-ray diffraction confirmed the formation of single-phase cobalt ferrite nanoparticles in the range 6-50 nm. The size of the particles varies depending on matrix disparity and mass content in the organic precursors. Single-crystal $CoFe_2O_4$, grown by the method of chemical transport reactions on MgO(100) substrate, was used for comparison. The average size of all nanoparticles was estimated from the BET specific surface area measurements. Raman spectra were measured at room temperature (300 K) through 50x microscope objective using Renishaw inVia micro-Raman spectrometer equipped with laser 830 nm. According factor group analysis are associated the cubic spinels $1A_{1g} + 1Eg + 3T_{2g}$ and tetragonal spinels $2A_{1}g + 3B_{1g} + 1B_{2g} + 4Eg$ [2]. We found that the Raman spectra the $CoFe_2O_4$ nanopowers have 10 lines and CoFe2O4 nanosized is tetragonal spinel.

References

1. V. Serga; M.Maiorov; A. Petrov; A. Krumina *Ferroelectrics*,Vol. 103, Is1 p.18–24 (2008).
2. Zhongwu Wang, R. T. Downs, R. T. Downs, R. Shetty, S. K. Saxena, C. S. Zha, Y. S. Zhao, D. Schiferl, and A. Waskowska4 Phys Rev. B68 094101 (2003)

PO-182

The Method of Glyceric Acid Preparation and Gold Supported Catalysts for its Realization

S.Čornaja[1], V.Kampars[1], J.Grabis[2], D.Jankoviča[2], S.Žižkuna[1], O.Muravjova[1], K.Dubencovs[1]

[1]Riga Technical University

[2]RTU Institute of Inorganic Chemistry

e-mail: Svetlana@ktf.rtu.lv

Glycerol is the main by-product of biodiesel fuel manufacturing. Glycerol catalytic oxidation by molecular oxygen is one of the feasible methods of glycerol utilization. A number of important and valuable products, which are used as a feedstock in various processes of organic synthesis, can be obtained in the process of glycerol oxidation. Currently the supply of these chemicals is limited due to high costs. Glycerol catalytic oxidation by molecular oxygen can substantially decrease the cost of oxidation products.

Kinetics of glycerol oxidation in presence of various gold based catalysts is studied in this research [1]. There are new synthesized gold nanoparticles supported on TiO_2 catalysts and commercial 1,5% Au/TiO_2 catalyst utilized.

According to the data presented in this research, activity of the new Au/TiO_2 catalyst is dependent on the catalyst specific surface (S_{sc}), gold nanoparticles size (d_{Au}), NaOH initial concentration, catalyst concentration and oxidation temperature. Activity of the catalyst increases along with decrease of the size of gold nanoparticles and increase of S_{cs}.

Research demonstrated that new gold containing catalysts are active, and yield of glyceric acid in presence of the new catalysts is equal to or higher than in presence of the commercial catalyst.

Glyceric acid is obtained as a main product with hight yield and selectivity.

Optimal parameters for the production of glyceric acid in closed thermostated gasometrical equipment and in barbotage type reactor have been determined.

References

1. S. Čornaja, V. Kampars, J. Grabis, D. Jankoviča, O.Muravjova, S. Žižkuna, R. Kampare, K. Dubencovs. Glicerīnskābes iegūšanas metode un katalizators tās realizācijai. *Pat.* LV 13956 (20.11.2009)

TABLE OF CONTENTS